Effects of Quorum Quenchers on Aspergillus fumigatus Conidia Aggregation, Adhesion to Surfaces, and Biofilm Formation

Tamimi, R.

Effects of Quorum Quenchers on *Aspergillus fumigatus* Conidia Aggregation, Adhesion to Surfaces, and Biofilm Formation

Roya Tamimi

A thesis submitted in partial fulfilment of the requirements of the University of Westminster for the degree of Doctor of Philosophy

January 2020

Abstract

Aspergillus fumigatus can produce in vitro an extracellular hydrophobic matrix with biofilm features under static growth conditions. Microbial quorum sensing (QS) system regulates genetic competence and biofilm formation. Notwithstanding, triclosan, as a synthetic antimicrobial, disrupts QS signal in some bacteria, yeasts, and dermatophytes through blocking the biosynthesis of amino acid and fatty acids in the microbes. In this study, triclosan quorum quenching role as well as the effects of microbial quorum quenchers, furanone, farnesol and tyrosol were investigated against *A. fumigatus* for the first time. Amphotericin B (AMB), a common antifungal agent used against *A. fumigatus* infection, carries adverse effects against human health. So, triclosan's antifungal effect in combination with AMB was also studied.

Microbial cells' detrimental attachment and biofilm formation on the indwelling medical implants, healthcare and hospital facilities, prompts interests to introduce feasible and cost-effective methods for eliminating/reducing microbial attachment to the surfaces. Using water contact angle (WCA) measurements, hydrophobicity of some hydrophilic surfaces (glass, acrylic, HDPE, nylon 6 and UPVC), and hydrophobic surfaces (PTFE and silicone) was measured following coating them with the mentioned antimicrobial agents.

A. fumigatus conidia were exposed to the agents and the subsequent changes in the conidial viability, biofilm biomass production, total and EPS-related protein/ polysaccharide/ and nucleic acid were studied. The effect of AMB was weaker than the other agents on mitigating the biofilm formation. eDNA release was observed from *A. fumigatus* mycelia treated with triclosan, tyrosol and farnesol as compared with untreated control group. This eDNA release appeared to be due to necrosis occurrence in the treated samples verified by gel electrophoresis and protein quantity analysis. As a novel finding, the necrosis induced by triclosan followed by apoptosis induced by AMB resulted in a synergistic interaction to reduce the conidia viability even at the sub-MIC doses of triclosan and AMB. Confocal microscopy of the *A. fumigatus* exposed to triclosan-AMB combination confirmed the synergistic interaction between them against the fungus biofilm. Assaying for hydrophobicity of the conidia cell wall revealed a change from hydrophobic to hydrophilic property. *ags3* down-regulation approved with real-time PCR assay showed triclosan's quorum sensing inhibitory role against *A. fumigatus*. This was through inhibiting conidia aggregation, and hence prohibiting initiation of quorum sensing signalling pathway. Through SDS-PAGE assay it was established that the conidia cell wall hydrophobic rodlet layer was absent in farnesol-treated sample.

This study revealed some of the physio-chemical properties that are involved in *A. fumigatus* conidia attachment to the surfaces. This work for the first time established that hydrophobic surfaces, PTFE and silicone, coated with farnesol showed hydrophilicity, while AMB changed UPVC surface charge from hydrophilic to hydrophobic. Taken together, besides influencing the conidia cell wall hydrophobicity, farnesol and AMB can also be used to coat the surfaces in clinical healthcare settings to diminish hydrophobic/hydrophilic microbial cells attachment to the surfaces.

“When knowledge strikes on the heart, it becomes a helper,
When knowledge strikes on the body, it becomes a burden.”

Jalal ad-Din Muhammad Rumi (1207–1273)

Table of Contents

List of figures

List of tables

List of equations

Acknowledgements

I would like to express my sincere appreciation to the University of Westminster Cavendish Scholarship, which funded my PhD tuition fees and to all those who have accompanied and encouraged me throughout my PhD adventure.

I wish to express my deepest gratitude to my supervisor, Professor Tajalli Keshavarz, whoes valuable comments and guidance encouraged me to learn and helped me at various stages of not only my research, but also my personal life. I am also indebted towards his wealth of experience and knowledge, which implies to me the passion for science can manifest in the form of literature.

Very special thanks to my second supervisor, Dr Godfrey Kyazze, for his invaluable guidance and numerous ideas throughout my PhD research. I wish to express my gratitude towards Dr Miriam Dwek for her valuable comments and feedbacks on my work through the upgrade report discussion meeting.

I acknowledge with appreciation the members of technical staff at the School of Life Sciences, University of Westminster particularly Burak, Joe, Jonathan, Luisa, Neville, Thakor, Umar, and Vanita for their help and support throughout my studies.

Many thanks to all members of the lab and research scholars, past and present, with whom I have shared the four-year of study. Special thanks go to Rachith, Tayebeh, and Zain. I would like to recognize the invaluable assistance that you all provided during my study. Special gratitude also goes to Dr Namdar Baghaei Yazdi, Dr Muhammad Javed, and Dr Nasim Farahmand, who were instrumental in defining the path of my career.

Finally, I am eminently grateful to my family, who kept me going on and this work would not have been possible without their precious support. Thank you for your constant unconditional love.

Author's Declaration

I declare that the present work was carried out in accordance with the guidelines and regulations of the University of Westminster. The work is original except where indicated by special reference within the text.

The submission as a whole or part is not substantially the same as any that I previously or am currently making, whether in published or unpublished form, for a degree, diploma or similar qualification at any University or similar institution.

Until the outcome of the current application to the University of Westminster is known, the work will not be submitted for any such qualification at another University or similar institution.

Any views expressed in this work are those of the author and in no way represent those of the University of Westminster.

Signed: Date:

List of abbreviations

- μ- Micro
- μL- Microlitre
- ABPA- Allergic bronchopulmonary aspergillosis
- ACP- Acyl carrier protein
- AFS- Allergic fungal sinusitis
- Air-liquid interface *(*ALI-biofilm*)*
- AMB- Amphotericin B
- AMPs- Antimicrobial peptides
- APS- ammonium persulphate
- BSA- Bovine serum albumin
- CAUTIs- catheter-associated urinary tract infections
- Cdna-Complementary DNA
- CFU- Colony forming units
- CFW- Calcofluor White
- CLSM-Confocal laser scanning microscopy
- CRBSI- catheter-related bloodstream infection
- CV-Crystal violet
- CVCs- central venous catheters
- DI water- De-ionized water
- DMSO-Dimethyl Sulfoxide
- DNA-Deoxyribonucleic acid
- eDNA- Extracellular DNA
- EDTA- Ethylene diamine tetra-acetic acid
- EDTA- Ethylenediaminetetraacetic acid
- EPS- Extracellular polymeric substances
- FCM- Flow cytometry
- FICI- Fractional inhibitory concentration index
- FPP- farnesyl pyrophosphate
- FSC- Forward scatter

- GAG- Galactosaminogalactan
- HAI- Healthcare Acquired Infections
- HDPE- High-density polyethylene
- HPLC- High performance liquid chromatography
- IPA- Invasive pulmonary aspergillosis
- MATH-Microbial adhesion to hydrocarbons
- MIC- Minimum inhibitory concentrations
- MOPS- mM 3-(N-morpholino) propanesulfonic acid
- mRNA- Messenger RNA
- NAG- N-acetylglucosamine
- OD- Optical density
- PBS- Phosphate-buffered saline
- PDA- Potato dextrose agar
- PDB- Potato dextrose broth
- PI- Propidium iodide
- PKA- Protein kinase A
- PTFE- Polytetrafluoroethylene
- QQ-Quorum quenching
- QQrs- Quorum quenchers
- QS- Quorum sensing
- QSC- Quorum-sensing-controlled
- QSI-Quorum sensing inhibitor
- QSM- Quorum sensing molecule
- RNA-Ribonucleic acid
- ROS- Reactive oxygen species
- Rpm-Revolution per minute
- RT-PCR- Real-time polymerase chain reaction
- SDS-PAGE- Sodium dodecyl sulfate polyacrylamide gel electrophoresis
- SSC- Side scatter
- TEMED- N,N,N′,N′-Tetramethylethylenediamine
- UPVC Unplasticized polyvinyl chloride
- UTIs- Urinary tract infections

- WCA- Water contact angle

List of publications

1. **Tamimi, R.,** Kyazze, G., and Keshavarz, T. "*Aspergillus fumigatus* mycelia molecular compartments and conidia surface charge are affected by antimicrobial agents, triclosan, tyrosol, farnesol and amphotericin B" *Under review.*

2. **Tamimi, R.,** Kyazze, G., and Keshavarz, T. "Anti-fungal effect of triclosan on *Aspergillus fumigatus*: quorum quenching role as a single agent, synergistic interaction with AMB" *manuscript in preparation.*

3. **Tamimi, R.,** Kyazze, G., and Keshavarz, T. "Hydrophobic surfaces coated with farnesol: anti-biofilm display against *Aspergillus fumigatus* hydrophobic conidia" *manuscript in preparation.*

Chapter 1

Introduction

1.1 Microbial cells attachment and biofilm formation

Biofilms can be defined as structured microbial communities attached to surfaces and encased within a matrix of exopolymeric materials (Yasir et al., 2018). Hydrophobins are involved in the formation of aerial structures and in the attachment of hyphae to hydrophobic surfaces (Wo¨sten, 2001) (section 1.7.3, Hydrophobins).

The microbial life cycle can be classified into two different phases:

- Unicellular (planktonic)
- Multicellular (biofilm or sessile cells) (Gestel et al., 2015)

To initiate biofilm formation, interchange between the two phases needs the transition from planktonic cells to sessile cells and from sessile cells to detached cells, which allows a return to the planktonic phase (Mcdougald et al., 2011).

Sessile cells within the biofilm, exist in a stationary or dormant growth phase (Hall-Stoodley et al., 2004) and exhibit phenotypes that are dissimilar to planktonic cells (Rollet, Gal and Guzzo, 2008). In biofilms, cells present an exceptional resistance to environmental stresses, especially antibiotics (Lebeaux et al., 2014).

There are differences in gene expression between planktonic cells and biofilm forming communities:

❖ Up-regulation of some genes. These genes are involved in iron-sulfur metabolism, lipid metabolism, amino acid and carbohydrate transport, biosynthesis of secondary metabolites, stress response (Guilhen, et al., 2016) and efflux system components (Rumbo-Feal et al., 2013). These factors are critical to the attachment stage of biofilm development. Several genes involved in iron acquisition are overexpressed in the biofilm compared to planktonic cells (Berlanga and Guerrero, 2016).

❖ Down-regulation of some genes. This includes down-regulation of the DNA repair genes, which lead to spontaneous mutations in biofilm forming cells. Therefore, novel genetic traits are raised within the biofilm (Nakamura et al., 2016).

1.2 Biofilm structure

Biofilm formation is commonly considered to occur in four main stages (figure 1.1):

1) Cells attachment to a surface: Within a niche, microbial cells encounter attractive or resisting forces that vary depending on ionic strength, pH, nutrient levels, and temperature. Medium properties accompanied by microbial cell-surface composition affect the direction toward or away from the contact surface (Davey and O'toole, 2000).

2) Microcolony formation: Adherence is mediated by additional extracellular adhesive attachments and secreted adhesins. However, the initial attachment is dynamic and reversible. During that, cells can detach and re-join the planktonic population if disturbed by repulsive hydrodynamic forces, or in response to nutrient availability. Irreversible attachment achieves by cells that can shear forces and preserve a stable grip on the surface (Kostakioti et al., 2013; Dunne, 2002).

3) Biofilm maturation: Surface contact generates responses that cause gene expression changes, up-regulating factors preferring sessility, such as those associated in the formation of the extracellular polymeric substances (EPS) (Martã-nez and Vadyvaloo, 2014).

4) Detachment (also termed dispersal): Detached cells may then colonise new areas (Kaplan, 2010). Biofilm detachment can be the consequence of various stress-inducing conditions including oxygen fluctuations, amendments in nutrient availability, and the increase of toxic products (Kostakioti et al., 2013).

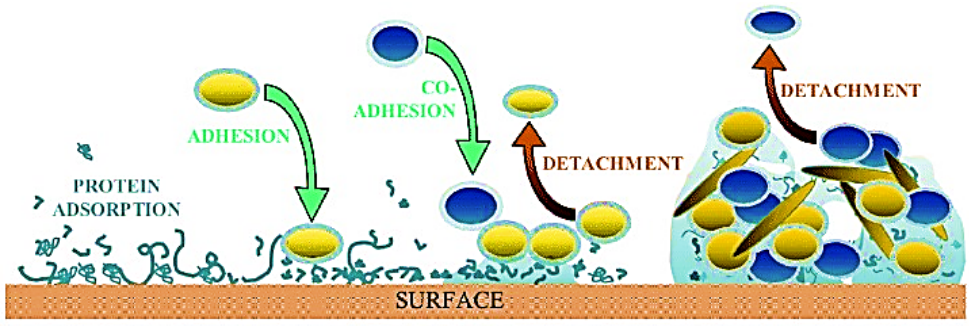

Figure 1.1 Biofilm formation stages. Unicellular (planktonic) and multicellular (biofilm or sessile cells) life phases alternate over time. Each phase is associated with a different transcriptional behaviour. In this two-phase cycle, microbs undergo physiological transitions from planktonic cells to sessile cells to form a biofilm structure, and from sessile cells to dispersed cells in returning to the planktonic phase (Berlanga and Guerrero, 2016) (Svensater and Bergenholtz, 2004)

Wimpenny (2000) described microbial biofilm formation by referring to the early development of micro-colonies, EPS production, and the formation of either internal channels or pores (Wimpenny, 2000). Biofilm formation in filamentous fungi has been demonstrated based on some structural features including aggregation, a surface-associated growth of cells, and cells embedded in self-secreted EPS. The features are related to altered gene expression resulting in boosted tolerance to antimicrobial compounds or biocides, changes in enzyme or metabolic production and/or secretion and physiological changes. Observing any of these phenotypic changes can confirm the biofilm formation phenomenon in filamentous fungi (Harding et al., 2009). Villena and Gutierrez-Correa (2007) studied *A. niger* biofilms under variable water activities and confirmed the filamentous fungal biofilm involvement in industrial processes (e.g. pipes, and cooling towers). They suggested that low water activity may affect enzyme biosynthesis and they used ethylene glycol as water activity depressor (Villena and Gutierrez-Correa, 2007). In liquid cultures, many filamentous fungi form structured pellets (hyphal aggregates); that have significantly different growth characteristics and metabolism compared to freely dispersed mycelia. Pellet formation depends on hyphae-hyphae interaction while biofilm formation is initiated by adhesion of spores and/or hyphae to surfaces (Priegnitz et al., 2012).

1.3 Comparing filamentous fungi biofilm with biofilms formed by yeasts and bacteria

(1) Propagule adsorption. This phase is comparable to the reversible attachment stage in bacterial models. For filamentous fungi, this includes deposition of spores or other propagules such as sporangia or hyphal fragments. This step essentially includes physical contact of the organism with a surface (Harding et al., 2009).

(2) Active attachment to a surface. This phase is equivalent to fixed attachment in bacteria. In filamentous fungi this often comprises secretion of adhesive substances by germinating spores and active germlings (newly germinated cells (Vahtera et al., 2014).

(3) Microcolony formation I. This phase is comparable to the early stages of micro-colony formation in bacteria. The initial stages of growth and surface colonization in fungi contain apical elongation and hyphal branching. Hyphae explore the substratum, ramify across surfaces as a monolayer, and/or become invasive. This stage includes the production of EPS that allows the growing colony to adhere tenaciously to the substrate

(Harding et al., 2009)

(4) Microcolony formation II (initial maturation). This phase is comparable to the later stages of micro-colony formation in bacteria. It includes the formation of compacted hyphal networks or mycelia and hypha–hypha adhesion. This contains layering, the formation of hyphal bundles 'glued' together by EPS, and the formation of water channels through hydrophobic repulsion between hyphae or hyphal bundles (Harding et al., 2009).

Within the asexual growth phases, filamentous fungi lack the growth dynamics resulting from binary fission or budding that are common in bacteria and yeasts (Harding et al., 2009). Many fungi produce invasive hyphal structures that extend beyond the liquid-air interface, or the specialised structures necessary for host penetration, sporulation, and nutrient acquisition at the host interface (Lin et al., 2014).

Hydrophobins are secreted from filamentous fungi and self-assemble into amphipathic layers at hydrophilic-hydrophobic interfaces. They modify hyphal surface properties in response to environmental and developmental signals (Linder et al., 2005; Bayry et al., 2012). These protein assemblies enable and support the fungal lifecycle at water-environmental and air-water interfaces.

Fungi generally have more than one planktonic form, including sexual spores, asexual spores (may be named conidia as well), sporangia (a sac-like cell which produces asexual spores) and hyphal fragments that can disperse to reinitiate the cycle (Siqueira and Lima, 2013). The dispersive forms are not unicellular and often float in the air rather than water. The aerial component of the lifestyle of many fungal species has a high dependency on aerial spore dissemination for dispersal (Rieux et al., 2014).

1.4 Biofilm role in filamentous fungi lifecycle

Fungal biofilms possibly represent much more than a simple biological coating (Hrding et al., 2009). For example, in *Aspergillus fumigatus* biofilm formation is required to be involved in the pathogenesis of localized as well as invasive diseases (Beauvais et al., 2007; Mowat et al., 2007; Chandrasekar and Manavathu, 2008). Aspergilloma, a localized infection, and invasive pulmonary aspergillosis (IPA) have been shown to contain highly agglutinated hyphae encased in EPS (Mowat et al., 2008; Loussert et al.,

2010).

Much of the knowledge about fungal biofilm formation has been gained through the studies of biofilms formed by *Candida* species on artificial surfaces (Negri et al., 2011; Das et al., 2014). Moreover, the increasing realisation of the significance of fungal biofilms is shown by reports on other yeasts, and filamentous fungi. This is including *Cryptococcus neoformans*, *Fusarium* species, *A. fumigatus, Pneumocystis* species, *Blastoschizomyces capitatus*, *Trichosporon asahii, Malassezia pachydermatis*, *Saccharomyces cerevisiae*, and *Coccidioides immitis* (Walsh et al., 1989; Reynolds, 2001; Davis, 2002; D'Antonio et al., 2004; Bonaventura et al., 2006; Cannizzo et al., 2007; Imamura et al., 2007; Mowat et al., 2007).

Biofilm formation involving molds such as *A. fumigatus* has been shown to include phase-dependent developmental stages like those of *C. albicans* (Ramage et al., 2011). The structural organisation of biofilms and the presence of flowing water channels may allow nutrient exchange and gas exchange while providing the fungal cells with a sheltered niche for protection against environmental predators, immune cells, shear forces, and antimicrobial drugs (Martinez and Fries, 2010). *A. fumigatus* also produces several mycotoxins, including the well-known fumitremorgins A and B, and verruculogen that act on the central nervous system, making sustained tremors, convulsions and death in animals. Verruculogen is the most toxic, causing tremors in swine and sheep (Tepsic, 1997).

Differences between the yeasts and *A. fumigatus* in regard to their vulnerability against antimicrobial agents have been studied. No effect has been observed for azoles against *C. albicans*. This may be because *C. albicans* biofilms consist of a combination of yeast cells and hyphae, therefore giving yeast cell the opportunity to divide and proliferate. However, for *A. fumigatus*, mature biofilms are entirely hyphal, showing no further signs of proliferation. Consequently, targeting of the ergosterol biosynthesis pathway would be useless, regardless of EPS and biofilm stability. So that, inhibition of defined fungal biofilm resistance mechanisms, such as heat shock proteins and efflux pumps have insignificant effects against mature *A. fumigatus* biofilms (Robbins et al., 2011; Rajendran et al., 2013). Also, caspofungin combined with a non-immunosuppressive analogue presented synergy against *C. neoformans*, whereas no synergistic interaction was seen against *A. fumigatus* (Steinbach et al., 2004). To improve

the effectiveness of antifungal drugs against fungal biofilms and biofilm-associated infections, treatment of early biofilm stages, novel formulations of antifungal drugs, and antifungal combinations have been successfully applied (Martinez and Fries, 2010). For instance, *in vitro* studies revealed that treatment of actively growing *A. fumigatus* biofilms with amphotericin B (AMB) was more effective than treating mature structures (Mowat et al., 2008). Regarding *C. albicans* biofilms, they presented greater susceptibility when treated with a combination of AMB and posaconazole than when treated with single drugs (Ibrahim et al., 2015).

1.5 *A. fumigatus* biofilm contamination of surfaces involved in medical devices

Investigation of *Aspergillus* species infections has grown in importance in recent years (Reyes-Montes et al., 2018). This increase probably results from a higher number of patients being at risk, including transplant recipients, neutropenic individuals, allergic patients and those treated with corticosteroids or other immunosuppressive regimens (Pasqualotto, 2009). As most of the *Aspergillus* infections are produced by *A. fumigatus*, majority of studies have focused on this species (Latgé and Steinbach, 2009). From a medical angle, *A. fumigatus* is an opportunistic pathogen of immunocompromised individuals, with a disease severity that depends on the host's immune status, demonstrating a 50-95% mortality rate (Gonzalez-Ramirez et al., 2016). *A. fumigatus* has become the most common airborne fungal pathogen, causing severe and usually fatal invasive infections in immunocompromised hosts in developed countries (Heinekamp et al., 2014). This fungus gives rise to diverse infections including local infections, such as nails dermatomycoses or fungal keratitis, and invasive infections, such as aspergillosis. An earlier report suggested that *A. fumigatus* was the second most common cause of fungal infections in hospitalised patients, after *C. albicans* (Ellis, 1999). *A. fumigatus* infection in the respiratory tract can induce lung fungal ball, asthma IPA, invasive aspergillosis, hypersensitivity pneumonitis, immunoglobulin E-mediated allergic rhinitis, chronic necrotizing pneumonia or allergic bronchopulmonary aspergillosis (ABPA). Additionally, it gives rise to osteomyelitis and endocarditis. It is also the most common *Aspergillus* organism causing allergic fungal sinusitis (AFS) (Peral-Cagigal, 2014). Viola and Sutton (2010) studied AFS, which showed that 100% of patients had a history of polyps, 54% had asthma, 27% had aspirin sensitivity, 65% had eosinophilia, and 69% had increased total IgE levels. So, most of the patients had a history of atopy, chronic sinusitis, nasal polyps, and intractable symptoms, despite adequate treatment for bacterial

sinusitis (Viola and Sutton, 2010). *A. fumigatus* sporulates plentifully on decaying organic matter. Conidia small size (2.0–3.0 mm in diameter with extremes up to 3.5 mm) enables this airborn dispersal, indoors and outdoors, and sedimentation on to various surfaces (Kwon-Chung and Sugui, 2013).

There is increasing interest from industrial, research and development and healthcare sectors in the development of feasible and cost-effective substitute methods of reducing Healthcare Acquired Infections (HAI). The most challenging areas tend to be high-touch points such as door handles, bed rails, bedding (mattress), table top surfaces, television controls and staff uniforms (Ramphal et al., 2014). Inside hospitals, although less numerous, the presence of *A. fumigatus* conidia may be related to contamination of ventilation systems and other factors such as renovation works inside or adjacent to the hospital (Fournel et al., 2010). The contaminated surfaces and the healthcare facility environment act as sources of direct or indirect contact with the patient. Hospitals have amended infection control practices to diminish and eradicate environmental microbial contamination. This is achieved mostly using disinfectants and detergents. The selection of the exact disinfectant dependents on multiple factors, e.g., areas of high risk such as operating theatres require multiple cleans, whereas patient waiting rooms may be cleaned only once per day (Murray et al., 2017). The choice of disinfectant agent is also multifactorial: body fluid spillages will normally need stronger disinfectants than those used in routine cleaning. Hence, hospitals use a variety of products including ethyl alcohol in hand rubs and gels, QACs (quaternary ammonium compounds), chlorine-releasing agents and peroxygen sterilants (Abreu et al., 2013).

However, given the available evidence for the ineffectiveness of cleaning and rapid recontamination of surfaces, there is much interest in substitute tactics to the problem. The development of intrinsically anti-microbial surfaces that incorporate a variety of agents to kill microbes may be considered a useful strategy. Also, the use of agents that can prevent surface contamination, or that exhibit a residual antimicrobial activity post-disinfection, could prove effective in the healthcare setting.

Likewise, deleterious effects of biofilm formation on medical devices such as indwelling vascular catheters, cardiac pacemakers, prosthetic heart valves, chronic ambulatory peritoneal dialysis catheters and prosthetic joints, voice prosthesis, and contact lenses have been studied (Donlan, 2002). Reported biofilm formation on silicon voice prosthesis

and penetration into the device are related to both fungi and bacteria (Chandra et al., 2012). There are few in vitro studies about the fungal colonisation of contact lenses. Fungal keratitis is counted as one of the most important causes of ocular morbidity and visual loss in developing nations, where particularly *Aspergillus* spp. and *Fusarium* spp. are the major offending organisms (Sengupta et al., 2012). While fungal colonisation adhesion to the contact lens surface can lead to the release of enzymes followed by generating products facilitating the growth of microorganisms, this invasion threat has not been observed in yeasts (Marqués-Calvo, 2002). The *A. fumigatus* infections of medical implant devices occurrence in the first month after lung transplantation suggests hospital acquisition, but *Aspergillus* may also be acquired at home after the patient's discharge (Remund et al., 2009). Other solid-organ transplantations, mainly liver, heart, and kidney also represent risk factors for invasive infection with *Aspergillus* spp. (Singh and Paterson, 2005).

1.6 Plastics used in medical devices and the biofilm controlling strategies applied there

In the past six decades, implantable medical devices or systems have been advanced through developments in science and engineering, especially in microelectronics, biotechnology, and materials (Joung, 2013).

Polyethylene (PE), which is used as the wear-bearing surface of hip and knee arthroplasty and total joint replacement (Chakrabarty, Vashishtha and Leeder, 2015), can be made in several ways with different physical properties. It can also have very small amounts of co monomers, which will alter its structure and physical properties. Among different types of PE, High-density polyethylene (HDPE) has densities ranging from 0.940 to 0.970 g/cm3 and may or may not contain co-monomer (McKeen, 2017).

Polytetrafluoroethylene (PTFE) polymer is an example of a linear fluoropolymer formed by the polymerization of tetrafluoroethylene (TFE). PTFE is a homopolymer, a polymer made from a single monomer, and the most common commercial name of it is Teflon, manufactured by Dupont Co. The vital properties of fluoropolymers differ from the atomic structures of fluorine and carbon and their covalent bonding in specific chemical structures (Modjarrad and Ebnesajjad, 2014). PTFE is hydrophobic and hence, neither water nor water-containing substances moisten it (Tzoraki and Lasithiotakis, 2018). Common applications of PTFE are in cardiovascular engineering containing heart valves

and vascular grafts. PTFE sutures are used in surgery for prolapse of the posterior or anterior leaflets of mitral valves and in the repair of mitral valve for myxomatous disease. PTFE is particularly used in implantable prosthetic heart valve rings. It has been effectively used as vascular grafts when the devices are implanted in high-flow, large-diameter arteries such as the aorta (Jaganatha, 2014).

Unplasticized polyvinyl chloride (UPVC) is one of the mostly produced plastics in the world. As it is highly resistant to chemical erosion and has smoother inner walls than PVCs is used in drinking water distribution systems as an alternative for metallic pipes (Zhang and Lin, 2014). Moreover, UPVC can also be used for doorframes and conservatories (Bortel and Szewczyk, 1996). The advantage of PVC-based medical devices has been evidenced by the fact that over 40% of plastic-based disposable medical devices used in hospitals are made from PVC (PVCMed Alliance, 2017). In real hospital practices, PVC medical devices can be effortlessly sterilised without affecting their properties such as flexibility and resistance to tears, scratches and kinks. However, the additives that are often necessary for PVC arouse concerns of its safety, thus quests the modifications of PVC itself (Zhang et al., 2018).

Reusable, disposable implant and packaging materials will need to be sterilised using various methods like steam, autoclave (dry heat which is usually performed at temperatures higher than 121°C), ethylene oxide (EtO), electron beam, and gamma radiation. They must be able to withstand these conditions and still maintain their properties (Modjarrad and Ebnesajjad, 2014). Table 1.1 shows sterilisation methods and their functionality on some plastics, which are used mostly in medical devices and indwelling, as discussed earlier.

Table 1.1 Sterilisation methods and their functionality on the surfaces used in this study (Modjarrad and Ebnesajjad, 2014)

Polymer	Abbreviation	Steam	Dry heat	Ethylene oxide	Gamma radiation	Electron beam
	Polyolefins					
High Density Polyethylene	HDPE	Poor	Poor	Good	Good	Good
Polyvinyl Chloride Unplasticized	UPVC	Poor	Poor	Good	Fair	Fair
	Fluoropolymer					
Polytetrafluoroethylene	PTFE	Fair	Fair	Good	Poor	Poor
	Polystyrene					
Acrylics	-	Poor	Poor	Good	Good	Good
	Polyamide					
Nylon 6 (Polyamide 6)	PA6	Fair	Fair	Good	Fair	Fair
	Elastomer					
Silicone	-	Good	Good	Good	Good	Good

Catheters are one of the most frequently used medical devices (figure 1.2). Central catheters, central venous catheters (also known as central venous pressure (CVP) catheters, and central lines) typically have one to three lumens and are created out of medical grade silicone or polyurethane (Wildgruber et al., 2016). These devices are notoriously prone to infection. Infection is the largest concern with catheter use, whether long term or short term. Urinary tract infections (UTIs) constitute the most frequently occurring nosocomial infections (Parida and Mishra, 2013). During long-term use of catheters, the risk of UTIs increases rapidly over time and reaches 50% after 7–10 days (Platt et al., 1983). These infections are considerably complicated by the fact that the patients in question often suffer from a compromised immune system, rendering the consequences of the infections even more severe (Brosnahan, Jull and Tracy, 2002). Consequently, it is highly desirable to be able to modify materials used for medical devices, e.g. urinary catheters, in a way that allows the production of catheters resistant to the initial microbial colonisation (Trautner, 2005). Presently, some commercial products with antimicrobial surface coatings are available. For anti-adhesive strategies, the use of polymer chains, or hydrogels is favoured, however using super-hydrophobic surfaces amended anti-adhesive activity. Antimicrobial peptides, antibiotics, chitosan or enzymes directly bound, tethered through spacer-molecules or encased in biodegradable matrices, nanoparticles and quaternary ammonium compounds have anti-microbial activities, as well (Swartjes et al., 2015).

Catheter-associated urinary tract infections (CAUTIs) are the most commonly faced HAIs or nosocomial infections (Jacobsen et al., 2008). CAUTIs can lead to numerous medical complications such as catheter encrustation, endotoxic shock, bladder stones, pyelonephritis, and septicaemia (Jordan et al., 2014). Fungi or bacteria, including both Gram-positive and Gram-negative bacteria, can cause CAUTIs. A urinary catheter can be constructed from any number of different polymers, with silicone being typically used, and latex rubber also common. All catheter types and brands are susceptible to CAUTIs and biofilm formation and existing methods to prevent these complications may just postpone the process without treating the problem (Stickler, 2012).

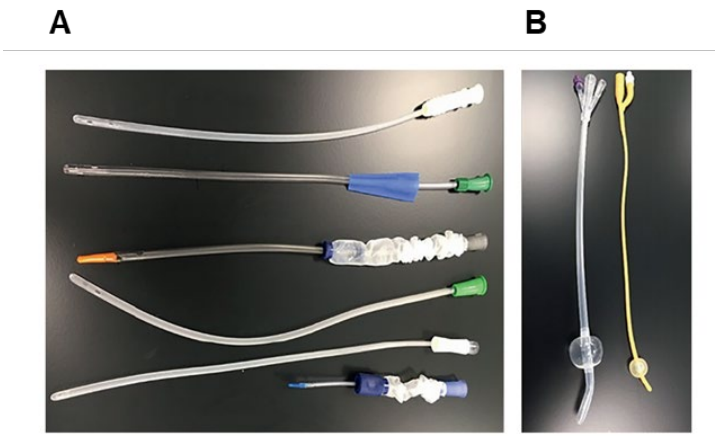

Figure 1.2 Different intermittent catheters (A): the upper five are male catheters; the lowest one is a female catheter (B): Two indwelling catheters with retention balloons inflated (Cortese et al., 2018)

Typically, in the bladder, microorganisms are freely suspended in the urine (planktonic state) and unable to cause a UTI unless they are present in large numbers and hence, overcome the bladder innate defences. When medical devices like an indwelling urinary catheter is within the body, microorganisms can attach to it, forming colonies bound together and enclosed in biofilm structures (Thomas-Whitel et al., 2016). Cortese et al., showed that the longer a urinary catheter is in place, the more likely it is to form biofilm on its surface and cause a CAUTI. Patients with short-term (≤ 7 days) catheterisation experience biofilm formation 10–50% of the time; yet, practically all patients with long-term (> 28 days) catheterisation are found to present with biofilm formation (Cortese et al., 2018). Microbial adhesion on catheter depends on physico-chemical characteristics, including hydrophobicity, electrostatic interactions, and surface roughness (Gominet et al., 2017) and on microbial cell properties; availability of the adhesins such as flagella, fimbriae, or surface-associated proteins or polysaccharides that helps anchoring the cell on catheter surface (Donlan, 2002). These microbial pioneers facilitate the arrival of other pathogens by providing more diverse adhesion sites. They multiply and produce the EPS that holds the biofilm together, leading to an irreversible attachment to the catheter surface (Flemming and Wingender, 2010). Once a mature biofilm is established, planktonic cells may disperse from the community, cause catheter-related bloodstream infection (CRBSI) and spread to other sites of the body. The most challenging feature of mature biofilms in case of CRBSIs is an increased ability of biofilm cells to survive the host immune system and antimicrobial agents (Lebeaux et al., 2014). This ability, named biofilm tolerance towards antibiotics, is the main reason explaining the difficulty to eradicate biofilms and control biofilm-related infections.

The organisms that attach to the catheter and develop the biofilm originate from one of several sources: (i) organisms travel intra-luminally from the inside of the tubing or collection bag, (ii) organisms are introduced into the urethra or bladder as the catheter is inserted, or (iii) organisms gain entry through the sheath of exudate that surrounds the catheter (Donlan, 2002). Extra-luminal contamination from the skin prevails in the first 10 days of catheter insertion and so frequently concerns short-term catheters (inserted for ≤ 14 days). Instead, intra-luminal contamination, mainly from the hub, increases with duration of catheterization and concerns long-term catheters (Safdar and Maki 2004; Helou et al., 2013).

Meta-analysis has demonstrated that catheters coated with chlorhexidine/silver sulfadiazine reduced the risk for CRBSI compared with standard non-coated catheters (Gominet et al., 2017). However, in a multi-centre randomised trial, central venous catheters (CVCs) impregnated with minocycline/rifampin on both the external and internal surfaces were associated with lower rates of CRBSI when compared with the first-generation chlorhexidine/silver sulfadiazine-impregnated catheters. Due to their broad-range spectrum of bactericidal activity, antimicrobial peptides (AMPs) have demonstrated a strong potential as anti-biofilm agents (Sanchez-Gomez and Martınez-de-Tejada, 2016). Catheters coated by AMPs killing microbes upon contact or through controlled release may consequently create promising future strategies to prevent catheter colonization. AMPs, though, might promote microbes' drug resistance. To overcome this resistance, drug combination strategies (chapter 3, section 3.2) or quorum sensing inhibitors (section 1.13) instead of AMPs may be applied for coating medical device surfaces.

Beside antimicrobial-impregnated catheters, preventive locks (instillation of highly concentrated antibiotic solutions left to dwell in the catheter for 12 to 24 hr) can be proposed for long-term catheters. However, the use of antibiotics (such as vancomycin or gentamicin) catheter flush or lock solutions could lead to the emergence of antibiotic-resistant organisms. In this context, non-antibiotic locks have been developed such as minocycline and Ethylenediaminetetraacetic acid (EDTA). This has been successful in avoiding catheter-related infection (Campos et al., 2011; Chatzinikolaou et al., 2003; Raad et al., 2002). Other non-antibiotic substances have been proposed such as ethanol or taurolidine-citrate (Liu et al., 2014; Souweine et al., 2015; Kavosi et al., 2016), but

extensive studies are needed to fully elucidate the benefits and the risks of such approaches.

1.7 *A. fumigatus* conidia and their cell wall components

The mycelia of *A. fumigatus* give rise to specialised hyphae, conidiophores, which produce conidia, small (~3µm) airborne dispersal cells that remain airborne for long periods and may enter human alveoli (Kohler et al., 2014). On average, a person is estimated to inhale several hundred *A. fumigatus* conidia each day; through contact with compost, grass cuttings, or leaf litter (Kohler, Casadevall and Perfect, 2014). They are recognised by innate immune system[1] of a human host only when they begin to germinate to produce a growing hypha after landing in an air-filled space like a paranasal sinus or lung (Aimanianda et al. 2009).

Conidia germinate to colonise new environments under favourable nutritional conditions. Conidial germination can be divided into four steps (Barhoom and Sharon, 2004; Harris and Momany, 2004):

- Breaking of the dormancy
- Isotropic swelling
- Establishment of cell polarity
- Formation of a germ tube

In liquid medium, germination of *A. fumigatus* conidia is related to conidial agglutination (Lamarre et al., 2008) that was defined in some filamentous fungi many years ago (Metz and Kossen, 1977). Conidial agglutination increases the size of the pellets produced under shake conditions and affects the use of filamentous fungi in biotechnology but does not affect the total germination (Papagianni, 2004; Kelly et al., 2006). Lin et al., (2007) suggestsed that in *A. niger* conidial aggregation corresponds to an agglomeration step but not a tight intergrowth of particles, suggesting a cell surface recognition (Lin et al., 2007).

[1] Nonspecific immune system; aposite to the adaptive immune responses, innate immune responses are not specific to a particular pathogen and anything that is identified as foreign or non-self is targeted by the innate immune system (Alberts et al., 2002).

The conidial cell wall is composed of two layers (Maubon et al., 2006):

- An external hydrophobic layer containing melanin and rodlet proteins, and
- An internal layer, electron translucent, containing polysaccharides such as α and β-glucans, chitin/chitosan and galactomannan.

Chitin is a vital component of the fungal cell wall, so that its synthesis has been proposed as a suitable target for the development of antifungal drugs, such as polyoxins and nikkomycins, which bind to the catalytic site of chitin synthesis (Ruiz-Herrera and San-Blas, 2003). In fungi, the chitin biosynthesis mechanism includes a multistep enzymatic conversion of glucose to uridine diphosphate-N-acetylglucosamine following with N-Acetylglucosamine units transfer from the uridine diphosphate form to growing chitin chains by chitin synthases (Catalli and Kulka 2010).

The fluorescent brightener Calcofluor White (CFW) has been a beneficial stain to study chitin biosynthesis and chitin localization. CFW is a disodium salt of 4,4′-bis-[4-anilino-bis-diethylamino-5-triazin-2-yl] amino]-2,2′-stilbene-disulfonic acid and binds to β-(1-3) and β-(1,4)-linked polysaccharides such as chitin and cellulose. At low concentrations (<25µg/ mL), CFW is a useful dye to stain fungal walls chitin and is used in medical mycology for recognition of fungal material in patient samples. At higher concentrations (>100µg/ mL), it inhibits fungi growth and has been used to screen mutant libraries for strains with cell wall defects. Overall, cells with low chitin concentrations are resistant to CFW comparing with the cells with high chitin levels, which are hypersensitive (Munro, 2013).

Conidia are coated with hydrophobic proteins and with the chemoprotectant melanin to endure harsh environmental stresses like freezing, sunlight, and desiccation (Kwon-Chung and Sugui, 2013).

The *A. fumigatus* cell wall polysaccharides moieties command the immune signature of the conidia depending on their morphological state (e.g. dormant, enlarged or germinating). Notably, most cell wall polysaccharides are biosynthesised from the monosaccharide glucose, which can be taken up from the extracellular environment and/or produced from gluconeogenesis and intracellular carbohydrate storage compounds such as trehalose and glycogen when necessary (Nelson and Cox 2012; Lee et al., 2013).

- Glucose is the basic unit of all types of glucans
- Glucose serves as a precursor for *N*-acetylglucosamine (NAG) in the chitin homopolyme
- Galactose, which is a glucose epimer, is also the major monosaccharide in galactomannans (Cabib and Arroyo, 2013).

Therefore, glucose is the major cell wall-associated monosaccharide, constituting more than 50% of all fungal cell wall polysaccharides (Gastebois et al., 2009; Schiavone et al., 2014; Lee and Sheppard, 2016). The biosynthesis of fungal cell wall polysaccharides is reached through a series of enzymatic steps that change glucose to glucan, NAG, and galactomannan (Orosz et al., 2014) (figure 1.3). Trehalose serves as an energy source during fungal germination at the first stages of development (Thevelein, 1984) and has been shown to be important for fungus-mediated infections (Foster et al., 2003; Puttikamonkul et al., 2010; Badaruddin et al., 2013). Glucose utilisation and trehalose and glycogen degradation are regulated by the protein kinase A (PKA) pathway (Wilson and Roach, 2002; Freitas et al., 2010; Assis et al., 2018). The presence of glucose is detected by a heterotrimeric G-protein, with the Gα subunit activating adenylate cyclase, resulting in an increase in intracellular cAMP pools and subsequent PKA activation (Fillinger et al., 2002; Krijgsheld et al., 2013). In eukaryotes, PKA is composed of a heterotetramer containing dimers of both a catalytic (PkaC1) and regulatory (PkaR) subunits. Binding of cAMP to PkaR results in the release of the active PkaC1 homodimer and subsequent downstream pathway regulation (Santangelo, 2006). Deletion of the *A. fumigatus pkaC1* causes defects in conidium germination and fungal cell wall organization and attenuates virulence in a mouse model of infection (Liebmann et al., 2004; Zhao et al., 2006; Grosse et al., 2008; Fuller et al., 2011). Likewise, glycogen breakdown and trehalose synthesis have been shown to be vital for *Magnaporthe oryzae* plant infection. In addition, *A. fumigatus* glycogen synthase kinase has been proposed to be a target for treating invasive aspergillosis, as it is important for *Aspergillus* growth (Sebastián-Pérez et al., 2016).

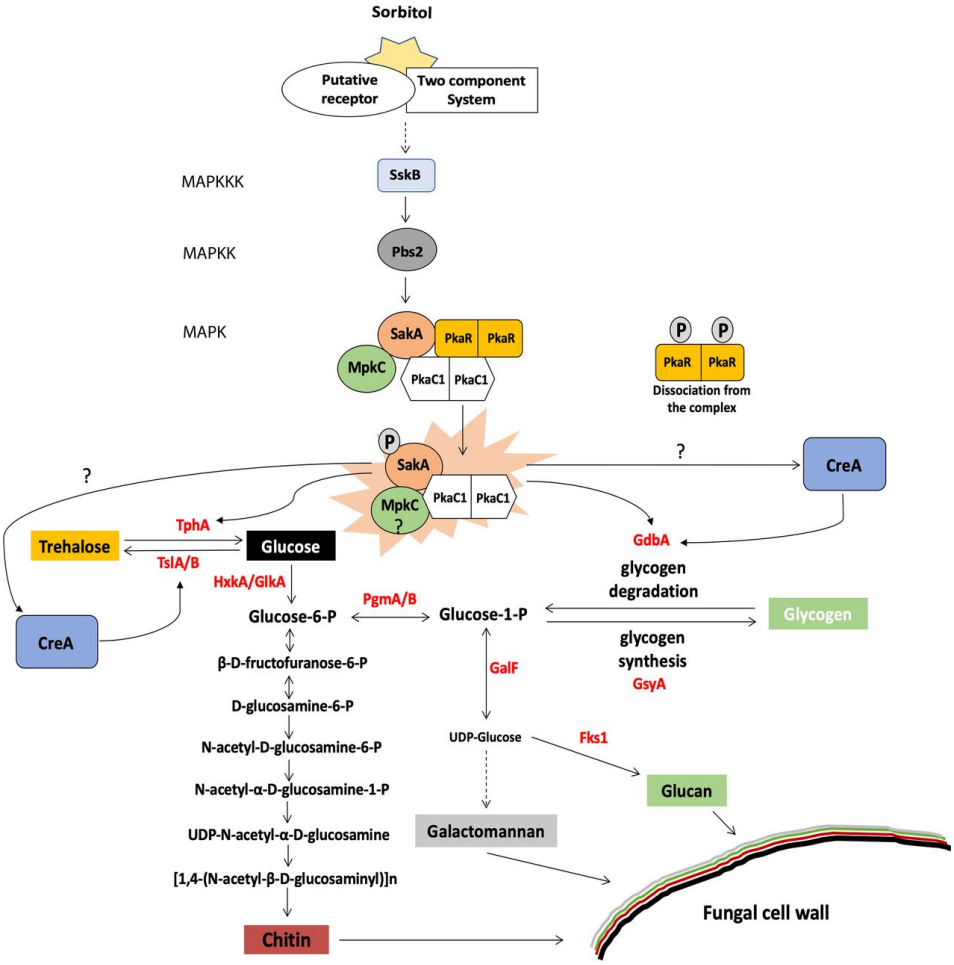

Figure 1.3 Glycogen and trehalose metabolism for cell wall polysaccharide precursor biosynthesis in *A. fumigatus*. In the absence of osmotic stress, a protein complex containing the PkaR and PkaC1 subunits with the HOG MAPK kinases SakA and MpkC forms. Upon the detection of osmotic stress, the HOG MAPK cascade is triggered, signalling to Pbs2, which in turn phosphorylates SakA. The active SakA acts upon the PKA regulatory subunit, resulting in the dissociation of PkaR from the complex and the activation of PkaC1. Now, the MpkC-SakA-PkaC1 complex controls trehalose and glycogen metabolism to offset the osmotic stress. Dashed arrows depict several steps in the pathway. TphA, trehalase phosphorylase; TslA/B, trehalose 6-phosphate synthase; HxkA, hexokinase; GlkA, glucokinase; PgmA/B, phosphoglucomutase; GalF, UTP-glucose-1-phosphate uridylyltransferase; Fks1, β-1,3-glucan synthase; GdbA, glycogen debranching enzyme; and GsyA, glycogen synthase (Assis et al., 2018)

During germination, swelling of conidia needs cell wall remodelling. During isodiametric growth, the conidial surface is changed. Scanning electron and atomic force microscopies have recognised that the outer rodlet/melanin layer of the resting conidia is increasingly lost, and the cell surface layer is transformed into a layer of amorphous material unmasking β-(1,3) glucan on the surface of the conidium (Rohde et al., 2002; Gersuk et al., 2006; Luther et al., 2007; Dague et al., 2008). It has been recommended that glucan

exposure or changes in hydrophobicity could be responsible for the agglutination process (Dynesen and Nielsen, 2003).

1.7.1 α-(1,3) glucan

α-(1,3) glucan (figure 1.4) is a major cell wall component of most ascomycetous and basidiomycetous fungi, e.g., *A. fumigatus*, *Blastomyces dermatitidis, Cryptococcus neoformans*, *Paracoccidioides brasiliensis*, *Histoplasma capsulatum*. These human pathogens establish their disease upon inhalation of their infective morphotypes. The role of this polysaccharide during infection has been confirmed and the mechanisms of its participation in establishing virulence have been promoted (Rappleye et al., 2007 and Reese et al., 2007).

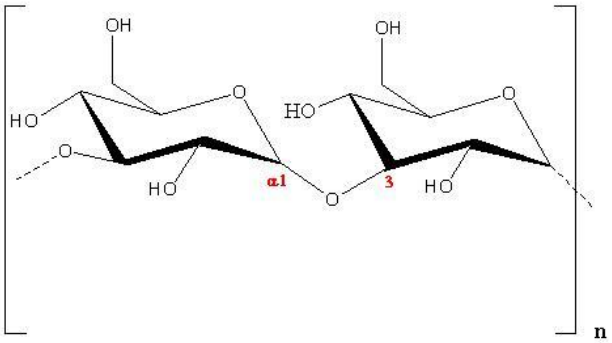

Figure 1.4 Structure of α-D-1-3-glucan polysaccharide. It is mainly found in the cell wall of microorganisms (http://polysac3db.cermav.cnrs.fr)

In *A. fumigatus*, α-(1,3) glucan is the main component of conidia and mycelium cell wall and accounts for 40% and 19% of the mycelial and conidial cell wall polysaccharides, respectively. In *A. fumigatus*, α-(1,3) glucan seems associated with melanin of the conidia cell wall (Maubon et al., 2006). They are also found in the matrix of the aerial-grown colony (Beauvais et al., 2007). In vivo, α-(1,3) glucan has been detected in the matrix of biofilm during pulmonary aspergilloma, where hyphae remain intensely aggregated but not during invasive aspergillosis where hyphae are dispersed in the lung (Loussert et al., 2010), suggesting that α-(1,3) glucans could be involved in the biofilm cohesion.

Adhesion to host tissues, mating, biofilm formation, colony morphology changes and fruiting body development require the interaction between fungal cells or fungi and host cells. Proteins and carbohydrates, due to their external location in the cell wall, are in interaction with the external environment. Except for the well-studied yeast mating

interaction, where protein-protein recognition is involved, most of the cell adhesion processes are controlled by a protein-carbohydrate complex (Dranginis et al., 2007). In *A. fumigatus*, α-(1,3) glucan are synthesized by three α1,3 glucan synthases (*Ags1p* [AFUA_3G00910], *Ags2p* [AFUA_2G11270], and *Ags3p* [AFUA_1G15440]). The lack of α-(1,3) glucan affects neither conidial germination nor mycelial vegetative growth and is compensated by an increase in β-(1,3) glucanand/or chitin content (Henry, Latge and Beauvais, 2011). α-(1,3) glucan chains interact among themselves and are accountable for the aggregation of swollen conidia without the involvement of any protein (Fontaine et al., 2010). Therefore, the physical properties of insoluble α-(1,3) glucan are implicated in the conidial aggregation.

Although α-(1,3) glucan carbohydrate binding modules (CBM-24) have been previously described in filamentous fungi (Fuglsang et al., 2000), the lack of an effect by any of proteinase, 0.1 M NaOH, or 0.1 M HCl treatments suggests that no protein is involved in conidial agglutination. α-(1,3) glucan-specific CBM have only been detected to date at the C-terminus of α-(1,3) glucanase.

Interaction between linear β-(1,3) glucan chains with the organisation of single and triple helix chain is well recognised (Sletmoen and Stokke, 2008). Despite the cell surface exposure of β-(1,3) glucan during conidial germination, this polysaccharide has no role in conidial recognition, signifying that α-(1,3) glucan–α-(1,3) glucan interaction should be stronger than β-(1,3) glucan interchain interaction (Fontaine et al., 2010).

1.7.2 Galactomannan

Galactomannan is a cell wall polysaccharide that is released by growing hyphae of *Aspergillus* spp. and has been used as a diagnostic marker of invasive aspergillosis. Levels are measured in the serum or respiratory samples of patients thought to be at risk of infection. The structural skeleton of the *A. fumigatus* cell wall consists of branched β-(1,3) glucan covalently bound to chitin, β-(1,3) /(1,4) glucan and galactomannan (Fontaine et al., 2000). This is embedded in an amorphous cement composed of α-(1,3) glucan and galactomannan (Beauvais et al., 2005). Galactomannan is itself formed by a linear chain of α-mannoside residues linked to short side chains of β-(1,5) galactofuranoses (figure 1.5) (Latge et al., 1994).

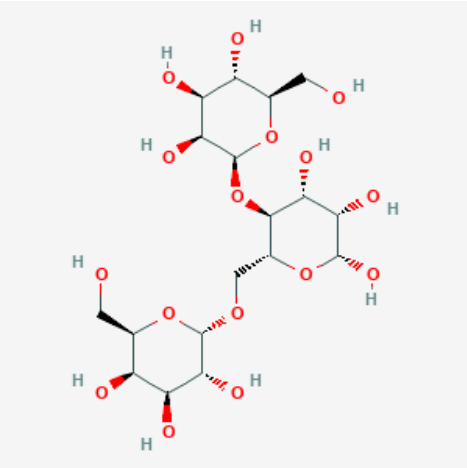

Figure 1.5 Structure of galactomannan (pubchem.ncbi.nlm.nih.gov)

Galactomannan is a useful biomarker in invasive aspergillosis as its levels associate with treatment response as well as disease progression. This has been revealed in an in vitro model using AMB and posaconazole (Hope et al., 2007; Lestner et al., 2010; Howard et al., 2011), as well as in animal models of IPA with triazole antifungals and AMB (Petraitiene et al., 2001; Vallor et al., 2008). Becker *et al* (2003) reported lower levels of serum and lung galactomannan in treated rats when AMB was commenced 16 hours after fungal inoculation (Becker et al., 2003).

1.7.3 Hydrophobins

Until 2010 it was thought that hydrophobins fit into two distinct classes. Jensen *et al*. (2010) and Littlejohn *et al*. (2012) introduced the concept that it is desirable to establish a classification system that can explain the full potential and subtle differences found within the hydrophobin proteins. While, after establishing that some *Aspergillus* proteins cannot be classified easily into either of the two classes, five hydrophobin classes were introduced (Jensen et al., 2010; Littlejohn, Hooley and Cox, 2012).

Hydrophobins have moderately large, exposed hydrophobic patches on the protein surface and display a clustering of surface charged residues that is expected to reinforce the detected high surface activity of these proteins (Lo et al., 2014). It is also likely that hydrophobins form layers intended to seal hyphal aggregations in more complex structures (Harding et al., 2009). If so, they would be obvious candidates for studies on the genes and molecules necessary for biofilm formation.

The rodlet surface is uniformly hydrophobic because of the presence of hydrophobins,

while the cell wall material synthesised upon germination is purely hydrophilic (Dague et al., 2008). Hydrophobins are secreted in a monomeric form, but once in solution they form dimers and in some cases tetramers. The tetramers are usually seen at higher concentrations (Torkkeli et al., 2002; Stroud et al., 2003). These oligomers help to sufficiently protect the hydrophobins' hydrophobic regions from contact with the polar substrate so that no further aggregation forms, even at concentrations as high as 100 mg/mL (Hakanpää et al., 2004; Corvis et al., 2006). As can be seen from figure 1.6, these molecules form films at interfaces very readily.

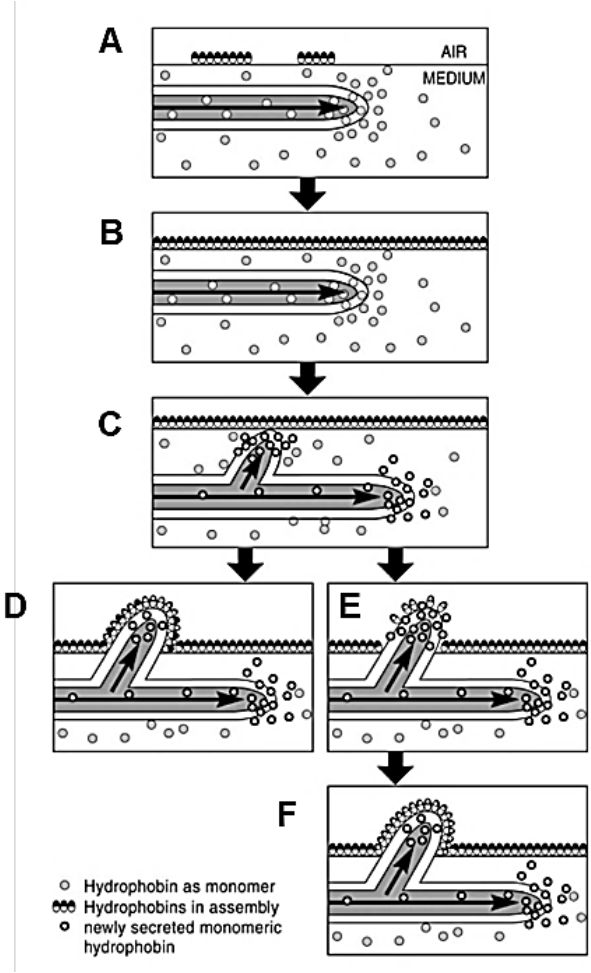

Figure 1.6 Model for fungal aerial structures formation. (A, B) The fungus secretes monomeric hydrophobin into the medium, after formation of a submerged feeding mycelium. (C) At the medium-air interface, the hydrophobin monomers self-assemble into an amphipathic membrane, which decrease the water surface tension. (D) Newly hydrophobin monomers are secreted without breaking the membrane. So, the hypha would never leave the aqueous environment. Instead, the hydrophobin membrane is punctured by the hypha, and the cell wall contacts the air. (E, F) Hydrophobin monomers secreted by such a hypha will self-assemble at the cell wall-air interface. The hydrophilic side of the hydrophobin film faces the hydrophilic cell wall, while its hydrophobic side is exposed to the air. The hydrophobin films covering the hyphae and the aqueous environment may combine (Wösten, 2001)

In *A. fumigatus* there are seven hydrophobins (RodA–RodG) fit in class I and III. *rodA* and *rodB* genes have been described to be upregulated in *A. fumigatus* biofilms comparative to planktonic forms. In comparison, the other hydrophobin genes were poorly expressed at far lower levels. *rodC* and *rodD* are mainly expressed in sporulating culture but present low expression level in biofilm. RodF is only expressed at moderate levels in planktonic and sporulating conditions. *rodE* and *rodG* are either not expressed or expressed at very low levels (Gibbons et al., 2012; Valsecchi et al., 2017).

Resistance of *A. fumigatus* conidia to desiccation and their capacity to reach the alveoli are partially due to the presence of a hydrophobic layer composed of RodA, which covers the conidial surface (Valsecchi et al., 2017). *rodA* encodes a cysteine-containing polypeptide that is assembled into a regular array of rodlets on the surface of conidia to render the surface highly hydrophobic (Paris et al., 2003). The disruption of *rodA* gene has been revealed to be related with a decrease in adherence of conidia to collagen and albumin, however not the basement membrane glycoprotein, laminin, fibrinogen or pulmonary epithelial cells (Sheppard, 2011). The *rodA* encodes a protein that forms the uniform rodlet structure on conidia that prevents the recognition of β- (1,3) glucan by immune cells (Aimanianda et al., 2009). The *A. fumigatus rodA* mutant did not show attenuated virulence in a murine model of Invasive Aspergillosis (IA), despite exposure of β-(1,3)-glucan in the mutant that resulted in immune response not seen with wild type spores (Beauvais et al., 2007).

RodB plays a role in the structure of the conidial cell wall. These rodletless mutants are more sensitive to be killed by alveolar macrophages, suggesting that the rodlet structure is also involved in the resistance to host cells. Nonetheless, *rodA* is the most highly expressed hydrophobin in sporulating culture, whereas *rodB* is up-regulated in biofilm conditions and in vivo. Only *rodA*, though, is responsible for rodlet formation, sporulation, resistance to physical insult or anionic dyes, conidial hydrophobicity, and immunological inertia of the conidia (Valsecchi et al., 2017).

Hydrophobins' binds to a polar surface are making it more hydrophobic. Binding onto submerged polar surfaces happens by self-assembly under specific conditions and this binding can cause a significant increase in water contact angle of the surface, henceforth making it more hydrophobic. In these cases, charged residues opposite of the hydrophobic patch (figure 1.7) of the amphiphilic proteins are thought to interact with the solid polar surface in such a way as the hydrophobic patch is turned outwards against the solution resulting in a hydrophobic surface coating (Grunér et al., 2012).

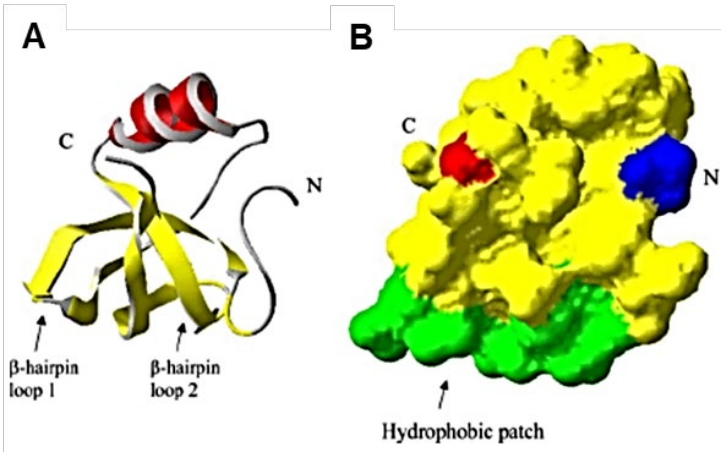

Figure 1.7 The structure of the *Trichoderma reesei* HFBII hydrophobin (class II hydrophobin). The figure shows an amphiphilic molecule with one hydrophilic and one hydrophobic part. (A) the secondary structure elements in HFBII. Two β hairpins form a central β sheet structure. The two loops of the hairpins (indicated) form most of the hydrophobic patch is. (B) A space-filling model of HFBII in the same scale and orientation. Green= the hydrophobic patch, yellow= the rest of the surface, blue= the N- and red= the C-termini (Linder et al., 2005)

Kulkarni and Shaw (2016) explained the contact angle measurement theory as follows: The contact angle between a liquid and a solid is the angle within the body of the liquid formed at the gas–liquid–solid interface. If the contact angle between a liquid and a solid is < 90°, the liquid will wet the surface and spread over it. If the contact angle is ≥ 90°, the liquid will stay on the surface as a bead and in case of water, the material is considered hydrophobic. Therefore, the contact angle between a liquid and a solid is dependent on the nature of the liquid as well as the surface characteristics of the solid. The solid surfaces should be prepared as smooth as possible so that the experimental advancing angles can be a good approximation of θ_γ. Also, penetration of the liquid into the solid, swelling of the solid by the liquid, and chemical reactions can all play a role. The solid surfaces should be as inert as possible so that effects, such as swelling and chemical reactions are minimized. There should be no physical or chemical reaction between the solid and the liquid to keep the values of γ_{lv}, γ_{sv} and γ_{sl} (figure 1.8) constant during the experiment (Kulkarni and Shaw, 2016).

A wetted and a non-wetted solid are mentioned as hydrophilic and hydrophobic, respectively. Surfaces with contact angles lower than 10° are referred to as super hydrophilic and surfaces higher than 150 are called super hydrophobic (Wo sten et al., 1994; Takahashi et al., 2005; Kisko et al., 2009). The water contact angle (WCA) is a method of presenting the energy of a surface and is also affected by the cleanness or

roughness of the surface. When depositing droplets on surfaces two different wetting cases can be distinguished, non-wetting and wetting (including partial wetting and complete wetting) (Kisko et al., 2009) (figure 1.8, B and C).

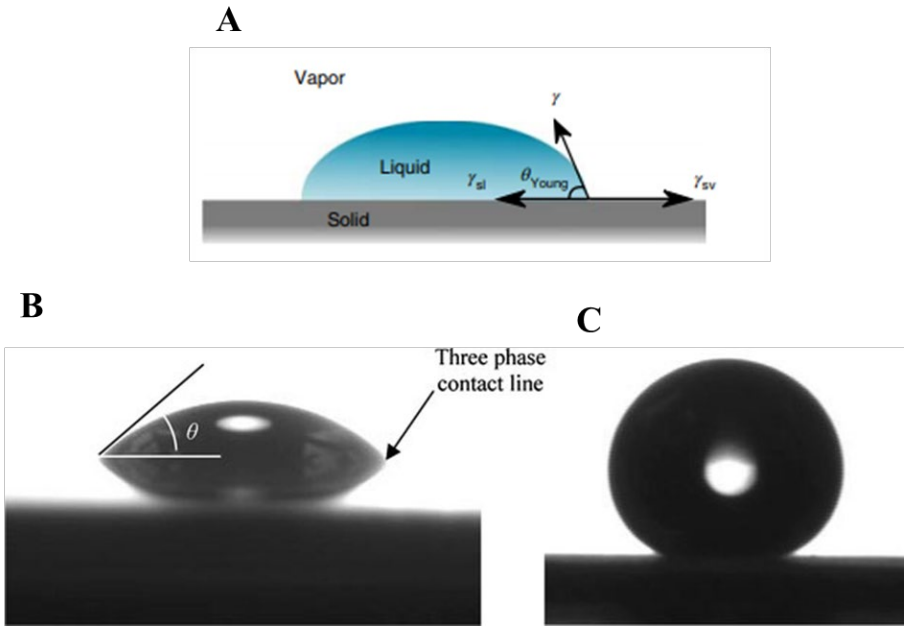

Figure 1.8 Droplet of water deposited on two surfaces with different energies. (A): γ_{sl} is the surface-liquid interfacial free energy, γ_{sv} is the surface-vapour free energy (tension) (B): wetting surface ($\theta < 90°$), (C): non-wetting surface ($\theta > 90°$). A non-wetting liquid forming a sessile drop on the surface of a solid forms a three-phase line, at which all three phases, solid, liquid and vapour are in contact (Huhtamäki et al., 2018). θ represents contact angle (Verplanck et al., 2007)

The static contact angle (θ) can be expressed by the Young equation (Grunér et al., 2012) (section 2.7.5.1, equation 3) (figure 1.8A).

Organic contaminants in general increase surface hydrophobicity, and their distribution might be non-uniform at the micro- and nano-scale. When droplets are obtained by condensation, there should be areas with little or no organic contamination, where water preferentially condensed, leading to reduced nano-scale contact angles (Yuan and Lee, 2013).

1.8 Extracellular polymeric substances

Cell-to-cell communication mechanisms (such as QS) play a key role in biofilm maturation and EPS production (Parsek and Greenberg, 2005). The EPS is composed of polysaccharides, proteins, extracellular DNA (eDNA) and lipids. Biofilms mechanical stability provides by EPS (Martino, 2018). It strengthens biofilm adhesion onto surfaces

and forms a cohesive, three-dimensional polymer network, which connects biofilm cells. It also protects microbial cells from external stresses including host immune defences and antibiotics (Gominet et al., 2017). Korstgens et al., (2001) showed that in *Pseudomonas aeruginosa*, biofilm architecture could be influenced by the interaction of anionic EPS, containing carboxylic groups, with multivalent cations. They discovered that Ca^{2+} ions could form a bridge between polyanionic alginate molecules, thus increasing mechanical stability of biofilm (Korstgens et al., 2001).

1.9 *A. fumigatus* extracellular polymeric substances components

In *A. fumigatus* biofilms, the hydrophobic EPS, as a heterogeneous substance composed of extracellular DNA, galactomannan, galactosaminogalactan (GAG), α -(1,3) glucans, monosaccharides, polyols, melanin, and proteins. It consists of glucose (74%), mannitol (18%), trehalose (3%), glycerol (5%), and melanin and proteins (2%) (Beauvais et al., 2007). Whereas in vivo studies suggested distinct chemical alterations, with GAG and galactomannan identified as the major EPS polysaccharides (Loussert et al., 2010; Beauvais and Latgé 2015). The EPS structure mediates adherence to inorganic substrates and host cells and increases resistance to host defences and antifungal agents. So, EPS components develop potential drug targets (Lu et al., 2014).

1.9.1 Extracellular DNA

eDNA is an essential component of both fungal and bacterial biofilms and is proposed to improve overall structural integrity (Martins et al., 2009). In *P. aeruginosa*, for example, it was shown to contribute less than 1 to 2% of the EPS composition (Rajendran et al., 2013). Besides, bacterial biofilm studies have shown that eDNA has a multifactorial purpose, specifically, as a facilitator of genetic information exchange (Molin and Tolker-Nielsen, 2003), a nutrient source (Mulcahy et al., 2010), contributor to biofilm establishment and dispersal (Whitchurch et al., 2002), and antimicrobial resistance factor (Mulcahy et al., 2008). It has also been shown in *C. albicans* that eDNA act as a regulator of biofilm antifungal resistance (Martins et al., 2011). Mechanistically, cell death and lysis, QS, and excretion from outer membrane vesicles have been suggested to be involved in eDNA release from bacteria (Rajendran et al., 2013).

Studies by Rajendran *et al*. (2014) have also demonstrated that eDNA is an essential structural constituent of *A. fumigatus* EPS and plays a critical efficient role in keeping the

structural and architectural integrity of its biofilms. Furthermore, the release of this eDNA by autolysis in biofilms is meaningfully linked with the levels of antifungal resistance, suggesting that eDNA plays an important role in biofilm resistance to antifungals. They also demonstrated phase dependent antifungal activity against *A. fumigatus* biofilms. It has been suggested that early resistance phenotypes are parallel with increased efflux pump activity. This association is not obvious in mature biofilms, so EPS may play a greater role in the later phases of biofilm growth (Ramage et al., 2011; Rajendran et al., 2014).

In *A. fumigatus*, eDNA leads to increased biomass, so in addition to providing structural support, it may also act as a nutrient source (Shopova et al., 2013). This designates that eDNA release may have a multifunctional role for *A. fumigatus*. Mechanisms of eDNA release in eukaryotic cells include active secretion, necrosis, and apoptosis (Tamkovich, Vlassov and Laktionov, 2008), with the possibility of more than one pathway being involved (Fink and Cookson, 2005). Bacterial autolysis is a commonly designated mechanism of eDNA release to promote biofilm formation (Lappann et al., 2010). For fungi such as *A. nidulans*, the molecular basis of autolysis has been studied, and it has been shown that the chitinase B (ChiB) plays a vital role in fungal autolysis in *A. nidulans* under conditions of carbon starvation (Szilagyi et al., 2010). Fungal chitinases are secreted enzymes that play a role in the digestion of exogenous chitin or utilisation of fungal chitin for energy during autolysis (necrosis) (Rajendran et al., 2013). Since chitinases are markers of autolysis, this process is a possible mechanism for eDNA release. eDNA release conferring structural support for the development and maintenance of the complex biofilm architecture (Adams, 2004). Rajendran et al., (2014) suggested a novel therapeutic strategy through digestion of biofilm eDNA by DNase may destabilise biofilm growth and improve antifungal sensitivity (Rajendran et al., 2014).

Propidium iodide (PI) fluorochrome is a membrane impermeable intercalator that binds with a good specificity to eDNA and damaged or dead hyphae, allowing the user to distinguish between abiotic and biotic particles (Rosenberg, Azevedo and Ivask, 2019). Flow cytometry is based on the use of specific antibodies, which are labelled with PI to identify cell types present in the sample and to measure changes in the expression of surface and intra-cellular markers (Menon et al., 2014).

1.9.2 Galactosaminogalactan

GAG is an -1,4-linked heteropolysaccharide composed of galactose and partially deacetylated GalNAc which is absent in *A. fumigatus* spores but is produced in plenty by growing hyphae (Sheppard and Howell, 2016).

A cluster of five co-regulated genes with predicted roles in synthesis and metabolism of polysaccharides is involved in GAG biosynthesis. One of these genes, *sph3*, encodes a protein belonging to the spherulin 4 family, a protein family with no known function. *Sph3* activity is required for functional GAG production (Bamford et al., 2015). The presence of gene clusters resembling bacterial operons is almost unusual in filamentous fungi and often suggests the acquisition of these genes happened through a horizontal gene transfer event (Sheppard, 2016). The presence of GAG gene cluster is found through a variety of taxonomically diverse fungal genomes, which has been approved by bioinformatics analyses. Through these analyses, gene deletion experiments, and the study of recombinant enzymes, a model for GAG biosynthesis is developing (Lee et al., 2013). This model shares some similarity with those described for the synthase-dependent production of hexosamine-containing polysaccharides found within bacterial biofilms. As *A. fumigatus* contains only a single plasma membrane, the model of GAG biosynthesis is most like exopolysaccharide synthesis by Gram-positive bacteria such as *Staphylococcus epidermidis* (Heilmann et al., 1996) and *Listeria monocytogenes* (Köseog˘lu et al., 2015).

Based on the Brown *et al* (2012) study the mortality of invasive aspergillosis is over 50%, besides using antifungal agents (Brown et al., 2012). The results demonstrated the necessity for new therapies that target *A. fumigatus*. In invasive aspergillosis, production of the exopolysaccharide GAG by *A. fumigatus* has been identified as an important pathogenesis factor as it increases the fungus ability to infect human hosts (Fontaine et al., 2011). Among *Aspergillus* spp., *A. fumigatus* produces higher levels of cell wall-associated GAG (Lee et al., 2016).

Here are two GAG functions related to *A. fumigatus* pathogenicity (Gravelat et al., 2013 and Gresnigt et al., 2014):

❖ GAG is required for biofilm formation and adherence to host cells. It plays an important role in the maintenance of the extracellular matrix of *A. fumigatus* biofilms.

Strains deficient in GAG production fail to produce extracellular matrix and are unable to form adherent biofilms on plastic or host cells in vitro.

❖ With other biofilm exopolysaccharides, GAG plays an important role in evading host defences. Strains deficient in GAG display attenuated virulence in mouse and invertebrate models of invasive aspergillosis. GAG functions as an immunosuppressive polysaccharide both indirectly, through masking -glucan from dectin-1 recognition, and directly by inducing neutrophil apoptosis and secretion of the immunosuppressive cytokine interleukin 1 receptor antagonist (IL-1RA).

Given the multiple roles that GAG plays in pathogenesis, the biosynthetic pathways governing GAG synthesis represent promising targets for novel antifungal therapies.

1.10 Quorum sensing and its role in biofilm formation and development

The term "quorum sensing" (QS) was introduced by Fuqua et al., (1994), who was putting together one of the first review articles on autoinduction in bacteria (Fuqua et al., 1994). Before 1994, QS was commonly referred to as "autoinduction" (Nealson et al., 1970).

Today, the QS definition explains bacterial ability to monitor and respond to changes in its environmental conditions through a cell density-related process. QS is a form of cell-cell communication regulated at the gene expression level to coordinate behaviour in a community (Dixit et al., 2017). Initiation and maturation of a structured microbial community needs cell-cell communication (Hoiby et al., 2011).

Biofilm formation is one of the most important virulence phenotypes of opportunistic human pathogens, and it is under the control of the QS system in several important pathogenic organisms (Papenfort and Bassler, 2016). The biofilm lifestyle poses a significant challenge to the effectiveness of conventional antibiotics and is considered a breeding ground for antibiotic resistance (Reen et al., 2018).

There are two reasons for lack/low effectiveness of antibiotics against biofilms of pathogens (LaSarre and Federle, 2013):

1) Biofilm matrix can act as a barrier to the diffusion of antibiotics into biofilms. Antibiotics either react chemically with biofilm matrix components or attach to anionic polysaccharides, which are available in EPS structure. Using transmission electron

microscopy in vitro, EPS was found to contain polysaccharides (for example, galactomannan and α-(1,3) glucan), melanin, proteins (for example, major antigens and hydrophobins), and monosaccharides.

2) Cells involved in biofilm structure do not grow, or grow slowly, hence their sensitivity to antibiotics decreases. To overcome these drawbacks, application of biofilm-matrix degrading enzymes, which can be used in combination with antibiotics, or the use of ultrasound with antibiotics, are suggested. Application of ultrasound can stimulate the metabolism of cells populations involved in biofilm structure.

Bioactive molecules produced by prokaryotes and eukaryotes are involved in biofilms disruption. These molecules act primarily by quenching the QS system. The phenomenon is also named as "quorum quenching" (section 1.13) (Kalia, 2013). Also, some synthetic compounds have been found to be effective in QQ.

1.11 Quorum sensing in yeasts and filamentous fungi

None of the discovered molecules or genes mediating bacterial QS seems to be found in dimorphic fungi. Indeed, fungi have evolved their systems to regulate fungal cell-cell communication (Sordi and Mühlschlegel, 2009; Tseng and Fink, 2008). The regulation of the shift between the yeast form and filamentous form in the parasitic fungus *Histoplasma capsulatum* presented the first example of an apparent QS mechanism in eukaryotes. The yeast form produces some unique cell wall polysaccharides (for example α-(1,3) glucan) in a cultured density-dependent fashion. This glucan is needed for virulence. It is abundant in yeast cells growing in a dense culture, but most cells lose the glucan when diluted to a low density in fresh medium (Sprague, 2006). However, QS in eukaryotic organisms was unknown until the discovery of farnesol as a quorum sensing molecule (QSM) (Section 1.12) in the pathogenic fungus *C. albicans* (Hornby et al., 2001). The other known fungal QSMs are all alcohols derived from aromatic amino acids tyrosine (tyrosol), as the second QSM described in *C. albicans*, phenylalanine (phenyl ethanol) and tryptophan (tryptophol); the last two molecules were found in *Saccharomyces cerevisiae* (Chen, 2006). Multicolic acid and related derivatives are reported as putative QSM in *Penicillium sclerotiorum* (Mehmood et al., 2019). It has been suggested that QSMs of dimorphic fungi are lipophilic isoprenes (Hornby et al., 2001 and 2004). They induce fungal apoptosis and modulate host immune cells

system (Wongsuk, Pumeesat and Luplertlop, 2016). Linoleic acid-derived signalling molecules and butyrolactone-I are potentially involved in *A. terreus* cell-cell communication. The use of linoleic acid-derived oxylipins in *A. terreus* during fungal fermentations improves the production of the secondary metabolite lovastatin (Sorrentino, Roy and Keshavarz, 2010). Exogenous addition of the oxylipin precursor linoleic acid to low cell density cultures can enhance lovastatin production up to 1.8- fold due to transcriptional up-regulation of the genes involved in lovastatin biosynthesis (Barriuso, 2015). An auto-stimulatory function has been suggested for butyrolactone I. Its exogenous addition results in 2.5- fold increase in lovastatin production, regulating transcription of the genes involved in its biosynthesis and increased endogenous levels of the butyrolactone I (2.5- fold). ɣ-heptalactone has been found to act as a QSM in *A. nidulans* regulating growth profile and secondary metabolite (penicillin) production in cultures at low cell density (Williams et al., 2012).

1.12 Quorum sensing molecules and their role as antifungal agents

QSMs have been investigated as antifungal agents in both yeasts and dimorphic fungi (tables 1.2 and 1.3, respectively). These autoregulatory molecules have been identified from a range of fungal pathogens, including *C. albicans* (farnesol and tyrosol), *Saccharomyces cerevisiae* (tryptophol and phenyl ethyl alcohol), *Cryptococcus neoformans* (11-mer) and *Penicillium paneum* (octen-3-ol) (Hornby et al., 2001; Chen et al., 2004; Chitarra et al., 2004; Alem et al., 2006; Lee et al., 2007). In *Candida* spp. farnesol inhibits drug efflux pump proteins (ABC drug transporters). A nontoxic concentration of farnesol may be used as an alternative anti-*C. albicans* (Wongsuk, Pumeesat and Luplertlop 2016). A few studies have demonstrated the requirement for a high minimum inhibitory concentration (MIC) for treatment of *C. albicans* biofilms (Chandra et al., 2001; Taff et al., 2013). Katragkou *et al*. showed a synergistic effect of farnesol combined with several antifungal agents (fluconazole, AMB, and micafungin) against *C. albicans* biofilms (Katragkou et al., 2015). Sterol biosynthesis mechanisms may be involved in reducing fluconazole resistance in farnesol-treated *C. albicans* biofilms by repressing the ERG11, ERG25, ERG6, ERG3, and ERG1 genes regulating ergosterol biosynthesis (Yu et al., 2012). Like farnesol, tyrosol was investigated in combination with antifungal agents and showed a synergistic effect when combined with AMB (90% reduction in *C. krusei* biofilm and *C. tropicalis* biofilm when 80mM tyrosol was coupled with 4 mg/L AMB) (Shanmughapriya et al., 2014). Cordeiro

et al. (2015) reported that exogenous tyrosol alone or combined with AMB inhibited planktonic cells and *Candida* biofilm growth. Interestingly, mature biofilms were also inhibited by tyrosol alone or combined with AMB, but tyrosol combined with azoles increased the biofilm activity in a dose-dependent manner (Cordeiro et al., 2015). In dimorphic fungi, Derengowski *et al.* (2009) showed the in vitro activity of farnesol against *P. brasiliensis* (an average MIC around 25mM and minimal lethal concentration around 30mM) (Derengowski et al., 2009). The combination of farnesol with antifungal drugs showed synergistic effects (fractional inhibitory concentration index [FICI] 0.5) in *C. posadasii* (Brilhante et al., 2013) and *H. capsulatum* (Brilhante et al., 2015).

Table 1.2 Role of QSMs on yeasts (Wongsuk, Pumeesat and Luplertlop, 2016)

Organism	QSMs	Role of QSMs on yeast cells
C. albicans	- Farnesol	- Inhibited hyphal development - Played role in morphogenesis - Inhibited biofilm formation - Induced apoptosis - Antifungal activity - Modulated drug extrusion
	- Tyrosol	- Promoted germ tube formation - Stimulated hypha production during the early stages of biofilm development - Antifungal activity
	- Isoamyl alcohol - 2-Phenyl ethanol - 1-Dodecanol E-nerolidol	- Played role in morphogenesis
C. dubliniensis	- Farnesol	- Inhibited hyphal development - Played role in morphogenesis - Inhibited biofilm formation - Antifungal activity
	- Isoamyl alcohol - 2-Phenyl ethanol - 1-Dodecanol E-nerolidol	- Played role in morphogenesis
C. tropicalis	- Farnesol - Tyrosol	- Antifungal activity
C. krusei	- Tyrosol	- Antifungal activity
S. cerevisiae	- Tryptophol - Phenyl ethanol	- Promoted pseudohyphal growth[2]
Debaryomyces hansenii	- Farnesol - Tyrosol - Tryptophol - Phenyl ethanol	- Played role in adhesion and sliding motility

[2] Pseudohyphal growth is a nutrient-regulated program in which budding yeast forms multicellular filament of connected cells (Norman et al., 2018).

1.12.1 Farnesol

Morphogenesis in *C. albicans* is under a complex positive and negative control by the actions of tyrosol and farnesol, respectively (Nickerson, Atkin and Hornby, 2006). Over 23000 individual isoprenoid compounds have been characterised and one of these, the sesquiterpene alcohol, farnesol ($C_{15}H_{26}O$), has been identified as the QSMs for *C. albicans* (Hornby et al., 2004). In 1983, Hazen and Cutler showed that the supernatant from a 48 hr culture of *C. albicans* prevents the yeast to hyphal interconversions of a fresh culture (Hazen and Cutler, 1983). The QSM responsible for this effect has since been identified as the autoregulatory molecule, farnesol (Ramage et al., 2002). Farnesol is a 15-carbon isoprenoid, a class of compounds naturally produced from mevalonate, which is part of the highly conserved sterol biosynthetic pathway (Semighini et al., 2006). Components derived from this pathway often act as signalling molecules that affect lipid synthesis, protein synthesis and degradation, developmental patterning, meiosis and apoptosis (Wang et al., 2014). Farnesol is generated within cells by enzymatic dephosphorylation of farnesyl pyrophosphate (FPP) (Ferriols et al., 2015). FPP plays a vital role as the precursor of protein prenylation, a post-translational modification of proteins (Nishinari and Tipton, 2000). Farnesol is extracellular and is produced continuously during growth and over a temperature range from 23 to 43°C (Abdel Rhman et al., 2015) and is itself very heat stable (Westwater, Balish and Schofield, 2005). Its production is not dependent on the type of neither carbon nor nitrogen source or the chemical nature of the growth medium (Hornby et al., 2001). In *C. albicans*, farnesol represses filamentation despite the presence of filamentation-inducing compounds such as serum and n-acetyl glucosamine (Shareck and Belhumeur, 2011). Therefore, it inhibits biofilm formation reversibly but does not block the elongation of pre-existing hyphae (Nickerson, Atkin and Hornby, 2006; Sordi and Mühlschlegel, 2009). Farnesol leads to a reduction of the size of biofilms, regardless of whether it is added to the cells before attachment to the surveys or to pre-formed major biofilms (Deveau and Hogan, 2010). In *C. albican* at a sufficiently high level (1 to 5 μM), it prevents mycelial development during growth (Hornby et al., 2004). It also blocks germ tube formation, while the presence of farnesol at concentrations of up to 250 μM prevents the yeast to mycelium conversion (Cugini, 2007; Joo and Jetten, 2010), resulting in actively budding yeasts, without influencing cellular growth (Hornby et al., 2001). Farnesoic acid, which is structurally related to farnesol, also blocks the yeast-to-hypha transition (Shareck and

Belhumeur, 2011). It has also been shown to impact properties other than the morphological switch, such as resistance to oxidative stress or apoptosis under planktonic conditions (Krom et al., 2015).

Although farnesol does not affect *C. albicans* growth (Davis-Hanna et al., 2007), its potent antifungal and antibacterial activity has been reported against several other organisms like *S. cerevisiae* and *A. nidulans* (Derengowski et al., 2009; Sordi and Mühlschlegel, 2009; Estrela and Abraham, 2016) conferring a selective advantage in the environment. An antagonistic relationship exists between *C. albicans* and ascomycete fungi, including *A. fumigatus*, *A. nidulans* and *Fusarium graminearum* (Ali Abdul Hussein, 2015). The response of these fungi to the presence of *C. albicans* can be mimicked by extracellular farnesol, which blocks the growth and development and triggers apoptosis (Semighini, Murray and Harris, 2008). Pure cultures of *C. albicans* are isolated from lesions, implying that *C. albicans* exerts an inhibitory effect on the growth of other microbes (Semighini et al., 2006). Dichtl et al., (2010) showed that farnesol inhibited the growth of wild-type cells of the human pathogen *A. fumigatus*, albeit to a lower extent of what was observed in *A. nidulans*. The toxicity was lower in osmotically stabilized medium and the addition of farnesol produced more profound inhibitory effects on cell wall mutants of *A. fumigatus* (Dichtl et al., 2010). Table 1.3 displays some molds and dimorphic fungi, which has been affected by farnesol.

Table 1.3 Farnesol effects against some molds and dimorphic fungi (Wongsuk, Pumeesat and Luplertlop, 2016)

Organism	Role of farnesol on molds and dimorphic fungi
A. nidulans	- Induced apoptosis - Oxidative and heat stress resistance
A. niger	- Inhibited conidiation - Reduced intracellular cAMP levels
A. fumigatus	- Altered growth phenotype - Perturbed cell wall
A. flavus	- Induced apoptosis
Coccidioides posadasii	- Antifungal activity - Decreased the amount of ergosterol - Affected the integrity of plasma membrane
F. graminearum	- Induced apoptosis - Inhibited germination of macroconidia - Decreased viability
H. capsulatum	- Inhibited biofilm formation - Antifungal activity
Paracoccidioides brasiliensis	- Inhibited growth - Delayed the dimorphic transition - Antifungal activity
Paracoccidioides expansum	- Induced apoptosis - Inhibited growth
Paracoccidioides destructans	- Inhibited growth
Shigella boydii	- Induced apoptosis - Inhibited growth
Lomentospora prolificans	- Induced apoptosis - Inhibited growth

Farnesol influences the intracellular localisation of AfRho1, and AfRho3, the apical actin cytoskeleton and the hyphal tip morphology. Specifically, in the presence of farnesol the predominant localisation of AfRho1, AfRho3 and tropomyosin to the hyphal tip disappear, and the hyphal tips change from a copped to a bulb-like morphology. This putatively happens because of an altered organisation of the actin cytoskeleton, a structure known to be regulated by Rho proteins (Taheri-Talesh et al., 2008). In *A. fumigatus* and *A. nidulans* the actin-binding protein tropomyosin spreads along the cytoplasm after farnesol treatment, while it normally focuses at the hyphal tip in untreated cells (Savoldi et al., 2008). Taken together, farnesol-induced misplacement of AfRho1 and other related regulatory proteins lead to the suppressed phosphorylation of AfMpkA, a cell wall integrity signalling kinase, under cell wall stress, the bulb-like tip morphology and the displacement of tropomyosin.

Farnesol can also induce apoptosis in several fungi via caspase stimulation (Joo and Jetten, 2010). Metacaspase Mca1p might be involved in the mechanism of farnesol-induced apoptosis (Léger et al., 2014). Furthermore, farnesol may interact at another point in the programmed cell death pathway by altering the levels of intracellular glutathione S-conjugate (F-GS) combined with transporter protein (Cdr1-p) (figure 1.9). These result in the decrease of intracellular reduced glutathione (GSH), leading to the activation of apoptosis pathways and fungal cell death (Shirtliff et al., 2009). In vitro studies of *C. albicans* have shown that farnesol can protect it from ROS (Westwater, Balish and Schofield, 2005) and increase its ROS resistance through suppression of the Ras1-cAMP pathway (Langford et al., 2009; Cottier and Mühlschlegel, 2012). In both yeast and *A. nidulans*, farnesol treatment induces intracellular ROS generation. The antioxidant N-Acetylcysteine (NAC) can ameliorate the effects induced by farnesol (Semighini et al., 2006). Therefore, ROS production is a major factor underlying farnesol-induced apoptosis.

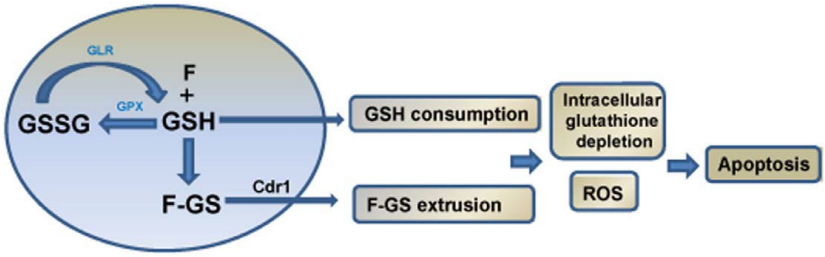

Figure 1.9 Farnesol apoptosis inducing mechanism. Farnesol conjugates with reduced glutathione (GSH) forming glutathione S-conjugate (F-GS) concomitant with oxidation of GSH to the disulphide form (GSSG), a reaction catalysed by GPX. GSSG is reduced to GSH by GLR as a recycling mechanism to maintain GSH levels. However, the oxidation and consumption of intracellular GSH coupled with the Cdr1p-mediated export of F-GS result in depletion of intracellular GSH, disruption of the redox balance and oxidative stress leading to apoptosis (Shirtliff et al., 2009)

Farnesol strongly inhibits germination and growth of *A. flavus* and induces markers for apoptosis including nuclear condensation phosphatidylserine externalisation, DNA fragmentation and intracellular reactive oxygen species (ROS) generation, metacaspase activation and abnormal cellular ultrastructure (Wang et al., 2014). Unlike *A. nidulans* and of *A. flavus*, farnesol increases the number of germ tubes per macroconidia in *F. graminearum* macroconidia, which suggests that the localisation or activity of monomeric GTPases involved in morphogenesis or cell wall stress signalling pathways could be altered (Semighini, Murray and Harris, 2008). In *A. niger* it has been shown that decreased conidiation and growth rates are associated with increased levels of cAMP (Oliver et al., 2002). Surprisingly, the reduction in conidiation brought about by farnesol is associated with dramatically decreased levels of intracellular cAMP and can be complemented by the addition of moderate amounts of cAMP, whereas conidia formation is again blocked by adding higher cAMP concentrations (Lorek et al., 2008). The mechanisms regulating fungal morphogenesis via farnesol and cAMP involve similar metabolic components but are different in different species. Some slight differences have been recognised between the effects of farnesol on *A. nidulans* and *Penicillium expansum*. Such that farnesol can induce the transformation of hyphal growth direction in *P. expansum*, but not in *A. nidulans*. In *P. expansum*, farnesol may affect sterol metabolism, membrane permeability and the lipid raft to disrupt the polarity of hyphae. This polarisation disrupted by farnesol may be the reason for hyphal growth conversion (Liu et al., 2009).

A synergistic effect is also observed with farnesol and antifungal drugs (azoles and polyenes) against *C. albicans* biofilms, as when farnesol is combined with antifungal agents, the MIC is decreased compared with antifungal agents alone (Saidi et al., 2006). The combination of farnesol with antifungal drugs also shows synergistic effects in dimorphic fungus *P. brasiliensis* (Derengowski et al., 2009), *C. posadasii* (Brilhante et al., 2013) and *Histoplasma capsulatum* (Brilhante et al., 2015). Farnesol shares several precursors with ergosterol in the biosynthetic pathway and it has been shown that in *Coccidioides posadasii* cells the concentration of ergosterol decreased when the strain is exposed to farnesol, even at subinhibitory doses. A similar effect was also observed when cells were exposed to itraconazole, which is known to inhibit the synthesis of ergosterol (Brilhante et al., 2013). Thus, it can be suggested that the two agents act similarly.

1.12.2 Aromatic alcohols

Yeasts cannot use branched chain or aromatic amino acids as their sole carbon source. However, they can be used as nitrogen sources under nitrogen- limiting conditions, with subsequent production of fusel alcohols as potentially toxic or regulatory by-products (Ghosh et al., 2008). The fusel alcohols 2-phenylethanol and tryptophol, derived from phenylalanine and tryptophan, respectively, were the first molecules reported to inhibit hyphal growth in *C. albicans* (Chauhan et al., 2013).

Tyrosol (2-[4-hydroxyphenyl] ethanol), a derivative of tyrosine is a QSM in *C. albicans*, which accelerates cell growth and hyphal development in the early stages of biofilm formation and stimulates the formation of germ tubes at low density (Bandara et al., 2012). Tyrosol also reduces the lag phase of growth in a diluted culture, which may account for its hypha-stimulating properties. In *C. albicans* on a per weight basis, biofilm cells secrete 50% more tyrosol than does planktonic cells. This 50% increase would be assumed if 30 to 40% of the biofilm cells were growing under anaerobic conditions (Alem et al., 2006).

The attachment of fungal cells on surfaces is the first step of biofilm development and QSMs play an important role in this phase (Davey and O'toole, 2000). Phenylethanol and tyrosol increased the ability of *D. hansenii* to attach to polystyrene while tryptophol and farnesol reduce this ability (Gori et al., 2011).

One Environmental clue that triggers the morphological transition from the yeast form to a filamentous form in *S. cerevisiae* is nitrogen-poor growth medium (Cullen and Sprague, 2012), a condition that activates several different signal transduction pathways. One of these pathways is the Ras-cAMP-dependent protein kinase (PKA) pathway (figure 1.10) (Budovskaya et al., 2004). Conditioned medium from *S. cerevisiae* stationary phase cultures considerably induces filamentous growth. At least in part, this induction is a result of the fivefold stimulation of transcription of *FLO11*, a gene essential for filamentous growth (Chen, 2006). Mutants unable to produce aromatic alcohols show significantly diminished filamentous growth and *FLO11* expression (Sprague, 2006). A second signal transduction pathway required for filamentous growth, a mitogen-activated protein (mapk)- based pathway, is not needed for induction of *FLO11* by aromatic alcohols (Cullen and Sprague, 2012). The active molecules were purified and shown to be phenyl ethanol and tryptophol (Wuster and Babu 2009). Phenylethanol and tryptophol are identified as QSMs in *S. cerevisiae* (Albuquerque and Casadevall, 2012; Avbelj, Zupan and Raspor, 2016). They switch morphology from yeast to filamentous form (pseudohyphal growth) in *S. cerevisiae* at relatively low concentrations, whereas tyrosol has no effect. The addition of both alcohols causes a more vigorous filamentous growth response and induction of *FLO11* than does either singly, implying some synergy in their action (Sprague, 2006).

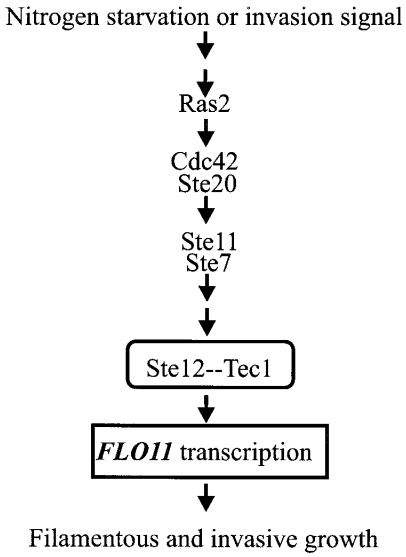

Figure 1.10 Aromatic alcohols mechanism of action in *S.cerevisiae* is a model for FLO11 action in the filamentous growth pathway. In the filamentous signalling pathway *flo11p* functions downstream of *ste12p* and is the primary target of *ste12p* to effect invasion (Lo and Dranginis, 1998)

Cell density regulates the biosynthesis of aromatic alcohols by controlling the levels of *ARO9* and *ARO10* transcripts, which are significantly greater in cells at high density than those at low density. The production of aromatic alcohols is auto-stimulated by tryptophol (but not phenylethanol) (Chen, 2006). The addition of tryptophan activates the biosynthetic pathway by upregulating the expression of *ARO9* and *ARO10*, required to convert tryptophan to tryptophol (Brunke et al., 2010). The key transcription factor in aromatic alcohol production is ARO80p, which directly controls the expression of *ARO9* and *ARO10* genes (figure 1.11) (Wuster and Babu, 2009). Autoinduction pathways have also been reported in bacteria. In the gram-negative bacterium *Vibrio fischeri*, N-acyl homoserine lactone (AHL), the QS signalling protein in gram-negative bacteria, induces its own production by binding to transcription factor *LuxR*, which activates the transcription of the luxICDABE operon (*luxI*) encodes the enzyme for the biosynthesis of AHL (Ng and Bassler, 2009).

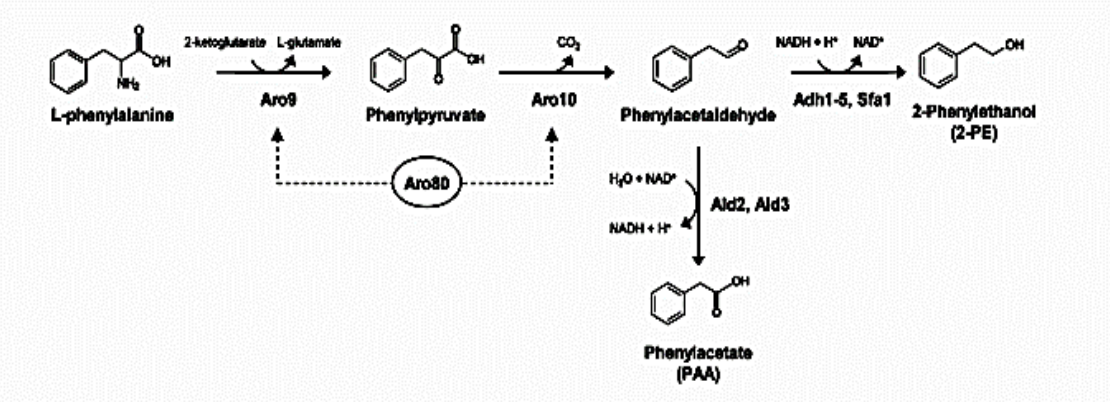

Figure 1.11 Biosynthesis of aromatic alcohols. Major metabolic pathways leading to the formation of 2-PE in *S. cerevisiae*. Enzymes involved in 2-PE and PAA production from L-Phe are indicated. Aro80 is a transcription activator involved in the expression of genes encoding Aro9 and Aro10 (Runguphan and Keasling, 2014)

In *C. albicans*, phenethyl alcohol, tyrosol, and tryptophol production are consistent with the use of the same pathway as in *S. cerevisiae*, i.e., transamination (*ARO8, ARO9*), decarboxylation (*ARO10*), and then reduction by alcohol dehydrogenase (ADH) (Ghosh et al., 2008; Egbe et al., 2015). Phenyl ethanol and tryptophol act opposite of tyrosol and inhibit the formation of germ tubes and biofilms (Alem et al., 2006). In *S. cerevisiae* tyrosol has no detectable effects, whereas phenyl ethanol and tryptophol are potent inducers of morphogenesis. Differential effects of alcohols between *S. cerevisiae* and *C. albicans* suggest that fungi, like bacteria, have evolved molecular signals that induce species-specific behaviours (Chen, 2006).

Tyrosol is investigated in combination with antifungal agents and showed a synergistic effect in combination with AMB (90% reduction in *C. krusei* biofilm and *C. tropicalis* biofilm when 80 M tyrosol is combined with 4 mg/L AMB) (Shanmughapriya et al., 2014). However, tyrosol combined with azoles increase the biofilm growth in *C. albicans* and *C. tropicalis* in a dose-dependent manner (Cordeiro et al., 2015).

1.13 Quorum quenching molecules and their role as antifungal agents

Quorum quenching (QQ) is a therapeutic approach, which has the potential to eliminate the disease, not the microbes causing the disease (Bhardwaj et al., 2013). For this reason, anti-virulence or anti-pathogeneses, such as using quorum quenchers (QQrs) are strategies that are thought to target components of microbes that are responsible for pathogenesis rather than those, which are involved in growth. Growth- inhibitory effects of agents can make microbes resistant to those specific agents. QS signals contribute directly to pathogenesis due to the synchronised production of virulence determinants, such as toxins, proteases, and other immune-evasive factors and QS mutants, in general, do not display growth defects. QQrs can act not by killing microbes but by slowing down the growing stage of them and reducing their metabolic activity, hence, suppressing their pathogenicity (Estrela and Abraham, 2016).

As all QS systems share a mechanism comprised of signal production, signal accumulation, and signal detection, QQrs belong to the following divisions (LaSarre and Federle 2013):

- Degradation and inactivation of QS signal (like proteases in case of enzymatic approach and antibodies in case of non-enzymatic approach)

- Inhibition of QS signal biosynthesis

- Inhibition of signal detection (generating agonists and antagonists of various QS systems)

1.13.1 Natural quorum quenchers

Furanone. The Australian red macroalga *Delisea pulchra* produces a range of halogenated furanone compounds (Nys, 1993). This alga originally attracted the attention of marine biologists because it was devoid of surface colonisation, i.e., biofouling, unlike other plants in the same environment. Biofouling is primarily caused by marine invertebrates and plants, but bacterial biofilms are believed to be the first colonisers of submerged surfaces, providing an initial conditioning biofilm to which other marine organisms may attach (Hentzer and Givskov, 2003). The natural furanone compounds were modified by chemical synthesis and screened for increased efficacy (figure 1.12). Furanone can inhibit QS of Vibrio harveyi and *E.coli* via Autoinducer-2 (AI-2). In *E.coli*, furanone inhibits phenotypes like air-liquid biofilm formation by interrupting (or blocking) AI-2 signalling. Also, it has been shown that furanone disrupts the expression of different AHL-regulated phenotypes in several Gram-negative species, without affecting their growth (Defoirdt et al., 2007). Hentzer et al., (2002) assessed the potential of furanone compounds as quorum sensing inhibitors (QSIs) (QQrs). For that, a synthetic halogenated furanone compound, which is a derivative of the secondary metabolites produced by *D. pulchra* was studied against *Pseudomonas aeruginosa* QS signal pathway (Hentzer et al., 2002). They showed that the compound reduces quorum-sensing-controlled (QSC) gene expression while having no effect on bacterial protein synthesis or growth, and hence reduces several QSC virulence factors. Classical antibiotics used to treat *P. aeruginosa* infections, e.g., tobramycin and piperacillin, are required at concentrations 100- to 1,000-fold higher to kill biofilm bacteria than to kill their planktonic counterparts. Hentzer and Givskov (2003) observed that furanone-treated biofilms were more susceptible to killing by tobramycin than their untreated counterparts (Hentzer and Givskov, 2003). This approach may lead to the development of novel non-antibiotic drugs, which aim at the attenuation of bacterial virulence rather than killing the pathogen.

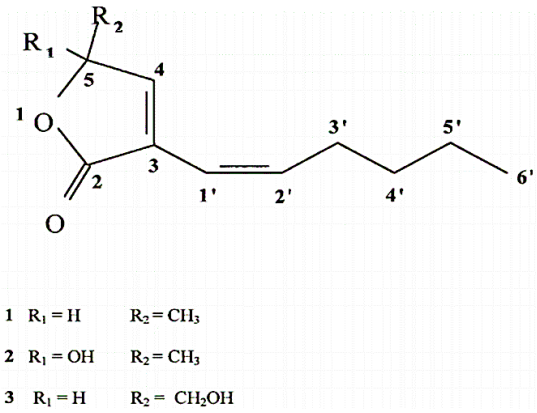

Figure 1.12 Structure of three antifungal furanones (1, 2, and 3) produced by *P. aureofaciens* (Paulitz et al., 2000)

Triclosan. Triclosan ($C_{12}H_7Cl_3O_2$) (figure 1.13) is a diphenyl ether derivative used as an antiseptic in toilet soaps and cosmetics. It has some bacteriostatic and fungistatic action. In gram-negative bacteria, it inhibits bacterial fatty acid synthesis by selectively targeting FabI encoded enoyl-acyl carrier protein (enoyl-ACP) reductase enzyme involved in bacterial fatty acid biosynthesis by synthesis of acyl-ACP, one of the essential intermediates in AHL biosynthesis; therefore, it can recuse AHL production (Darouiche et al., 2009). Triclosan exhibits an antifungal effect as well. Triclosan exhibits an antifungal effect in vitro against azole-resistant *C. albicans* when combined with fluconazole (Yu et al., 2011). *P. aeruginosa* is resistant to triclosan due to the activity of a multidrug efflux pump (LaSarre and Federle, 2013).

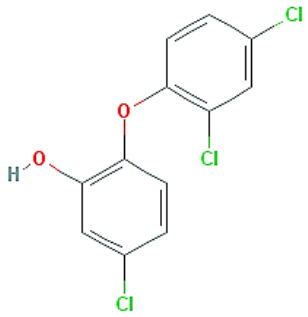

Figure 1.13 Triclosan biochemical structure (https://pubchem.ncbi.nlm.nih.gov)

The triclosan + DispersinB (DspB) combination displayed synergistic efficacy against *S. aureus*, *S. epidermidis*, *E. coli* and *C. albicans* and indicated a significant decrease in the adherence of each organism to triclosan+DspB-coated catheters, which has been made of silicone, compared with uncoated control catheter (Darouiche et al., 2009). These results show that triclosan has antibiofilm effect against both gram positive and

gram negative, as well as yeast strains. In another studies, Renko et al., (2017) and Guo et al., (2016) have demonstrated that triclosan-containing sutures in comparison with the ordinary sutures reduce the surgical site infections in children and adults (Guo et al., 2016; Renko et al., 2017). This finding shows in vivo efficacy of triclosan. Triclosan effect on fungi (Jones et al., 2000) has been reported against *Candida tropicalis*, *Blastomyces dermatitidis*, *Epidermophyton floccosum*, *Microsporum audouinii*, *Microsporum canis*, *Trichophyton mentagrophytes*, *Trichophyton rubrum* and *Trichophyton tonsurans.*

Triclosan has been reported to be harmless in topical and surface-coating applications (Gilbert and Mcbain, 2002). Biodegradation of triclosan by *A. versicolor* has been investigated. HPLC analysis showed that fungal triclosan biodegradation yield was 71.91% at about 7.5 mg/L concentration in the semi-synthetic medium and was 37.47% in simulated wastewater. The fungus could tolerate the highest triclosan concentration (15.69 mg/L) (Taştan and Dönmez 2015).

1.14 Amphotericin B

AMB (figure 1.14) is a polyene antibiotic, which binds to ergosterol, the principal sterol in the fungal cell membrane, and forms aqueous pores in the lipid bilayers. Subsequently, amino acids and proteins leak out, which in turn leads to disrupted membrane proton gradients (Reeves et al., 2004). Although, AMB is known as a fungicidal drug by causing ion leakage, studies have shown that forming channels in the cellular membrane is not the only mechanism of AMB activity (Palacios et al., 2007). Addition of antioxidants, such as reduced glutathione (GSH), cysteine, etc., could revive endospores of *Coccidioides immitis* treated with AMB (Graybill et al., 1997), indicating the involvement of cellular oxidative stress in AMB activity.

Biofilms are highly resistant to antimicrobials in the comparison of planktonic counterparts (Spoering and Lewis 2001). Drug-tolerant or persister cells, usually ≤ 1% of the overall population that neither grow nor die in the presence of microbiocidal agents are being considered as a possible reason for a drug resistance (Keren et al., 2004; Lewis, 2007). Persisters can withstand drug concentrations substantially greater than the MIC and represent specialised survivor cells that are phenotypic variants of the wild-type rather than mutants. The existence of persisters in *C. albicans* biofilms has been reported (Khot et al., 2006). Hence, these persisters may play a role in the resistance of the

candidal biofilm to AMB. It has been also suggested that for *A. flavus* and *C. albicans*, the ergosterol content (Gray et al., 2012), the composition of the fungal cell wall (Seo et al., 1999), and the ability to produce catalase might play a role in AMB resistance.

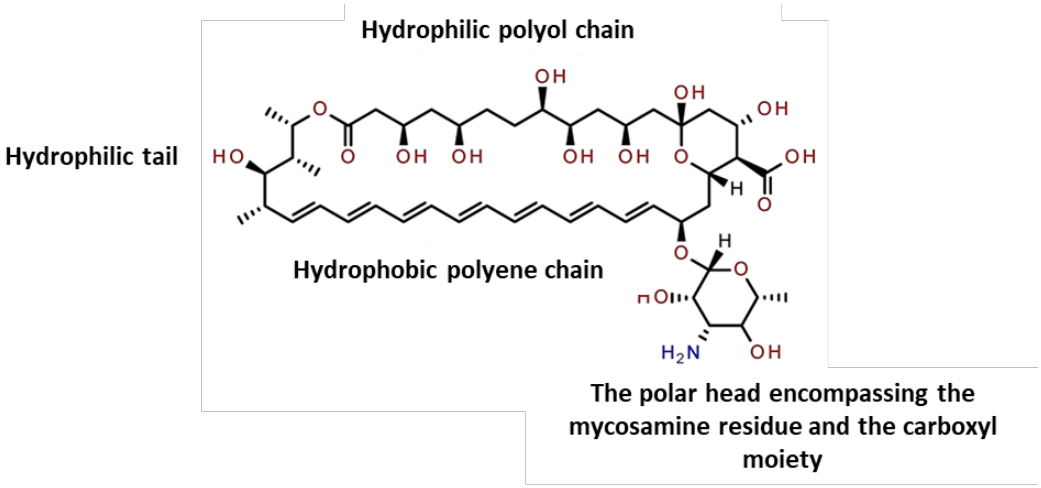

Figure 1.14 Chemical structure of AMB (Zielińska et al., 2016)

Aim

The overall aim of this progect was to investigate the effect of some antimicrobial agents (triclosan, AMB, furanone, tyrosol and farnesol) on a clinical strain *A. fumigatus* to mitigate its biofilm formation on a variety of surfaces (hydrophilic surfaces, glass, acrylic, HDPE, nylon 6 and UPVC, and hydrophobic surfaces, PTFE and silicone). The antifungal effect of triclosan and AMB were compared, as well.

Objectives

- The assessment of the antimicrobials' fungicidal role through analysing *A. fumigatus* conidia viability.
- *A. fumigatus* biofilm depth and EPS formation with and without triclosan and AMB under single-agent and combination treament.
- Triclosan and AMB influence on α(1, 3)-glucan (involved in conidia aggregation) and galactosaminogalactan (involved in biofilm attachment to biotic/abiotic surfaces as well as EPS production) synthesis.
- The antimicrobials' role on composition of *A. fumigatus* EPS.
- Analysing the *A. fumigatus* conidia surface hydrophobic rodlet layer synthesis influenced by the antimicrobials.
- The effect of the antimicrobials on the chitin content of the *A. fumigatus* mycelium cell wall.
- The impact of applied antimicrobials on manipulating the hydrophobicity of medicaly relevant surfaces.

Chapter 2

Materials and methods

2.1 Materials

Appendices 1 and 2 (appendix 1) show respectively the materials used in this study and the chemicals and reagents used in this study. Table 2.1 shows the surfaces used in this study. The surfaces coated with the antimicrobial agents and the fungus biofilm formation on them was assayed then.

Table 2.1 Surfaces used in this study. They all were provided by Goodfellow Cambridge Ltd, Huntingdon, UK

Surface	Application	Reference
Acrylic	Transparent items such as lenses, automotive trim, household items, light fixtures, decorator items	Houck, 2001
Glass	Medical technology, optical glass; Packaging (jars for food, bottles for drinks, flacon for cosmetics and pharmaceuticals); Tableware (drinking glasses, plate, cups, bowls); Housing and buildings (windows, facades, conservatory, insulation, reinforcement structures)	Benvenuto, 2015
High density polyethylene (HDPE)	Plastic bottles, corrosion-resistant piping, geomembranes, and plastic lumber	Hopewell et al., 2009
Nylon 6 (Polyamide 6)	Automotive Electrical appliances Textiles	Guo et al., 2009
Polytetrafluoroethylene (PTFE) (Teflon®)	Medical implants like heart valves and vascular grafts	Jaganatha, 2014
Silicone elastomer	Cardiovascular devices, prosthetic devices, general medical care products, transdermal therapeutic systems, orthodontics, and ophthalmology	Yoda 1998
Un-plasticized poly (vinyl chloride) (UPVC)	Pipe, window, door frame and wire insulator	Bortel and Szewczyk 1996; Zhang and Lin 2014

2.2 Fungus strain

A. fumigatus ATCC46645, available in the Culture Collection of the University of Westminster, London, UK, was stored in 20% (v/v) glycerol stocks; 170 µL glycerol and 680 µL stock spore solution in phosphate-buffered saline (PBS). The preparations were mixed and stored at -80°C. Stock cultures of *A. fumigatus* maintained on Potato Dextrose Agar (PDA) medium were propagated in Potato Dextrose Broth (PDB) medium or RPMI-1640.

2.3 Antimicrobial agents used in this study

Table 2.2 shows the antimirobials applied in this study. Farnesol and tyrosol were prepared in dimethyl sulfoxide (DMSO) and Triclosan, AMB and furanone were prepared in DI water. The final solvent background was < 0.5%.

Table 2.2 Antimicrobial agents used in this study

Agent	Company
(Z-)-4-Bromo-5-(bromomethylene)-2(5H)-furanone	Sigma-Aldrich, Dorset, UK
5-Chloro-2-(2,4-dichlorophenoxy) phenol, Irgasan, Triclosan	Sigma-Aldrich, Dorset, UK
Amphotericin B loaded liposomes, AmB-LLs	Thermo Fisher Scientific, Leicestershire, UK
Farnesol	Merck, Dorset, UK
Tyrosol [2-(4-hydroxyphenyl) ethanol]	Merck, Dorset, UK

2.4 Solutions and buffers used in this study

Tables 2.3 and 2.4 list respectively the solutions and buffers used in this study.

Table 2.3 Solutions used in sodium dodecyl sulfate- polyacrylamide gel electrophoresis (SDS-PAGE) preparation and in silver staining of the gel

Solution	Recipe
SDS (10% w/v)	SDS (100 g) was dissolved in 900 ml water with gentle stirring and brought to 100 ml with DI water
Ammonium persulfate (APS) (10% w/v)	100 mg ammonium persulfate was dissolved in 1 mL of DI water. It should be used fresh
Fixer	Ethanol (40% v/v), acetic acid (10% v/v), DI water (50% v/v)
Sodium thiosulfate (0.02% w/v)	$Na_2 S_2O_3$ (0.04 g), DI water (200 mL)
Silver nitrate (0.1% w/v)	$AgNO_3$ (0.2 g), DI water (200 mL), and formaldehyde (0.02% v/v) (40 µL 35% (v/v) was added just before use)
Sodium carbonate (3% w/v)	Na_2CO_3 (7.5 g), DI water (250 mL), and formaldehyde (0.05% v/v) (125 µL 35% (v/v) was added just before use)

Table 2.4 Buffers used in this study

Buffer	Recipe
Buffer used for conidia cell wall protein extraction	Tris -HCl (0.1 M). The pH was adjuste by using 8 M urea
EDTA (Ethylenediaminetetraacetic acid) (0.5 M)	EDTA (232.8 g) was added to DI water up to 1000 mL, then NaOH was added until pH reached 8.0.
Lysis buffer	Tris-acetate (40 mmol/L), sodium acetate (20 mmol/L), EDTA (1 mmol/L), and SDS (1% w/v), pH 7·8
PBS (Phosphate-buffered saline) (1X)	NaCl (8 g), KCl (0.2 g), Na2HPO4 (1.44 g) and KH_2PO_4 (0.24 g) were added to ddH2O (800 mL). The pH was adjusted to 7.4 with HCl. DI water was added to make a total volume of 1 litre.
Extraction buffer	Tris-HCl (0.1 M), KCL (0.1 M), EDTA (10 mM), Polyvinylpolypyrrolidone (PVPP) (1%), β-mercaptoethanol (0.4%).
SDS-PAGE (sodium dodecyl sulfate-polyacrylamide gel electrophoresis) sample loading buffer (2X) (SDS reducing buffer)	Tris-HCl (50 mM) (pH 6.8), sucrose (23% w/v), SDS (4% w/v), bromophenol blue (0.01% w/v), dithiothreitol (DTT) (100 mM). The SDS gel-loading buffer without DTT was kept at room temperature; DTT was added from a 1 M stock just before the buffer was used.
SDS-PAGE running buffer (10X)	Tris-base (30.3 g), glycine (144.0 g), SDS (0.1% w/v) (10.0 g) were dissolved. Then, DI water was added to make a total volume of 1 litre. The running buffer was stored at room temperature and dilute to 1X before use
TBE (Tris/Borate/EDTA) (10X)	Tris-base (108 g) and boric acid (55 g) were dissolved in 900 mL DI water. Na2EDTA 0.5M (40 mL) (pH 8.0) was added. Then, DI water was added to make a total volume of 1 litre.
Tris-HCl (0.5 M) (pH 6.8)	Tris-base (60 g) was added to 800 mL DI water. pH was adjusted to 6.8 with 6 N HCl. Then, DI water was added to make a total volume of 1 litre and stored at 4°C.
Tris-HCl (1.5 M) (pH 8.8)	Tris-base (181.5 g) was added to 800 mL DI water. pH was adjusted to 8.8 with 6 N HCl. Then, DI water was added to make a total volume of 1 litre and stored at 4°C.

2.5 Growth condition of *A. fumigatus*

2.5.1 Potato Dextrose Broth

Potato dextrose (24 g/L) broth powder (1% (w/v) yeast extract, 2% (w/v) peptone and 2% (w/v) dextrose) was added to make up 1000 mL de-ionized water (DI water). The solution was autoclaved for 15min at 121°C.

2.5.2 HEPES-buffered RPMI-1640 with L-glutamine

RPMI- 1640 was prepared based on Sigma product information sheet. Deionized water (DI) water (900 mL) was measured out. Water temperature was between 15-20°C. While gently stirring the water, the powdered medium was added and stirred until dissolved (without heating). RPMI- 1640 medium was then supplemented with 50 mM 3-(N-morpholino) propanesulfonic acid (MOPS) buffer. After it was dissolved completely, the pH was raised to 7.2 with NaOH (1 N). While stirring, the pH of the medium was adjusted to 0.1-0.3 pH units below the desired pH since it may rise during filtration. Additional water was added to bring the solution to final volume (1 L) and sterilised immediately by filtration using a Millipore membrane filter with a porosity of 0.22 microns. Then, the medium was aseptically dispensed into a sterile container.

2.6 Long term storage of *A. fumigatus* culture and preparation of working stock

A. fumigatus was stored as 20% (v/v) glycerol stocks (150 µL glycerol and 700 µL stock spore solution in PBS were added into cryotubes). The solutions were mixed and stored at -80°C. Stocks were maintained for months by plating a loopful of the frozen fungus onto agar slopes in 5 mL bottles. The slopes were stored at 4°C after the cultures have grown.

2.7 Methods

2.7.1 Culture and treatment of *A. fumigatus*

Spore suspensions were prepared from 5-day-old cultures grown on PDA. Prior to use in the susceptibility assay/biofilm experiments, conidia were washed twice in sterile PBS and harvested. The cells were then suspended in DI water, counted in a haemocytometer and adjusted to the desired cell density (a suspension containing ~10^6 of conidia in 1 mL solution served as inoculum). For liquid cultures, *A. fumigatus* was grown in 100 mL RPMI-1640 medium or PDB medium, in 500 mL conical flasks, and inoculated with 1 mL

inoculum. Flasks were then incubated with shaking (150 rpm) at 37°C for appropraie times. For conidial-related analysis treated inoculums were plated on PDA plates and incubated for seven days at 37°C. Subsequently, the surfaces of the agar plates were washed three times with PBS. Then, a scraper was used to detach the conidia from the agar surface. The conidia were added to 5 mL deionised water, counted and stored at 4°C for fourteen days.

To determine MIC_{50} of each of the antimicrobials (table 2.2), the inoculation of *A. fumigatus* on 96-well polystyrene plates was carried out in RPMI-1640 medium at 37°C under static condition. The mature biofilms formed after 48 hr. The MIC_{50} determination assay was followed by the effective time determination assay viability assay to measure the effective time for the calculated MIC_{50}. Both effective doses and times of the agents for sessile (biofilm) cells and conidia were measured by the resazurin reduction assay.

2.7.2 Assying antifungal role of the agents against *A. fumigatus*

2.7.2.1 Growth curve of *A. fumigatus*

A. fumigatus growth curve was obtained based on optical densities, OD at 405 nm, changes. *A. fumigatus* was cultured in PDB medium under static condition in t175 culture flask at 37°C for 48 hr. Samples were taken at 4 hr intervals.

2.7.2.2 Serial dilution method to measure the metabolic activity

Using serial dilution method effective doses of triclosan, furanone, AMB, tyrosol and farnesol were determined. Doses ranged between 0.5 to 32 mg/L, 0.6 to 20 mg/L, 0.125 to 16 mg/L, 0.005 to 0.32 mg/L and 0.1 to 3.2 mg/L for triclosan, furanone, AMB, tyrosol and farnesol, respectively were prepared in 96-well plates. The results were used to determine the effective doses for agents when they introduced to the medium either before or after biofilm formation.

In one experiment each antimicrobial agent was added to the RPMI-1640 medium containing *A. fumigatus* clinical strain (200 µL in total) at t_0 and incubated at 37°C for 24 hr, which is enough time for *A. fumigatus* biofilm formation.

In another experiment, the non-treated medium containing inoculum was removed from wells after 24 hr of incubation, and fresh medium containing the agents' different doses were added (200 µL) to the biofilm. Viability determined after 24 hr at 37°C.

In both tests, resazurin dye solution was added in an amount equal to 10% (v/v) of the culture medium volume 24 hr after adding the antimicrobial agents. The 96-well plates incubated at 37°C on a shaker at 50 rpm for 50 min (figure 2.1), and the absorbance of multi-well was measured spectrophotometrically by monitoring the decrease in absorbance at a wavelength of 590 nm. Resazurin, a nonfluorescent dye, can penetrate living cells and reduce to fluorescent product, resarufin, probably by the action of mitochondrial, cytosolic and microsomal enzymes. The dye can diffuse from cells and back into the surrounding medium (Cell Viability Assay, Promega Corporation).

The conversion of resazurin to fluorescent resorufin is proportional to the number of metabolically active, viable cells present in a population. The signal was recorded using a standard multiwell fluorometer.

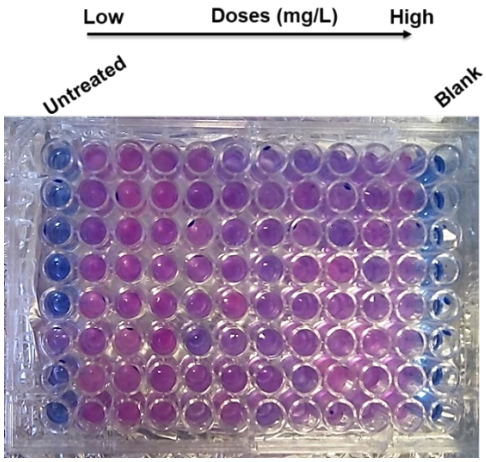

Figure 2.1 Measurement of metabolic activity using antifungal resazurin dye solution

2.7.3 *A. fumigatus* biofilm analysis upon treatment with the agents

2.7.3.1 Biofilm quantification by crystal violet (CV) assay

The effect of agents (triclosan, AMB, tyrosol and farnesol at their MIC_{50} concentrations) on the biofilm was estimated using the crystal violet (cv) assay. To determine the ability to form biofilms, an inocula was added to 200 µL PDB medium in a 96-well polystyrene microtiter plate, which was incubated, without agitation, at 37°C for 36 hr. Subsequently, to

determine the effect of agents on the biofilm formation, following the initial incubation period, the medium was aspirated and non-adherent cells removed by thoroughly washing the formed biofilm three times with PBS. After fixation with glutaraldehyde (70% in H_2O) for 20 min and air-drying, the biofilms were stained with 200 µL, 0.5% w/v crystal violet for 15min, followed by rinsing with sterile PBS, and de-stained with ethanol (96% v/v). The absorbance of the crystal violet stained biofilm in the treated and untreated control groups was measured at 590nm using a spectrophotometer.

Percentage biofilm biomass in the treated samples was calculated using the following equation:

(A590 of the test/A590 of untreated control) × 100 **Equation 1**

where A590 is the absorbance of the crystal violet stained biofilm matrix at 590 nm.

2.7.3.2 Biomass assay

To study the biomass weight, conidial inoculum was added in a 35 mm Petri dish containing 20 mL of RPMI-1640 medium (treated with triclosan, AMB, tyrosol and farnesol, nontreated=control+); no inoculation= control-, which was incubated at 37°C for 36 hr. The Petri dishes were then weighted.

2.7.3.3 Biofilm dry weight assay

For biofilm formation, inoculum was added to 20 mL RPMI medium and dispensed on flat, pre-sterilised polystyrene petri dishes. Following an initial adherence phase of 4 hr during static incubation at 37°C, unbound conidia were washed three times with sterile PBS. Fresh RPMI medium with the indicated additives was added to the adhered conidia, and static submerged cultures were grown for up to 48 hr at 37°C (figure 2.2). Mycelia were harvested by scraping from the surfaces of the petri dishes and filtered through filter papers (55 mm). The dry weight of biofilm produced was determined.

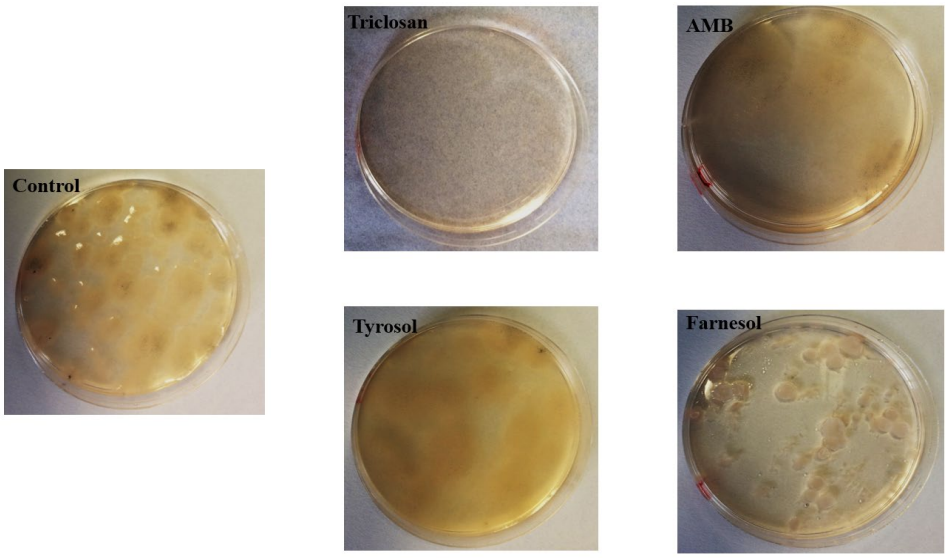

Figure 2.2 *A. fumigatus* conidia were grown in RPMI-1640 while treated with the agents' MICs for 48 hr at 37˚C. Colonies formed at the liquid- air interface. Though, there was no growth in triclosan-treated medium. The growth was obvious in the other treatments, while the morphology of the farnesol- treated colonies looks different with that in the untreated control Petri dish

2.7.3.4 Protein quantification assay

The Bradford protein assay was used to measure the concentration of total protein in a sample. The principle of this assay is that the binding of protein molecules to Coomassie dye under acidic conditions results in a colour change from brown to blue (Bradford, 1976). To draw the standard curve based on the Bradford micro-assay 5 µL from different doses of bovine serum albumin (BSA) (0.1, 0.2, 0.5, 1 and 1.5 mg/ mL) were added to 5 wells of 96-well microplate and 250 µL 1x Bradford dye reagent added to them. DI water (5 µL) was added for blank sample preparation. The samples were incubated at room temperature for at least 5 min (absorbance will increase over time; samples should incubate at room temperature for no more than 1 hr). The absorbance was measured at 595 nm. For treated and untreated control sample preparation, the inocula were added to 1.8 mL RPMI in a 2 mL Collection Tube and treated with triclosan, AMB, tyrosol and farnesol. After 0, 4, 16, 28 and 40 hr static incubation in RPMI at 37°C, the fungal cultures' proteins were extracted as explained in section 2.7.5.4 and used for the Bradford and phenol-sulphuric acid assays.

2.7.3.5 Carbohydrate quantification assay

The method described by Masuko et al., 2005 was adopted for this study. Samples were prepared as described in section 2.7.1 and diluted (40 µL/ mL). First, phenol 5% (v/v) (200 µL) was added to Falcon tubes (15 mL). Subsequently, culture broth samples (200 µL) were added. Finally, concentrated H_2SO_4 (1 mL) was added quickly into each tube. The tubes were shaken gently until solution look homogenised and kept still for 10 min at room temperature. The absorbance of the solution was read at a wavelength of 490 nm. A standard curve was prepared using glucose.

2.7.3.6 Extraction of *A. fumigatus* EPS for DNA, protein and carbohydrate assays

Each sample grown under static condition in t175 polystyrene tissue culture flasks containing inocula in PDB treated with agents' MICs for 48 hr was transferred to 50 mL conical tubes. Harvested biofilms were washed in situ twice with 32 mL PBS to remove planktonic and loosely adherent cells. The sessile cells were then flooded with 13 mL of 10 mM Tris (pH 7.4) per flask and mixed mildly with a vortex mixer for 60 sec. Each sample was transferred to a 50 mL conical tube and stored at 4°C until processing. For the EPS extraction, the tubes containing the *A. fumigatus* biofilm were subjected to sonication for 10 min. Followed by high speed mixing on a vortex mixer for 30 sec. The tubes were then centrifuged at 3600 xg at 4ºC for 15 min. The supernatant was poured into new tubes. Centrifuged again to remove additional cells. The resulting supernatant was dialyzed against distilled water using SnakeSkin™ Dialysis Tubing for 2 days (3.5-kDa molecular mass cut off), then, lyophilized (Reichhardt et al., 2015). The amounts of DNA, protein, and carbohydrate extracted from the EPS were then calculated.

2.7.3.7 NanoDrop DNA and RNA quantification

Asexual spore suspensions (10^6 spores/mL) were added to 1.8 mL RPMI in a 2 mL Collection Tube and treated with triclosan, AMB, tyrosol and farnesol effective doses. After 18 hr static incubation the fungal cultures were analysed with NanoDrop™ spectrophotometer for DNA and RNA quantification.

To accurately assess sample quality, 260/280 or 260/230 ratios should be analysed in combination with overall spectral quality. Pure nucleic acids typically yield a 260/280 ratio of ~1.8 and a 260/280 ratio of ~2.0 for DNA and RNA, respectively. This ratio is

dependent on the pH and ionic strength of the buffer used to make the blank and sample measurements. In this measurement EB Solution from Allprep Fungal DNA/RNA/Protein Kit, and DI water were used as blanks for DNA and RNA measurments. Acidic solutions will under-represent the ratio by 0.2-0.3, while a basic solution will over-represent the ratio by 0.2-0.3. Significantly different purity ratios may indicate the presence of protein, phenol or other contaminants that absorb strongly at or near 280 nm (Desjardins et al., 2010).

2.7.3.8 DNA agarose gel electrophoresis

Agarose (500 mg) was dissolved in Tris/Borate EDTA buffer (50 mL; TBE) by heating in a microwave until boiling, this solution was allowed to cool, and then gel red was added (0.02 µL/mL). Gels (1% w/v) were then cast in a 10 x 20 cm gel tank, any bubbles were removed with a pipette tip and then gel comb was added, and the gel allowed to set. Gel electrophoresis was carried out in a horizontal tank containing TBE buffer and was run at 120 V for 40 min. Gels were imaged using a UV transilluminator.

2.7.3.9 Flow cytometry (FCM)

To assess conidia viability without the use of culture media, DI water was used instead. Based on the method defined by Mesquita et al., (2013) flow cytometery tubes (3.5 mL) included control tubes and experimental tubes were prepared (1 mL of DI water+1 mL of the corresponding spore suspension (section 2.7.3.11)) and marked as follows:

Tube 1: no antimicrobial added - this is control

Tube 2: Triclosan- treated sample

Tube 3: AMB- treated sample

Tube 4: Tyrosol- treated sample

Tube 5: Franesol- treated sample

Samples (100) µL of each treated (test) and untreated (control) groups were added to a flow cytometry tube with 50 µL of propidium iodide (PI) stock solution (1mg/ mL) and 1.85 mL distilled water. Tubes were mixed by inversion and analysed in the cytometer, after 10 min of staining with PI. PI excites by a 488-523 nm laser (Mesquita et al., 2013).

When excited, it can be detected with in the PE/Texas Red® channel with a bandpass filter 610/10 (BioLegend, California, US). To remove any particles smaller than spores from the analysis, the discriminator was defined for the particle size just under the lowest spore signals. Conidial viability was defined by the FSC (forware scatter) and SSC (side scatter) characteristics and the mean fluorescence intensity (MFI) of PI in treated and untreated conidia.

2.7.3.10 Calcofluor White (CFW) staining of the chitin

For chitin detection of the cell wall of *A. fumigatus*, 1x10^6/mL conidia were inoculated onto glass coverslips that were placed in a 6-well plate containing 3 mL of RPMI-1640 medium (figure 2.3), which were then incubated at 37°C for 12, 24 and 36 hr.

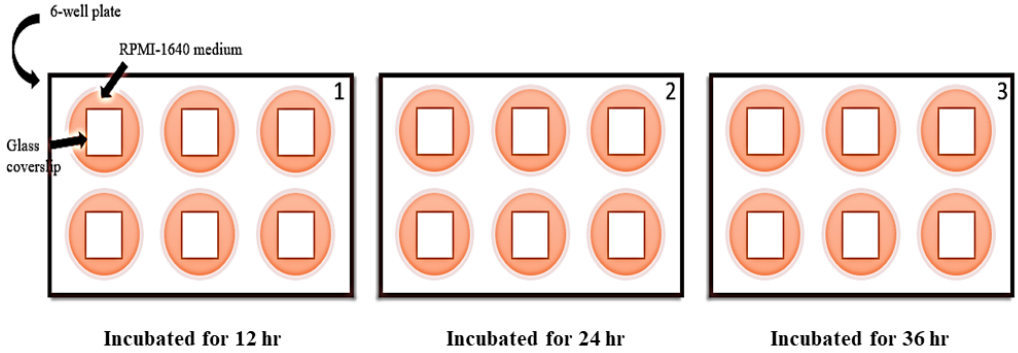

Figure 2.3 CFW staining of the cell wall of *A. fumigatus* biofilm to assess the synthesis of chitin

After incubation, the coverslips were transferred to fixation solution [PBS 1X, DMSO 5% (v/v), and formaldehyde 3.7% (v/v)]. Calcofluor white stain at the concentration of 1 µg/mL was added to the coverslips. They were kept at room temperature for 15 min, and then rinsed briefly with PBS buffer, mounted, and observed in a dark room under UV light using Zeiss Model AxioVert 100 at 40X magnification (figure 2.4).

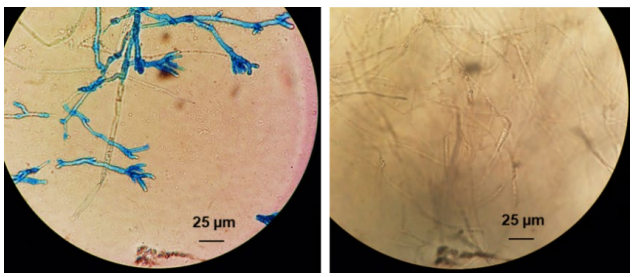

Figure 2.4 CFW staining of the chitin in *A. fumigatus* cell wall. The left picture shows non-treated control sample, which has been stained with CFW as blue; while the picture on the right, farnesol-treated sample: no response to stain (100X magnification)

2.7.3.11 High performance liquid chromatography (HPLC)

The isolates, MIC_{50} of the agents and untreated control test group added to the PDB medium were re-cultured in PDA medium plates and incubated at 37°C until sporulating cultures were obtained (three days). Fresh conidia were harvested by washing with a sterile saline solution (0.9% w/v). The original concentration of the spore's suspensions was estimated and subjected to 6 $x10^6$ spores/mL. This corresponding spore suspensions were used in FCM analysis, as well. The corresponding spore suspensions were stored in 4°C without light. Samples were prepared with 1 mL of PDB liquid culture medium, and 1 mL of the corresponding spore suspension, for final concentration of 5 x 10^6 spores/mL. Samples were incubated at 37°C, for the duration of this experiment (36 hr). Samples were taken at three different time points, 4, 18 and 36 hr of incubation.

For HPLC analysis of glucose, *A. fumigatus* spore suspensions prepared from 4-, 18- and 36-hr old sporulating PDA cultures were diluted in HPLC grade water (resistivity of 18.2 MΩ ×cm) and syringe filtered through 0.22-micron filter to avoid the particulate matter. Glucose at different concentrations (0.01, 0.025, 0.05, 0.1 and 0.25 M) were prepared as conrol standards.

HPLC analysis was carried out using a Dionex™ ICS-5000+DC detector. A reverse phase column (Phenomenex Rezex RHM Monosaccharide H^+ 300 x 7.8 mm) was maintained at 37°C with a solvent flow rate of 0.8 mL/min. A linear solvent gradient of 5–40% (v/v) CH_3CN in 2% (v/v) acetic acid was used for the first 30 min, then 40–100% (v/v) was used for the next 10 min. Thermo Scientific™ Dionex™ Chromeleon™ 7 Chromatography Data system software was used to set and run the device.

2.7.4 Triclosan effect alone and in combination with AMB against *A. fumigatus*

2.7.4.1 Slide culture method

Slide cultures (figure 2.5) were made by setting up a small Petri dish moist chamber containing a V-shape piece of tubing resting on a layer of moisturised filter-paper. A sterile block of PDA medium, about 1 cm^2, was placed on a flame-sterilised microscope slide and the slide was then set in the moist chamber (some drops of DI water were added to the petri dish to keep the culture moist) on the tubing. *A. fumigatus* treated with

effective dose of triclosan and untreaed control were inoculated near the four edges of the agar block and a sterile cover slip was put over it. Then, incubated for seven days at 37°C.

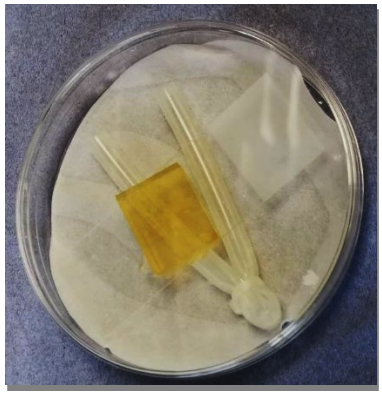

Figure 2.5 Slide culture technique for morphological assessment

2.7.4.2 Colony forming unit (CFU) determination assay

A. fumigatus conidia (treated with AMB and triclosan and untreated control test group) were grown in PDB medium in an orbital shaker (150 rpm) at 37°C. Samples (100 µL) were taken from PDB subnatant (after filtration through a Whatman cellulose filter) after 24 and 36 hr of incubation; then resuspended in PBS and were plated on PDA plates. The fraction of viable biofilm cells was determined by counting the colonies and calculating the percentage of surviving *A. fumigatus* cells relative to the control drug-free cells and also colony diameter was determined after incubation at 37˚C for 24 hr.

2.7.4.3 Cell dry weight assay

Culture broth (40 mL) from each flask containing *A. fumigatus* mycelia (treated with AMB and triclosan and untreated control test group) were filtered through Whatman cellulose filters after 24 and hr 48 incubation. For dry weight assay performing, the filter papers were maintained in an oven at 50°C for an overnight.

2.7.4.4 Single and combination treatment of *A. fumigatus* with triclosan and AMB

For single treatment, 200 µL RPMI-1640 medium containing the first antimicrobial MIC_{50} and inoculum was added per well. After 24 hr RPMI-1640 medium was replaced with fresh medium, this time without any antimicrobial or conidia. By using resazurin assay cell viability was determined after 24 hr (48 hr in general) of incubation at 37°C.

Simultaneous combination treatment was performed by addition of both triclosan and AMB MICs, simultaneously, to the 200 µL RPMI-1640 medium containing *A. fumigatus* conidia. After 24 hr RPMI-1640 medium was replaced with fresh medium, this time without any antimicrobial or conidia.

For continuous combination treatment, 200 µL RPMI-1640 medium containing the first antimicrobial and conidia was added per well (after 24 hr incubation biofilms were already formed, which means that the first antimicrobial worked on the conidia attachment and/or biofilm formation, which means it has a pre-biofilm formation effect). After 24 hr the medium was replaced with the fresh one containing the second antimicrobial (the second antimicrobial has its effect on the developed biofilm since by removing medium the unattached conidia were removed from the wells).

For both simultaneous and continuous combination treatment strategies, viability was determined by using resazurin assay after 24 hr treatment with the second agent. Replacing the medium with fresh medium before adding resazurin leads to removal of the unattached conidia.

2.7.4.5 Disk-diffusion assay

Five single colonies were picked and inoculated into PDB. Cells are grown overnight in a rotary shaker at 150 rpm at 37°C. An aliquot of 100 µL of the conidia inoculum was prepared and applied onto the PDA plate and spread uniformly using a cell spreader. Then, 6-mm Whatman® antibiotic assay discs impregnated with triclosan and AMB (at their MIC_{50} and sub-MIC_{50s}, alone and in combination) were positioned on an agar plate to evaluate the antifungal effect of triclosan. After incubation at 37°C for 48 hr, the diameters of the growth inhibition zone were measured.

2.7.4.6 Synergy assays

To study the interaction between triclosan and AMB when they were adding sequentially or continuously, checkerboard assay was performed. CompuSyn software was used to confirm the results.

Checkerboard assay. Triclosan-AMB interactions were evaluated using the checkerboard assay. Checkerboards were prepared by using serial dilutions of AMB and triclosan. Triclosan and AMB dilutions were prepared as recommended in the EUCAST (European

Committee on Antimicrobial Susceptibility Testing) protocol to give final drug concentrations of 1 to 64 mg/L and 0.25 to 16 mg/L for triclosan and AMB, respectively, in 100 µL of double-strength RPMI medium containing 10^6 conidia/mL fresh spore suspension. Antifungal dilutions were transferred to the wells of a 96-well flat-bottom microplate. Subsequently, 100 µL of RPMI medium containing fresh spore suspension (10^6 conidia/mL) were added to the 0.2 mL vertical wells, resulting in concentrations in the range of 0.5 to 32 mg/L and 0.125 to 8 mg/L for triclosan and AMB, respectively. Plates were read after 24 hr of incubation at 37 ºC, and the wells without visible signs of growth were identified by placing the plate on a mirrored surface. Each well was resuspended and agitated for 5 min, and the OD at 570 nm wavelength was determined with a spectrophotometer.

The fractional inhibitory concentration index (FICI) was calculated as follow:

$$FICI = (MIC\ A_{com\ A/B} / MIC_{agent\ A}) + (MIC\ B_{com\ A/B} / MIC_{agent\ B}) \qquad \textbf{Equation 2}$$

According to the equation, FICI ≤ 0.5 indiates synergy, FICI > 4 indicates antagonism whereas 0.5 < FICI < 4 suggests no interaction.

Synergistic assay based on CompuSyn software. The Chou-Talalay method for drug combination is based on the median-effect equation, derived from the mass-action law principle, which is the unified theory that provides the common link between single entity and multiple entities, and first order and higher order dynamics. The resulting combination index (CI) theorem of Chou-Talalay offers quantitative definition for additive effect (CI=1), synergism (CI<1), and antagonism (CI>1) in drug combinations (Chou, 2010).

2.7.4.7 Biofilm visualization and thickness measurement

A. fumigatus biofilm prepareation on glass surfaces The *A. fumigatus* biofilms formed on coverslips were challenged with the different agents' MICs. Sterile coverslips (13mm diameter) were used as growth surfaces for the biofilm formation and were inserted into the 6-well tissue culture plate. Approximately 3 mL of the *A. fumigatus* inoculum was added to each well of a polystyrene, flat-bottom, 6-well tissue culture plate. Subsequently, the plates were incubated at 37°C. The biofilms were checked after 24 hr incubation at 37°C.

Confocal laser scanning microscopy (CLSM) CLSM was used to examine the fluorescent filamentous biomass and hence the biofilm and its thickness. Microscopic visualization and image acquisition of biofilms were conducted using an upright scanning Leica DMRE confocal microscope equipped with an argon/krypton laser and detectors, and filter sets for monitoring of green (excitation 480nm, emission 517nm) and red (excitation 633nm, emission 676nm). The biofilms on the surfaces were washed three times in sterile PBS and stained using a fluorescent stain, FUN-1 [2-chloro-4-(2,3- dihydro-3-methyl-(benzo-1,3-thiazol-2-yl)-methylidene)-1-phenylquinolinium iodide] stain prepared according to the manufacturer's instructions. For biofilm visualization, FUN-1 (1 μL) from a 10mM stock was mixed in 1 mL of PBS. Three drops of the mixture were added on the top of the biofilm, which was then mounted on a coverslip. The slides were incubated for 45min at 37°C in the dark. The biofilm, formed as explained above, was washed again with PBS and mounted on a slide. An excitation wavelength of 488 nm using an argon ion laser at a magnification of 200x was used to examine the biofilms. The FUN-1 exposed the morphology of *A. fumigatus* biofilm.

The FUN-1 stain passively diffuses into cells and initially stains the cytoplasm with a diffusely distributed green fluorescence. However, in several common species of yeast and fungi, subsequent processing of the dye by live cells results in the formation of distinct vacuolar structures with compact form that exhibit a striking red fluorescence, accompanied by a reduction in the green cytoplasmic fluorescence. Formation of the intravacuolar structures requires both plasma membrane integrity and metabolic capability. A bright green cytoplasmic stain is produced after passive diffusion. Dead cells would have fluoresced bright yellow-green, with no red structures.

Horizontal (xy) view of reconstructed 3-dimensional images of FUN1-stained biofilms, with filter set to capture green fluorescence. Thickness of the biofilm can be observed in the side view of the reconstruction. Sections on the xy plane were taken at 1 μm intervals along the z-axis of the sections taken parallel to the x-y plane to determine the depth of the biofilms. Images were taken every micrometer throughout the whole biofilm depth. Three-dimensional images were assembled using Leica TCS SP5 software (Leica Microsystems, Heidelberg, Germany). Quantitative analyses of image stacks were performed using the COMSTAT software (Heydorn et al., 2000).

2.7.4.8 Polymerase chain reaction (PCR) assay

A. fumigatus was treated with triclosan and AMB MICs and cultivated in PDB medium in universal tubes for 24 hr at 37°C. Genomic DNA was then extracted by using Allrep fungal DNA/RNA/protein kit.

To optimise the reaction setup, PCR assay was repeated several times and finally the agarose gel concentration, voltage and time of operation was calculated as 1% w/v, 120 v and 50 min, respectively. Thin-walled PCR tubes were placed on ice. A fragment of the gene encoding *ags3* and *sph3* were isolated from genomic DNA; the master mix was prepared by adding FastStart SYBR Green and the forward and reverse primers (appendix 1, table 3). Each 25-µL PCR mixture contained: 12.5 µL SYBR Green Master, 2 µL Template DNA (target DNA) (10 ng-500 ng), 2.5 µL Forward Primer (5 pmol/µL stock), 2.5 µL Reverse Primer (5 pmol/µL stock) and 5.5 µL DI water. For the negative control the amounts were 12.5, 0, 2.5, 2.5 and 7.5 µL, respectively. Amplifications were performed on a Techne™ 5PrimeG Gradient Thermal Cycler.

ags3 amplification. Reaction tubes were placed in the PCR machine and the machine was set as follows: samples were heated to 95°C for 2 min to activate the FastStart Taq DNA Polymerase. Thirty cycles of PCR were then performed with a melting step at 95°C for 20 s, annealing at 55°C for 20 sec, and extension at 72°C for 30 sec, with a final extension of 72°C for 10 min. PCR products were visualized by agarose gel electrophoresis.

sph3 amplification. PCR was performed under the following cycling conditions: samples were heated to 95°C for 2 min to activate the FastStart Taq DNA Polymerase. Thirty cycles of PCR were then performed with a melting step at 94°C for 30 s, annealing at 45°C for 30 sec, and extension at 72°C for 1 min, with a final extension of 72°C for 10 min. PCR products were visualized by agarose gel electrophoresis.

2.7.4.9 Real-Time -PCR

Expression of the genes of interest (*ags3* and *sph3*) was quantified by relative real-time (RT-PCR) analysis. The primers used for each gene are shown in appendix 1, table 3. RNA was extracted by using Allrep fungal DNA/RNA/protein kit. First strand synthesis was performed from total RNA with Quantitec Reverse Transcription kit (Qiagen) using random primers.

Total RNA extraction. RB, RW and MB solutions were provided in the Allrep fungal DNA/RNA/protein kit.

- Untreated control, triclosan- and AMB- treated fungal cultures (1.8 mL) were centrifuged (3 min at 15,000 xg) in 2 mL Collection Tubes (provided in the kit) and all of the supernatant were removed with a pipette tip.
- β-mercaptoethanol (a key reagnt in denaturing RNases) and HaltTM Protease Inhibitor Cocktail (10 µL/mL) were added to the cells' aliquots. The cell pellets were re-suspended by vortexing. The re-suspended cells were then transfered to a PowerBead Tube (provided in the kit).
- RB Solution (350 µL) was added to the flow through and vortexed briefly on high to mix. The lysate was added to a new spin filter and centrifuged at 15,000 xg for 1 min at room temperature. The spin filter basket was transferred to a clean 2 mL Collection Tube.
- RW Solution (650 µL) was then added to the spin filter and centrifuged at 15,000x g for 1 min at room temperature. The flow through was discarded.

Ethanol 100% (v/v) (650 µL) was added to the spin filter and centrifuged at 15,000x g for 1 min at room temperature. The flow through was discarded. The empty spin filter was centrifuged at 15,000 xg for 2 min at room temperature to remove any residual solution. Then, the spin filter was placed in a new 2 ml Collection Tube.

- RNase-Free Water (100 µL) was added to the center of the white filter membrane ad then, incubated for a minimum of 1 min at room temperature and centrifuged at 15,000 xg for 1 min at room temperature.

Preparing the genomic DNA. Template RNA was thawed on ice. gDNA Wipeout Buffer, Quantiscript Reverse Transcriptase, Quantiscript RT Buffer, RT Primer Mix, and RNase-free water (all provided in the Quantitec Reverse Transcription kit) were thawed at room temperature (15–25°C). Each solution was mixed by flicking the tubes and centrifuged briefly to collect residual liquid from the sides of the tubes, and then stored on ice. The genomic DNA elimination reaction was prepared on ice (table 2.5), stirred and then stored on ice. Subsequently, the appropriate volume of this master mix was distributed into individual tubes followed by each RNA sample. The tubes were kept on ice.

Table 2.5 Genomic DNA elimination reaction components

Component	Volume/ reaction	Final concentration
gDNA Wipeout Buffer, 7X	2 µL	1X
Template RNA	Up to 1 µg	-
RNase-free water	Variable	
Total volume	14 µL	-

Reverse-transcription preparation. The prepared tubes were incubated for 2 min at 42°C and then placed immediately on ice. The reverse-transcription master mix was prepared on ice according to table 2.6, mixed and then stored on ice.

Table 2.6 Reverse-transcription master mix

Component	Volume/reaction	Final concentration
Quantitative Reverse Transcriptase (also contains RNase inhibitor)	1 µL	
Quantitative RT Buffer, 5x (Induces Mg^{2+} and dNTPs)	4 µL	1x
RT Primer Mix	1 µL	

The reverse-transcription master mix contains all components required for first-strand cDNA synthesis except template RNA. The template RNA (14 µL) was added to each tube containing reverse-transcription master mix, mixed and then stored on ice. The tubes were incubated for 15 min at 42°C, and for 3 min at 95°C to inactivate Quantiscript Reverse Transcriptase.

Reverse-transcription reactions were stored on ice and proceeded directly with RT-PCR. For long-term storage, they were stored at –20°C.

Master mix was prepared as follows (for one reaction): SYBR Green 12 µL; DI water 4 µL; Template 4 µL; Rverse Primer 1 µL; Forward Primer 1 µL

RT-PCR was then performed using a 7500 Real-Time-PCR System. Fungal gene expression was normalized to *A. fumigatus ags3*/*sph3* expression. For relative quantification comparative threshold cycle (Ct) method was used. This method, based on ThermoFisher guideline (2014) compares the Ct value of one target gene to another (using the formula: $2^{-\Delta\Delta Ct}$) (e.g., an internal control or reference gene (housekeeping gene)) in a single sample. Multiple reference genes (Llanos, François and Parrou, 2015) were used to calculate their Ct depends on their stability. Among them. the expression level of a given reference gene (appendix 1, table 3) did not change between the studied conditions (control, and treated). The reference gene had stable mRNA expression and the amount of its mRNA was strongly correlated with the total amounts of mRNA in the samples.

Relative expression was estimated using the formula ($2^{-\Delta\Delta Ct}$), where $\Delta\Delta Ct = [Ct_{\text{target gene, treated}} - Ct_{\text{reference gene, treated}}] - [Ct_{\text{target gene, control}} - Ct_{\text{reference gene, control}}]$. In each qPCR assay, test samples were run in duplicate with four no-template controls. To verify the absence of genomic DNA contamination, negative controls were used for each gene set in which reverse transcriptase was omitted from the mix.

2.7.5 The antifungals' effect on the hydrophobicity of the cells and abiotic surfaces

2.7.5.1 Contact angle and wetting properties

Wettability studies usually involve the measurement of contact angles as the primary data, which indicates the degree of wetting when a solid and liquid interact. Small contact angles (<90°) correspond to high wettability, while large contact angles (>90°) correspond to low wettability (Yuan and Lee, 2013) (figure 2.6).

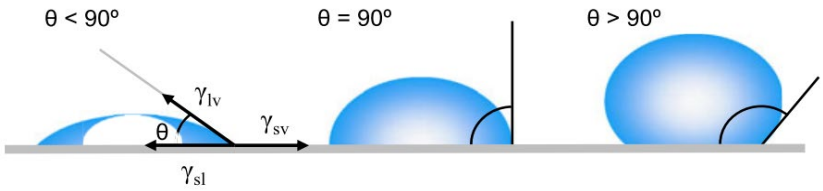

Figure 2.6 Diagram of contact angles formed by sessile liquid drops on a smooth homogeneous solid surface (Yuan and Lee, 2013)

As first described by Thomas Young in 1805, the contact angle of a liquid drop on an ideal solid surface is defined by the mechanical equilibrium of the drop under the action of three interfacial tensions (Young, 1805):

$$\gamma_{lv} \cos \theta_Y = \gamma_{sv} - \gamma_{sl} \qquad \textbf{Equation 3}$$

where γ_{lv}, γ_{sv}, and γ_{sl} represent the liquid-vapor, solid-vapor, and solid-liquid interfacial tensions, respectively, and θ_Y is the contact angle (1) is usually referred to as Young's equation, and θ_Y is Young's contact angle (Yuan and Lee, 2013).

Roughly speaking, a wetted solid is referred to as hydrophilic and a non-wetted solid is called hydrophobic. Surfaces with contact angles lower than 10° are referred to as superhydrophilic and surfaces higher than 150° are referred to as superhydrophobic. The WCA is a method of presenting the energy of a surface and is also affected by the cleanness or roughness of the surface (Grunér et al., 2012).

WCA measurements were studied where a 6 µL drop of MQ water (Millipore) was put on the surface of choice (Silicone, UPVC, PTFE, HDPE, Glass, Nylon 6 and Acrylic), which were coated with the agents (triclosan, AMB, tyrosol and farnesol). Untreated surfaces

were used as the controls. Three water contact angles were measured per coating at room temperature via the sessile- drop method using a FTA 100 optical contact meter (5 µL water droplet). The average contact angle was calculated for each surface. The reported WCA values were determined as the average of three measurements.

2.7.5.2 Transmission flow-cell preparation

Flow-cell device (figures 2.7 and 2.8) was purchased (table 2.1) and used to mimic the initial features of in vivo environment. Stirilization and preparation were performed based on the method applied in the lab for the first time. Ethanol sterilisation at the rubber insertion points was used to prevent unwanted contamination. A peristaltic pump was added to pump the ethenol through at a velocity of 0.3 mL/min. The intended surfaces (PTFE and UPVC surfaces) were cut to the standard microscope slide size (75 mm × 25 mm) and placed in the chamber spots of the flow-cell device. The device was put in the incubator at 37°C. For equilibration the PDB medium was flowing through the device for 4 hr. The conidia suspension was then inserted to the device. Subsequently, the flowing was stopped for 4 hr, which is a sufficient time for conidia to attach to the different surfaces applied in this study. The agents at their MIC_{50} levels were added to the feeding bottles containing PDB medium and the medium was passed through the flow-cell device at a rate of 150 µL/min for 48 hr, which was calculated as the effective process time.

Upon completion of the desired time of treatment, the flow-cells were washed with 0.9% saline solution and stained using cv (%0.5 w/v). Images from the biofilms were taken by the optical microscopy.

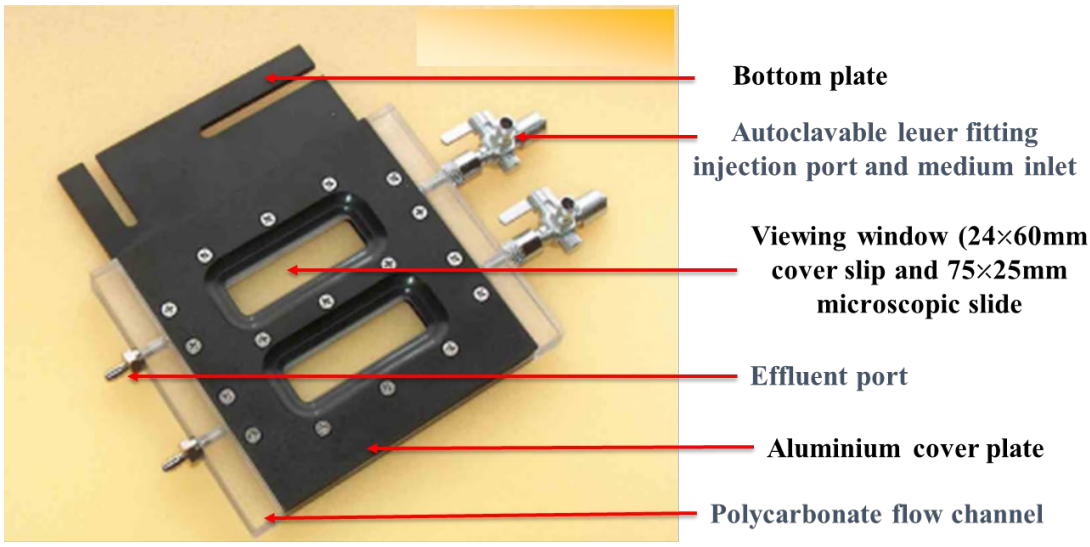

Figure 2.7 FC 281-PC transmission flow-cell

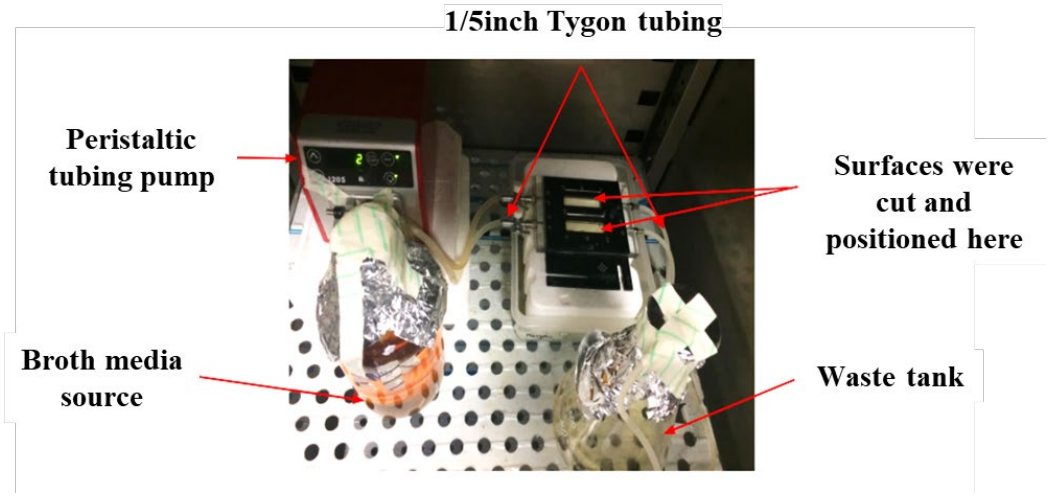

Figure 2.8 Flow-cell device to mimic the initial features of in vivo environment

2.7.5.3 Determination of hydrophobicity by using microbial adhesion to hydrocarbons (MATH) assay

The microbial adhesion to hydrocarbons (MATH) assay (Das and Kapoor, 2004) was used to characterize microbial cell hydrophobicity. The MATH assay involves spectrophotometric absorbance measurements of the initial and final cell concentrations in an aqueous cell suspension that has been contacted with a hydrocarbon liquid, hexadecane. Conidia of 14-day cultures were taken from PDA plates. Treated and untreated control isolates were washed with saline solution (0.9% w/v). Then, saline solution aliquots (3 mL) contains conidia were dispensed individually into acid-washed glass tubes (12 mm ×

75 mm) and covered with 300 µL hexadecane. The tubes were vortexed for at least three periods of 30 sec. After standing for 15 min at room temperature (figure 2.9) the hexadecane phases were carefully removed and discarded. The tubes were cooled to 5°C and any residual solidified hexadecane were removed. The tubes were then returned to room temperature and absorbance of the resulting conidial suspension was determined at 470 nm. PBS was used as a negative control, and *A. fumigatus* untreated strain was used as a positive control. The hydrophobic index was calculated using the equation:

$(A_{470}$ of control) - (A_{470} of hexadecane treated sample)/A_{470} of control **Equation 4**

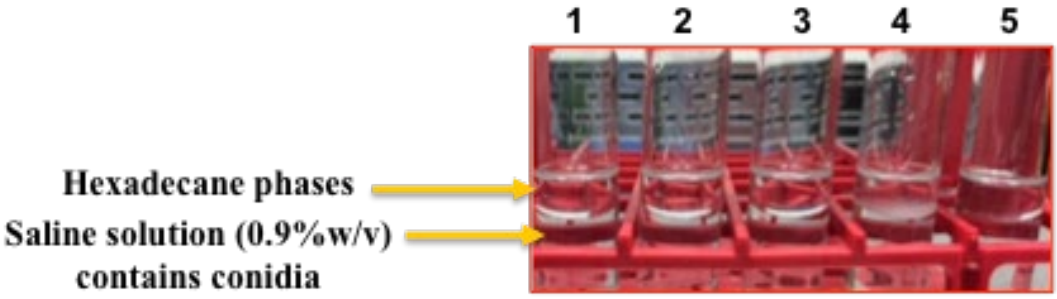

Figure 2.9 Tubes used for MATH assays of conidia of *A. fumigatus*. Tubes 2–5 contain conidia of a 14-day culture isolate were treated with the effective doses of triclosan, AMB, farnesol and tyrosol, respectively (tube 1 is untreated control test) and then, MATH assay was performed. In this assay, entities with Hydrophobic Index or HI>0.7 are considered hydrophobic (HI= no. cells in organic phase/total no. cells)

2.7.5.4 Extraction of proteins from *A. fumigatus* mycelia for the protein assay

Mycelia were prepared from (1) colonies grown under treatment with the agents' MICs on PDA plates and (2) untreated colonies grown on PDA made with the agents' MICs, as follows:

A single colony was removed from the agar with a scalpel, freed from traces of agar, suspended in 1 mL of distilled water in an Eppendorf tube and fragmented by pipetting. CsCl (1 g) was added and followed with centrifugation at 20,000 xg for 10 min. Then, the bulk of the mycelium was removed from the surface of the CsCl solution, leaving behind the agar at the bottom and a few mycelial stands dispersed in the solution. After washing twice with DI water in an Eppendorf tube, the mycelia were freeze-dried for a minimum of 12 hr and stored at −20°C. One colony yielded approximately 15 mg of dry mycelia. Freeze-dried mycelia were powdered using pre-cooled pestle and mortar (Al-Samarrai and

Schmid 2000). To extract proteins from the mycelia, trichloroacetic acid (TCA) precipitation method was used (Li et al., 2018). Accordingly, the fine poweder was hemogenized by using extraction buffer (table 2.7) and centrifuged at 20000 xg for 20 min at 4°C. The liquid phase were collected and precipitated with four volumes of 20% TCA for 20 min at −20°C and followed with centrifugation at 20,000 xg for 20 min at 4°C. The precipitate was collected and suspended in 80% acetone. Then, centrifuged at 20000 xg for 20 min at 4°C. These suspending and centrifuging steps were repeated for seven times. The final protein extracts were stored at -80°C. The total protein amount calculated using Bradford reagent (section 2.7.3.4).

2.7.5.5 Extraction of proteins from *A. fumigatus* conidia surface for the protein and SDS-PAGE assays

Using the prepared samples as described in section 2.7.1, total proteins from the fungal conidial surface were extracted. Inocula from treated and untreated control test groups were incubated with 200 µL of 0.5 M NaCl solution for 2 hr at room temperature at a ratio of 2×10^9 conidia/mL. The supernatant was collected by centrifugation at 17,000 xg for 5 min, lyophilized, and re-suspended in 50 µL of buffer (0.1 M Tris -HCl, pH 8.8, using 8 M urea) (Bom et al., 2015).

Acetone precipitation of proteins. Protein samples were placed in acetone-compatible tube and four times the sample volume of cold (-20°C) acetone added to the tube. Then, the tubes were vortexed and incubated for 60 min at -20°C. After centrifuging for 10 min at 13,000-15,000 xg, the supernatant disposed decently and properly. The acetone was allowed to evaporate from the uncapped tube at room temperature for 30 min. Care was taken to avoid the pellet getting over-dried. PBS (100 µL) was added and vortexed thoroughly to dissolve protein pellet. The samples (25 µL) were mixed with 25 µL of 2x concentrated sample buffer in an Eppendorf tube and placed in a rack in the boiling water bath for 2-3 min. The samples then were subjected to SDS-PAGE

2.7.5.6 Sodium dodecyl sulphate polyacrylamide gel electrophoresis (SDS-PAGE)

Preparing gels for electrophoresis. The Polyacrylamide gel was used to separate the protein molecules based on size as first described by Laemmli (1970). The gel comprises a resolving gel and a stacking gel. The resolving gel was poured into the apparatus first (up to around 3 cm from the top of the glass plate). The resolving gel was allowed to

polymerise and then the stacking gel was poured on top. Referring to the table 2.7 the buffers for the resolving gel and the buffers for the stacking gel were prepared. Polyacrylamide gel was used as a support medium and SDS was used to denature the proteins. An appropriate volume of APS and TEMED, as shown in table 2.7, were added to the resolving/stacking gel mixture at the last**.** Considering the comb thickness (gel thickness) (1.0 mm) and the number of the wells (10), 44 μL of the samples were added to each well. To completely fill a gel cassette 5.6 mL of resolving gell was needed. Acording to table 2.7, 8 mL resolving, and 5 mL stocking gels were prepared; table shows the reagents volumes, which were used to prepare 10 mL of monomer solution per gel. Light (4% v/v) and heavy (20% v/v) acrylamide solutions of resolving gels were also prepared to make a gradient gel.

Table 2.7 Reagents to prepare resolving (in different polyacrylamide percents needed) and stacking gels for SDS-PAGE assay (enough for one gel preparation)

Reagent	Stacking gel (4%)	Resolving gel		
		4%	12%	20%
30% Acrylamide stock	0.67 mL	1.07 mL	3.2 mL	5.33 mL
Stacking gel buffer (0.5 M Tris-HCl pH 6.8)	1.25 mL	-	-	-
Resolving gel buffer (1.5 M Tris-HCl pH 8.8)	-	2 mL	2 mL	2 mL
DI water	3.0 mL	4.8 mL	2.6 mL	0.5 mL
10% w/v SDS	50 µL	80 µL	80 µL	80 µL
10% w/v ammonium persulphate (APS)	50 µL	80 µL	80 µL	80 µL
TEMED (N,N,N′,N′-Tetramethylethylenediamine)	5.0 µL	8 µL	8 µL	8 µL

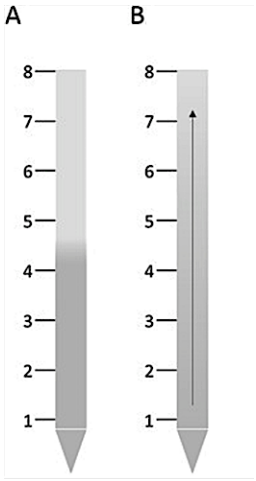

Figure 2.10 Generating separate resolving gel buffers differing in acrylamide concentration (Miller, Roman and Norstrom, 2016). Refer to the text, for more explaining

***Gradient gel preparation*.** Gels were made with a single, continuous percentage throughout the gel (single-percentage gels), and with a gradient through the gel (gradient gels). Gradient gels were used to separate samples containing a broad range of molecular weights. The larger pore size toward the top of the gel permits resolution of larger molecules, while pore sizes that decrease toward the bottom of the gel restrict excessive separation of small molecules.

Using the method described by Miller, Roman and Norstrom (2016), to easy customizable gradient gel electrophoresis, the lower concentration gel buffer was drawn into a serological pipet until a desired volume was reached (half of the resolving gel volume) (figure 2.10A). Using the same pipet, the higher acrylamide concentration was drawn up until the final gel volume was reached (figure 2.10B). When the gel solution was ejected into the casting plate sandwich, the higher acrylamide concentration was placed on the bottom followed by the lower concentration on top. This created a fixed concentration gradient with very little mixing of the phases at the interface (Miller, Roman and Norstrom, 2016).

Silver staining of the SDS-PAGE Silver staining is used for sensitive detection of proteins separated by 1D and 2D SDS PAGE with detection limits from 0.5-5 ng. Silver staining was applied based on the method reported by Mortz et al., (2001).

The SDS-PAGE gel was incubated in fixer for 1 hr. The gel was washed in H_2O for at least 30 min (Overnight washing with several changes of water will remove all acetic acid, reduce background staining and increase sensitivity. the gel got sensitized in 0.02% (w/v) sodium thiosulfate for only 1min (Longer time will decrease peptide recovery from the gel). The gel was washed in H_2O for 3x 20 sec and then, incubated for 20 min in 4 ºC cold 0.1% (w/v) silver nitrate solution (Staining is enhanced with cold $AgNO_3$). The gel was washed in H_2O for 3x 20 sec and placed in a new staining tray (Residual $AgNO_3$ on the gel surface and staining tray will increase background staining). The gel was washed in H_2O for 1 min and developed in 3% sodium carbonate, 0.05% (v/v) formaldehyde. The developer solution was changed immediately when it turns yellow. The gel was washed in H_2O for 20 sec. The staining was terminated in 5% (v/v) acetic acid for 5 min. The gel was left at 4 ºC in 1% (v/v) acetic for storage. Prior to analysis the gel was washed in water for 3x 10 min to ensure complete removal of acetic acid (Mortz et al., 2001).

2.7.6 Statistical ananlysis

The SPSS software was used for paired sample T-Test calculation (in all the graphs the samples were compared with their control groups, except for figure 3.33) showing data sets that were deemed not significantly different (N.S; > 0.05) and data sets that were significant at different levels: *$P \leq 0.05$, **$P \leq 0.01$, ***$P \leq 0.001$ and ****$P \leq 0.0001$. Standard error of the mean (SEM) bars are related to three independent repeats for each test.

Chapter 3

Results

Introduction to results; sections 3.1, 3.2, and 3.3

The results of this work are divided into three distinct sections (3.1, 3.2, and 3.3), and they are discussed separately in the relevant section.

Section 3.1 One of the main aims of this study is to investigate the antifungal activities of triclosan, furanone, AMB, tyrosol and farnesol against *A. fumigatus*. The antifungal activities could be inhibition/destruction of any phases involved in biofilm formation. These activities include a) inhibition of biofilm formation by affecting the conidial attachment to, or conidial accumulation on the substrates or b) interrupting the pre-formed biofilm structures by effecting the early or mature biofilm structure. First, the effects of growth conditions, in liquid (dynamic) and on agar (static) media are presented on growth of *A. fumigatus*. The *A. fumigatus* growth curve is provided for a period of 48 hr. Resazurin-based viability assay was applied to determine the agents' potential MICs and effective times of their action. Then, antifungal effects of the agents were studied by analysing their effects on the *A. fumigatus* growth profile. Next, *A. fumigatus* biofilm following treatment with the agents was studied. Biofilm biomass, indirectly (cv stain) and directly (through weighting the biomass), and proteins and carbohydrate concentrations in EPS were determined in liquid medium. The DNA and RNA quantities in the mature biofilm structure were studied as well. Then, the agents' effect on *A. fumigatus* conidia was assessed. The viability of agents-treated fungal conidia was studied using PI staining and flow cytometry. Subsequently, the agents' effect on the *A. fumigatus* cell wall was investigated. To study the cell wall chitin content of the treated fungus, morphological alterations after treatment with the agents were investigated using CFW, which stains the chitin content in *A. fumigatus* cell wall. HPLC analysis was carried out to find the effects of the agents on the fungus glucose uptake from the culture.

Section 3.2 Triclosan and AMB combined effect against *A. fumigatus* was studied and is presented and discussed in this section. Other researchers have already determined triclosan antimicrobial effects against yeasts and dimorphic fungi, but no such investigation was attempted on *A. fumigatus.* In this study, first, the effect of triclosan on growth and morphology of *A. fumigatus* on solid and in liquid media was studied. Next, triclosan activity against germinated *A. fumigatus* conidia was investigated. Potential synergistic activity, using synergy checkerboard assay and CompuSyn software, was assayed on combination treatment with triclosan and AMB. Susceptibility testing using

discs on agar plates was used to confirm their effect (when they were added in single or in simultaneous combination treatment) on the fungus growth. Finally, the fungus morphological changes and biofilm thickness were observed using FUN-1- based confocal microscopy. Finally, RT-PCR was carried out to investigate the genes coding for α(1, 3)-glucan and GAG in the fungus cell wall before and after treatment with triclosan and AMB.

Section 3.3 A different approach for control of biofilm formation is based on treatment of surfaces prone to microbial attachment. This section is devoted to the results and discussion of this strategy. Common solid surfaces (Glass, acrylic, HDPE, Nylon 6, PTFE, silicone and UPVC) used in indwelling devices and medical utensils were exposed to the agents. The aim of this study was to determine strategies to control biofilm formation on these surfaces. For that, hydrophobicity of the solid surfaces and of the conidial surfaces following coating and treatment with the agents were analysed using contact angle assay and MATH assay, respectively. Also, *A. fumigatus* biofilm formed on some of these surfaces in transmission "flow-cell" device analysed by using optical microscopy. The conidial surface total protein concentration after treatment with the agents was quantified and SDS-PAGE was run to study *rodA* expression in the treated and untreated control samples.

3.1 Antifungal activity of triclosan, furanone, AMB, tyrosol and farnesol against *A. fumigatus* through diminishing biofilm formation

3.1.1 Introduction

A. fumigatus resistance to environmental alterations within biofilms is tightly regulated. *A. fumigatus* biofilm has a heterogeneous architecture, in terms of distribution of fungal cells and extracellular polymeric substances (EPS). Germination of conidia (12-24 hr) happens before biofilm formation stage. *A. fumigatus* biofilm formation on biotic and abiotic substrates develops through early (24-48 hr) and maturation (48-72 hr) phases (figure 3.1). During early to intermediate phases of biofilm development, efflux pumps are formed and EPS material are produced towards fungi maturity stage (Ramage et al., 2011). Different fungal factors including cell wall components and secondary metabolites contribute to the biofilm formation (Kaur and Singh, 2013).

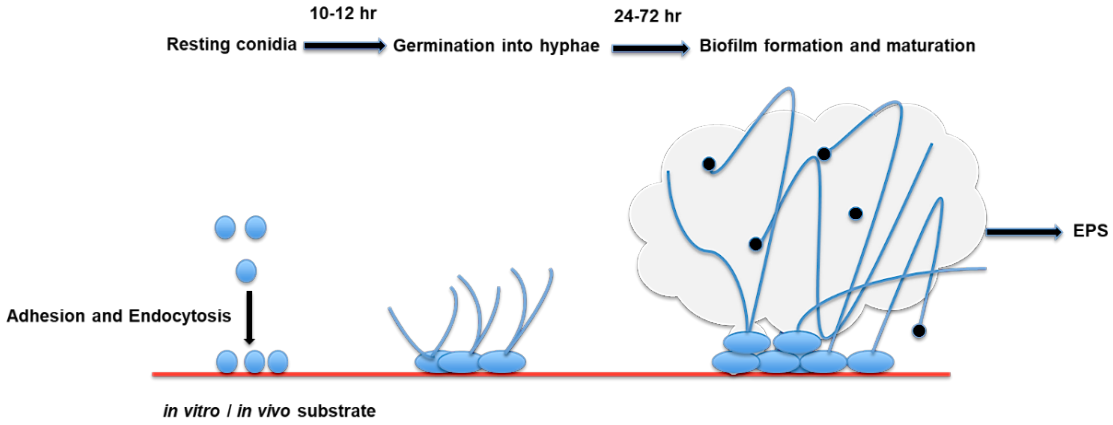

Figure 3.1 Different phases of *A. fumigatus* biofilm formation

Using resazurin-based viability assay triclosan, furanone, AMB (Amphotericin B loaded liposomes, AmB-LLs), tyrosol and farnesol MICs against *A. fumigatus* have been calculated from the provided doses range (table 3.1).

Table 3.1 Agents applied in this study with their doses to determine their MICs

Agents	Doses range (mg/L)
Triclosan	0.5 to 32
Furanone	0.6 to 20
AMB (Trade name: Fungizone) *	0. 125 to 8
Tyrosol	125 to 4000
Farnesol	0.75 to 24

* Amphotericin B contains 250 µg of amphotericin B and 205 µg of sodium deoxycholate per mL of distilled water

3.1.2 Results

3.1.2.1 *A. fumigatus* growth under dynamic and static conditions

In filamentous fungi, biofilm mycelia are distributed in a way, which form surface and inner channels. This is in stark contrast to fungal pellets, which are composed of a compactly packed deep mycelium and highly intertwined hyphae (Mowat et al., 2009). In this study, tissue culture flasks and Petri dishes were used to investigate *A. fumigatus* biofilm formation (figure 3.2).

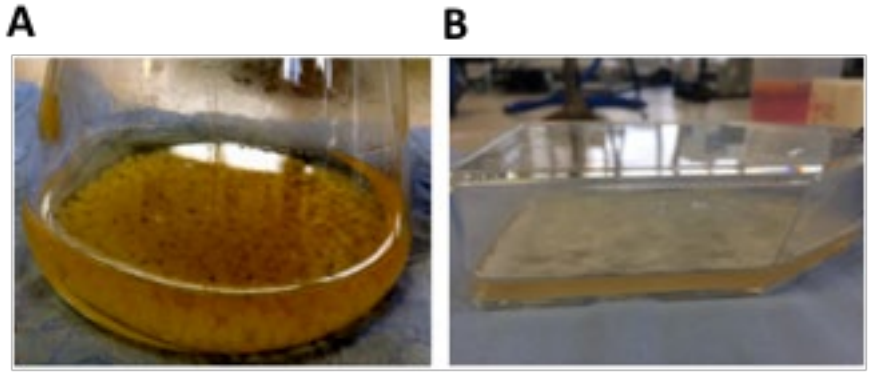

Figure 3.2 *A. fumigatus* growing in PDB medium for 48 hr under dynamic (left, pellets are formed) and static (right, biofilm is formed) conditions in conical and t175 tissue culture flasks, respectively

3.1.2.2 *A. fumigatus* development stages

Figure 3.3 shows *A. fumigatus* development stages at different time points, 12-, 24-, 36-, and 48-hr of incubation. For that, the fungus dormant conidia (100 µL), taking from PDB medium after 4 hr of cultivation, was inoculated on PDA plates and incubated at 37°C.

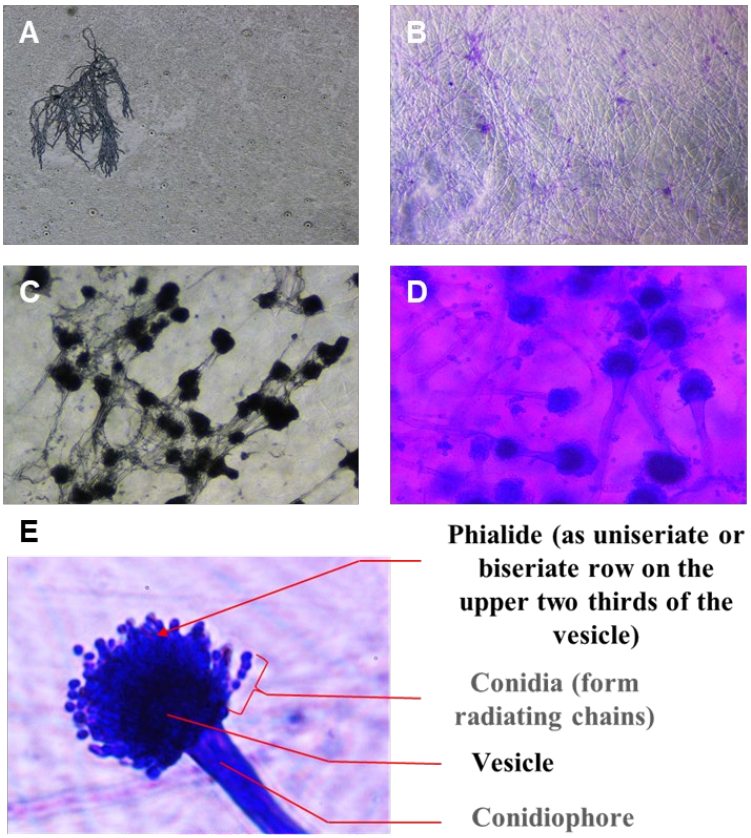

Figure 3.3 different developmental stages of *A. fumigatus* were collected at the following time points: (A) 12 hr (vegetative hyphae), 100X; (B) 24 hr, 100X (competent hyphae); (C) 36 hr (early conidiophores) 400X. and (D) 48 hr (mature conidiophores and spores 400X. (E) *A. fumigatus* mature conidiophore structure 1000X

Competent hyphae, which has been mentioned in figure 3.3, is morphologically indistinguishable from pre-competent hyphae. Competent hypha is a form in the growth cycle from conidia to fully hyphal state. Many recognised virulence factors including genes encoding mycotoxins and proteases are up-regulated in response to the onset of developmental competence and some of the genes expressed by competent hyphae control the production of conidiophores (Gravelat et al., 2008).

3.1.2.3 *A. fumigatus* growth in PDB and RPMI-1640 media

It has been reported that *Aspergillus* spp have a poor growth in RPMI-1640 (Meletiadis et al., 2001). However, it is used for viability studies. RPMI-1640 was used in this work to investigate its potential compared to PDB for growth of *A. fumigatus*.

To assay the effect of growth medium on protein production by the fungus, the conidia were inoculated in RPMI-1640 (the medium was prepared according to the manufacturer's

instructions and buffered to pH 7.0 with 0.165 M morpholino propane sulfonic acid (MOPS)) and PDB medium at 37°C for 48 hr. Based on the standard curve for the protein assay (appendix 2, figure 1A), the protein quantities were higher for the fungus growing in either PDB or RPMI-1640 medium than the control medium with no fungus inoculation (figure 3.4). Also, the growth was better in PDB than in RPMI-1640 medium.

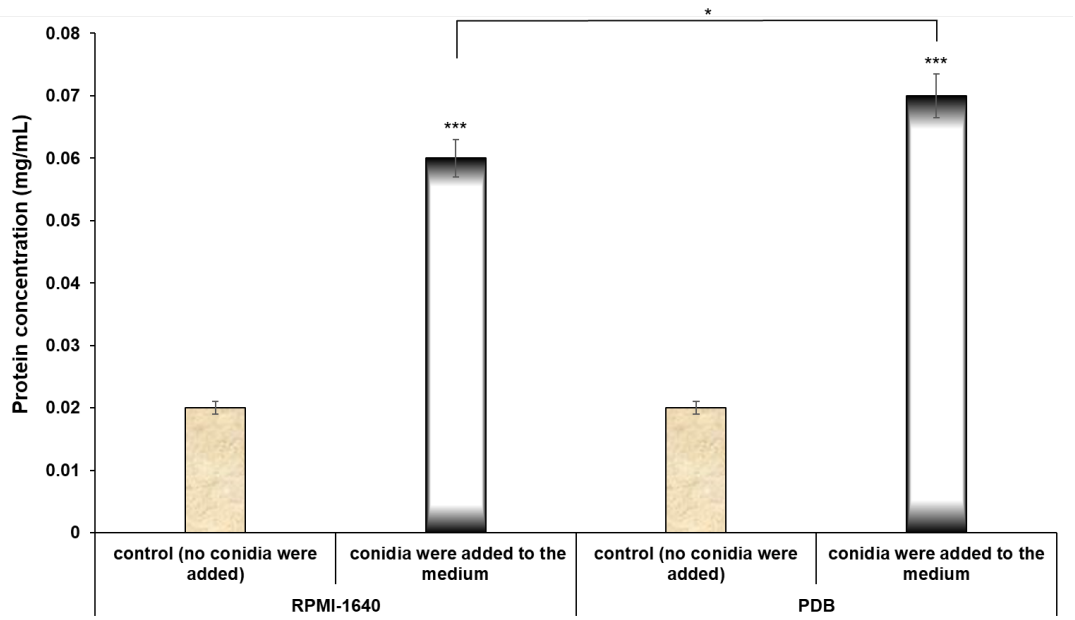

Figure 3.4 Comparison of *A. fumigatus* growing in RPMI-1640 and PDB media in case of its total protein quantity after 48 hr of incubation at 37 ˚C. They were compared with their controls (no conidia were added). ***P ≤ 0.001 (SEM bars are shown for n = 3)

Based on the presented results, the total protein of *A. fumigatus* cultivated in RPMI-1640 after 48 hr of incubation (mature biofilm formation stage) was less than that in PDB, while the difference was not significance.

Figure 3.5 shows the growth curve of *A. fumigatus* when it was grown in RPMI-1640. The following phases in the growth of the fungus were distinguished: Lag phase: the first phase in which no changes in OD were measured. During this phase germination of spores and conidia happened followed by elongation of hyphae to a maximal length. First transition period: further elongation of hyphae was detected spectrophotometrically and resulted in a rapid increase in OD. Log phase: the growth curve reached the maximal slope. OD values increased linearly over time and the growth rate was constant at its highest value. Second transition period: the slope of the growth curve decreased, and the OD tended to reach a plateau. Stationary phase: no linear changes in OD were observed.

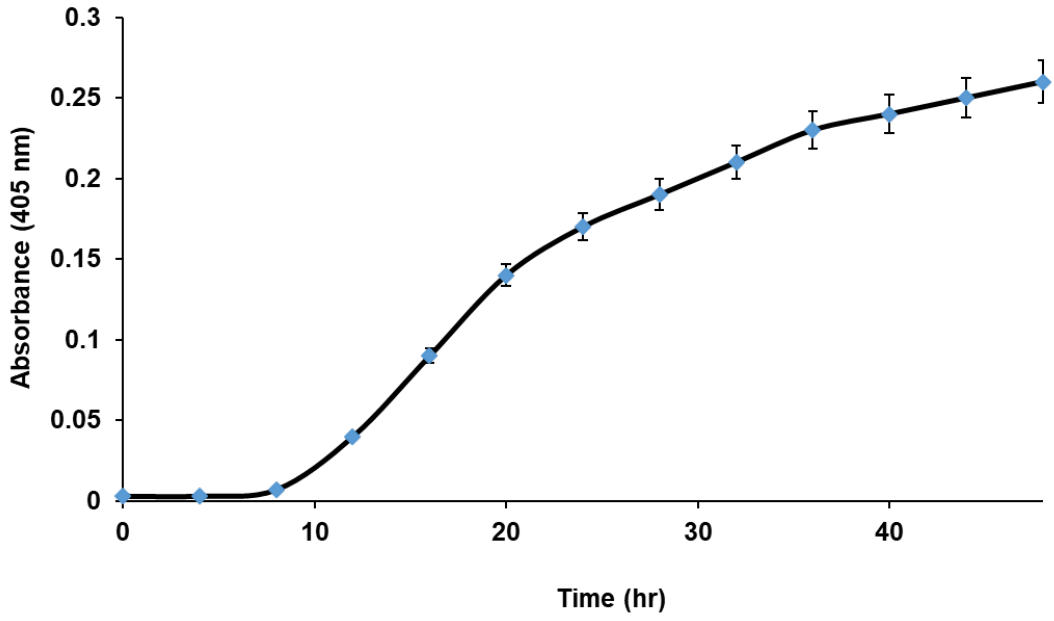

Figure 3.5 *A. fumigatus* growth curve in PDB medium (SEM bars are shown for n = 3)

3.1.2.4 Evaluation of *A. fumigatus* susceptibility against the agents

Following adhesion and germination of the fungal conidia on the 96-well plates, mature biofilms formed after 48 hr embedded in a thick EPS. In the presence of various concentrations of the antimicrobial agents (table 3.1), their inhibitory effects were determined against *A. fumigatus*. For antimicrobial susceptibility testing, the MICs should be read when the growth control is in the log phase and not in the transition periods (between lag phase and log phase or between log phase and stationary phase) (Meletiadis et al., 2001). The lowest variation was observed during the log phase of the growth curve, which was between 8 to 20hr for the control group. Thus, the optimal reading time of antifungal susceptibility testing of *A. fumigatus* was determined over this period. To assess the agents' MIC_{50s}, they were added to the culture at t_0 of incubation and the fungus viability was calculated after 18 hr of incubation at 37°C. The agents' potential effects on the early or mature biofilm were tested after 24 and 48 hr of incubation, respectively.

Based on this assay, triclosan, AMB, tyrosol and farnesol had their best effects against *A. fumigatus* when they were added at t_0 and incubated for 18 hr, except for tyrosol that its effective time was 12 hr. Furanone showed only weak activity towards *A. fumigatus* (figures 3.6 to 3.10). Figures 3.6 to 3.10 represent different doses added to the conidia at t_0, before biofilm formation and after 24 and 48 hr of incubation at 37°C when early and

mature biofilms were formed, respectively. Then, they were incubated for more 24 hr. To confirm the agents' effective time, different time points were applied.

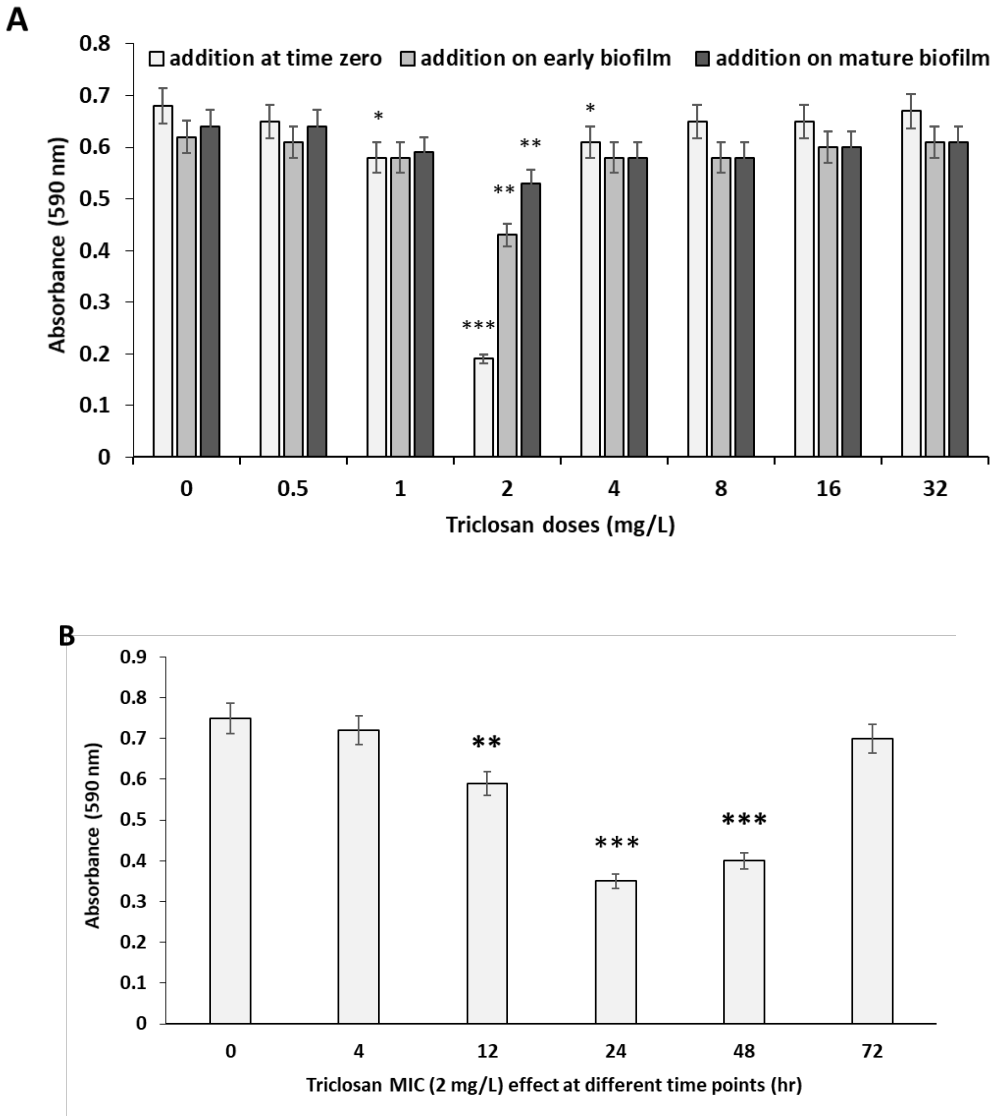

Figure 3.6 *A. fumigatus* inoculum was cultured and treated with triclosan doses in RPMI-1640 medium at 37˚C under static condition. Effective (A) dose and (B) time of triclosan against *A. fumigatus* were determined by resazurine- based viability assay. Its MIC_{50} was calculated as 2 mg/L, which inhibits the viability by ~ 70% after 18 hr of incubation. **P ≤ 0.01 and ***P ≤ 0.001 (SEM bars are shown for n = 3)

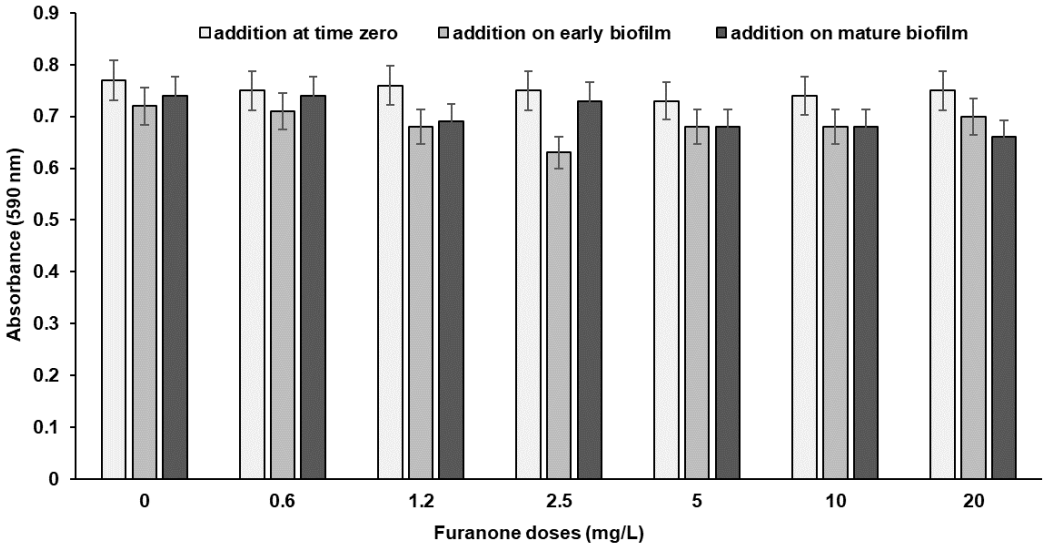

Figure 3.7 *A. fumigatus* inoculum was cultured and treated with furanone doses in RPMI-1640 medium at 37˚C under static condition. Resazurin-based viability assay of furanone against *A. fumigatus*. No effective activity against the fungus viability was observed (SEM bars are shown for n = 3)

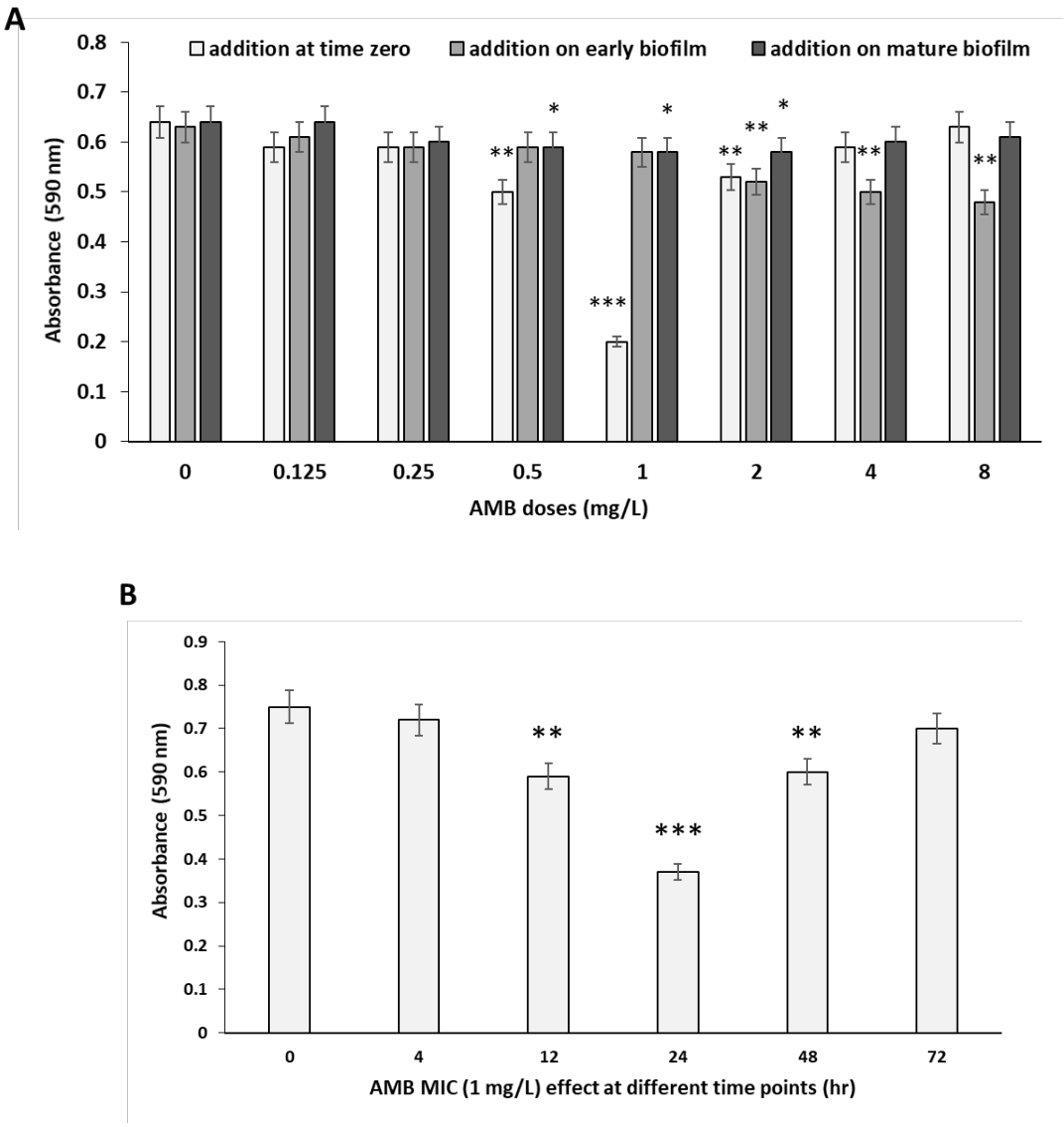

Figure 3.8 *A. fumigatus* inoculum was cultured and treated with AMB doses in RPMI-1640 medium at 37˚C under static condition. Effective (A) dose and (B) time of AMB against *A. fumigatus* were determined by resazurine- based viability assay. Its MIC_{50} was calculated as 1 mg/L, which inhibits the viability by 46% after 18 hr of incubation. *P ≤ 0.05 and **P ≤ 0.01 and ***P ≤ 0.001 (SEM bars are shown for n = 3)

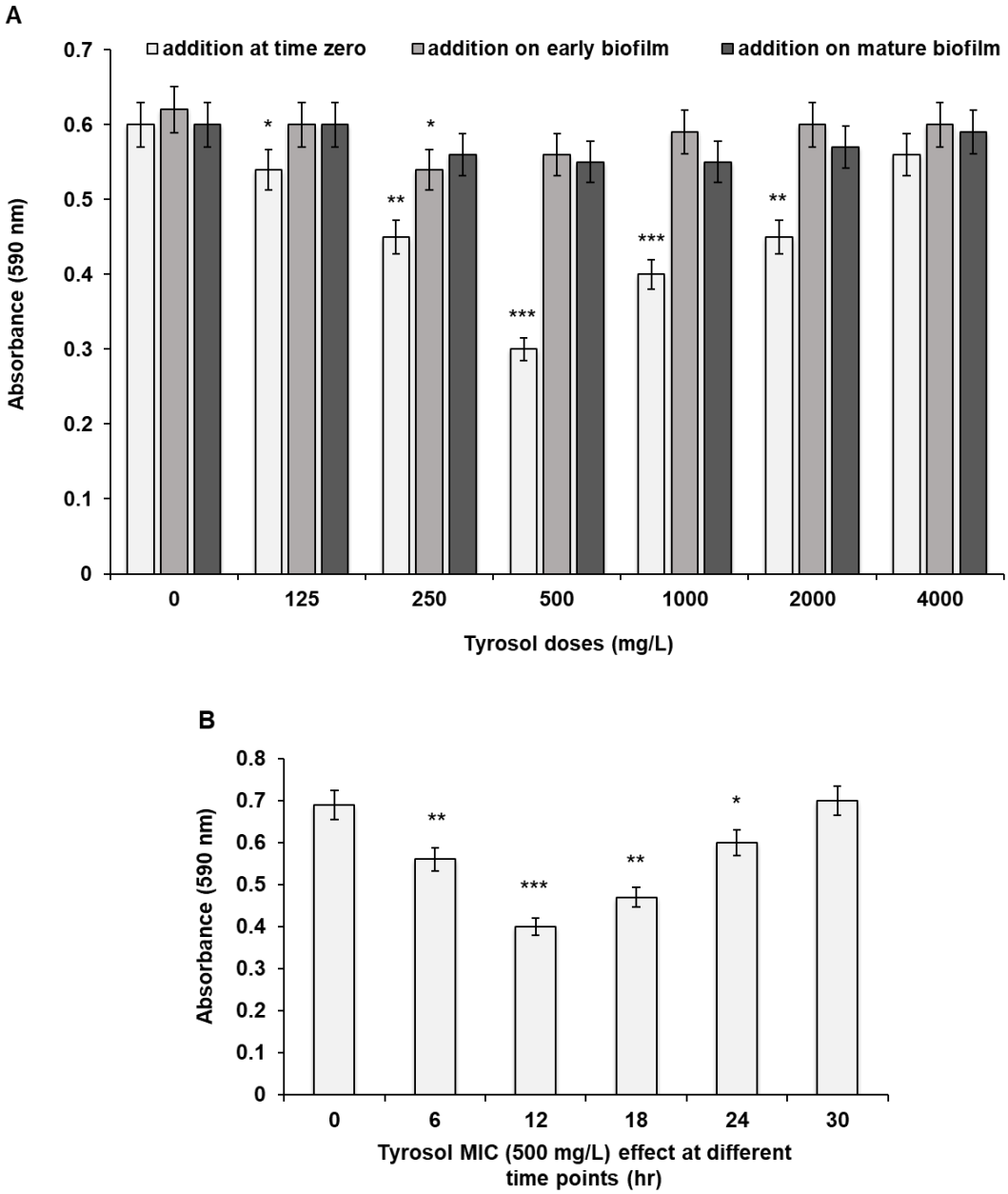

Figure 3.9 *A. fumigatus* inoculum was cultured and treated with tyrosol doses in RPMI-1640 medium at 37˚C under static condition. Effective (A) dose and (B) time of tyrosol against *A. fumigatus* were determined by resazurine- based viability assay. Its MIC_{50} was calculated as 500 mg/L, which inhibits the viability by 50% after 12 hr of incubation. *P ≤ 0.05, **P ≤ 0.01 and ***P ≤ 0.001 (SEM bars are shown for n = 3)

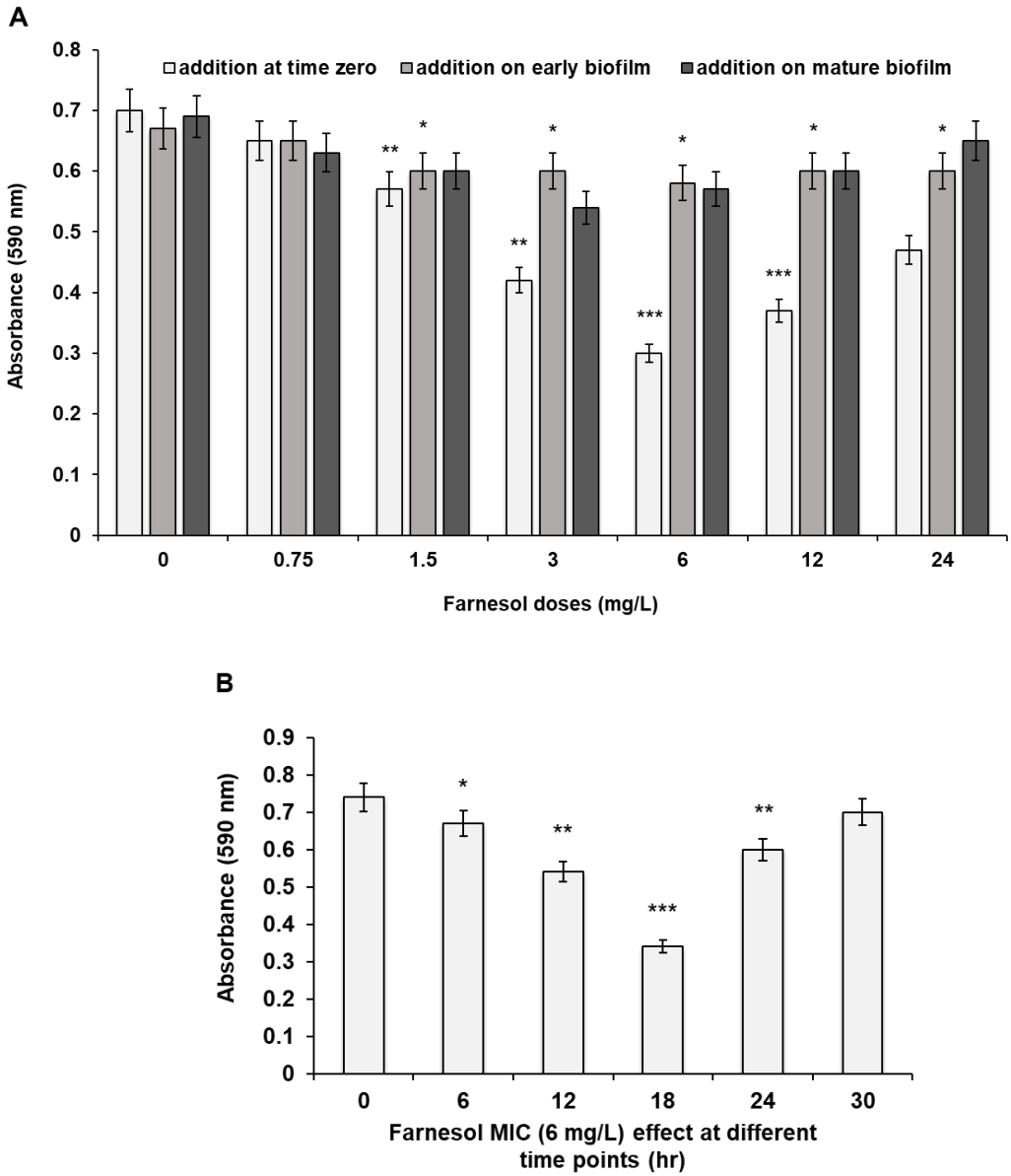

Figure 3.10 *A. fumigatus* inoculum was cultured and treated with farnesol doses in RPMI-1640 medium at 37˚C under static condition. Effective (A) dose and (B) time of farnesol against *A.fumigatus* were determined by resazurine- based viability assay. Its MIC_{50} was calculated as 6 mg/L, which inhibits the viability by 40% after 18 hr of incubation. *P ≤ 0.05, **P ≤ 0.01 and ***P ≤ 0.001 (SEM bars are shown for n = 3)

3.1.2.5 *Growth* pattern of *A. fumigatus* following treatment with the agents' MICs

A. fumigatus was treated with the agents' MIC_{50s} at t_0 in PDB medium. The growth curves (figure 3.11) were split and analysed.

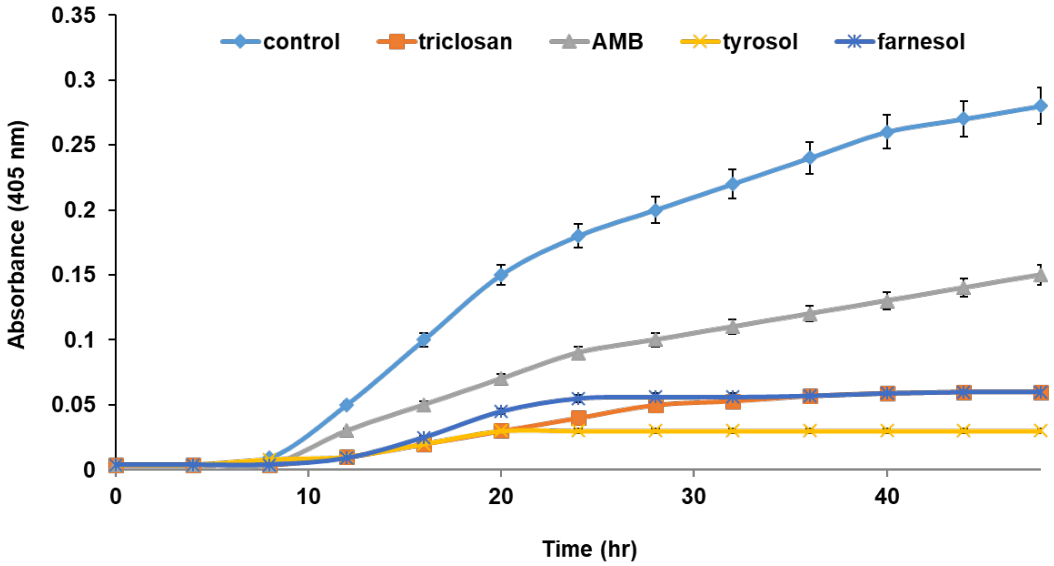

Figure 3.11 Representation of the growth curve of treated *A. fumigatus* expressed as OD (SEM bars are shown for n = 3)

3.1.2.6 Analysing the agents' effect on *A. fumigatus* static biofilm

For biofilm quantification, cv assay in microtiter plate containing PDB was applied to determine the effect of the agents on the mature biofilm (36 hr of incubation) (figure 3.12). The assay stains both live and dead cells as well as some components present in the biofilm matrix, thus it is well suited to quantify total biofilm biomass.

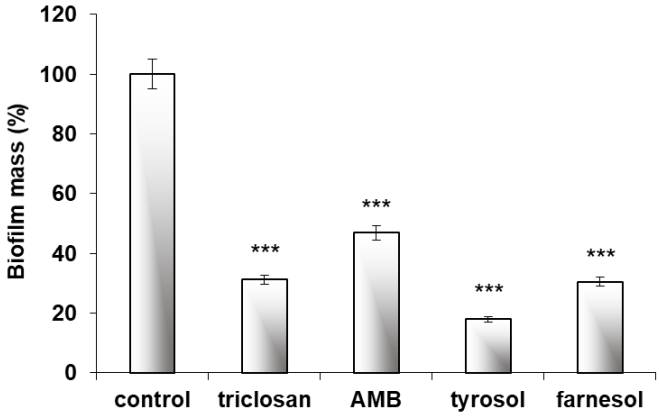

Figure 3.12 Indirect measurement of biofilm mass by adsorption/desorption of cv. The graph shows that the fungus attachment and biofilm formation were less in the agent-treated samples than the untreated (control) test group. Among the agents, tyrosol showed better anti-biofilm effect. The SPSS software was used for paired sample. ***P ≤ 0.001 (SEM bars are shown for n = 3)

3.1.2.7 Quantification of the agents' effect on the biomass of *A. fumigatus* growing in RPMI-1640

The biomass assay results are shown in figure 3.13. This experiment was repeated three times and the weight average for the negative control (control-) was 24.45 g. Control- was the autoclaved medium under the same condition as the culture but without growing the strain or treating with any of the agents. The control negative biomass was then subtracted from the biomass weights of the treated and untreated cultures. The final values represent the biofilm formed in the Petri dishes. The results were in correlation with cv assay results, except for tyrosol.

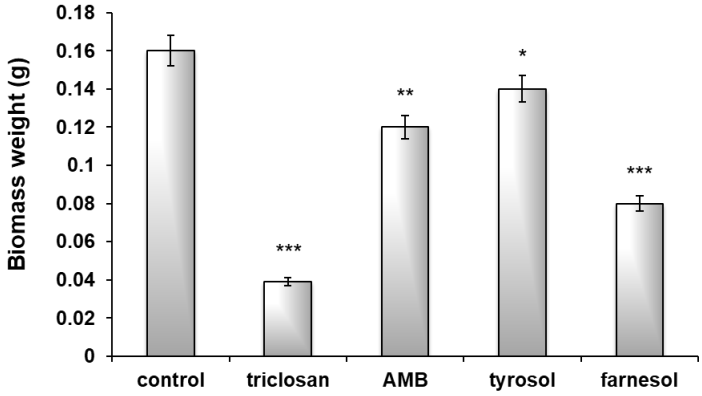

Figure 3.13 Biomass assay to study the total weight of *A. fumigatus* treated (test) and untreated (control) groups after 36 hr of incubation in RPMI-1640. The SPSS software was used for paired sample. *P ≤ 0.05, **P ≤ 0.01 and ***P ≤ 0.001 (SEM bars are shown for n = 3)

3.1.2.8 Effect of the agents on total protein concentration of *A. fumigatus* growing in liquid medium

The total protein concentration of the agents-treated and untreated control test groups grown in RPMI-1640 was determined (figure 3.14) based on the standard curve (appendix 2, figure 1B). Total protein concentrations in the treated (test) and untreated (control) samples were studied in 40 hr. The time points applied were correlated to the lag phase (4 hr), log phase (16 hr) and stationary phase (28 and 40 hr).

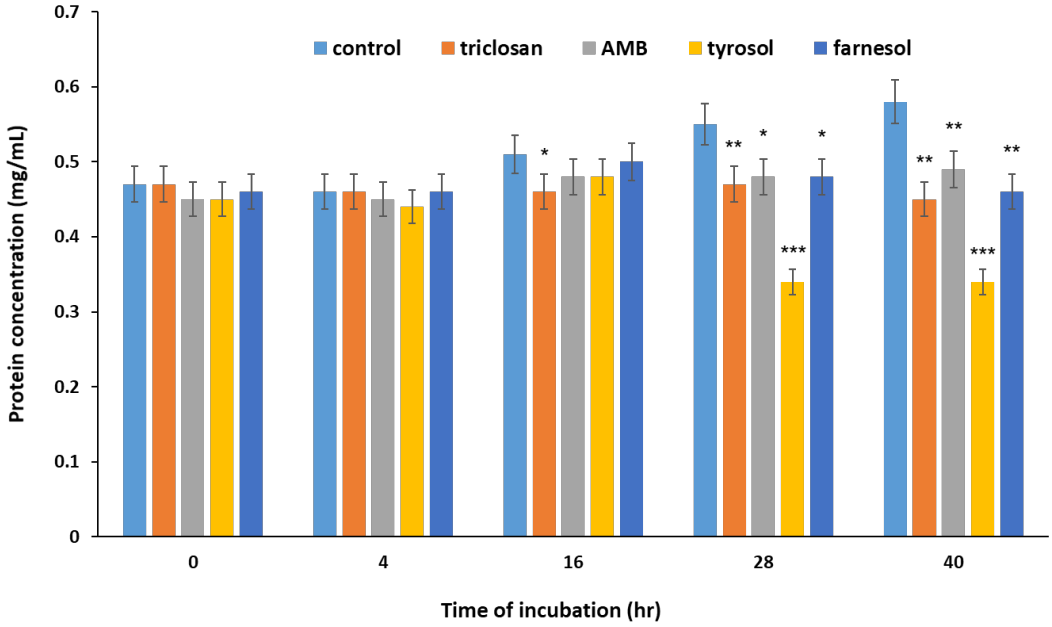

Figure 3.14 Total protein concentration *A. fumigatus* conidia in agents- treated and untreated control groups growing in RPMI-1640 medium studied at 0, 4-, 16-, 28- and 40-hr of incubation. Each treatment is compared with the control related to each time point *P ≤ 0.05, **P ≤ 0.01 and ***P ≤ 0.001 (SEM bars are shown for n = 3)

3.1.2.9 Effect of the agents on EPS-related protein quantity of *A. fumigatus* growing in PDB medium

EPS of each treated and untreated samples grown in PDB for 48 hr were extracted. Figure 3.15 shows the EPS-related protein concentrations in each sample calculated based on the standard curve (appendix 2, figure 1C).

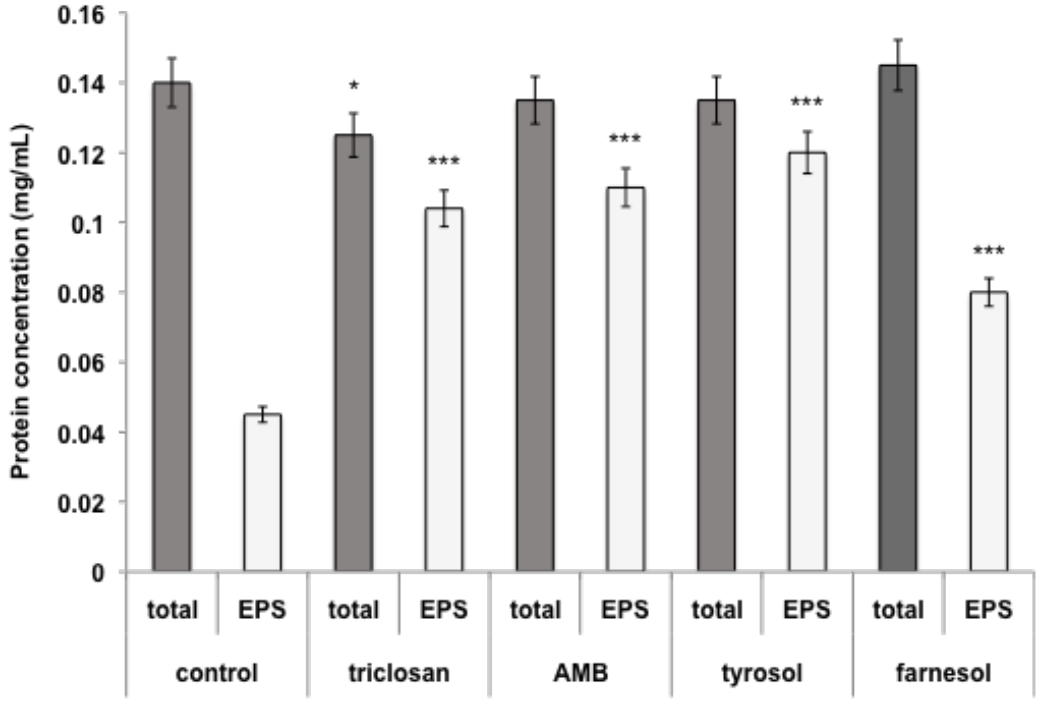

Figure 3.15 Total protein concentrations from *A. fumigatus* EPS extracts in the treated and untreated control test groups growing in PDB medium for 48 hr. ***P ≤ 0.001 (SEM bars are shown for n = 3)

3.1.2.10 Effect of the agents on EPS-related carbohydrate quantity of *A. fumigatus* growing in PDB medium

Based on the standard curve (appendix 2, figure 2), total and EPS-related carbohydrates for each of the treated and untreated control test groups were determined (figure 3.16).

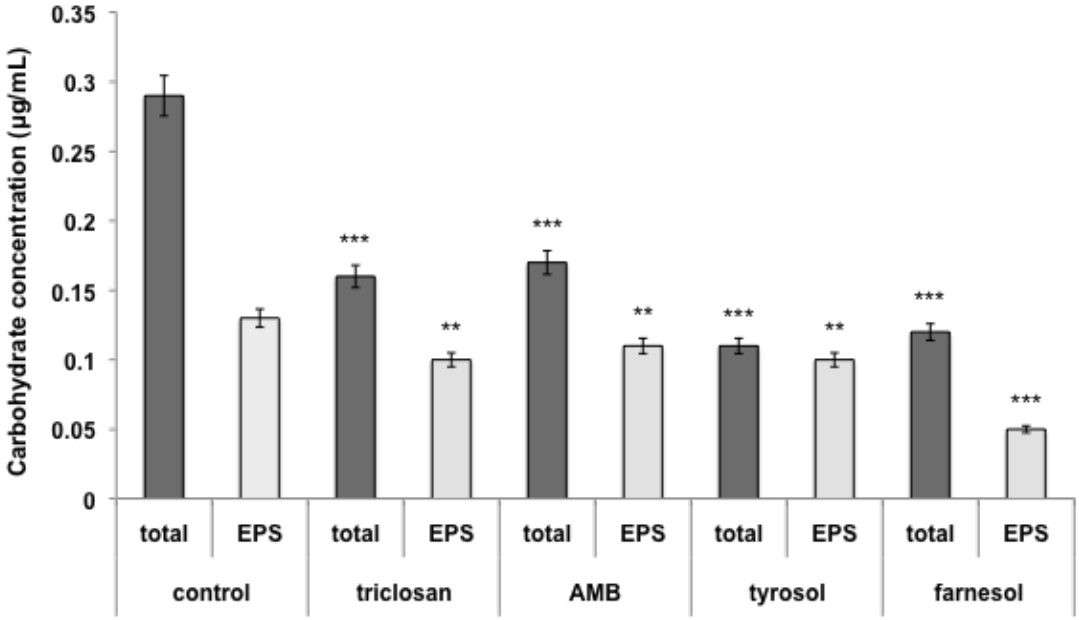

Figure 3.16 *A. fumigatus* total carbohydrate and carbohydrate related to the extracted EPS in PDB medium incubated for 48 hr. **P ≤ 0.01 and ***P ≤ 0.001 (SEM bars are shown for n = 3)

3.1.2.11 The agents' effect on the *A. fumigatus* DNA and RNA quantification

Samples were prepared as described earlier (section 2.7.3.7). Using a NanoDrop spectrophotometer, DNA and RNA quantities were analysed, respectively and are shown in figures 3.17 and 3.18. Results demonstrated that tyrosol caused release of nucleic acids leading to an increase in absorbance at 260 nm, reaching values higher than those obtained for the fungal growth control or treated with the other agents.

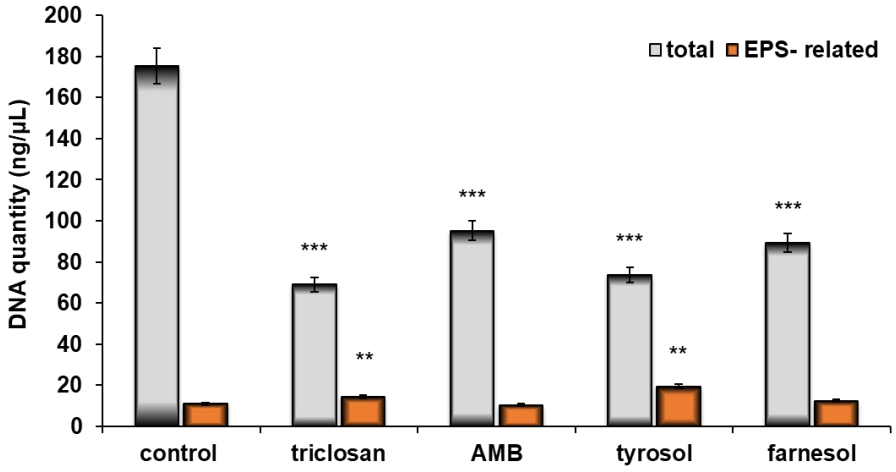

Figure 3.17 NanoDrop DNA concentration at 260 nm. Amounts are related to the total and EPS-extracted samples both from agents-treated and untreated fungus growing in PDB medium for 18 hr. ***P ≤ 0.001 (SEM bars are shown for n = 3)

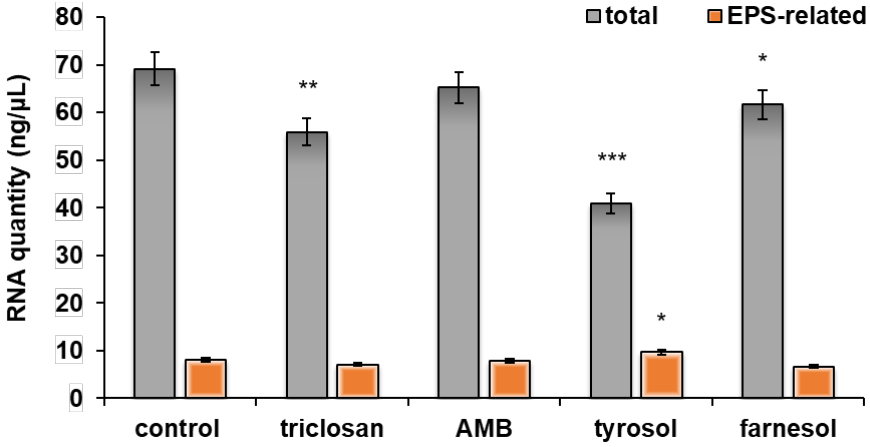

Figure 3.18 NanoDrop RNA concentration at 260 nm. Amounts are related to the total and EPS-extracted samples both from agents-treated and untreated fungus growing in PDB medium for 18 hr. *P ≤ 0.05, **P ≤ 0.01 and ***P ≤ 0.001, (SEM bars are shown for n = 3)

3.1.2.12 Agarose gel electrophoresis of *A. fumigatus* DNA after treatment with the agents and when it is in stationary phase of its growth

Agarose gel electrophoresis of DNA extracted from *A. fumigatus* treated with different agents, and, from the fungus at stationary phase of its growth was performed (figure 3.19). DNA isolated from *A. fumoigatus* grown on PDB medium in shake flask culture at 37°C, separated on a 1% (w/v) agarose gel and visualised by GelRed staining.

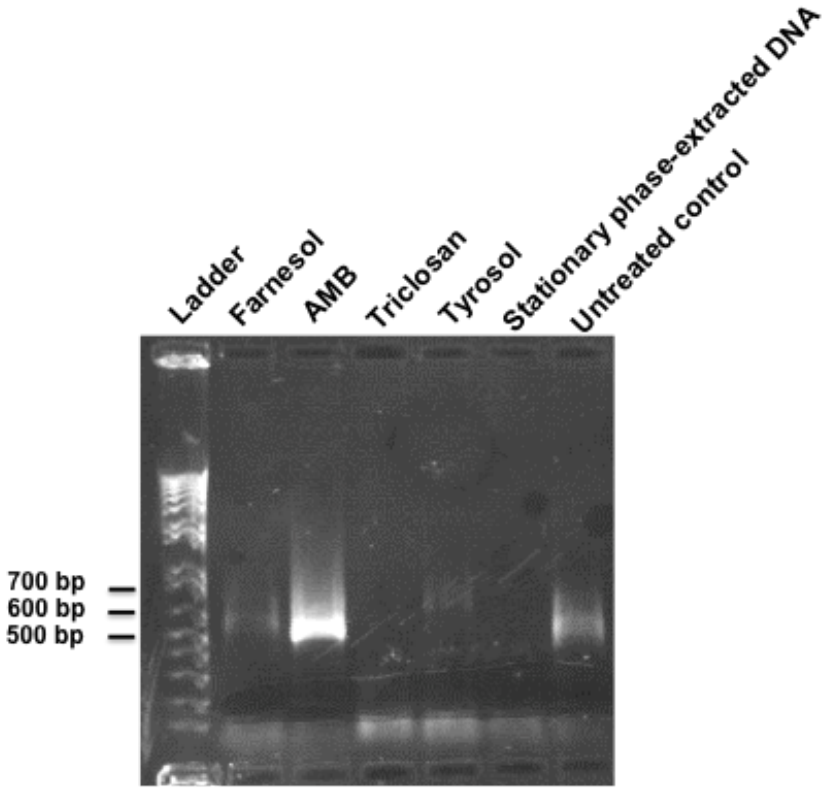

Figure 3.19 Agarose gel electrophoresis of DNA extracted from *A. fumigatus* mycelium exposed to agents. DNA smearing represents DNA fragments formation when the fungus was treated with AMB

3.1.2.13 Assessment of the agents' effect on the viability of *A. fumigatus* conidia

Flow cytometry (FCM) was used to analyse the viability of agent-treated fungal conidia (figures 3.20 to 3.22). The particles considered for the count were selected by relying on three parameters (PI staining, FSC, and SSC). It is often suggested that FSC indicates cell size whereas SSC relates to the complexity or granularity of the cell. Within scatter parameters, the pulse height *vs* pulse width plots (forward versus side scatter (FSC *vs* SSC)) are used to identify cells of interest based on size and granularity (complexity) and to isolate single cells passing through the cytometer, thereby remove any non-single cells (doublets, clumps and debris). FSC *vs* SSC can also be used to exclude debris, as they tend

to have lower forward scatter levels. They are often found at the bottom left corner of the plot (Rowley, 2012).

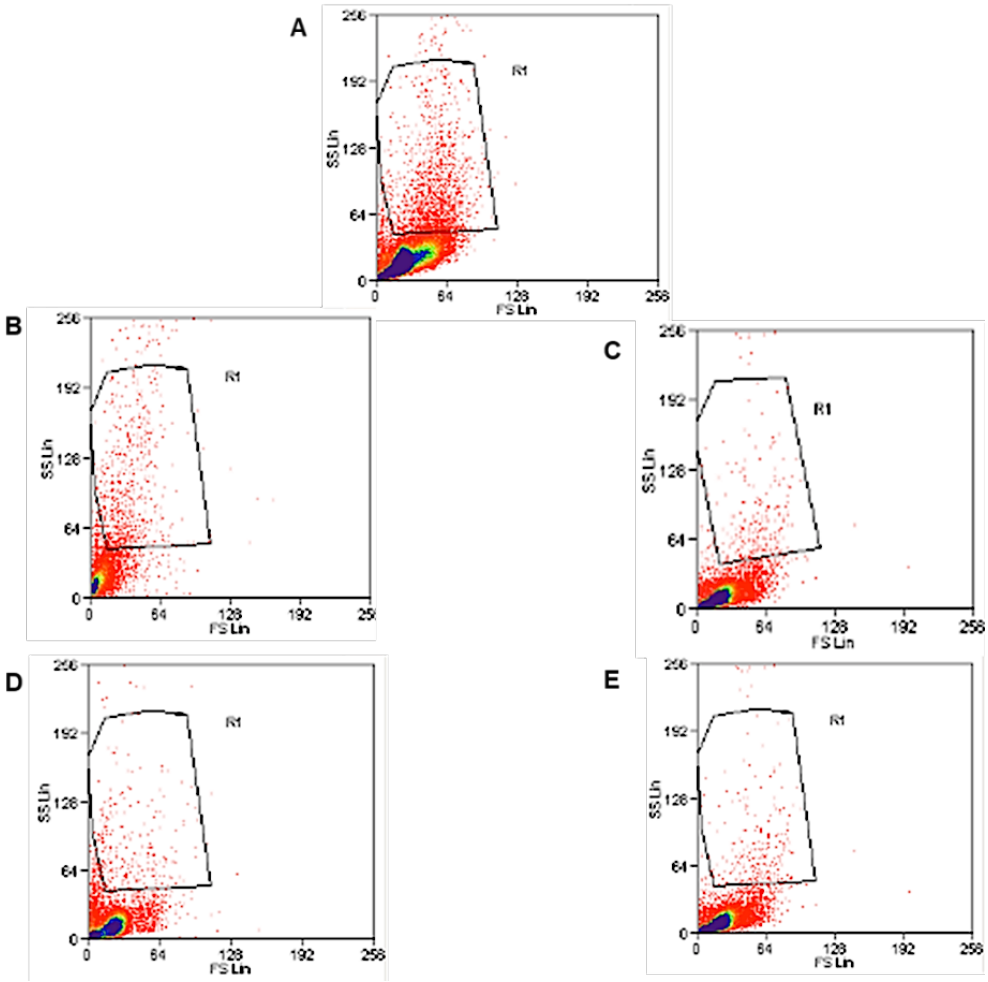

Figure 3.20 FSC vs SSC density plots. The plots show the effect of agents on the conidia cells population; PI binds by intercalating DNA and RNA, where it fluoresces red. The test groups were as follows: (A) non- treated control group, and (B) triclosan-treated, (C) AMB-treated, (D) tyrosol-treated, and (E) farnesol-treated test groups. On the x-axis, individual events go from small to large, and on the Y-axis individual events go from less complex to more complex; R1, the *A. fumigatus* single conidia cells passing through the cytometer isolated based on the cells' size and granularity

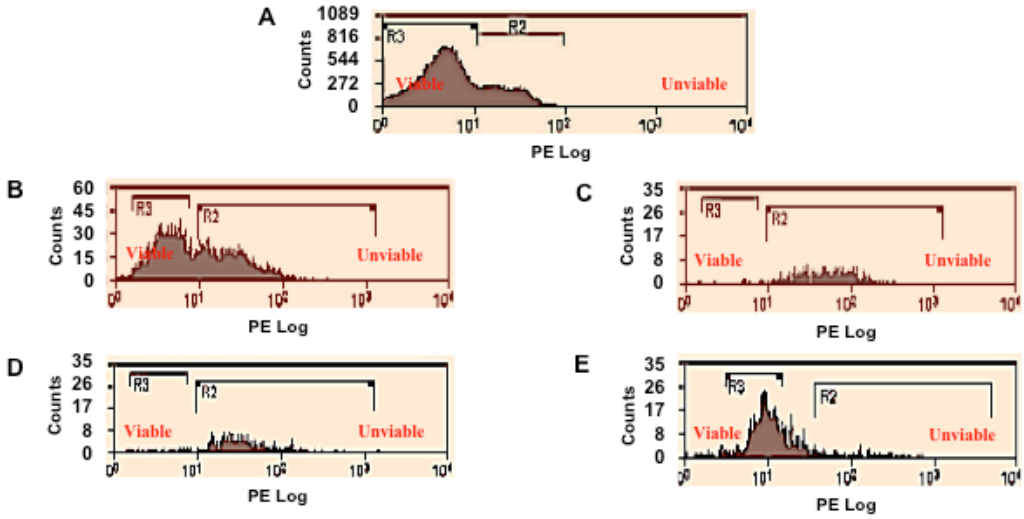

Figure 3.21 FCM measurements of antifungal effects of the agents on *A. fumigatus* after 18 hr of incubation. Histograms obtained by flow cytometric analysis of sample after PI staining. PI was used in the evaluation of cell viability and to assess DNA content in the cell cycle. The FSC frequency histogram allowed discriminating between the conidial population going through the flow chamber one by one, represented by the higher peak, and the population of coupled conidia, represented by the lower peak. The test groups were as follows: (A) non-treated control group, and (B) triclosan-treated, (C) AMB-treated, (D) tyrosol-treated, and (E) farnesol-treated test groups. Approximately 30,000 particles were analysed in each run. Counts, number of particles; R3, conidia passing singly through the flow cytometer; R2, conidia passing in pairs through the flow cytometer

Relative susceptibility to agents was measured by forward- and side-scatter characteristics of the conidial population and by mean fluorescence intensity (MFI) of the dye (figure 3.22).

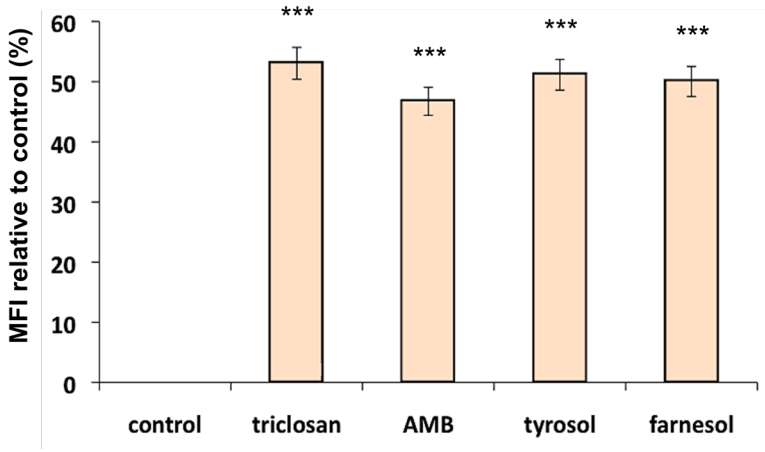

Figure 3.22 MFI of PI in the agents-treated conidia in relative to the growth control (standardised to 0% flurescent). MFI analysed in both FL-1 and FL-2 channels shows eDNA increase in agents-treated groups comparing with the untreated control group. ***P ≤ 0.001 (SEM bars are shown for n = 3)

3.1.2.14 Screening the agents' effect on the chitin of the *A. fumigatus* mycelia cell wall

For detection of chitin in the cell wall of *A. fumigatus*, CFW stain was used and the treated and untreated control test groups were observed under UV light (figure 3.23).

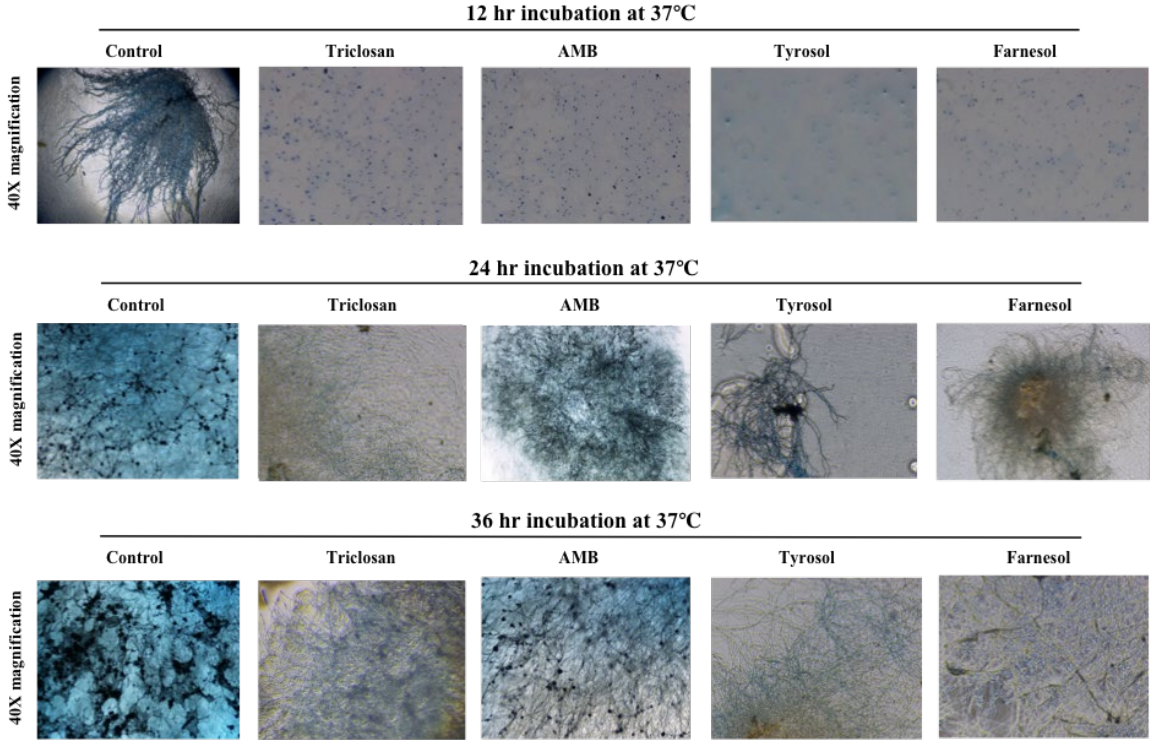

Figure 3.23 CFW staining of the *A. fumigatus* cell wall chitin. Triclosan, AMB, tyrosol and farnesol at their MIC_{50s} (section 3.1.2.4) were added to the fungus at t_0. The CFW-related morphological analysis showed that there was no growth after 12 hr of incubation in any of the treated samples while vegetative interwoven hyphae structures were formed in the untreated control group. The blue dots represent the attached conidia. In the untreated control group, the competent hyphae without EPS structure was formed after 24 hr of incubation, while the treated samples were at the vegetative hyphae formation phase. After 36 hr, the early conidiophore structure with EPS structure and hypha-hypha interactions were clearly observed in the control test group, while competent hyphae structures without hypha-hypha interactions were obvious in the treated samples

3.1.2.15 Quantification of glucose in *A. fumigatus* cultures treated with the agents

Samples of the treated (test) and untreated (control) groups were measured for constituent sugar concentrations (glucose) by the HPLC method. Samples were prepared with 1 mL of PDB culture medium, and 1 mL of the corresponding spore suspension, for final concentration of 5x 10^6 spores/mL. Sampling was performed at three time points, 4, 18 and 36 hr of incubation (figures 3.24 and 3.25).

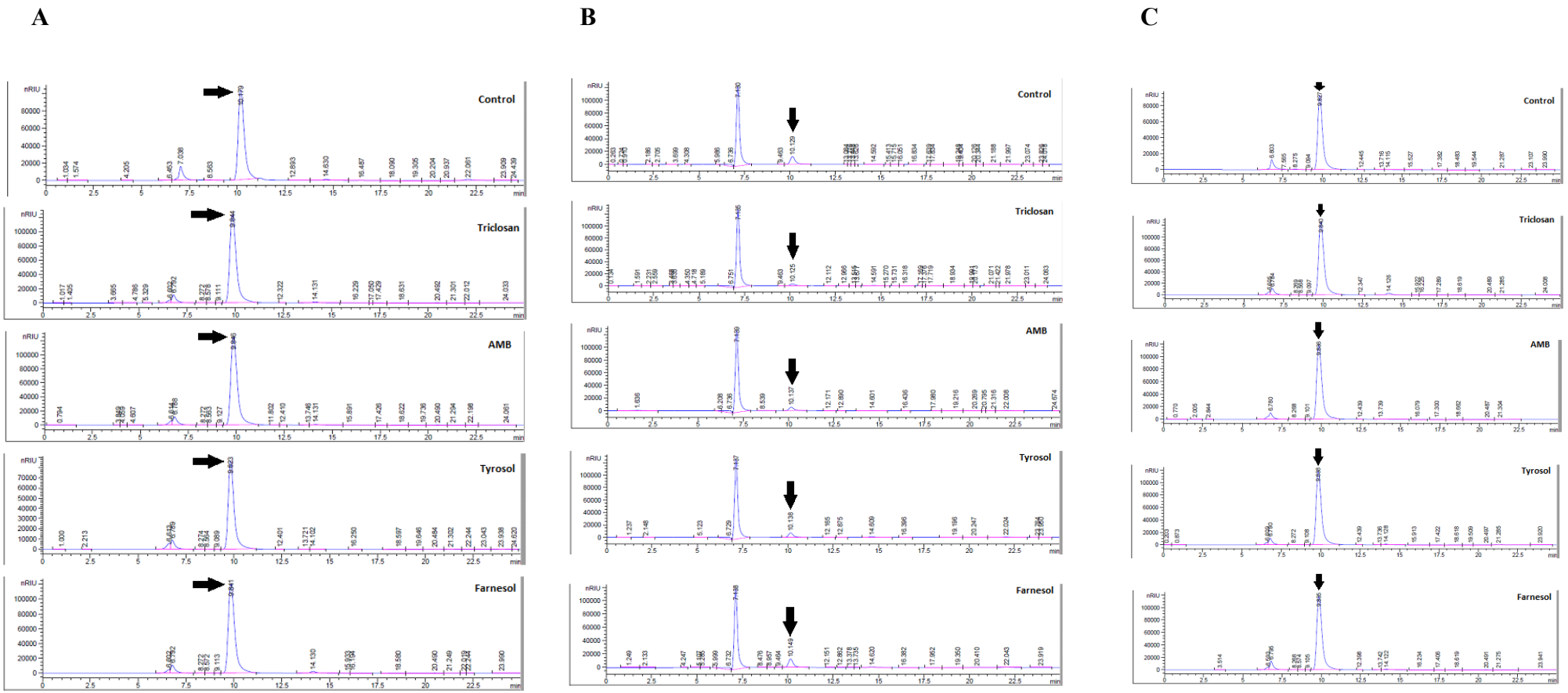

Figure 3.24 HPLC analysis of the treated and non-treated samples. Results after (A) 4, (B) 18 and (C) 36 hr of incubation at 37°C. The arrows show the peaks which correspond to the retention time for the glucose

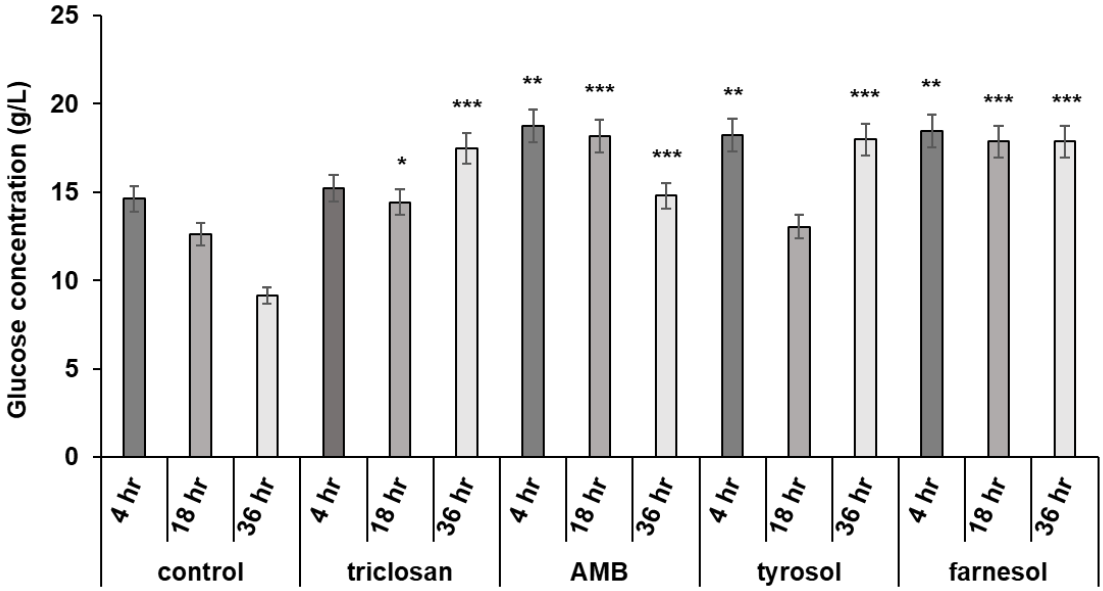

Figure 3.25 The amount of glucose in 1 litre of the treated medium after 4, 18 and 36 hr of incubation at 37°C. *P ≤ 0.05, **P ≤ 0.01 and ***P ≤ 0.001 (SEM bars are shown for n = 3)

3.1.3 Discussion

For antimicrobial susceptibility testing, the MICs should be read when culture growth is in the log phase (also called exponential phase). The growth curve phases are correlated to conidia (fungus in the lag phase) and hyphae (fungus in the log or stationary phase). Since the growth curves of filamentous fungi are characterized by long transition periods, the precise determination of these periods is crucial to obtain an accurate growth curve (Meletiadis et al., 2001). It has been already shown, for example, that actively growing cells are AMB's targets to interfere with their ergosterol biosynthesis pathway (Ren et al., 2014).

Resazurin-based viability assay used to determine effects of triclosan, AMB, furanone, tyrsol and farnesol against *A. fumigatus*. Table 3.2 shows the effective doses of each agent.

Table 3.2 Agents' effective doses and times determined based on resazurin assay (NE: None Effective)

Agents	Effective dose (mg/L)	Effective time (hr)
Triclosan	2	18
Furanone	NE	NE
AMB	1	18
Tyrosol	500	12
Farnesol	6	18

Based on the growth curve (figure 3.5), in the untreated control group, the highest rate of increase in OD was observed during the log phase. The log phase was from 8 hr to 20 hr for the control group. So, the viability of the agents was determined 18 hr after the agents' addition to the fungus culture at time zero. Each antimicrobial has its effect on the log phase duration of the fungus growth (figure 3.11). This is reported in table 3.3. Among the agents, triclosan-related treatment showed the slowest log phase. The other conclusion from the growth curves is that after 20 hr for tyrosol and farnesol and after 28 hr for triclosan the OD values did not change, which means there was no further growth. Also, comparing with the untreated control goup, logarithmic phase initiated with delay in the all treated samples.

Table 3.3 Agents' MICs effect on *A. fumigatus* log phase duration

Agents	Log phase duration (hr)
Control	8 to 20
Triclosan	12 to 28
AMB	12 to 24
Tyrosol	12 to 20
Farnesol	16 to 20

Biofilm biomass was determined indirectly using cv stain and directly through weighing the Petri dishes containing RPMI-1640, with and without biomass. Although, all treated groups showed an extremely significant reduction as compared with the untreated control group, cv assay resulted in the least biomass production in the tyrosol-treated sample (figure 3.12). As stated above, regarding the effect of the agents on the fungus log phase, tyrosol curtailed log phase duration (from 12 hr in the control group to 8 hr in the tyrosol-treated group). Hence, the biofilm biomass related to this antimicrobial was predicted to be less than the other agents. This was confirmed through cv assay, as well. Weighing the biomass formed in Petri dishes, though, showed significant reduction for triclosan in comparing with the other treated and untreated control groups. Remarkably, cultivating *A. fumigatus* in Petri dishes to study the fungus biomass led to brownish colour colonies (figure 2.2). *A. fumigatus* possesses specific physiological and molecular characteristics which make this fungus an aggressive pathogen. These include the biosynthesis of a certain type of melanin. *A. fumigatus* can produce two types of melanin, dihydroxynaphthalene melanin (DHN-melanin) and extracellular (although this pigment can be retained also on the surface of hyphae causing blackish-brown pigment, pyomelanin (Schmaler-Ripcke *et al*. 2008; Perez-Cuesta et al., 2019). These pigments are secondary metabolites made up of complex polymers of phenolic or indolic monomers (Bayry *et al*. 2014) and considered important resistance mechanisms to stress and virulence factors (Monod *et al*. 2002; Wartenberg *et al*. 2011; Sueiro-Olivares *et al*. 2015; Guruceaga *et al*. 2018). It has been shown that DHN-melanin from *A. fumigatus* is able to reduce the effects of ketoconazole and itraconazole (Sande et al., 2007). Some studies conducted on *Sporothrix* species have demonstrated that pyomelanin can protect the fungus from antifungals such as AMB (Almeida-Paes *et al*. 2016). In this study, as it is shown in figure 2.2, anti-biofilm effect of triclosan was more obvious compared to the

other agents. These results might be applicable to pyomelanin production. Based upon Sande et al., (2007) and Almeida-Paes *et al*. (2016) observations, and the findings provided in figures 3.13 and 3.14, it could be suggested that pyomelanin protects the fungus against AMB and tyrosol while it is ineffective against triclosan and farnesol.

Aspergillus asexual reproductive cycle can be divided into two phases: Vegetative growth, which involves the germination of a conidium and the formation of an undifferentiated network of interconnected hyphal cells, which form the mycelium structures; and developmental phase, which happens under proper PH, temperature, and media conditions when some of the vegetative cells stop growing. This phase includes conidiophore formation and spore maturation (Yu, 2010). The microscopical observations showed that the germination of conidia started after 5 hr of incubation and completed after 13 hr, in RPMI-1640 and PDB media. The first detectable growth for the strains of *A. fumigatus* was after 10 hr (pictures not provided).

Overall, the viability assay results demonstrated that treatment of actively growing *A. fumigatus* cells with antifungal agents is more effective than treating them in their mature state in vitro. The agents were significantly more effective against germinated conidia after immediate drug exposure (0–4 hr) than against intermediate and complex filamentous populations. However, as the agents' exposure time increased (8–24 hr), there was no significant difference in their activity against the cellular populations.

The results reported in this section revealed that during the log phase, triclosan-treated samples showed statistically significant reduction in the total amount of proteins compared to the other treated and untreated control groups. However, in the case of tyrosol, the reduction was significant over the stationary phase. This work (please note figures 3.5 and 3.11 regarding log and stationary phases) has shown that regarding the proteins involved in attachment of the fungus to the surfaces, triclosan affects conidial stage while tyrosol and farnesol restrict biofilm formation and maturation (decrease in total protein during the period from 16 hr to 28 hr was observed). This observed diminution at log phase could be due to increase in the activity of proteases. Schwienbacher et al., (2005) revealed that mitogillin, chitosanase and aspergillopepsin are three major proteins secreted by *A. fumigatus* during the log phase of growth under different growth conditions. Chitosanases have been discussed as molecules with anti-fungal activity. Mitogillin is a ribotoxin, which blocks eukaryotic protein synthesis in cell-free extracts. It is expressed

during human infections and has been discussed as a potential virulence factor. Also, chitinase and β(1–3) endoglucanase are other proteins, which based on sequence analysis, are released during the stationary phase of growth. The analysis (Schwienbacher et al., 2005) revealed no evidence of these proteins attachement to the cell wall trough glycosylphosphatidylinositol (GPI)-anchors, which is a lipid anchor for many cell-surface proteins in eukaryotes. So, these proteins might localize in the cell envelope and release by cell wall reorganisation that might take place during stationary phase. Thus, lack of proteins in the tyrosol- and farnesol- treated test groups during stationary phases of growth could be applicable to the down-regulation of chitinase and β(1–3) endoglucanase, or to protein degradation as Bradford assay does not quantify the protein degradation products. For triclosan, in the other hand, the steady level of proteins content during the log and the stationary phases, could be as a result of dysfunctionality of the genes coding these proteases.

The protein release could be achieved through calculation of the EPS-related protein concentration over the total protein concentration ratio (figure 3.15). These amounts were determined in percentages and reported in table 3.4. The data shows the highest release is related to the cells treated with tyrosol and it is followed by triclosan and AMB. This could be because of autolysis.

Table 3.4 Agents' effect on proteins release from *A. fumigatus* after 48 hr of incubation

Agents	EPS/total protein concentration x 100
Control	32.14
Triclosan	83.20
AMB	81.50
Tyrosol	88.90
Farnesol	55.18

Figure 3.16 shows the total carbohydrate (intra- and extra-cellular) concentration was the lowest for tyrosol, among the agents, as compared with the untreated control group. Also, the concentration of EPS-related carbohydrates (extra-cellular) was the lowest for farnesol compared to the control. The carbohydrate release was calculated as percentage of EPS-related to the total carbohydrate ratio and reported in table 3.5.

Table 3.5 Agents' effect on carbohydrates release from *A. fumigatus* after 48 hr of incubation

Agents	EPS/total carbohydrate concentration x 100
Control	44.83
Triclosan	62.5
AMB	64.70
Tyrosol	90.90
Farnesol	41.67

Considering the protein and carbohydrate contents of EPS/total concentration percentages as provided in tables 3.4 and 3.5 respectively, tyrosol penetrates and disrupts cell walls, as showed the highest release of the protein and carbohydrate content from cytoplasm to EPS environment. Release of essential cellular metabolites can disrupt critical cell functions.

Based on the NanoDrop data (figures 3.17 and 3.18), among the agents, the highest DNA and RNA release happened in tyrosol-treated samples (tables 3.6 and 3.7). Farnesol has been reported to induce mitochondrial fragmentation, nuclear condensation and other signs of apoptosis in *A. nidulans* (Semighini *et al.*, 2006; Savoldi *et al.*, 2008). Triclosan, also, demonstrated apoptotic-like cell death (ALCD) mechanism in *Cryptococcus neoformans*, as encapsulated yeast (Movahed et al., 2016). The results were provided based on DNA and RNA release contents as a sign of apoptosis suggested programmed cell death in the samples treated with the agents. The release of eDNA by autolysis in biofilms plays an important role in biofilm resistance to antifungals (Rajendran et al., 2013). Effect of tyrosol on the permeability of the cell membrane of dimorphic fungi has been already demonstrated. Tyrosol acts on the fungal membrane and reduces the ergosterol content of the fungal strains and hence causes release of intracellular molecules (Brilhante et al., 2016). This release has also been shown in the samples treated with the other three agents.

Table 3.6 Agents' effect on DNA release from *A. fumigatus* after 18 hr of incubation

Agents	EPS/total DNA concentration x 100
Control	6.20
Triclosan	20.81
AMB	10.87
Tyrosol	26.35
Farnesol	13.91

Table 3.7 Agents' effect on RNA release from *A. fumigatus* after 18 hr of incubation

Agents	EPS/total RNA concentration x 100
Control	11.63
Triclosan	12.78
AMB	12.02
Tyrosol	23.71
Farnesol	10.80

A hallmark of apoptosis is inter-nucleosomal fragmentation of nuclear DNA. This DNA fragmentation is occurring as a result of induced nuclease activity early during cell death. DNA smearing has been reported as a late response in *A. nidulans*, following treatment with phytosphingosine (Cheng et al., 2003). Mousavi and Robson (2003) have been reported that *A. fumigatus* viability in liquid culture decreased rapidly when the fungus entered stationary phase. The authors explained this viability decrease because of the apoptotic-like programmed cell death (Mousavi and Robson, 2003). In their study, *A. fumigatus*, DNA smearing was also absent during cell death in the stationary phase. So, considering DNA smearing is associated with the induction of an apoptotic-like phenotype, AMB caused death in *A. fumigatus* through inducing apoptosis (figure 3.19).

To inhibit biofilm formation, a method is treatment of the conidial cells with the agents with the aim to reduce the conidial cells' viability and hence biofilm formation. To quantify viable cells in a cell suspension PI labelling was followed by FCM analysis as a quantitative technique. PI is a positively charged, membrane-impermeable fluorochrome that can only pass through the membranes of stressed, injured, or dead cells. Base on the principle that apoptotic cells, among other typical features, are characterized by DNA fragmentation and, thus, loss of nuclear DNA content (Riccardi and Nicoletti, 2006), FCM assay was perfomed on the treated conodia stained with PI. It has been already shown that FCM can be applied on conidia cells to assay their viabilities (Balajee and Marr 2002; Mesquita et al., 2013; Vanhauteghem et al., 2017). Dot plots and histograms obtained by the combination of SSC and FSC are shown in figures 3.20 and 3.21, respectively. Detection and quantification of airborne fungi conidia by FCM was obtained. Based on the results, the viability of fungal conidia treated with the agents showed triclosan and farnesol were less effective than tyrosol and AMB to reduce conidial viability.

A. fumigatus cell wall is composed of two layers (Maubon et al., 2006): An external hydrophobic layer containing melanin and rodlet proteins, and an internal layer, electron

translucent, containing polysaccharides including α and β-glucans, chitin/chitosan and galactomannan.

Chitin is a vital component of the fungal cell wall, which can be stained using CFW stain (figure 2.4). Biosynthesis of chitin is the primary event in the organization of the cell wall (Bernard and Latgé, 2001).

The CFW-related morphological analysis (figure 3.23) confirmed the growth curve studies discussed earlier and demonstrated that the agents slowed down/delay the growth phase of *A. fumigatus* to initiate the log phase.

As it was explained in section 1.7, glucose is the main unit of galactomannan, glucan and mannose in the fungus cell wall. HPLC results (figure 3.25) were in correlation with the results provided in table 3.4 and table 3.6; the decrease in the glucose uptake in triclosan- and tyrosol-treated samples at 36 hr and 4 hr and 36 hr, respectively, which could be because of the cell wall disruption. Triclosan and tyrosol might promote glucose attachment to their transporters, but without crossing through the cell wall. Thus, the following sampling from the cultures showed decrease in the glucose content. Following cell walls reorganisation at the stationary phase, the attached glucose was released from the transporters into the culture, which could explain the increase in the concentration of glucose in the culture at 36 hr. Tables 3.4 and 3.6 showed cell wall reorganisation was disrupted under triclosan and tyrosol treatment, at the stationary phase (36 hr).

3.2 Triclosan antifungal activity alone and in combination with AMB against *A. fumigatus*

3.2.1 Introduction

Treatment with the AMB has been reported to be associated with the side effects, like neurotoxicity, nephrotoxicity, and/or hepatoxicity (Dupont, 2002; Allen, 2010); the effect of AMB on mortality has also been reported (Brown et al., 2012). In this study AMB loaded liposomes, AmB-LLs, was applied to investigate its effect alone and in combination with triclosan against *A. fumigatus*. AMB penetrates more efficiently to various organs and across the cell wall (Walker et al., 2018). It shows reduced toxicity at higher, more effective doses compared to the second most commonly used AmB product, deoxycholate detergent-solubilized AMB (Ambati et al., 2019). However, AmB-LLs still brings about AmB human toxicity, such as renal toxicity in 50% of patients (Tonin et al., 2017).

Triclosan, a phenoxyphenol antimicrobial agent, was first developed in the early 1960s and has been widely used as an antibacterial or antifungal agent since the 1970s (Kim et al., 2015).

The prospect of combined drug therapy as an alternative approach to the treatment of systemic mycoses began from the pioneering work of Medoff, Comfort and Kobayashi (1971) (Medoff, Comfort and Kobayashi, 1971). Although single-agent antimicrobial therapy is more feasible, a combination of two or more antimicrobial agents is suggested under certain conditions (Leekha, Terrell and Edson, 2011), such as:

i) When agents exhibit synergistic activity against a microorganism. Synergy between antimicrobial agents means that, when studied in vitro, the combined effect of the agents is greater than the sum of their independent activities when measured separately. When infections caused by more than one organism, a combination regimen may be favoured because it would extend the antimicrobial spectrum beyond that reached by a single agent.

ii) When critically ill patients (comprising 5 to 10% of the patients admitted into intensive care units) (Boniatti et al., 2011), need empiric therapy before microbiological aetiology and/or antimicrobial susceptibility can be determined. Antibiotic combinations are used in empiric therapy for healthcare–associated infections that are frequently caused by bacteria

resistant to multiple antibiotics. Combination therapy is used in this setting to ensure that at least one of the administered antimicrobial agents will be active against the suspected organism(s).

iii) To prevent emergence of resistance. The emergence of resistant mutants in a bacterial population is commonly the result of selective pressure from antimicrobial therapy. Provided that the mechanisms of resistance to two antimicrobial agents are different, the chance of a mutant strain being resistant to both antimicrobial agents is much lower than the chance of it being resistant to either one. In other words, use of combination therapy would afford a better chance that at least one drug will be effective, in so doing avoiding the resistant mutant population from emerging as the dominant strain and causing therapeutic failure.

For instance, AMB–tyrosol possess antibiofilm properties in *Candida* spp, although such properties are better suited for preventive strategies rather than for treatment. The biofilm density was severely altered by high concentrations of tyrosol in the combined therapy at early stages of biofilm formation. As the concentration of tyrosol increased, the density of biofilm decreased in a dose-dependent manner. Time of addition of antibiofilm agents should be considered as well. The initial adherence time was found to be important regarding the ability of AMB–tyrosol to inhibit biofilm formation. As another example, combinations of amphotericin B with 5-fluorocytosine, rifampin, and tetracycline acted synergistically against certain yeast-like fungi including *Candida* spp., *Aspergillus* spp., and *Coccidioides immitis* in vitro (Beggs, Sarosi and Walker, 1976; Kitahara et al., 1976; Dupont and Drouhet, 1979).

In this section, the antifungal activity of AMB and triclosan against *A. fumigatus* was compared. Also, their combination was studied to see if there is any synergistic interaction between them against the fungus.

To study triclosan and AMB mechanism of action, expressions of two dominant carbohydrates, galactosaminogalactan (GAG) and α-1,3-Glucan, in *A. fumigatus* conidia cell wall were studied after treatment with triclosan and AMB.

GAG is a heteropolysaccharide composed of α-1,4-linked galactose, *N*-acetylgalactosamine, and galactosamine residues that is found both in a secreted form and bound to the cell wall of hyphae (Fontaine et al., 2011). *A. fumigatus*

produces higher levels of cell wall associated GAG than other *Aspergillus* species (Lee et al., 2015). GAG is required for biofilm formation and adherence to host cells. A co-regulated five-gene cluster has been identified and proposed to encode the proteins required for GAG biosynthesis. One of these proteins is spherulin 4. *Sph3* (Afu3g07900) is annotated as a gene encoding this protein (Bamford et al., 2015).

A. fumigatus has three α-1,3-glucan synthase genes (*ags1–3*). α-1,3-Glucan of *A. fumigatus* has a role in the aggregation of germinating conidia. This aggregation is important at the microcolony formation stage of the biofilm formation. The *Δags* strain lacks α-1,3-glucan and is less pathogenic than the parental strain (Miyazawa et al., 2018).

3.2.2 Results

3.2.2.1 *A. fumigatus* morphological identification and growth in triclosan-treated solid and broth media

Slide cultur method and microscopic analysis were performed to study the morphological alterations after treatment of the fungus with triclosan. Slide culturing method preserves the morphological features relatively undisturbed comparing with other techniques used for microscopic examination of fungal colonies (tease mounts[3] and cellotape mounts[4]). Figure 3.26 demonstrates the appearance in both inoculated conditions (treated and untreated). In any one microscopic field only a few hyphal filaments were in focus signifying that as the hyphae grew they branched extensively forming a network of mycelial growth producing a three dimensional structure.

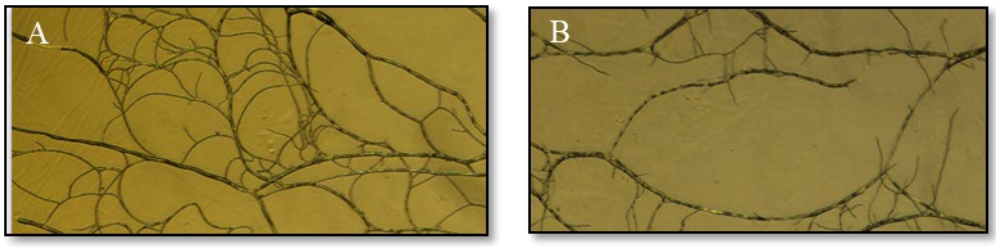

Figure 3.26 Day 7 growth of *A. fumigatus* on PDB agar. (A) Non-treated inoculum was added to the agar; control (B) Triclosan-treated inoculum was added to the agar. Microscopic analysis show that more branched patterns with shorter branched absorbing structures (BAS) at the tip were seen in the control biofilm than in the triclosan-treated biofilm

Figure 3.27 shows the triclosan-treated *A. fumigatus* grown in either RPMI-1640 or PDB formed no biofilm structure on the liquid-air surface of the media. While, the layers of biofilm were obvious in the both untreated control broth media.

[3] A small portion of a colony is digged out with a pair of dissecting needles or pointed applicator sticks. The colony is placed on a microscopic slide, teased apart with the dissecting needle and overlaid with a coverslip (Winn and Koneman, 2006)

[4] A piece of clear Scotch tape is cut and folded back on itself with the adhesive side turned outward. Then, the adhesive side of the tape is pressed onto the surface of the colony. The aerial hyphae of the colony will stick to the adhesive surface. The tape adhesive side is then placed down on a glass slide (Ghannoum and Isham, 2009)

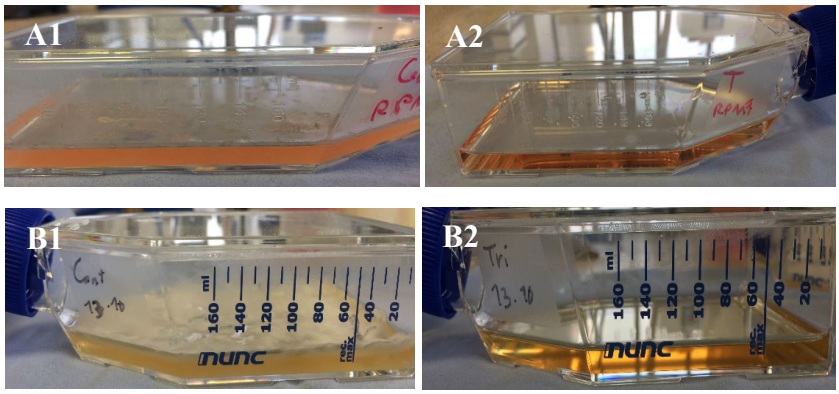

Figure 3.27 *A. fumigatus* biofilm formation in RMPI-1640 (first row) and PDB (second row). Comparing non-treated control media (A1 and B1), and media treated with triclosan MIC_{50} (A2 and B2) shows less biofilm structure were formed at the air-liquid interface (ALI-biofilm) in the treated media

3.2.2.2 Investigation of triclosan activity against germinated *A. fumigatus* conidia growth

Figures 3.28 and 3.29 show respectively the colony forming units (CFU) and the colonies diameter related to the samples taken from the 24- and 36-hr incubated control and treated groups in PDB medium, which subsequently incubated for more 24 hr on PDA plates. Figure 3.28 shows that competent hyphae, taken after 24 hr from broth medium, formed more CFU compared with early conidiophores, taken after 36 hr (for further information on this, see section 3.1.2.2).

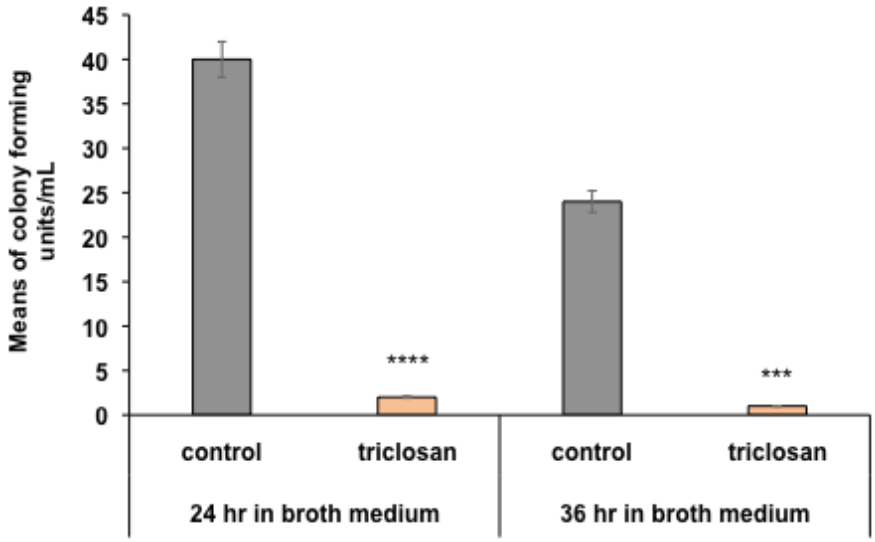

Figure 3.28 *A. fumigatus* colony formation on PDA plates. The SPSS software was used for paired sample T-Test calculation (in all the graphs the samples were compared with their control groups) showing data sets that were deemed not significantly different (N.S; > 0.05) and data sets that were significant at different levels: ***P ≤ 0.001 and ****P ≤ 0.0001 (SEM bars are shown for n = 3)

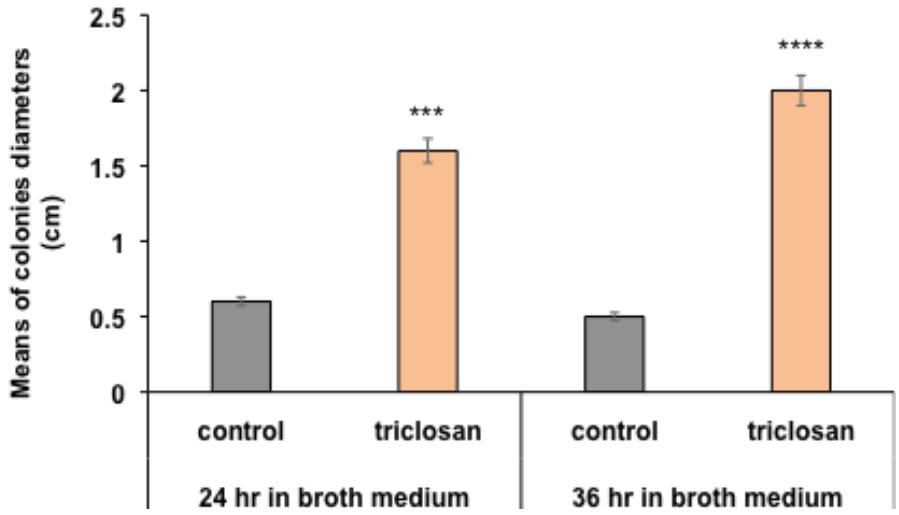

Figure 3.29 Growth rate of the treated and untreated test groups expressed as radial growth rate on solid PDA medium. ***P ≤ 0.001 and ****P ≤ 0.0001 (SEM bars are shown for n = 3)

3.2.2.3 Biomass quantification of triclosan-treated *A. fumigatus* at its early and mature developmental stages

Cell dry weight assay was performed on *A. fumigatus* mycelia grown in PDB medium (figure 3.30).

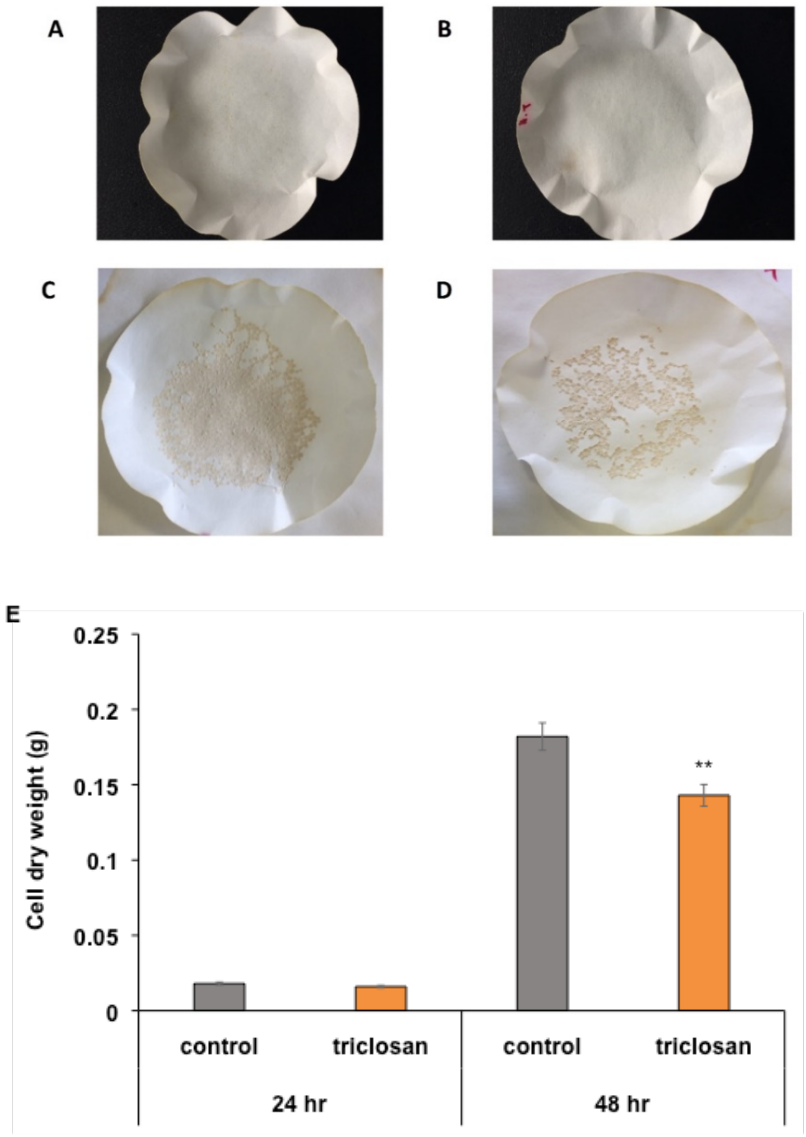

Figure 3.30 Cell dry weight assay. *A. fumigatus* mycelia filtered through Whatman cellulose flters related to A) control group related to 24 hr of incubation, B) triclosan-treated sample after 24 hr of incubation, C) control group after 48 hr of incubation, and D) triclosan-treated sample after 48 hr of incubation. Since no mycelia is forming after 4 hours incubation this test was not performed on the samples taken at 4 hr incubation of untreated control and treated samples. (E) Cell dry weight **P ≤ 0.01 (SEM bars are shown for n = 3)

3.2.2.4 Combination treatment of *A. fumigatus* with triclosan and AMB

Figures 3.31 and 3.32 show the effectiveness of triclosan and AMB alone and in combination against *A. fumigatus* biofilms formed in 96-well plates in PDB. The results were determined by resazurin-based viability assay.

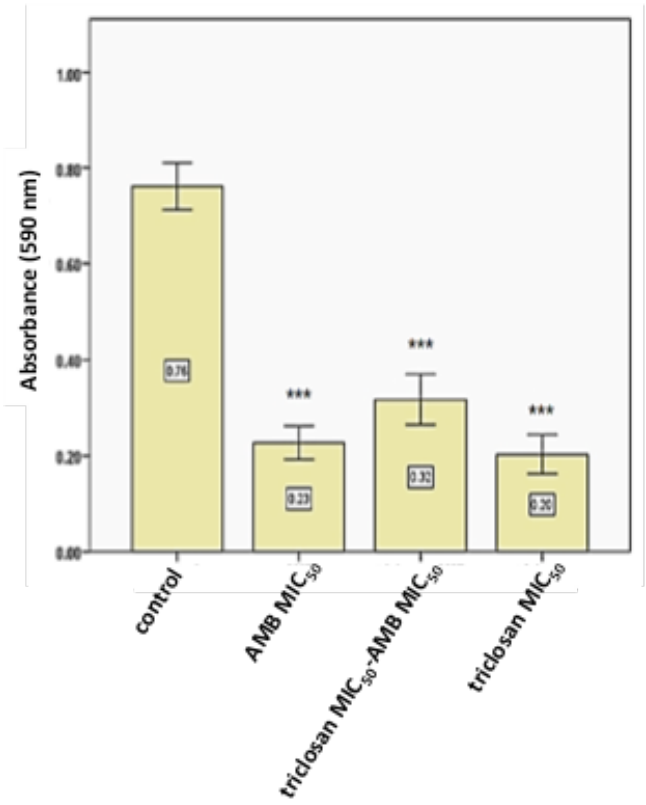

Figure 3.31 Simultaneous combination treatment (triclosan-AMB). The antimicrobial agents were added at their MIC_{50} level, as a single agent or in the combination manner. The SPSS software was used for paired sample T-Test calculation (the samples were compared with the untreated control group) showing data-sets that were deemed not significantly different (N.S; >0.05) and data-sets that were significant at different levels: ***P ≤ 0.001 (SEM bars are shown for n = 3)

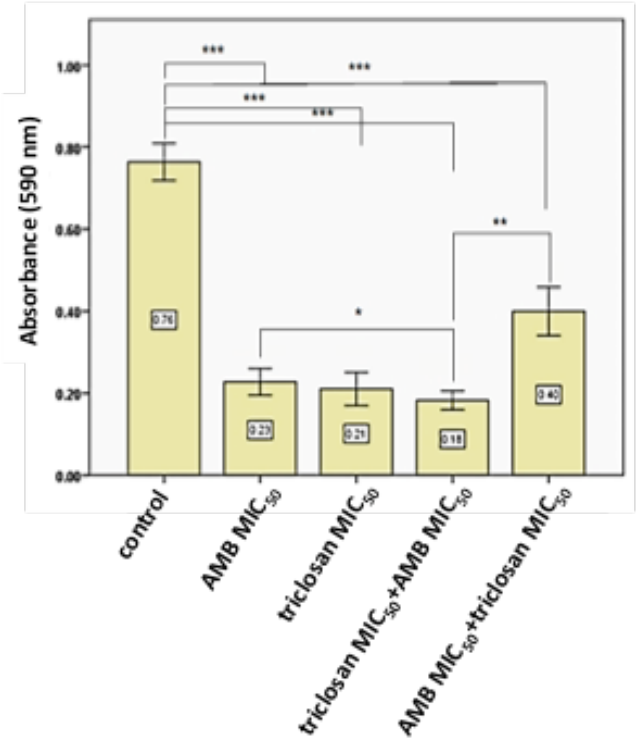

Figure 3.32 Sequential combination treatment (with drug regimens administered one after another; triclosan+AMB and AMB+triclosan). Adding triclosan MIC_{50} following with AMB MIC_{50} is more effective than adding each of the antimirobials MIC_{50} alone and also than AMB MIC_{50} following with triclosan MIC_{50}. The graph shows the average of three separate tests. The SPSS software was used for paired sample T-Test calculation (in all the graphs the samples have been compared with their control groups) showing data sets that were deemed not significantly different (N.S. > 0.05) and data sets that were significant at different levels: *P ≤ 0.05, **P ≤ 0.01 and ***P ≤ 0.001 (SEM bars are shown for n = 3)

3.2.2.5 Susceptibility testing of *A. fumigatus* treated with various doses of triclosan and AMB alone and in combination

Agar plates were inoculated with a standardized inoculum (100 μL) of the test microorganism. Then, filter paper discs (6mm in diameter) containing the test compound at a desired concentration, were placed on the agar surface (figure 3.33). Generally, antimicrobial agent diffuses into the agar and inhibits germination and growth of the test microorganism.

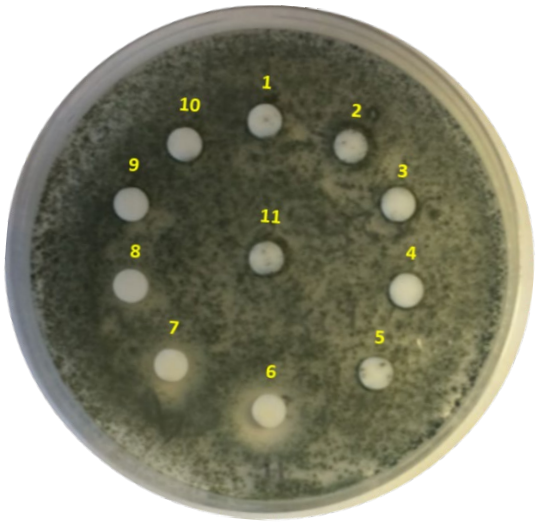

Figure 3.33 Disk-diffusion assay. There was no *A. fumigatus* growth around the disk impregnated with AMB MIC_{50} (1 mg/L) or triclosan MIC_{50} (2 mg/L) after 48 hr of treatment. Triclosan and AMB combination treatment partially inhibited the growth. 1: triclosan 1 mg/L; 2: triclosan 4 mg/L; 3: triclosan 1 mg/L+AMB 0.5 mg/L; 4: triclosan 1 mg/L+AMB 1 mg/L; 5: triclosan 2 mg/L+AMB 0.5 mg/L; 6: triclosan 2 mg/L; 7: AMB 1 mg/L; 8: triclosan 2 mg/L+AMB 1 mg/L; 9: AMB 0.5 mg/L; 10: AMB 2 mg/L; 11: untreated control

3.2.2.6 Synergistic effect analysis

Synergy Checkerboard assay. The MIC_{50} has been defined as the minimal concentration that results in 50% of growth inhibition. When MICs in the combination treatments were established, the FICI was calculated based on them by using equation 1 (section 2.7.3.1). The MICs for triclosan and AMB were already calculated (section 3.1.2.4) as 2 and 1 mg/L, respectively. Based on the checkerboard assay to calculate FICI, a synergistic activity between the agents could be achieved if triclosan and AMB were applied at doses equal or less than 0.6 and 0.2 mg/L, respectively. The minimum inhibition effect, when they were added simultaneously (triclosan dose at 0.6 mg/L plus AMB dose at 0.2 mg/L were added to the cells) or sequentially (AMB dose at 0.2 mg/L following with triclosan dose at 0.6 mg/L were added to the cells), revealed ~ 60% viability (~ 40% inhibition) (tables 3.8 and 3.9). This means the 50% growth inhibition was not obtained.

Table 3.8 Checkerboard assay analysis of the simultaneously combination treatment

AMB dose (mg/L) addedat t0 \ Triclosan dose (mg/L) added at t0	0	0.15	0.3	0.6
0	100 *	95.5	93	88
0.05	90.5	70	66	67
0.1	87.7	70	65.5	69
0.2	83	81.5	73	60.5

* Numbers are presented the cells' viability (%)

Table 3.9 Checkerboard assay analysis of the sequential combination treatment (first AMB following with triclosan)

AMB dose (mg/L) added at t0 \ Triclosan dose (mg/L) added at t18	0	0.15	0.3	0.6
0	100 *	96.5	95	95
0.05	92.5	80	77	77
0.1	90.7	70	65.5	65
0.2	90	85	70	60

* Numbers are presented the cells' viability (%)

Sequential addition of triclosan-AMB to *A. fumigatus* cells (first triclosan (0.6 mg/L) following with AMB (0.2 mg/L)) disclosed 48.5% viability (counted as MIC_{50}), resulting in a FICI= 0.5; hence a synergistic interaction was formed. The triclosan and AMB MIC_{50}s were reduced 30% and 20%, and dropped to 0.6 and 0.2 mg/L, which present sub-MIC_{50} doses, respectively in this combination treatment (table 3.10).

Table 3.10 Checkerboard assay analysis of the sequential combination treatment (first triclosan following with AMB)

AMB dose (mg/L) added at t18 \ Triclosan dose (mg/L) added at t0	0	0.15	0.3	0.6
0	100 *	90.5	89.5	80
0.05	95	87	70	67
0.1	93	70	65	60
0.2	93	67	55	48.5

* Numbers are presented the cells' viability (%)

Using CompuSyn software for data analysis. To confirm checkerboard assay results, various doses (table 3.11) of triclosan were combined with AMB (0.2 mg/L), sequentially (first triclosan following with AMB) and relevant ODs were analysed using CompuSyn software.

The Combination index (CI) values at all effect levels can be simulated as Fa (the default effect)-CI Plot. The default setting for the CompuSyn is fa = 0.05, 0.1, 0.15…0.95 and 0.97. CI < 1, = 1, and > 1 indicate synergism, additive effect and antagonism, respectively. The Fa-CI plot with Fa increment of 0.05 showed synergistic effect (CI < 1) (figure 3.34).

Table 3.11 CI data for constant combination (1:1) of triclosan+AMB

Triclosan dose (mg/L)	AMB dose (mg/L)	Effect	CI
0.00	0.20	0.52	27.36
0.15	0.20	0.50	40.50
0.30	0.20	0.59	0.09
0.60	0.20	0.63	0.002
1.20	0.20	0.53	160.27

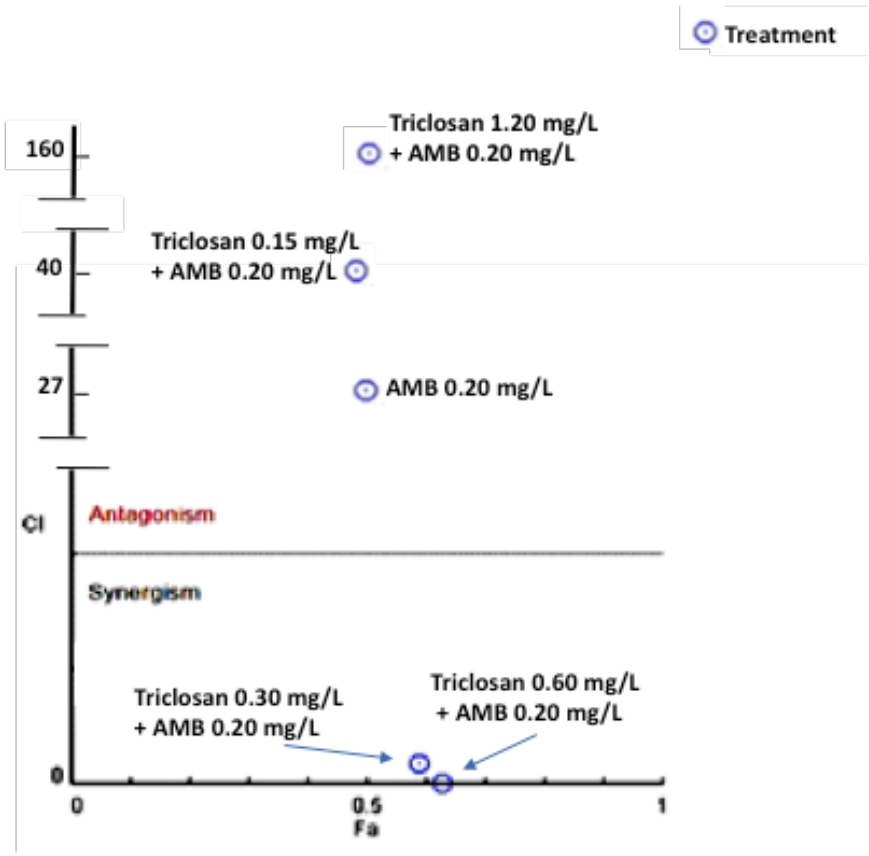

Figure 3.34 Combination Index Plot. CI values for synergism is 0-1, and for antagonism is 1-∞. Among 5 combination data points, 2 of them were on the synergy side (CI < 1): triclosan (0.6 and 0.3 mg/L) followed by AMB (0.2 mg/L). Fa= the fraction affected or inhibited

3.2.2.7 Phenotype modifications of *A. fumigatus* biofilm in the presence of triclosan- and AMB- MICs

A. fumigatus biofilm formation on glass slides after 48 hr of incubation at 37°C were analysed using FUN-1-based confocal laser scanning microscopy (CLSM). Free FUN-1 stain is almost nonfluorescent in aqueous solution, but when complexed with DNA or RNA and excited with light between 470 and 500 nm, its fluorescence at 530 nm increases as much as 400-fold (Millard et al., 1997). The kinetics of formation of *A. fumigatus* biofilm was observed by CLSM (figure 3.35). Also, 3D surface plots showing the biofilm depth in triclosan-treated sample in comparison with AMB-treated and control groups are shown in figure 3.36.

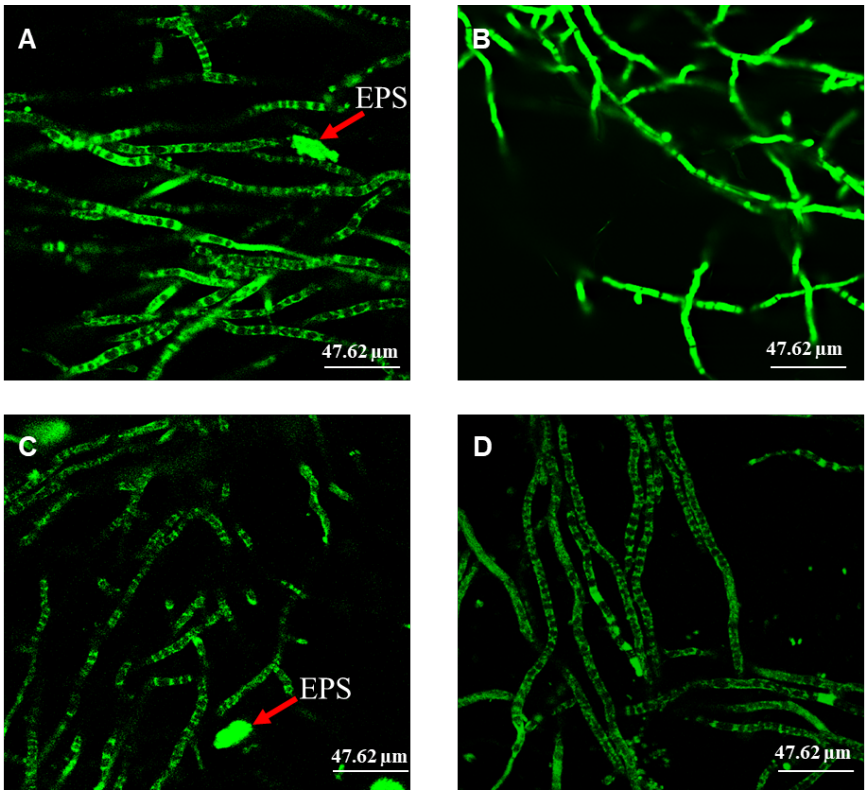

Figure 3.35 *A. fumigatus* growing on glass surface after 48 hr of incubation. Confocal laser scanning fluorescence microscopy images of *A. fumigatus* FUN-1-stained from (A) control, (B) treated with triclosan MIC_{50}; (C) treated with AMB MIC_{50} and (D) treating with triclosan sub-MIC_{50} following with AMB sub-MIC_{50}

The CLSM analysis of the biofilms allowed to measure and to compare the means of thickness of the triclosan-treated and the combination-treated test groups (figure 3.36).

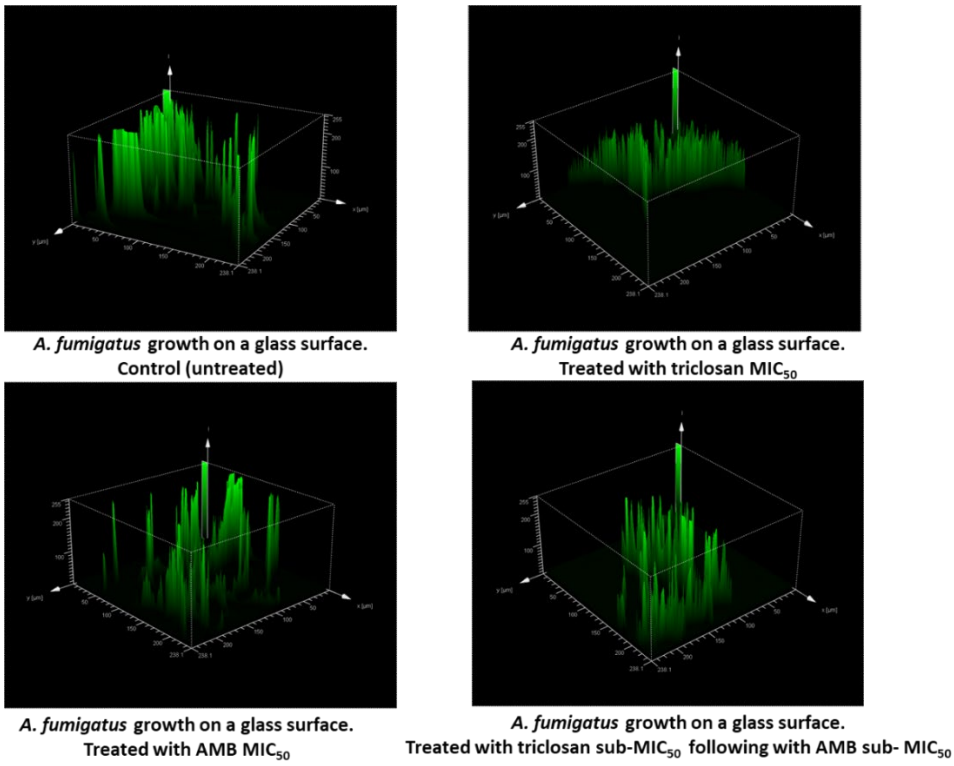

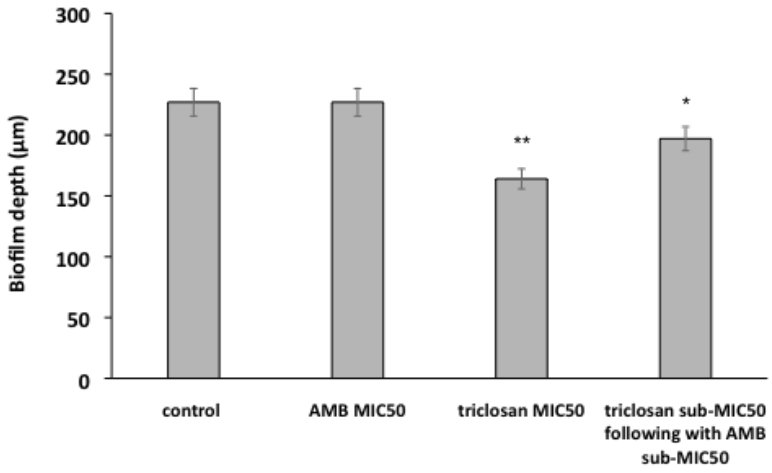

Figure 3.36 CLSM observations of 18 hr-old biofilms thicknesses inoculated on glass coverslips. The figure demonstrates CLSM microscopy 3D surface plots images of *A. fumigatus* FUN-1-stained from control and treated with the combination of triclosan and AMB MICs, sequentially at 48 hr growth. The graph shows average projections of confocal laser scanning fluorescence microscopy 3D surface. *P ≤ 0.05 and **P ≤ 0.01 (SEM bars are shown for Three image stacks from each of three independent experiments (nine stacks in total))

3.2.2.8 Real-time-PCR and expression levels of *A. fumigatus* genes coding cell wall proteins (α-(1,3) glucans and GAG) following treatment with AMB and triclosan

Polymerase chain reaction (PCR) is a technique used to amplify a single copy or a few copies of a segment of DNA across several orders of magnitude, producing thousands to millions of copies of a particular DNA sequence. PCR was used to study the availability of the *ags 3* (which codes α-(1,3) glucan) and *sph3* (which codes GAG) in *A. fumigatus* (figure 3.37).

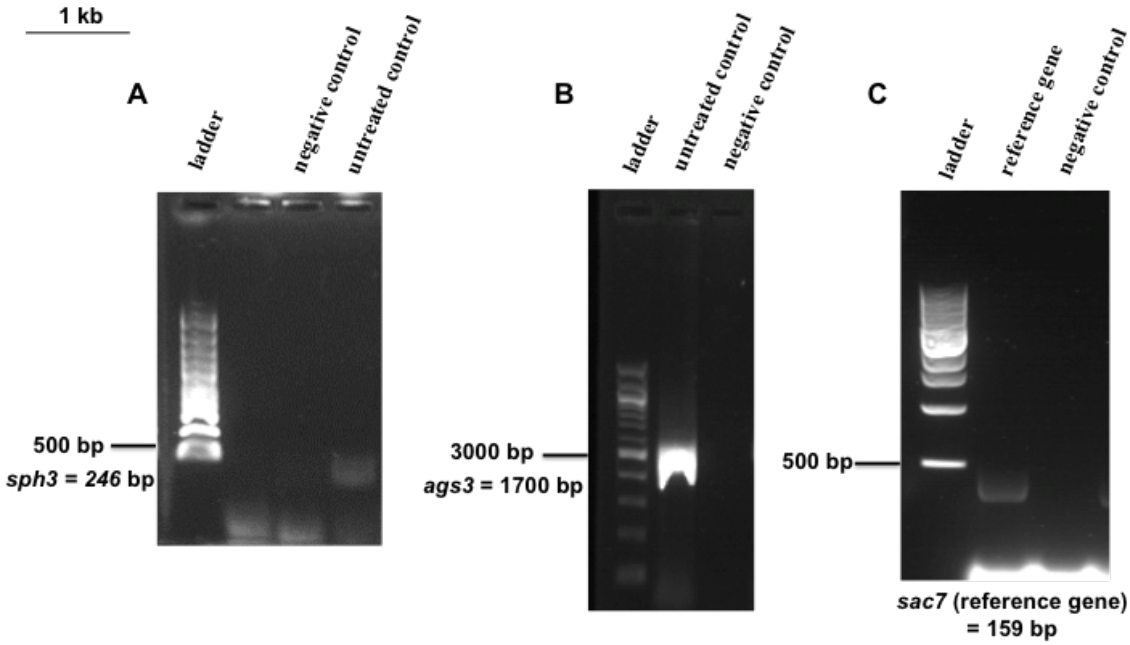

Figure 3.37 Gel electrophoresis pictures of (A) *sph3* and (B) *ags3* availability in *A. fumigatus*. (C) reference gene related band is depicted (*sac7*). Negative control = dH_2O and forward/reverse primers were added without template

The PCR results showed *ags3* and *sph3* availability in *A. fumigatus* grown in PDB for 48 hr at 37°C (figure 3.37). RT-PCR was performed for *A. fumigatus* cDNA. Table 3.12 shows the C_T values, fractional cycle umbers at which the fluorescence passes the fixed threshold.

Table 3.12 C_T (threshold cycle) values of DNA extracted from *A. fumigatus* samples in RT-PCR. C_t values obtained for the experiment were expressed as mean ± standard deviation (n=3)

Experiments / Genes	Reference gene, *sac7* C_T Mean	*ags3* C_T Mean	*sph3* C_T Mean
Untreated control	15.82	22.62	20.92
Triclosan	15.47	30.65	29.49
AMB	22.40	33.12	32.39

RT-PCR analysis represents the *ags3* and *sph3* expression qualities when the fungus was treated with triclosan and AMB (figure 3.38).

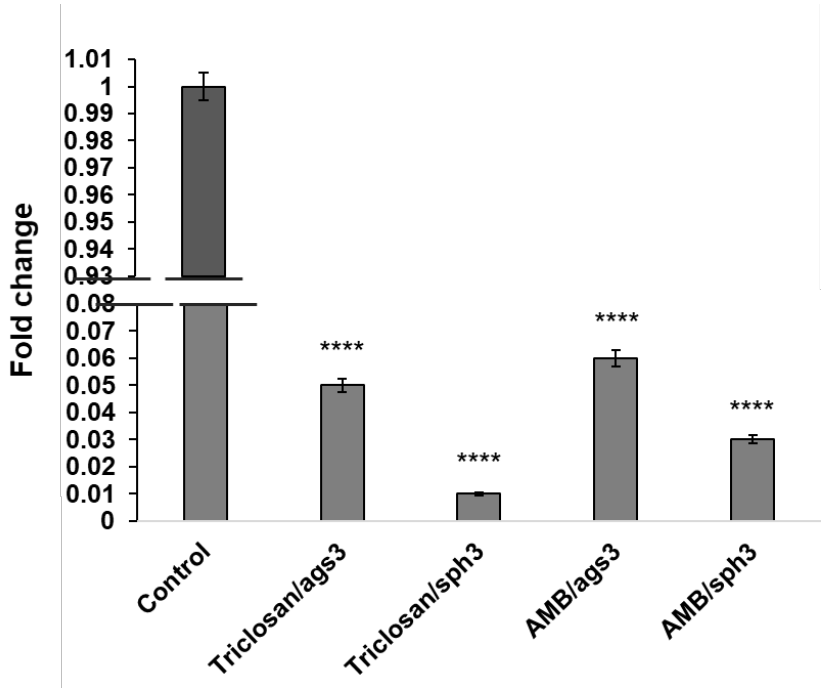

Figure 3.38 Relative expression of *ags3* and *sph3* in *A. fumigatus* treated with triclosan and AMB compared with untreated control. The expressions after treatment with these agents were diminished (= genes were down-regulated), while this decrease was more in the samples treated with triclosan. $\Delta\Delta C_T$ was calculated by subtracting ΔC_T untreated test group (control) from ΔC_T of each treated group. $R = 2^{-\Delta\Delta CT}$ corresponds to the fold change. To verify the absence of genomic DNA contamination, negative controls were used for each gene set in which reverse transcriptase was omitted from the mix. ****$P \leq 0.0001$ (SEM bars are shown for n = 3)

3.2.3 Discussion

To study the effect of triclosan and AMB on the morphology, CFU and diameters of the colonies, samples were prepared in PDB medium and then introduced to a substrate, on PDA plates. Treated samples taken from 4 hr cultured broth medium did not show any significant differences in the matte of CFU than the control group; 4 hr was not sufficient time for triclosan to enter the conidial or disrupt with their bioactivity. The number of colonies were less in the samples taken from 24 hr- and 36 hr-incubated groups treated with triclosan in PDB compared to untreated control groups while the mean size of the colonies diameters in the treated groups were bigger than that in the control groups (figures 3.28 and 3.29). In the case of morphology, all samples formed greenish grey colonies. Based on these results, comparing with the control, triclosan inhibited conidial growth on the agar while the growth rate of the resistant conidia was higher than that in untreated control group. As the growth rate decrease is a defining trait of persister cells to increase antibiotic tolerance (Balaban *et al*., 2004), so, impact of *A. fumigatus* triclosan treatment could be on reducing persister levels or affecting their gene expression. In bacteria, however, Westfall *et al* (2019) showed that triclosan promoted *E. coli* and *Staphylococcus aureus* tolerance to bactericidal antibiotics, and that triclosan increased persister frequency to all tested antibiotics, ampicillin, ciprofloxacin, kanamycin and streptomycin.

As discussed in section 3.1, AMB and triclosan exhibited the best spectrum of activity against germinated conidial growth (forms after 5 hr of incubation). This inefficiency was observed for 48 hr-related samples growing in the medium. This suggests that triclosan loses its effectiveness over time and to get the best antifungal effect of triclosan, the fungus should be exposed to triclosan every 24 hr.

The mass weight analysis showed a significant reduction in triclosan-treated samples compared to control groups after 48 hr of incubation but not in the samples incubated for 24 hr (figure 3.30) (since no mycelia had been formed after 4 hr of incubation this test was not performed on the samples taken from 4 hr incubated control and treated test groups).

Using checkerboard assay and agar disk-diffusion test, Yu *et al*., 2011 have already shown that triclosan exhibits an antifungal effect in vitro against azole-resistant *C. albicans* when combined with fluconazole.

Synergistic activity is beneficial to extend the antimicrobial spectrum beyond that achieved by use of a single agent for treatment of infections. In this study, antifungal effect was observed when triclosan and AMB were added sequentially, first triclosan then AMB. Resazurin-based viability assay was performed to study the triclosan-AMB combination treatment against *A. fumigatus*. A comparison of the A590 values obtained for treated samples as a function of triclosan or AMB concentrations alone showed that the biofilm formation was susceptible to the fungicidal activity of the antifungal agents ($P \leq 0.001$) as compared with untreated control group. Similarly, triclosan in combination with AMB was active against biofilm compared to the untreated test group ($P \leq 0.001$). However, single treatments were more effective than the simultaneous combination treatment on reducing the fungus growth. The fungus showed ≃ 30% and ≃ 26% viability when it was treated with AMB and triclosan alone, respectfully, and ≃ 42% viability when it was treated with triclosan-AMB combination, simultaneously (figure 3.31). Under sequential treatment condition, adding triclosan-MIC followed by AMB-MIC_{50} (≃ 23% viability) was more effective against *A. fumigatus* than adding AMB-MIC_{50} followed by triclosan MIC_{50} (≃ 52% viability). This type of combination treatment was also more effective than adding agents, alone (figure 3.32).

Reducing the agents' effective doses is advantageous since it decreases the microbial potency and resistance against those agents. The agar disks-diffusion results were compatible to what was obtained in the resazurin-based viability assay. Both tests showed *A. fumigatus* was susceptible to triclosan and AMB at 2 mg/L and 1 mg/L, respectively, while triclosan-AMB simultaneous addition to the fungus revealed a partial growth inhibition. Other treatment doses (sub-MIC_{50s} and above the MIC_{50s} of triclosan and AMB) allowed normal mycelium formation, stunted and highly branched colonies (figure 3.33).

The resazurin assay-based results were obtained when the agents were applied at their MIC_{50s}. But, based on the checkerboard assay, to see the synergistic interaction among the agents, they had to be applied at their sub-MIC doses (tables 3.8, 3.9, and 3.10). These doses were ≤ 0.6 mg/L and ≤ 0.2 mg/L for triclosan and AMB, respectively. Based on this assay, FIC_{AMB} and $FIC_{triclosan}$ obtained in the sequentially treatment manner revealed a synergistic interaction between triclosan and AMB. This synergistic interaction formed when they were added sequentially, first triclosan then AMB. The results showed that the

effective dose of triclosan and AMB could be reduced by 30% and 20% and dropped to 0.6 and 0.2 mg/L, respectively in this combination treatment. This finding is beneficial, as it has been shown that AMB and triclosan have some adverse effects against human/human environment. Although, AMB is more toxic to fungal cells than the mammalian sterol cholesterol and binds the fungal plasma membrane sterol ergosterol more efficiently, its side effects of neurotoxicity, nephrotoxicity, or hepatoxicity against mammalian cells have been reported (Dupont 2002; Allen 2010). Triclosan might affect immune responses, ROS production, and cardiovascular functions. It would pass go through both biotic and abiotic transformation, producing a multitude of by-products. Some of these by-products were found to be more toxic than the parent triclosan compound (Weatherly and Gosse, 2017). Triclosan effects on endocrine disruption were reviewed, as well (Ruszkiewicz et al., 2017).

CompuSyn software confirmed synergistic activity between triclosan (0.6 mg/L) and AMB (0.2 mg/L) against *A. fumigatus*. Although, by using this software triclosan at 0.3 mg/L dose revealed synergistic interaction with AMB (0.2 mg/L), as well (table 3.11 and figure 3.34).

Together, these data support a synergistic activity between triclosan and AMB in *A. fumigatus*. This synergism could be through triclosan triggering persister cells and make them vulnerable to AMB.

The effect of these agents on the fungus' EPS production were observed by confocal images, where samples were analysed by FUN-1, a fluorescent stain. Based on the provided results in section 3.1, following initial conidial seeding, there was a lag phase of approximately 8 hr (conidial adhesion and germination) before the hyphae began to intertwine forming a monolayer (8-20 hr) followed by increased structural complexity over the subsequent 16 hr. With maturity of the biofilm structure, the hydrophobic EPS concentration is increased (Sheppard and Howell, 2016). This cohesively bound the hyphae together. The EPS possess mannose and glucose residues. At 48 hr of growth, a highly branched mycelium was observed, and the production of EPS increased. The biofilm formation is known to increase with the duration of culturing. In this section, the confocal microscopy images showed that the number of hyphae structures as well as EPS formation diminished in triclosan MIC-treated samples in comparison to the AMB MIC-treated and the untreated control groups (figure 3.35). Although, the number of

impaired and dead hyphae were more in the both treated samples than the untreated control group. Confocal microscopy was also applied to assess triclosan and AMB activity by measuring hyphal length. Hyphal length assays showed that triclosan treatment of the fungus was far more effective at inhibiting hyphal growth than addition of AMB (figure 3.35). The biofilm thickness for triclosan-treated and the combination-treated test groups were 170 μm and 190 μm, respectively. This was 230 μm for both AMB-treated and untreated control test groups (figure 3.36).

Taken together, the confocal results demonstrated that the length of the hyphae and the biofilm thickness were decreased and the EPS production was inhibited more efficiently in triclosan treated samples compared to the AMB-treated, combination-treated and untreated control group tests. However, the sequential combination treatment (triclosan following with AMB), which contains sub-MIC doses of triclosan and AMB, reveals a synergistic interaction between them. This combination showed antifungal effects by diminishing the EPS production and the biofilm depth, as compared with addition of AMB, as a single agent. Considering adverse effects of AMB on human health, reducing its effective dose, while achieving more antifungal effect is beneficial.

Expression of the genes coding the two main carbohydrates, α-(1,3) glucans and GAG, in *A. fumigatus* cell wall was also studied. For that, expressions of *ags3* and *sph3*, which involve in α(1–3)-glucan and GAG biosynthesis respectively, were analysed using RT-PCR method (figure 3.38).

Cell wall α-(1,3) glucans play an essential role in conidia aggregation in a liquid medium, Sabouraud medium (Fontaine et al., 2010; Henry, Latgé and Beauvais et al., 2011). In particular, three α(1–3)-glucan synthase genes, *ags1*, *ags2*, and *ags3*, have been identified and were found to be responsible for cell wall α(1–3)-glucan biosynthesis. The *Δags1* and *Δags2* strains were not defective in virulence (Beauvais et al., 2005), while the *Δags3* mutant was hypervirulent in an experimental mouse model of aspergillosis (Maubon et al., 2006). In *A. fumigatus*, the triple *ags* deletions do not show a distinct growth phenotype in vitro (Henry, Latge and Beauvais, 2011)

EPS, a hydrophobic matrix, cohesively binds hyphae together in the biofilm structure. GAG is a major polysaccharide of the in vivo *A. fumigatus* EPS (Loussert et al., 2010). GAG plays a critical role in the maintenance of the EPS of *A. fumigatus* biofilms.

Strains deficient in GAG production fail to produce EPS and are unable to form adherent biofilms on plastics or host cells in vitro (Gravelat et al., 2013). Enzymatic activity of *sph3* is required for the synthesis of functional GAG (Bamford et al., 2015).

RT-PCR results revealed that α(1–3)-glucan and GAG production were down- regulated in AMB- and triclosan-treated test groups. As mentioned earlier, α(1–3)-glucan, as a major cell wall polysaccharide in *A. fumigatus*, is involved in conidia aggregation; its absence affects microcolony formation stage of biofilm formation. GAG is involved in EPS production and its absence lead to a reduction in biofilm attachment to the biotic or abiotic substrates. GAG-mediated adherence is largely a consequence of charge-charge interactions between the polycationic polysaccharide and negatively charged surfaces (Lee et al., 2016).

It has been shown that the deletion of one cell wall gene does not only result in the loss of the encoded gene's product but leads to a complete restructuring of the fungal cell wall (Beauvais et al., 2013). α(1–3)-glucan normally covers β-(1,3)-glucan and chitin (Alsteens et al., 2013). So, lack of α-(1,3) glucan is compensated by an increase in β-(1,3) glucan and/or chitin content, while does not affect conidial germination or mycelial vegetative growth (Henry, Latge and Beauvais, 2011). As α-(1,3) glucan absence does not result in cell death, putative drugs which trigger α-(1,3) glucan regulation in the cells can be considered as QQrs.

In vivo studies have been revealed that in *Δags* strains, the surface rodlet layer on the resting conidia during vegetative growth is masked by a layer of glycoproteins. This hydrophilic layer of glycoprotein oversees the initiation of pro-inflammatory cytokine production immediately after conidial phagocytosis. This leads to conidial death during germination phase of its growth (Beauvais et al., 2013). In vitro effect of *ags3* down regulation on *A. fumigatus* biofilm formation can be explained via formation of a hydrophilic layer of glycoprotein on top of the cell wall rodlet layer upon α(1–3)-glucan absence on the conidia cell wall. This alteration on the cell wall charge will lead to hetregenicity and hence reduce conidia aggregation. As this mutant reveals its effect on the resting conidia during its vegetative growth, the conidia attachment to the surfaces is not affected by this mutant.

Taken together, due to triclosan and AMB adverse effects on the human health and environment reducing their effective doses would be ideal. The combination of sub-MIC levels of AMB and triclosan against *A. fumigatus* showed a decrease in EPS production and biofilm depth as compared with the AMB at its MIC_{50}. Triclosan revealed the least biofilm depth and no EPS structure was formed in the samples treated with triclosan MIC. QQ activity of triclosan against bacteria has been described through inhibition of acyl-homoserine lactone molecules (AHLs) synthesis, while its QQ mechanism in filamentous fungi is not known yet. In *A. fumigatus* triclosan down-regulated two major conidia cell wall polysaccharides (α(1–3)-glucan and GAG) which are acting through changing conidia cell wall charge and hence interrupting the conidia aggregation, EPS production and biofilm formation.

3.3 Analysis of the antimicrobials' effect on *A. fumigatus* conidia attachment to the hydrophobic and hydrophilic surfaces

3.3.1 Introduction

Biofilm formation cycle which could initiate the disease process include detachment of cells or cell aggregates, production of endotoxin, improved resistance to the host immune system, and provision of a niche for generation of resistant organisms. The unique and persistent nature of biofilms should be considered to find efficient strategies to prevent or control biofilms on medical devices. Recent intervention strategies are designed to avoid initial device colonization, minimize microbial cell attachment to the device, penetrate the biofilm extracellular polymeric substances (EPS) and destroy the related cells, as well as remove the device from the patient or to treat based on inhibition of genes involved in cell attachment and biofilm formation (Donlan and Costerton, 2002). For example, to hinder biofilm formation on urinary catheters, following control tactics have been used: bladder instillation or irrigation, antimicrobial ointments and lubricants, impregnating the catheter with antimicrobial agents (silver oxide), using systemic antibiotics for prophylaxis in catheterised patients and antimicrobial agents in the collection bags (Kaye and Hessen, 1994). Sedor and Mulholland (1999) noted that the material of catheter construction might be important too; in patients prone to catheter encrustation, silicone catheters obstruct less often than latex, Teflon, or silicone-coated latex (Sedor and Mulholland, 1999).

Using non-biocidal approaches could be counted as a new defensive strategy to prevent catheter colonisation and catheter-related bloodstream infection (CRBSI). Examples include:

Treatment of abiotic surfaces through the adsorption of different bacterial polysaccharides, which have a long-lasting anti-adhesive effect and significantly inhibit mature biofilm development in a broad spectrum of pathogenic bacteria (Chauhan et al., 2014).

Using non-leaching polymeric sulfobetaine (polySB), which coordinates water molecules on the catheter surface. It reduces in vitro and in vivo microbial cell adherence on both the external and the internal surfaces of polySB-modified catheters compared to unmodified catheters (Smith et al., 2012).

Coating of Totally Implantable Venous Access Ports (TIVAP) by methylcellulos, a

polymer with both eukaryotic and bacterial cells anti-adhesive property. This is effective to reduce in vivo adhesion and hence biofilm formation of *P. aeruginosa* and *S. aureus* (Chauhan et al., 2014).

Prophylaxism in urinary catheter could be used to contaminate the catheter by a preventive microbiota that would interfere with pathogenic bacteria colonization (Gominet et al., 2017). Indeed, adhering appropriate bacteria can prevent entry of inbound bacteria into the already formed biofilms layer through several mechanisms comprising downregulation of adhesion and biofilm formation genes; release of molecules interfering with bacterial QS; degradation of components of the matrix; and production of dispersion signals (Rendueles and Ghigo, 2012 and 2015).

Contact angles are typically measured simply by depositing a drop of liquid on a given solid surface following with placing a tangent to the drop at its base using a so-called goniometer (the sessile drop technique) (Busscher et al., 1984). Apart from the subjectivity of the technique, it normally yields contact angle accuracy of no better than ±2°. This technique does not reflect the complexities of solid-liquid interactions (Mittal, 2000).

3.3.2 Results

3.3.2.1 Investigating the effect of the agents on dynamic nature of the variety of abiotic surfaces

To determine the hydrophobicity of the selected materials, contact angles of a water drop on the solid surfaces (Glass, acrylic, HDPE, Nylon 6, PTFE, silicone and UPVC), covered with agents were investigated (figures 3.39 and 3.40 and table 3.13).

The results showed that among the surfaces, UPVC's hydrophilic surface turned hydrophobic after coating with AMB, which theoretically should attract the hydrophobic conidia. While hydrophobic surfaces (PTFE and silicone) coated with farnesol became hydrophilic which supposedly should repel the hydrophobic conidia.

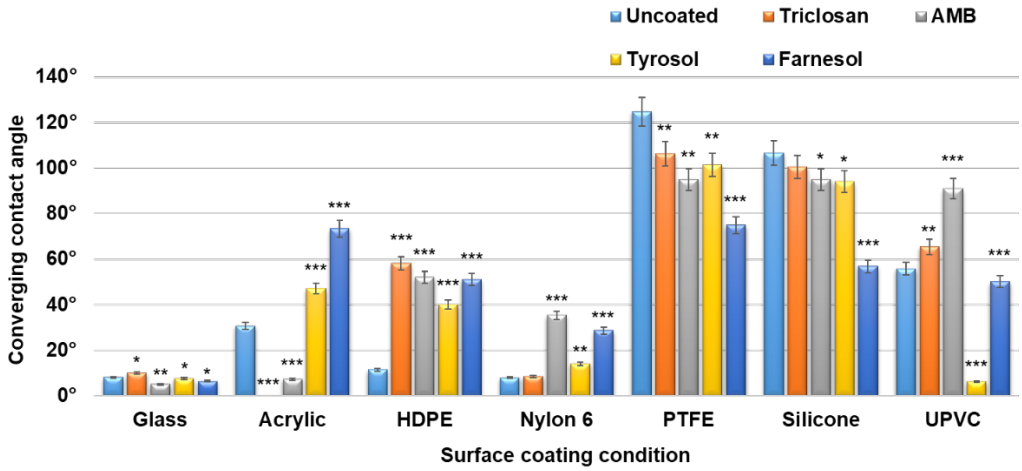

Figure 3.39 Angle values for the treated surfaces with triclosan, AMB, tyrosol, and farnesol. Hydrophobic surfaces have the property of repelling water, which means they do not easily become wetted in contact with water (contact angle ≥ 90°) (SEM bars are shown for n = 3)

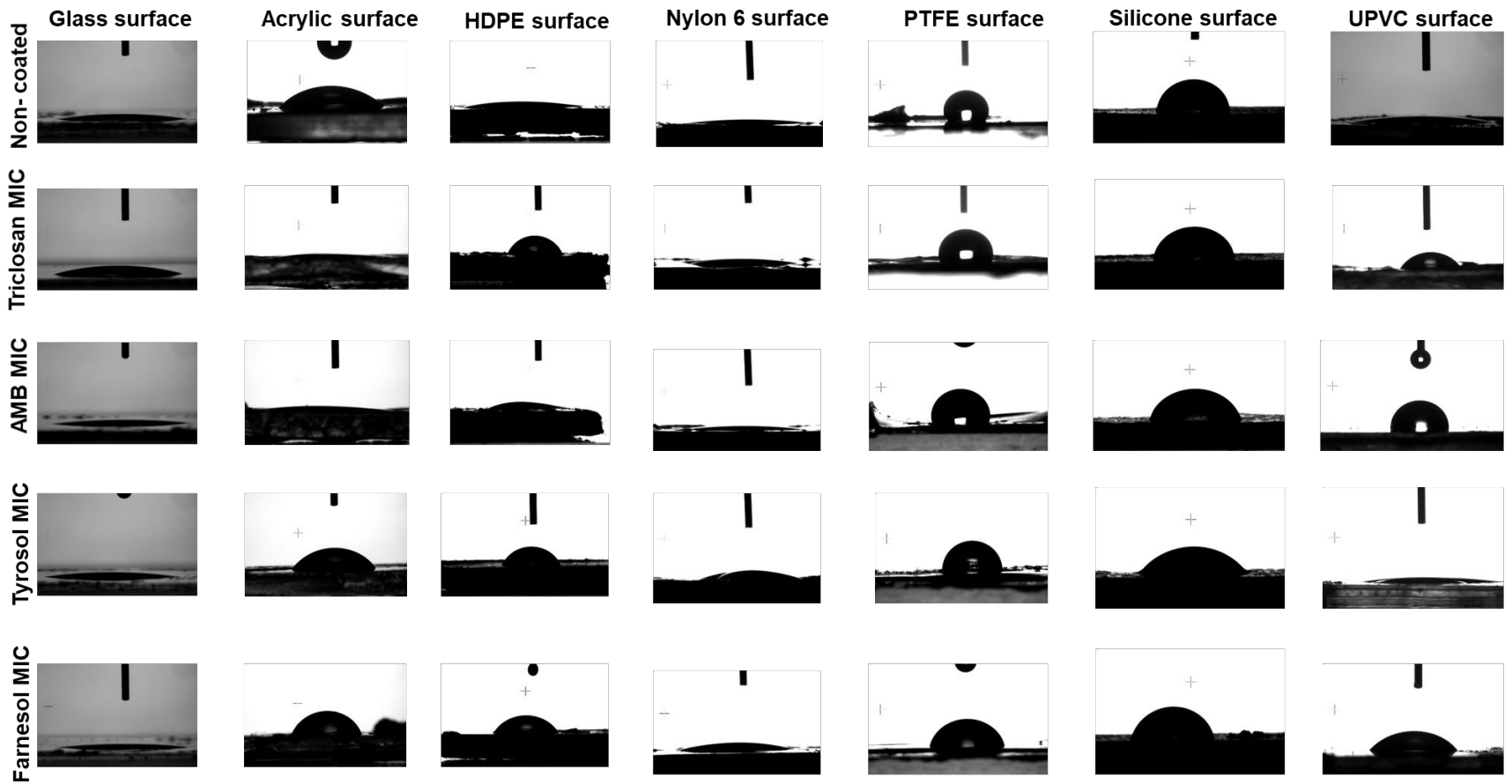

Figure 3.40 Water droplet contact angle measurement on different surfaces

Table 3.13 Dynamic natures of the surfaces when coated with the selected agents (n = 3)

	Uncoated	Triclosan	AMB	Tyrosol	Farnesol
Glass	Super hydrophilic	Super hydrophilic	Super hydrophilic	Super hydrophilic	Super hydrophilic
Acrylic	Hydrophilic	Super hydrophilic	Super hydrophilic	Hydrophilic	Hydrophilic
HDPE	Super hydrophilic	Hydrophilic	Hydrophilic	Hydrophilic	Hydrophilic
Nylon 6	Super hydrophilic	Super hydrophilic	Hydrophilic	Hydrophilic	Hydrophilic
PTFE	Hydrophobic	Hydrophobic	Hydrophobic	Hydrophobic	Hydrophilic
Silicone	Hydrophobic	Hydrophobic	Hydrophobic	Hydrophobic	Hydrophilic
UPVC	Super Hydrophilic	Hydrophilic	Hydrophobic	Super hydrophilic	Hydrophilic

3.3.2.2 Microscopic comparison of *A. fumigatus* biofilm formed on uncoated PTFE and farnesol- coated PTFE surfaces in transmission flow-cell

As reported in section 3.3.2.1, PTFE is a hydrophobic surface and attracts the *A. fumigatus* conidia. Two pieces of PTFE were cut to 75 mm × 25 mm size (the standard size of microscope slides) and one of them coated with farnesol. Using flow-cell device, the *A. fumigatus* biofilm was formed in 48 hr on them and compared morphologically by microscopic analysis. The flow-cell device can mimic the in vivo condition through the flowing of the PDB medium over the applied surfaces. Figure 3.41 shows hyphal interwoven structures on the uncoated PTFE surface is more than farnesol- coated PTFE surface.

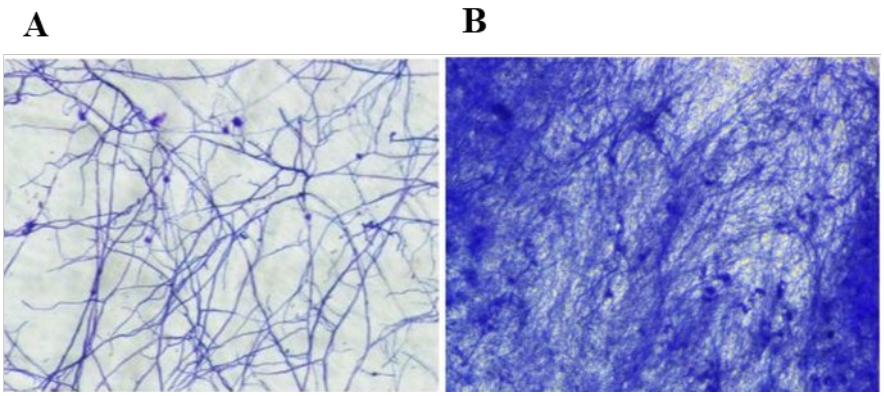

Figure 3.41 Flow-cell device analysis of (A) a PTFE surface coated with farnesol and (B) an uncoated PTFE surface. Cv (%0.5 w/v) dye was applied on the surfaces after 48 hr of incubation with the fungus conidia in the flow-cell device (100X magnification)

3.3.2.3 Screening *A. fumigatus* biofilm formation on agents-coated UPVC surfaces in transmission flow-cell

UPVC coupons were prepared in size 75 mm × 25 mm. One of them was used as the uncoated control and the other was coated with the agents for two days at room temperature. In section 3.3.2.1 UPVC coated with AMB showed hydrophobic nature. Figure 3.42 shows photomicrographic images of *A. fumigatus* biofilm on UPVC surfaces coated with the agents (uncoated UPVC surface was used as the control). The surfaces were incubated for 48 hr at 37°C in a flow-cell device while inoculated PDB medium passed over them. Tyrosol-coated UPVC surface showed super hydrophilicity as well as the uncoated UPVC surface, hence repelled the conidia and no biofilm formed on it, while AMB-treated surface attracted conidia and formed a proper substrate for their growth.

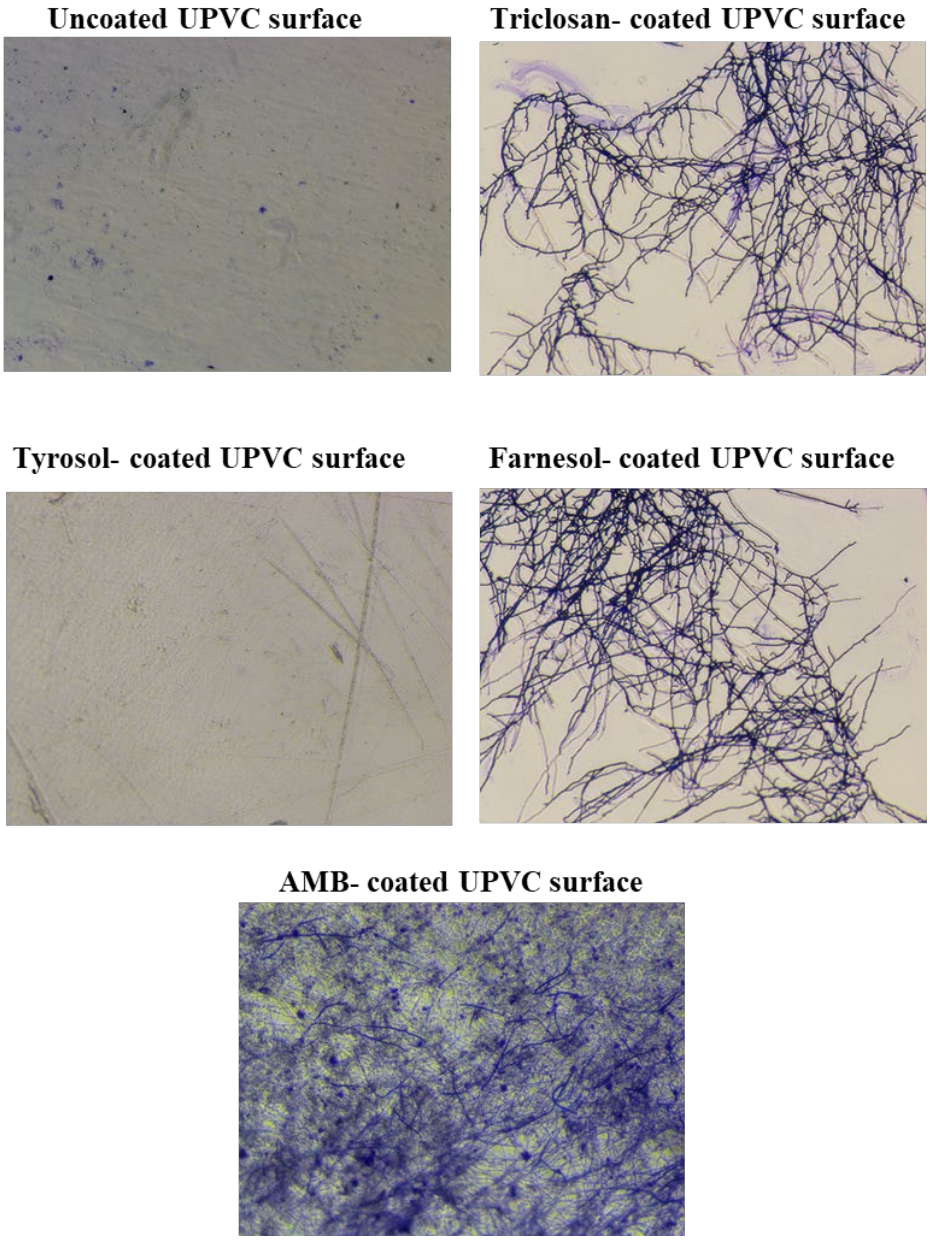

Figure 3.42 Flow-cell device analysis of *A. fumigatus* growth on UPVC surfaces coated with triclosan, AMB, tyrosol and farnesol. Uncoated UPVC surface was considered as positive control (100X magnification)

3.3.2.4 Investigating the effect of the agents on dynamic nature of the conidia surfaces

MATH hydrophobicity measurement is based on determination of microbial hydrophobicity by differential partitioning at an aqueous-hydrocarbon interface and the results yield the hydrocarbon interaction affinity of the microbes. PBS was used as a negative control, and *A. fumigatus* strain was used as a positive control. In *A. fumigatus* biofilm formation, prior to beginning conidial germination, the conidia surface is markedly hydrophobic and is composed of 40% hydrophobic methyl groups.

The data demonstrated that *A. fumigatus* conidia become more hydrophilic after treatment with effective doses of the applied agents (Figure 3.43).

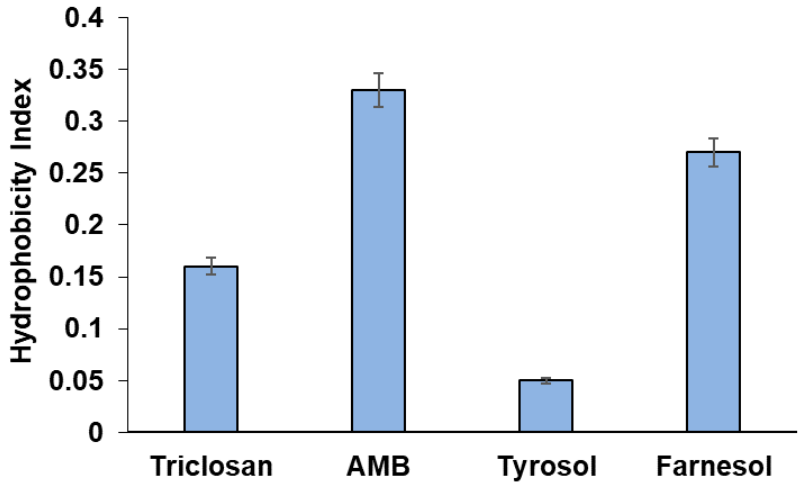

Figure 3.43 MATH assay analysis of the conidial hydrophobicity after treatment with the agents. The treated samples have been normalised based on control (untreated fungus). The assay indicates that after treatment with the agents, the surfaces of aerial conidia were clearly hydrophilic and did not distribute into the organic phase and predominantly localized at the aqueous phase (HI < 0.7) (section 2.7.5.3 for the equation 4) (SEM bars are shown for n = 3)

3.3.2.5 *A. fumigatus* mycelia proteins extraction for the protein quantity assay

Agar plates were prepared as explained in the layout:

Two sets of PDA plates were prepared

- Agar plates supplemented with the agents. Untreated inocula (100 µL) were added to the plates
- Agar plates prepared without the agents. Agents-treated inocula (100 µL) were added to the plates

The Petri dish plates were incubated for one week and then, mycelial proteins were extracted (section 2.7.5.4). The proteins were quantified based on the standard curve (appendix 2, figure 1B) and the results are provided in figure 3.44.

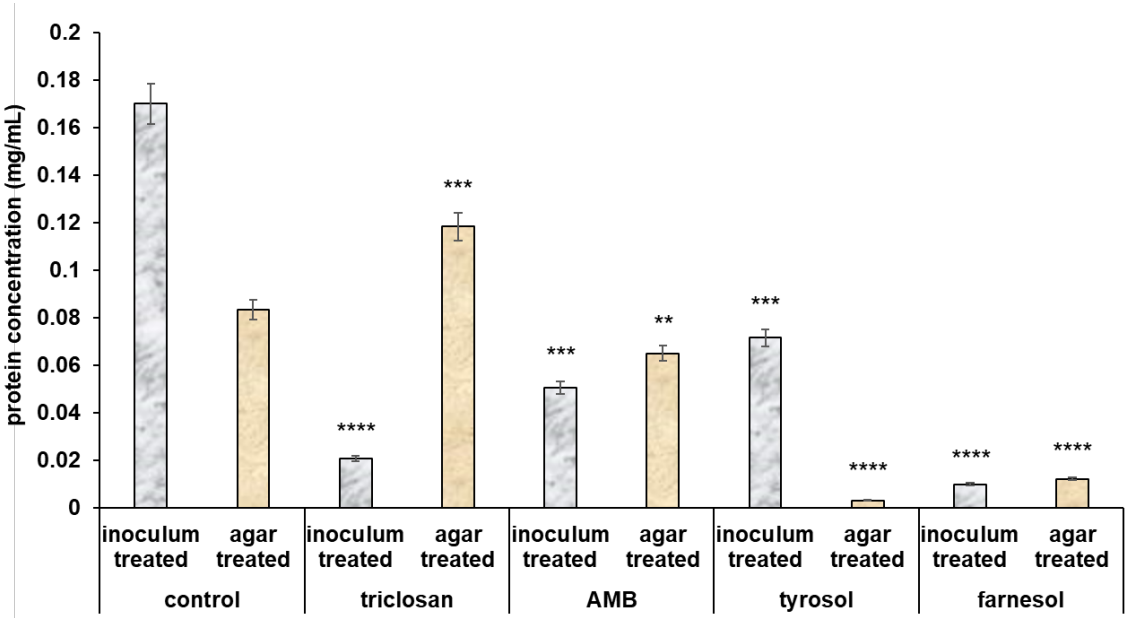

Figure 3.44 Total protein quantification under two conditions: inocula were treated with agents at their MICs levels and added on PDA (100 µL) vs. agars treated with agents at MICs following with addition of untreated inocula (100 µL). Control groups applied for both groups. ***P ≤ 0.001 and ****P ≤ 0.0001 (SEM bars are shown for n = 3)

3.3.2.6 The antimicrobials' effect on the *A. fumigatus* conidia surface hydrophobins, *rodA* expression

Conidial surface proteins were extracted a described in section 2.7.5.5 and purified using acetone precipitation. A 2-D SDS-PAGE experiment was used for analysis of conidial surface proteins from *A. fumigatus* with or without treatment with the agents. The purified proteins migrated as a major protein band in SDS-PAGE. This fraction showed two bands with an apparent molecular mass of 16-kDa described RodA protein in the presence of triclosan and tyrosol but not in the presence of AMB, farnesol, and in the absence of the agents (figure 3.45A). Using graient gel, the bands observed in the control group as well as triclosan-, AMB-, and tyrosol- treated groups, while no band was observed in the farnesol-treated sample (figure 3.45B).

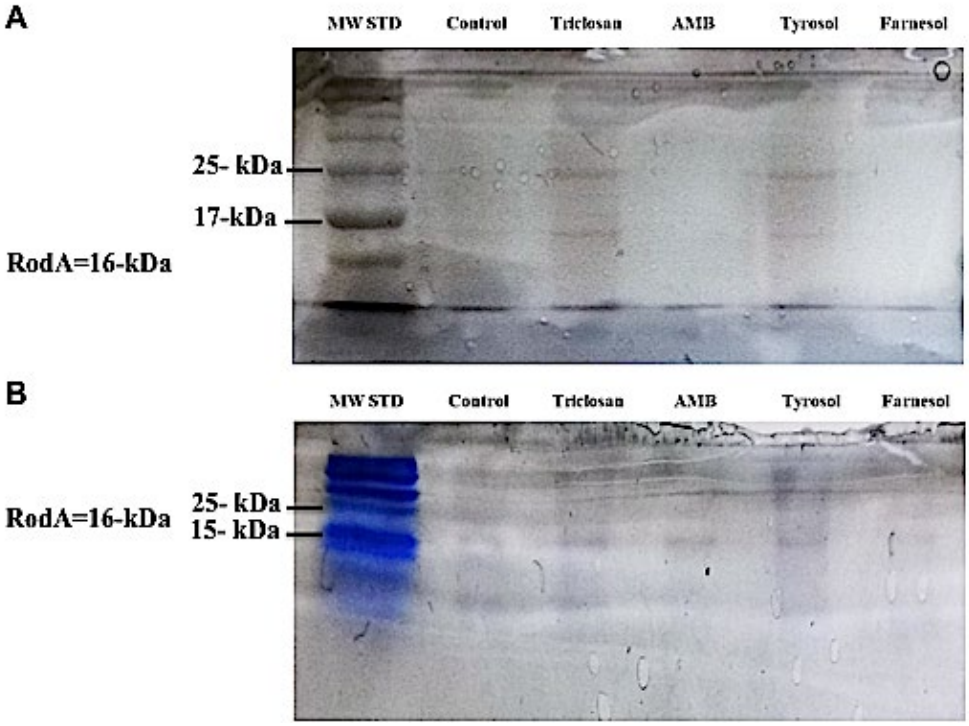

Figure 3.45 SDS-PAGE analysis of RodA protein in treated and untreated control *A. fumigatus*, separated by one-dimensional-polyacrylamide gel electrophoresis using A) 12% gel ad B) gradient gel (4% v/v and 20% v/v polyacrylamide). Proteins stained with silver nitrate solution. Based on the gradient gel, there was no band for farnesol-treated test group. Sodium dodecyl sulphate molecular weight standard (MW STD)

3.3.3 Discussion

The outermost cell-wall layer of the *A. fumigatus* conidium is characterized by the presence of interwoven rodlet fascicles. This layer, which is composed of hydrophobic proteins (hydrophobins), confers hydrophobic properties to *A. fumigatus* conidia. Based on the hydrophilic or hydrophobic property of the surfaces, conidia may be repelled or attracted to them, respectively. The hydrophobicity of the surfaces was confirmed based on the water contact angle (WCA) measurement (section 3.3.2.1). Electrostatic forces are important for the interaction between hydrophobins and polar surfaces. The binding and resulting WCA values are highly dependent on the ionic strength of the solution (Grunér et al., 2012). The surface wettability is mostly measured by means of water contact angle on a solid surface. When the water contact angle is >150, the surface becomes superhydrophobic (Falde et al., 2016).

The microscopic analyses showed that the *A. fumigatus* biofilm formed in flow-cell transmission in 48 hr produced an extensive firmly adherent mycelial growth on the PTFE surface (hydrophobic) and, also, showed that the hyphae was totally embedded in the EPS. While no EPS structure was found on the farnesol-coated PTFE surface (hydrophilic) (figure 3.41).

A. fumigatus conidia adhesion occurs more often to hydrophobic surfaces than to hydrophilic ones. It has been shown that binding onto submerged polar surfaces occurs by self-assembly and that the binding can result in a significant increase in water contact angle of the surface, hence making it more hydrophobic. Briefly, charged residues opposite of the hydrophobic patch (described in section 1.7.3) of the hydrophobins are thought to interact with the solid polar surface in such a way that the hydrophobic patch is turned outwards against the solution resulting in a hydrophobic surface coating (Grunér et al., 2012).

AMB coating of UPVC led to a change in the surface property from hydrophilic to hydrophobic (table 3.13). The microscopic analysis of the biofilm formed in flow-cell transmission after 48 hr confirmed the contact angle results (figure 3.42). On the UPVC surface coated with AMB cell attachment and biofilm structure were formed in the higher extend than the UPVC surfaces coated with the other agents. The hyphal network appeared less dense with less conidiation of *A. fumigatus* on all triclosan- and farnesol-coated than the AMB- coated UPVC surfaces at 48 hr.

In the biofilm formation process, the initial adhesion of the conidia on a bio- or non-bio surface is a critical step. So, finding a way to diminish this attachment could be counted as a preventive strategy to control biofilm formation. The contact angle measurement assay demonstrated that apart from UPVC, silicone and PTFE the agents do not change the property of the surfaces (table 3.13).

To study the agents' effect on conidial surface hydrophobicity, MATH assay was carried out (figure 3.43). The results showed a transformation of the treated conidia from hydrophobic to hydrophilic. Therefore, except for PTFE and silicone, which are hydrophobic surfaces, a repellent interaction is expected to happen between the conidia treated with the agents and the surfaces.

The structure of the cell wall of conidia and mycelia is different (Beauvais and Latgé, 2018). For protein analysis of the mycelia cell wall, mycelia cell wall protein extraction and quantification were carried out. To study agents' effect on mycelia attachment to a surface, agar plates were prepared in two sets. One set was treated with the agents and the other was left untreated but treated inocula were added to them. Figure 3.44 shows that although in all the plates the inhibitory effects against *A. fumigatus* were significant as compared with their controls, when triclosan, AMB and farnesol were added to the inocula they showed stronger inhibitory effect compared to the agar treated cases. As regards tyrosol, agar treatment revealed better effect. Agar is a hydrophilic colloid extracted from certain marine algae of the class Rhodophyceae (Selby and Whistler, 1993). This inhibitory effect, which was recognised through lower concentrations of the mycelia cell wall protein, led to diminished attachment of the mycelia to the agar. Taking together, treatment of conidia/agar with the agents were both led to form mycelia with lower protein concentrations than the untreated conidia/agar.

In *A. fumigatus* hydrophobic rodlet layer-forming gene (*rodA*) encodes the rodlet protein. Absence of this rodlet layer results in the formation of conidia that become more hydrophilic than the conidia of the parental strain (Girardin et al., 1999). Voltersen et al., (2018) performed liquid chromatography-tandem mass spectrometry (LC-MS/MS) analysis on conidial cell wall proteins extracts. They studied proteins located in the cell wall, containing GPI-anchored proteins and proteins exposed on the conidia surface. Among all types of proteins, RodA was found to be the most abundant protein (Voltersen et al., 2018). They also identified a novel protein, conidial cell wall protein A (CcpA) to

be nearly as abundant as RodA. CcpA encodes a protein with molecular mass, 25.7 kDa. Based on their report, CcpA demonstrated a role in virulence and conidial innate immune recognition but was not linked to cell surface structure. In this study, conidial surface proteins were extracted (section 2.7.5.5). Then, SDS-PAGE analysis was performmed to study the agents' effect on RodA protein availability in the extracted proteins from the conidial cell wall. The results showed that RodA protein were absent in the farnesol-treated test group (figure 3.45). Thus, farnesol might affect the hydrophobins (or their hydrophobic patches, exclusively) through, for example, inhibition of their expression or translation.

Chapter 4

General discussion

Figure 4.1 shows *A. fumigatus* general growth stages.

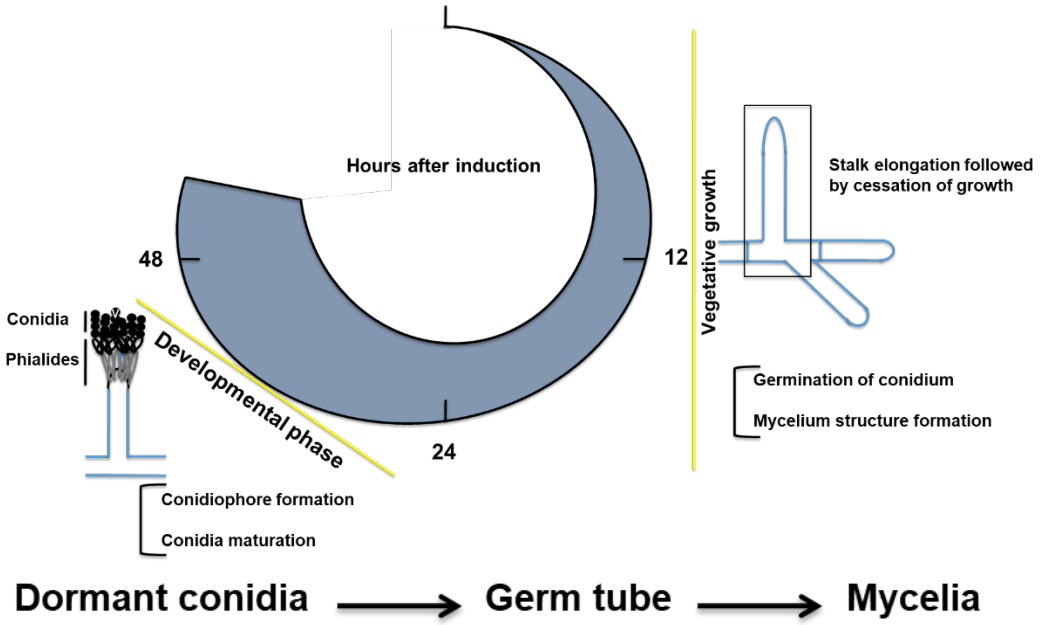

Figure 4.1 *A. fumigatus* growth stages in PDB medium

Dormant conidium starts to grow isotropically 2 hr after inoculation in liquid/broth medium. The first morphological change in spore germination is isotropic growth (also called swelling) (Leeuwen et al., 2013). The transcriptome of conidia changes dramatically, during the early stage of germination. Initiation of protein synthesis and respiration are important at this stage. Synthesis of ingredients for metabolic activities such as DNAs, RNAs, and proteins are initiated during isotropic growth, as well (Mirkes, 1974, Osherov and May, 2000). Isotropic growth is followed by polarised growth resulting in germ tube formation after 6hr of incubation (Leeuwen et al., 2013). Next, establishment of cell polarity, and formation of a germ tube are happening.

This study employed the use of five antimicrobials; triclosan, furanone, AMB, tyrosol and farnesol, which except for furanone the rest showed antifungal activities against *A. fumigatus* (table 4.1).

Table 4.1 Agents' effects on *A. fumigatus* conidia and mycelia

AMB	
Total protein concentration	Decreased during stationary phase (late developmental phase), which might be through chitinase and β(1–3) endoglucanase down-regulation or degradation.
Conidia viability	The least among the agents.
Apoptosis	Happens at the late developmental phase. So, biofilm structure has already formed, and cell components released to the extracellular environment can be captured in the biofilm.
Down- regulation of α-(1,3)-glucan synthesis	Led to increase in mycelial chitin content.
Down- regulation of GAG synthesis	EPS structure was not affected. So, an alternative potential molecule might replace the GAG role in EPS formation
Biofilm	Biofilm not affected as the released cell components were captured in the biofilm structure and revealed the highest biomass concentration among the agents, as compared with the untreated control group.
Triclosan	
Total protein concentration	Decreased during log phase (early developmental phase).
Conidia viability	The highest among the agents.
Necrosis	Happens at the early developmental phase. Led to increasein chitinase activity, hence cell wall disruption and less chitin availability in mycelia cell wall.
Down- regulation of α-(1,3)-glucan synthesis	Unlike AMB, mycelial chitin content did not increase due to necrosis- induced chitinase activity. So, conidia cell wall (re)structuring and aggregation were inhibited.
Down- regulation of GAG synthesis	Mediating conidia (mycelia) attachment to negatively charged surfaces. Resulted in less conidia (biofilm) attachment and EPS production.
Quorum quenching role	Inactivating QS signalling pathway.
Tyrosol	
tal protein concentration	Decreased during stationary phase (late developmental phase). Might be through chitinase and β(1–3) endoglucanase down-regulation or degradation.
Necrosis	Led to increase in chitinase activity; cell wall disruption led to less chitin availability in mycelia cell wall.
Farnesol	
Total protein concentration	Decreased during stationary phase (late developmental phase). Might be through chitinase and β(1-3) endoglucanase down-regulation or degradation.
Necrosis	Led to increase in chitinase activity; cell wall disruption led to less chitin availability in mycelia cell wall.
Down- regulation of rodlet protein synthesis	Resulted in hydrophilic conidia unlike untreated conidia, which hydrophobic.

4.1 Protein release at the developmental phase in the treated cultures of *A. fumigatus*

The viability of the fungal cells was half of the untreated control group (the agents were applied at their MIC_{50} levels) after 18 hr of incubation, while their protein concentrations were not significantly affected by the antimicrobials (except for triclosan, $*P \leq 0.05$) as compared with the control, after 16 hr of incubation (figure 3.14).

Total protein concentration was affected by triclosan during the log phase, and by AMB, tyrosol and farnesol during the stationary phase of the *A. fumigatus* growth (figure 3.14). Thus, considering any roles for proteins in conidial attachment to the surfaces, triclosan affects conidial attachment while tyrosol and farnesol restrict biofilm formation and maturation (it has been explained in section 4.4 that the biofilm production was not interrupted by AMB).

One possibility is that biosynthesis of a protein molecule under treatment by the agents could be responsible for the reduced viability of the culture through apoptosis or necrosis. At later stages of development, the growth rate of the germ tube increases, and the functional organisation of the hyphal tip area acquires its full potential. A fungal mycelium is established through branching and inter-hyphal fusions (Glass, 2004). Developmental phase includes the log (exponential) phase and the stationary phase, when the fungus growth curve is studying. Exponential growth of *A. fumigatus* (figure 3.5) was initiated after 8 hr of inoculation and entered stationary phase after 20 hr as determined by optical density at 590 nm.

It has been revealed that mitogillin, chitosanase and aspergillopepsin are three major proteins secreted by *A. fumigatus* during the log phase of growth under different growth conditions (Schwienbacher et al., 2005). Chitinase and β(1–3) endoglucanase are also produced at late developmental phase (the stationary phase). As these proteins are not GPI-anchors to the cell wall, cell wall reorganization which happens at stationary phase (Schwienbacher et al., 2005) may let them release to the extracellular environment. Thus, increase in the amount of proteins in the untreated control group over the time, could be applicable to these proteins production during log and stationary phases. Effect of tyrosol on the permeability of the cell membrane of dimorphic fungi is known already (Brilhante et al., 2016). Tyrosol acts on the fungal membrane through reducing the ergosterol content of the fungal cell wall and hence causes release of intracellular molecules (Brilhante et al., 2016). We have demonstrated that the protein release can occur in *A. fumigatus* treated

with triclosan and AMB and to a lesser extent with farnesol, as well (Table 3.4). Total protein decrease was happened during the period from 16 hr to 28 hr in tyrosol- and in a lesser extent in farnesol- treated samples. This could be explaind through tyrosol and farnesol effect on causing protein degradation at the stationary phase and that the Bradford assay does not quantify the protein degradation products.

4.2 Antifungal effect of triclosan, tyrosol and farnesol on *A. fumigatus* is through chitinase-involving necrosis induction

Based on the NanoDrop assay, eDNA release has happened in all the treated cultures, remarkably in tyrosol- treated samples in comparing with the untreated control test group (table 3.6). The QS system plays critical roles in the adaptation of microbes to the surrounding environment. One of the consequences of QS, which helps microbial cells to adapt to the environmental stresses, is producing biofilm structures. As mentioned earlier, biofilms are communities of microbes encased in a matrix of extracellular DNA (eDNA), exopolysaccharides and proteins (Harmsen et al., 2010). Rajendran et al., (2013) have explained mechanisms of eDNA release in eukaryotic cells as active secretion, necrosis, and apoptosis, with the possibility of more than one pathway being involved (Rajendran et al., 2013). This includes autolysis as another possible mechanism for the release of local eDNA. eDNA release in biofilms promote microbial biofilm formation and plays an important role in biofilm resistance to antifungals. Therefore, QS mechanism inducing a programmed cell death through autolysis (Pang et al., 2016; Zemke and Bomberger, 2016) is in favor of biofilm formation and increase the resistance of the microbes against antimicrobial agents. So, the autolysis induced by QS is a programmed cell death. When the cells undergo treatment with the QQrs, the QS signalling is affected and therefore there is no biofilm structure to be conserved with the released eDNA.

In Mousavi and Robson's (2003) study, *A. fumigatus* was treated with AMB and agarose gel electrophoresis of the extracted *A. fumigatus* conidial DNA revealed smear DNA, which they counted it as a sign of apoptotic cell death (Mousavi, 2004). While, Ohyama et al., (2001) clarified laddering DNA, not smear DNA, as a sign for apoptotic cell death. This DNA laddering is not usually found when looking at DNA from intact cells or cells killed by necrosis, which contain only high molecular weight DNA or a smear of randomly degraded DNA, respectively (Ohyama et al., 2001). Table 4.2 shows main differences between necrotic and apoptotic cells.

Table 4.2 Molecular and phenotypic differences between necrosis and apoptotic-like programmed cell death (Collins et al., 1997)

	Induction stimuli	Morphological changes	Molecular changes
Necrosis	- Viral or chemical exposure - Radiation - Endogenous or pathological factors	-Before any significant alterations in nuclear morphology necrotic cells show early lysis of the plasma membrane - Necrotic cells initially swell before lysis - Necrotic cells eventually exhibit swelling of the nucleus	- DNA cleavage is occurred by random DNA fragmentation - Agarose gel electrophoresis demonstrates a "smear" on agarose gels
Apoptosis	- Chemotherapy - Oxidative stress - Death receptor ligands	- Apoptotic cells show cell shrinkage - Apoptotic cells exhibit characteristic nuclear morphological changes, like: - Chromatin condensation - Hyper segmentation of nuclear chromatin of irregular size - Hyper segmented nuclear structures may bud from the rapidly blebbing cell surface and form "apoptotic bodies"	- DNA cleavage is occurred at sites between nucleosomes, protein-containing structures in chromatin at ~200 bp intervals - Agarose gel electrophoresis demonstrates a "ladder" pattern at ~200 bp intervals

Based on the gel electrophoresis results (figure 3.19), AMB-treated samples revealed DNA smear assigned to necrosis. DNA extracted from *A. fumigatus,* at its stationary phase, and also when treated with triclosan and tyrosol formed no band in gel electrophoresis. Based on the other studies, DNA laddering was absent during cell death in *S. cerevisiae* and in *Pichia pastoris* (Martinet et al., 1999; Madeo et al., 1999), and also during cell death in the stationary phase in *A. fumigatus* (Mousavi & Robson, 2003). The absence of a DNA band for triclosan-treated sample and the sample taken from the stationary phase of the fungus growth could be due to the lower DNA content. Based on the NanoDrop results (figure 3.17), among the agents, triclosan and tyrosol showed the least amount of DNA in the treated samples compared to the untreated control group (**$P \leq 0.01$ and ***$P \leq 0.001$, respectively). The absence of the stationary phase-related *A. fumigatus* DNA band on the electrophoresis gel could be related to breaking the bonds between nucleotides in nucleic acids as a DNA cleavage activity of endonuclease (Nagamalleswari et al., 2017) or to the ratio of viable cells vs. dead fungal cells.

Fungal chitinases are secreted enzymes that play a role in the digestion of exogenous chitin or utilisation of fungal chitin for energy during necrosis (Rajendran et al., 2013). CFW staining assay performed after 36 hr of incubation revealed less chitin content in hyphae cell wall in triclosan-, tyrosol-, and farnesol-treated samples as compared with untreated control group. While chitin in AMB-treated samples were present in the mycelial cell wall (figure 3.23). Tyrosol and farnesol's role in chitinase secretion from the cell walls is already discussed in the section 4.1. Since chitinases are markers of necrosis (Rajendran et al., 2013), this process is a possible mechanism for eDNA release.

Accepting the apoptotic activity of AMB against *A. fumigatus*, Mousavi (2004) suggests the presence of two apoptotic-like pathways in *A. fumigatus*. The author showed increase in intracellular activity of caspase substrates, as cultures entered the stationary phase, which was different from the development of the apoptotic-like phenotype induced by AMB (Mousavi, 2004). However, it has been reported that fungi do not encode true caspases and "apoptosis" applied to fungi presumably has a different definition. Therefore, fungal-related caspases appear not to behave or to be regulated like mammalian caspases (Hardwick, 2018).

Taking the involvement of the two independent apoptotic- pathways into consideration, a caspase-independent manner might be involved in *A. fumigatus*. In this manner, like in mammalian cells, mitochondrial DNA fragmentation-inducing factor; EndoG and apoptosis-inducing factor (AIF) might be involved. These factors are released from mitochondria and then they induce DNA fragmentation (Kitazumi and Tsukahara, 2010).

Figure 3.25 shows the results for HPLC analysis of the agent's effects on *A. fumigatus* glucose uptake from the culture over 36 hr of incubation. Sampling was performed at three time points; 4- (germination phase), 18- and 36-hr (both are refered to as the developmental phase) of growth. In the untreated control groups, the glucose concentration showed decreased over the period from 4 hr to 36 hr of culturing, suggesting that glucose was transmitted from the culture to the fungal cells and consumed in the cells. Glucose uptake from the culture was decreased in triclosan- and tyrosol-treated samples over the time points of 18 hr to 36 hr. Triclosan and tyrosol, yet, showed better glucose uptake at around 18 hr than the other time points. In correlation with the results provided in table 3.4 and table 3.6, the decrease in the glucose uptake under triclosan and tyrosol at 36 hr and 4 hr and 36 hr, respectively, may be because of the cell wall disruption, and not the disruption of the cell wall glucose (sugar) transporter(s). Triclosan and tyrosol might promote glucose attachment to their transporters, but without crossing through the cell wall. In this situation, the glucose transference across the cell wall might be disrupted with triclosan and tyrosol, thus, resulting in depiction of decrease in glucose concentration. The following sampling from the cultures showed decrease in the glucose content. Then, following cell walls reorganisation at the stationary phase, the attached glucose was released from the transporters into the culture. This could explain the increase in the concentration of glucose in the culture at 36 hr. In correlation with the results provided in tables 3.4 and 3.6, at the stationary phase (36 hr), cell wall reorganisation was disrupted under triclosan and tyrosol treatment.

Glucose can act as a precursor for chitin biosynthesis in fungi (section 1.7). In *A. fumigatus*, unlike the other *Aspergillus* spp. (Wei et al., 2004; Dos Reis et al., 2013 and Sloothaak et al., 2015), there are no published reports on putative glucose transporters. In *A. niger*, glucose uptake is mediated by a high-affinity and a low-affinity transport system, while the latter is only evident at high glucose concentrations (15 %) (Torres et al., 1996). In humans, the SLC2 family glucose transporters (GLUTs) catalyse facilitative diffusion

of glucose and other monosaccharides across biomembranes (Hediger et al., 2013 and Mueckler and Thorens 2013). Structures of XylE, the *E. coli* homologue of GLUTs, are available in three states: ligand-bound and outward-occluded, inward-open and partly inward-occluded (Sun et al., 2012; Quistgaard et al., 2013 and Wisedchaisri et al., 2014). The conformation of the transporters at any of their states may be disrupted by chemicals and reagents. The effect of chemicals and reagents on GLUT3, which is stated to as the 'neuronal glucose transporter' and is also responsible for glucose uptake in circulating white blood cells, sperm and preimplantation embryos (Simpson et al., 2008), was further studied. It has been shown that D-glucose, D-galactose, D-mannose, D-xylose and D-fucose blocked more than 90% of the [^{3} H]glucose uptake activity, and L-arabinose and D-lyxose inhibited more than half of the activity of GLUT3. Among the chemicals tested, L-dehydroascorbic acid, as a substrate for GLUTs, effectively inhibited the counterflow of D-glucose by GLUT3 (Deng et al., 2015).

Figure 3.23 suggests that in AMB-treated samples, the cell wall glucose transporters' makeover at 36 hr could culminate in the uptake of glucose. The fungi cell wall reorganisation at its stationary phase is confirmed with the protein and DNA release results (Tables 3.4 and 3.6) in AMB-treated samples. Figure 3.23 confirms that, after 36 hr of treatment, the chitin content and hence the chitin precursor (glucose) availability was obvious in AMB-treated samples. In farnesol-treated samples, remarkably, glucose uptake was apparently the least at any of the applied sampling time points. Farnesol showed the least protein or DNA release (Tables 3.4 and 3.6) amongst the treated samples. Therefore, farnesol effect against *A. fumigatus* might be through inhibition of the glucose attachment to their transporters, rather than the disruption of the fungus cell wall integrity.

4.3 AMB-induced cell death in *A. fumigatus* is empowered when the persister cells initially been affected by triclosan

Table 4.1 shows that *A. fumigatus* treatment with AMB led to increase in mycelial chitin content. Since increase in chitin content may result in decreased antifungal sensitivity (Walker et al., 2008 and 2013), exposing *A. fumigatus* to AMB would increase the risk of fungus resistance against this agent. Reducing AMB's effective dose, may lead to increase in chitin content too. On the other hand, the use of sub-lethal concentrations of the antimicrobial may lead to increase in cell autolysis, eDNA release and biofilm formation in the microbial systems (Hsu et al., 2011). Accordingly, combination treatment seems

favourable. Triclosan at 15% of its MIC_{50}, and AMB at 20% of its MIC_{50} showed synergistic interaction to induce cell death in *A. fumigatus*. The fungus resistance against AMB alone, and the side effects of the individual use of triclosan and AMB on the environment and human health is another concern, which can be overcome through combination therapy.

Table 3.10 reports checkerboard assay results for sequential combination treatment of *A. fumigatus* with triclosan- AMB. Based on the checkerboard assay, a synergistic interaction exists between triclosan and AMB when they are applied at their sub-MIC_{50s}. The analysis performed based on CompuSyn software confirms the checkerboard results that triclosan, at 15% of its MIC_{50} and AMB, at 20% of its MIC_{50} can induce cell death in the fungus cells. This result become more valuable when the adverse effects of triclosan on human health and environment and AMB on human health are considered.

The reason of triclosan improving the AMB-inducing cell death could be due to triclosan effect on persister cells, which make them vulnerable to undergo apoptosis when AMB has been added to the culture. Persister cells can tolerate aggressive conditions (e.g. antimicrobial agents) and revive under their proper conditions (e.g. clearance of the antimicrobial agent from the environment). Persister cells usually contain $\leq$ 1% of the overall population. These cells that neither grow nor die in the presence of microbiocidal agents, are considered as a possible reason for drug resistance (Keren et al., 2004; Lewis, 2007). Persisters can endure drug concentrations much higher than the MIC_{50} and represent survivor cells, which are phenotypic variants of the wild-type rather than mutants (Al-Dhaheri and Douglas, 2009). Combination of triclosan-AMB revealed less viability (**$P \leq 0.01$) than the combination of AMB-triclosan, when they were added sequentially (figure 3.32).

Molecular characterization of apoptosis has been suggested to be related to a specific DNase (CAD, caspase-activated DNase), which cleaves chromosomal DNA in a caspase-dependent manner. CAD is synthesized with the help of ICAD (inhibitor of CAD) in proliferating cells. Cleavage of ICAD results in the release and activation of CAD, which induces DNA fragmentation (Kitazumi and Tsukahara, 2010). Thus, considering that AMB apoptosis is happening through the caspase pathway triclosan may influence ICAD (e.g. up regulate its expression) in the persister cells. As explained in section 6,

microscopic and molecular analysis can be performed to study apoptotic activities of the antimicrobials in the cells.

RT-PCR analysis (figure 3.38) revealed that in both triclosan- and AMB-treated samples α-(1,3)-glucan synthesis was down-regulated. In *A. fumigatus*, α-(1,3)-glucan accounts for 40% and 19% of the mycelial and conidial cell wall polysaccharides, respectively. α-(1,3)-glucan is a major adhesive involved in the aggregation of germinating conidia and in biofilm formation (Maubon et al., 2006) and is one the EPS components (Beauvais, Schmidt, and Guadagnini, 2007). Lack of α-(1,3) glucan affects neither conidial germination nor mycelial vegetative growth which are compensated by an increase in β-(1,3) glucan and/or chitin content (Henry, Latge and Beauvais, 2011). So, chitin synthesis in AMB-treated fungi (figure 3.23) (as discussed in section 4.2) could be a result of *ags3* down regulation. In triclosan-treated samples, on the other hand, β-(1,3) glucan content might be increased as a result of *ags3* down regulation; or the chitinases enhanced activity (as discussed in section 4.2) may degrade cell wall chitin. If the case of the second scenario, sever necrosis activity induced by triclosan in correlation with the *ags3* down- regulation prohibits both cell wall structuring and conidia aggregation. The necrosis induced by triclosan followed by necrosis (or apoptosis) induced by AMB can provide the synergistic interaction to reduce the cells' viability even at their sub-MIC_{50} levels.

4.4 Quorum quenching effect of triclosan on *A. fumigatus* through inactivation of QS signal

Figure 3.11 shows that *A. fumigatus* cultures treated with the agents (triclosan, AMB, tyrosol, farnesol) formed the same growth pattern as the untreated control group, although the cells viability was decreased at 590 nm under treating conditions. Accordingly, the agents showed QQ effect and acted by slowing down the growing stage of the fungus and reducing their metabolic activity, hence, suppressing their pathogenicity. Diminishing of metabolic activity has been reported for different microbes treated with triclosan, AMB, tyrosol and farnesol (Han, Cannon and Villas-Bôas, 2012; Cordeiro et al., 2015; Kovács et al., 2017; Westfall et al., 2019). QS signals contribute directly to pathogenesis due to the production of virulence determinants, such as toxins, proteases, and other immune-evasive factors. Targeting components of microbes that are responsible for pathogenesis makes QQrs better candidates compared to the agents with growth- inhibitory effects as microbes

can become resistant against these agents. It is not clear, however, if the lack of viability in the treated samples compared to the untreated control group was because of lack of cells attachment to the surface, or their dead by the agents.

Also, cv binding assay on the mature biofilm structure resulted in the least biomass production in the tyrosol-treated samples among the agents, which is in correlation with the flowcytometry results. However, AMB-treated cultures revealed highest biomass concentration. Cv does not measure the biofilm viability as it stains the microbial cells and the extracellular matrix (Welch, Cai and Strømme, 2012). CV binds to proteins, polysaccharides and nucleic acids (Kvasničková et al., 2016). As discussed in section 4.2, among the agents, the highest and the lowest eDNA release are from the cultures treated with tyrosol and AMB, respectively. Accordingly, AMB-related eDNA release was encapsulated in the biofilm structure, which means the biofilm production had not been interrupted by AMB. While in tyrosol-treated sample, no biofilm structure was formed to capture the released cell components.

PI-based flow cytometry analysis of the conidial viability (figures 3.20 to 3.22) revealed viability affected, from the most to the least, in triclosan- (MFI~52% more then control), tyrosol- (MFI~51% more than control), farnesol- (MFI~50% more than control), and AMB- (MFI~48% of the control) treated conidia. Persister cells (as discussed in section 4.3), likely, are affected by tyrosol but not by AMB, so, upon removal of AMB (or losing its effectivness), the persister cells can proceed growing.

Consequently, AMB reduced the conidial viability, whereas the viable (attached) conidia were able to form biofilm structure. eDNA released and captured in the biofilm structure in AMB-treated culture, so, the biomass seemed less affected in AMB compared to other agents; untreated samples formed the control group. Tyrosol, also, reduced the conidial viability, which led to less attached cells to the well bottom of well-plates where eventually less biofilm (biomass) structure was formed.

There has been no report so far on the effect of tyrosol on *A. fumigatus*. Cordeiro et al., (2015) have reported that exogenous tyrosol alone or combined with AMB inhibited planktonic cells as well as mature biofilms in *Candida* spp. However, tyrosol combined with azoles increased the biofilm formation in a dose-dependent manner (Cordeiro et al., 2015).

Triclosan effect on *A. fumigatus* is unclear, as well. As one of triclosan's commercial applications, triclosan is the active ingredient in Microban (Microban Products Co, Huntersville, N.C.). Microban provides resistance to growth of gram-positive and gram-negative bacteria, molds, and fungi (Lefebvre et al., 2001). While its mechanism of action has been studied in bacterial strains, there is a need for further studies in fungi.

Based on the previous studies (Stewart et al., 1999; Dong, Wang and Zhang 2007) and the results reported here, triclosan's QQ effects could be through two pathways:

1) *Inactivation of QS signal*: The QS signalling is initiated through cells accumulation. This accumulation is followed by auto inducers secretion. When the autoinducer's concentration reach at a specific threshold, the expression and the transcription of the selected microbial genes will be regulated. So, if an agent inhibits the cell communication it interferes with/inhibits QS signalling to initiate. It is found that α-(1,3) glucans interact among themselves and are accountable for the aggregation of swollen conidia without the involvement of any protein (Fontaine et al., 2010). As no protein is involved in conidia agglutination and this role is restricted to α-(1,3) glucan, the physical properties of insoluble α-(1,3) glucan are implicated in the conidial aggregation. RT-PCR results (figure 3.38) show that α-(1,3) glucan's expression was down-regulated in triclosan-treated sample.

Other examples of the agents, which inactivate the QS signals, are proteases in the case of enzymatic process and antibodies in the non-enzymatic case. Furanone, also, interfere (block) microbial QS signalling (Manny et al., 1997; Hentzer et al., 2002).

2) *Disruption of QS signal synthesis*: QQ activity of triclosan against gram-negative bacteria has been described through inhibition of acyl-homoserine lactone molecules (AHLs) synthesis. Therefore, triclosan blocks the metabolism of amino acids and fatty acids in the bacteria. One of the primary signals for *Aspergillus* spore and sclerotia development are oxylipins (oxygenated polyunsaturated fatty acids), which act as autocrine and paracrine mediators in eukaryotic organisms (Dagenais et al., 2008). In *A. flavus* and *A. niger* oxylipins have been suggested to regulate secondary metabolism and spore development via QS (Affeldt et al., 2012). Linoleic acid in *A. terreus* (Sorrentino, Roy and Keshavarz, 2010), γ-heptalactone in *A. nidulans* (Williams et al., 2012), and butyrolactone in *A. terreus* (Raina et al., 2012) are other known QSMs (also

known as secondary metabolite or autoinducer) in *Aspergillus* spp. The occurence of these QSMs has not yet been reported in *A. fumigatus*. However, gliotoxin has been reported as a secondary metabolite in *A. fumigatus*, where it has an important role in fungal pathogenesis and in modulating biofilm formation (Bugli et al., 2014).

Farnesol effects on different *Aspergillus* spp cultures through different mechanisms. Farnesol is reported to induce mitochondrial fragmentation, nuclear condensation and other signs of apoptosis in *A. nidulans* (Savoldi et al., 2008). While, in *A.niger* cultures, it shows no signs of apoptosis, but decreased in cAMP levels (Lorek et al., 2008). In *A. fumigatus*, farnesol disturbes the signalling pathway related to cell wall integrity (Dichtl et al., 2010). The previous studies have showed that combination of farnesol with antifungal drugs lead to a synergistic interaction (fractional inhibitory concentration index [FICI] of 0.5) in *C. posadasii* (Brilhante et al., 2013) and *H. capsulatum* (Brilhante et al., 2015). In general, no QQ role for farnesol has been defined yet.

4.5 Farnesol treatment of *A. fumigatus* conidia: *rodA* down-regulation, hydrophilic conidia

RT-PCR results performed on triclosan- and AMB-treated samples revealed *ags3* down regulation in both test groups. The rodlet surface is uniformly hydrophobic because of the presence of hydrophobins (rodlet proteins). In *A. fumigatus rodA* encodes the rodlet proteins. Absence of this rodlet layer results in the formation of conidia that become more hydrophilic than the conidia of the wild type strain (Girardin et al., 1999). Farnesol could influence either expression or translation of hydrophobins in the treated *A. fumigatus* conidia samples. But except from hydrophobin modulation at its molecular level, lack of hydrophobicity of the conidia can be because of rodlet layer hiding. Hiding of the rodlet layer has been shown with Beauvais et al., (2013) that can be a result of a hydrophilic glycoprotein layer, which is usually secreted during vegetative growth. This glycoprotein secretion is a consequence of either *ags3* or chitin synthase mutants. The rodlet structure of the mutants, if it forms, is less organized than the rodlet of the wild type strain, which putatively modified the ionic strength of the hydrophobin layer in the mutant strains (Beauvais et al., 2013). So, conidia become hydrophilic upon treatment with triclosan and AMB, as a result of rodlet layer hiding by a hydrophilic layer, or modification of the ionic strength of the rodlet layer. Through SDS-PAGE results, hydrophobic rodlet layer-forming protein (RodA), among treated and untreated control groups, was absent in the

farnesol-treated sample. The absence of RodA rejects the possibility of hiding of the rodlet layer. So, farnesol effect on *A. fumigatus* conidia cell wall can be through interrupting the rodlet protein translation or through down regulation of *rodA* expression.

MATH assay revealed that all the agents changed the ionic charge of the conidia surfaces from hydrophobic to hydrophilic. This change in the hydrophobicity of the conidia cell wall can be explained through of the conidia rodlet protein layer presence or absence and *ags3* down-regulation. Given the SDS-PAGE results the rodlet protein absence was only confirmed in farnesol-treated test groups. As regards to triclosan, AMB and tyrosol, down-regulation of *ags3* or chitin synthase pathway was followed by glycoprotein layer formation. Therefore, in triclosan-, AMB- and tyrosol- treated conidia, the rodlet layer had been formed (as the SDS-PAGE bands confirmed it) but was covered by a hydrophilic glycoprotein layer.

Triclosan and tyrosol effect on inducing chitinase' enhanced activity in the mycelia structures was discussed in section 4.1. If this overactivity does happen in the vegetative conidia as well, degradation of the chitin (as one inducers of formation of a glycoprotein layer over the rodlet layer) can result in the conidial charge change after treating with these agents.

4.6 Hydrophobic surfaces coated with farnesol: anti-biofilm display against hydrophobic microorganisms

In WCA study, the surfaces were coated with the MIC_{50} of each agent. Therefore, both the surfaces' charges and the viability of the potential microbes on them may be affected if they are used in vivo. It is not clear, at this stage, if the changes observed on the surfaces' properties by the agents were concertation dependent.

Cell surface hydrophobicity plays a key role in the attachment to, or detachment from a surface. The impact of cell surface hydrophobicity on adhesion of microorganisms to biotic and abiotic surfaces has both negative and positive aspects. Hydrophobic microorganisms are more invasive, they cause diseases difficult to treat and damage surfaces by biofilm formation. On the other hand, high cell surface hydrophobicity enables microorganisms to adsorb on organic pollutants (they move from water to organic, hydrocarbon phase) and degrade them (Kobayashi et al., 1999 and Doyle, 2000). Under some circumstances, increasing the hydrophobicity is beneficial. The formation and

structure of biogranules[5] are associated closely with cell hydrophobicity. So, cell surface hydrophobicity plays a vital role in wastewater treatment in microbial granular reactors (microorganisms aggregate there in aerobic and anaerobic granules). One of the problems is the slow formation of the granules, which takes many weeks. With increasing cell hydrophobicity, cell-cell aggregation is observed to grow (Liu, Sheng and Yu, 2009). It has been shown that application of cultures of microorganisms with high cell surface hydrophobicity accelerates the formation of the granules (Adav et al., 2005).

MATH assay revealed the agents' effect on *A. fumigatus* conidia is through making them hydrophilic (this has been discussed in section 4.5). It has been revealed that the more hydrophobic the cells are the stronger adherence to hydrophobic surfaces, while hydrophilic cells strongly adhere to hydrophilic surfaces (Kochkodan et al., 2008; Giaouris, Chapot-Chartier and Briandet, 2009).

[5] Biogranulation is a promising biotechnology developed for wastewater treatment. Biogranules exhibit a matrix microbial structure. EPS is a major component of the biogranule matrix material in both anaerobic and aerobic granules.

Table 4.3 WCA measurement of (hydrophobic/hydrophilic) surfaces upon coating with the agents (triclosan, AMB, tyrosol and farnesol)

	WCA (θ) measurement of solid surface (original property)	WCA (θ) measurement of solid surface (coating with the agents)
Glass	Super hydrophilic	Although, the surface was still super hydrophilic, triclosan increased but AMB, tyrosol and farnesol decreased its hydrophobicity.
Acrylic	Hydrophilic	Triclosan and AMB made it super hydrophilic. Although, the surface was still hydrophilic, tyrosol and farnesol increased its hydrophobocity.
HDPE	Super hydrophilic	Although, the surface was still super hydrophilic, triclosan, AMB, tyrosol and farnesol increased its hydrophobicity.
Nylon 6	Super hydrophilic	Although, the surface was still super hydrophilic, AMB, tyrosol and farnesol increased its hydrophobicity.
PTFE	Hydrophobic	Although, the surface was still hydrophobic, triclosan, AMB, and tyrosol decreased its hydrophobicity. Farnesol changed the surface property into hydrophilic state.
Silicone	Hydrophobic	Although, the surface was still hydrophobic, AMB, tyrosol and farnesol decreased its hydrophobicity.
UPVC	Super hydrophilic	Although, the surface was still super hydrophilic, triclosan increased, but, tyrosol and farnesol decreased its hydrophobicity. AMB changed the surface property into hydrophobic state.

Triclosan, AMB, tyrosol and farnesol were applied for coating some hydrophobic and hydrophilic surfaces, with differing effects as stated in table 4.3. Based on the WCA measurements, triclosan and AMB provides better coating results for acrylic, as compared with tyrosol and farnesol through changing the surface property from hydrophilic to super-hydrophilic. In certain situations, such as water near protein surface or inside nanochannels, it is difficult to establish a contact angle, and some other suitable metrics should be applied (Granick and Bae, 2008). Given to the WCA results, there were no interaction between the agents' and the surfaces' molecules. This lack of interaction can be explained through WCA results related AMB-coated surfaces. On biotic surfaces, AMB binds to fungal membranes that contain ergosterol (also binds to membranes with cholesterol). In some

papers AMB (as a polyene) is reported as a circular molecule consisting of a hydrophobic and hydrophilic region. This makes polyene an amphoteric molecule (Kamiński, 2014; Yeagle, 2016). While in some other publications, AMB is reported as a highly hydrophobic antifungal (Tan et al., 2106; Selvam, Andrews and Mishra, 2009). Accepting AMB as an amphoteric chemical, in AMB-coated surfaces, AMB molecules were expected to adsorb with their polar head onto oppositely charged surfaces rendering the surfaces more hydrophobic. Figure 3.39 and table 3.13 show that HDPE, Nylon 6 and UPVC coated with AMB became more hydrophobic, while glass and acrylic surfaces coated with AMB showed no change and less hydrophobicity, resoectively, than their uncoated state. The chemical heterogeneity of the films (the polymer surfaces consist of hydrophilic (anhydride) and hydrophobic (alkyl) moieties) affects WCA measurement. The surfaces' heterogeneity, for example in acrylic and glass surfaces, might be the reason for AMB not increasing hydrophobicity of these surfaces.

Microorganisms interact with food components such as lipids and proteins. Therefore, microbial hydrophobicity plays an important role in food production chain and spoilage. For example, bacteria with more hydrophobic surfaces have a higher affinity for milk fat and aroma compounds. Lactic acid bacteria tend to adsorb on lipid droplets but do not cause a destabilization of the emulsion. But, when the bacterial surface charge is opposite to an emulsion, the emulsion's droplets with ionic surface-active compounds become unstable (Ly et al., 2006). Microbiological contamination costs the food industry many millions of dollars annually (Brooks and Flint, 2008).

Among the surfaces, untreated conidia (hydrophobic) attachment to silicone and PTFE (Teflon) (both are hydrophobic) was expected. While, as the other surfaces were hydrophilic, less conidia attachment was expected on those surfaces. Medical implants such as catheters, mechanical heart valves or pacemakers are mostly constructed from materials like silicon and PTFE. So, it is expected that conidial adhering to PTFE is happening relatively easily compared to hydrophilic surfaces. WCA measurements revealed that hydrophobic surfaces, PTFE and silicone, coated with farnesol showed hydrophilicity. Microscopic analysis confirmed less biofilm structure was formed on PTFE surface coated with farnesol than on uncoated PTFE surface (figure 3.41).

PTFE is a fluorocarbon solid as it is of a high molecular weight composed entirely of carbon and fluorine (figure 4.2). The PTFE molecules on its surface are completely encased in fluorine atoms. The fluorine atoms are strongly electronegative, and so carry some degree of negative charge.

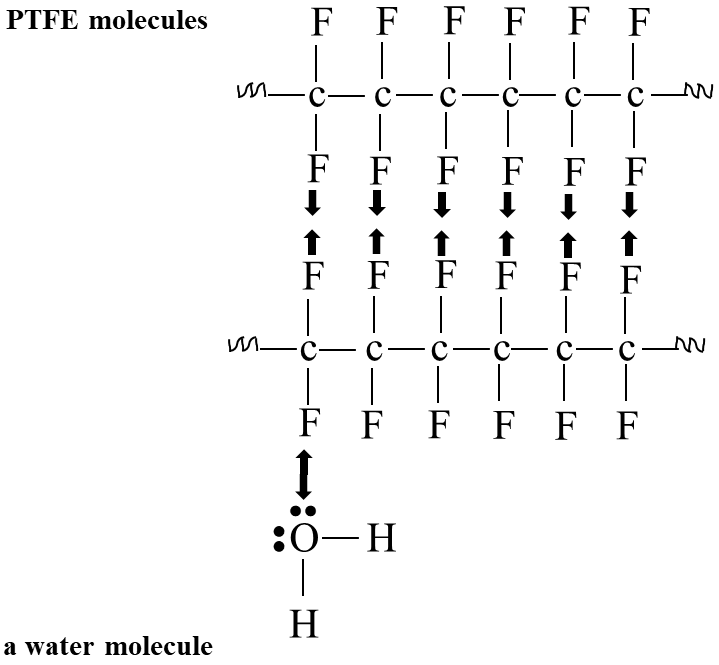

Figure 4.2 The fluorine atoms of PTFE attract each other, while repelling water molecule

Farnesol has been reported to have hydrophobic property (Langford et al., 2009). PTFE, as a hydrophobic surface became hydrophilic when coated with farnesol. This could be because of molecular attraction between farnesol and PTFE surface. WCA results showed that farnesol-coated surfaces, depart from the ionic charge of the surfaces can reveal hydrophilicity. If farnesol function in changing hydrophobic surfaces to hydrophilic was not through the farnesol's and surfaces' molecular interactions (independent of the surface chemical composition) it could be considered as a general coating solvent to reduce hydrophobic microorganisms' attachment to the hydrophobic surfaces.

Regarding AMB-coated UPVC surface, AMB turned the surface charge from hydrophilic (polar) to hydrophobic (non-polar). The attachment of microbial cells to surfaces depends on several factors including Brownian movement, van der Waals attraction, gravitational forces and surface electrostatic charges. One of the important factors is the hydrophobicity of the cells (Van Loosdrecht, Norde and Zehnder 1990). Microscopic analysis under

dynamic conditions using a transmission flow-cell confirmed that conidia (hydrophobic) formed no biofilm structures on triclosan-, tyrosol- and farnesol- coated UPVC surfaces (hydrophilic), while biofilm structure was formed on AMB-coated UPVC surface (figure 3.42). So, in order to diminish growth of hydrophilic microorganisms on UPVC surface, coating it with AMB seems effective.

The polymers' surfaces are characterized based on their surface structure (morphology, roughness, swelling) and surface chemistry (elemental surface composition, acid–base characteristics) (Grundke et al., 2015). UPVC Chemical composition consists of PVC (resin), $CaCO_3$ (calcium carbonate) and titanium dioxide (TiO_2) (Yang and Li, 2011). In the published studies, TiO_2 thin film has been applied to denture base, acrylic resin, resulting in increased hydrophilic properties and decreased attachment of food accumulation, as well as an inhibitory effect on adhesion of microorganisms (Arai et al., 2009). A TiO_2 coating has been used in several medical products. For instance, TiO_2 coating of catheters exerts an antimicrobial effect (Sekiguchi et al., 2007). The AMB role in changing UPVC property from hydrophilic to hydrophobic state might be because of TiO_2 presence in UPVC and its reaction with AMB polar bonds.

4.7 Triclosan and AMB affecting *A. fumigatus* conidia

Confocal microscopy (figures 3.35 and 3.36) showed that *A. fumigatus* biofilm formation on glass surfaces was more affected by triclosan than AMB. The conidia become hydrophilic upon treatment with triclosan and AMB, and the glass surface is hydrophilic, the question is posed as to what makes triclosan to diminish conidial attachment to the glass better than AMB. Microbial adhesion to surfaces involves physio-chemical phenomena, which can effectively mask the influence of cell surface hydrophobicity. Thus, although the primary adhesion of hydrophobic cells to a hydrophilic surface is weak, the bridging polymers give rise to long-range attraction, which will effectively anchor the cells to the surface.

Phylogenetically distant species in the phyla, *Proteobacteria, Bacteroidetes, Chloroflexi, Firmicutes*, and *Actinobacteria*, produce amyloids proteins in the sludge. Amyloids play an important role in activated sludge wastewater treatment plants (Larsen et al., 2007). The function of amyloid fibrils is assumed to be related to enhanced adhesion to surfaces and biofilm formation (Prigent-Combaret et al., 2001). Several filamentous bacteria such

as *Meganema perideroedes, Gordona amarae* and *Skermania piniformis* are known to be highly hydrophobic due to the presence of amyloid- like material (Iwahori et al., 2001; Nielsen, Mikkelsen and Nielsen 2001; Kragelund et al., 2006). In filamentous/multicellular fungi rodlets formed by class I hydrophobins (RodA, RodB, and RodC) show the hallmarks of amyloid fibres. RodA, however, is the only hydrophobin responsible for rodlet formation, sporulation, and conidial hydrophobicity in *A. fumigatus*. In the infective morphotype conidia, the cell wall is covered by a melanin layer and an outer layer with rodlet morphology consisting of amyloid fibres composed of the protein RodA (Valsecchi et al., 2017; Shanmugam et al., 2019). As discussed earlier in section 4.5, RodA protein was present in both AMB- and triclosan- treated samples. So, amyloid fibres' misfunctioning is not a reason for the diminished conidia attachment to the glass surface. As discussed in section 4.3, triclosan activity through inducing necrosis and, also, down-regulating the *ags3* expression inhibit both cell wall structuring and conidia aggregation.

As RT-PCR results revealed, *sph3* was downregulated in both triclosan- and AMB-treated samples. GAG is encoded by *sph3*, which its absence affects biofilm attachment and EPS production. Based on confocal microscopy (figure 3.35), EPS production did happen in AMB-related samples (which is in correlation with the results discussed in section 4.4), while in triclosan-treated samples EPS was absent. So, AMB might trigger an alternative pathway in *A. fumiagtus*, through which the fungus overcomes GAG absence. Through an alternative potential molecule, the EPS production, and biofilm formation could happen in AMB-treated sample.

The surface charge density at different solid–liquid interfaces is related to the dielectric properties of the surface (Li and Bhushan, 2015). AMB and triclosan both made conidial surface property hydrophilic. Given to conidia- treated with AMB and triclosan hydrophilic and glass surface hydrophilic property, attachment of treated conidia was expected on the glass surface. On glass surface, though, triclosan- treated conidia resulted in less conidial attachment. The glass surface was submerged in deionized water (as the main component of PDB) when prepared for both the WCA measurement and confocal microscopy. Silicon dioxide (SiO_2) is a common essential chemical composition of glass (Philipp, 1997). It has been known that silicate glass surfaces immersed in water attain a negative surface charge density (Behrens and Grier, 2001). When immersed in water,

glass would have surface silanol groups (SiOH). The hydrogen nucleus breaks free, (pH is decreased) and leaves an SiO^- behind. Therefore, the surface of the glass becomes negatively charged.

GAG is mediating adherence via charge-charge interactions, between the polycationic polysaccharide and negatively charged surfaces. So, the conidial attachment to the glass surface through GAG was predictable as figure 3.35 shows. The triclosan- and AMB-treated conidia are hydrophilic as well as the glass surface. The general physio-chemical effects, though, led to less conidia (biofilm) attachment to the glass surface in triclosan-treated than AMB- treated samples. Triclosan-induced necrosis in comparison with AMB-induced apoptosis might happen at the earlier stages of the conidial growth. In section 4.3 addition of triclosan following with AMB revealed better effect than AMB following with triclosan. Triclosan-AMB sequence effectivity shows that triclosan triggers cells at earlier stage but AMB at late stage of their growth. In section 4.4 triclosan's and AMB's role on diminishing total protein concentartion during the log phase (early developmental phase) and stationary phase (late developmental phase) of *A. fumigatus* growth were discussed. In the same section, it was also explained that the biofilm production was not interrupted by AMB through PI-based flow cytometry and cv binding assays. Therefore, less conidial attachment, aggregation and availability was observed on triclosan- than AMB-treated samples on glass surfaces.

In addition to the contribution of the physio-chemical phenomena contribution in microorganism attachment to a surface, microbial ability to reconstruct their cell wall is another challenge in inhibiting cells attachment to a surface. A pathogenic bacterium, *Staphyloccocus aureus*, was found to attach to both hydrophobic indium tin oxide (ITO)-coated glass and hydrophilic glass surfaces, with stronger adhesion to hydrophobic surface (Zmantar et al., 2011). As reported through studying *Burkholderia* strains adhesion to *n*-hexadecane, the microorganisms are able to adapt to the presence of hydrocarbons by modifying their cell surface composition to increase or decrease adhesion (Chakarborty et al., 2010). This mechanism of adoption is not reported on *A. fumigatus* yet.

Chapter 5

Conclusion

A. fumigatus, the most important airborne fungal pathogen of humans (Baldin et al., 2015), was subjected to four agents (triclosan, AMB, tyrosol and farnesol). Each of these agents' effect on the fungus was different (table 4.1). Among the agents, triclosan's effect on *A. fumigatus* was not studied before. This study has revealed that triclosan triggers cells to undergo necrosis at the early stage of the fungal growth (vegetative growth phase). Also, α-(1,3)-glucan and GAG were down-regulated which resulted in less conidia aggregation and mycelia attachment to the abiotic surfaces, respectively in triclosan- treated samples. All together triclosan may inactivate QS signalling in *A. fumigatus*.

Quorum quenchers are counted as agents which effect the QS pathway and hence biofilm formation. As they do not kill the cells they are not trigger resistance. Farnesol's QQ role through inhibiting the cell wall integrity signalling in *A. fumigatus* has been reported (Dichtl et al., 2010) but its mechanism of action is not fully understood so far. In this study, a potential mechanism of action for farnesol is proposed through SDS-PAGE analysis, which showed down-regulation of RodA biosynthesis. The data showed RodA, the most abundant protein found both in the cell wall and surface of the conidia (Voltersen et al., 2018), was absent in the presence of farnesol. RodA is the only essential hydrophobin in *A. fumigatus*, conditioning the structure, permeability, hydrophobicity, and phialides modifications (Valsecchi et al., 2017). Conidia rodlet layer absence may result in a heterogeneous culture, comprising both hydrophobic and hydrophilic conidia. Conidia with different surface properties repel each other and hence conidia aggregation and consequently biofilm formation is interrupted by farnesol.

Among the agents used in this study farnesol may directly trigger the hydrophobic rodlet layer formation on conidial surfaces, while triclosan, AMB and tyrosol may act indirectly. Farnesol could influence either expression or translation of conidia cell surface hydrophobins in *A. fumigatus*. The conidial surface charge, as regards to triclosan and AMB can turn hydrophilic due to down-regulation of *ags3*. Triclosan and tyrosol may induce chitinase activity during the vegetative phase. Chitinase activity and *ags3* down-regulation would result in a hydrophilic glycoprotein layer formation, which covers the conidia hydrophobic rodlet layer.

Overall, antibiofilm effect of triclosan, tyrosol and farnesol against *A. fumigatus* resulted in diminishing biofilm formation, while the biofilm structure was formed in the

AMB-treated culture, under static condition. The biofilm formed in AMB-treated samples contained the EPS structure. This suggests the possibility of an alternative process for AMB to overcome GAG synthesis down-regulation in the treated samples. Triclosan and AMB synergistic interaction may provide better antibiofilm treatment against *A. fumigatus* with decreasing the possibility of the fungus resistance. Triclosan may trigger necrosis (or/and affect the persister cells) and thus make microbial cells more vulnerable against AMB to undergo apoptosis.

As a general approach, changing hydrophobic microbial cells to hydrophilic is appropriate. Hydrophobic microbes, contrary to hydrophilic ones seem to be more resistant to the solvents' toxic effects (in the bacterial strains, the resistance can be due to the modification of the cell membrane lipopolysaccharides, which protect the microbes from the attachment of organic molecules) (Kobayashi et al., 1999).

Hydrophobic (low-energy) surfaces applied in this study, PTFE and silicone, coated with farnesol turned hydrophilic (high- energy). AMB, on the other hand, changed UPVC surface property from hydrophilic to hydrophobic. AMB might interact with TiO_2, involved in UPVC chemical structure and through that increase UPVC hydrophobicity. In the food industry, PTFE is a typical material used in installations. It has been demonstrated that hydrophobic pathogens such as *Salmonella* spp. and *Listeria monocytogenes* easily attach to this material (Sinde and Carballo, 2000). Similar to the case of medical implants, surfaces of materials used in the food industry can be modified. For instance, bioactive surfaces can utilize immobilized enzymes, stainless steel can be augmented by ions lowering surface energy, or antimicrobial chemicals can be used to coat the surfaces (Yazdankhah et al., 2006; Zhao and Liu, 2006; Srinivasan and Swain, 2007; Tabak et al., 2007). Relationships between hydrophobicity of microbial surfaces and adhesion to different materials are very difficult to be evaluated, since many parameters are involved in these processes in regards interfacial responses. In pure water, repulsive forces are often observed between hydrophobic polystyrene and hydrophilic surfaces. Remarkably, Thormann et al., (2008) found an interaction between hydrophobic polystyrene particles and a hydrophilic surface, which is regulated by addition of salt. In the presence of the salt, secondary adhesion processes are observed and the loosely bound

polystyrene molecules attach to the surface (Thormann *et al.* 2008). Consequently, when the concentration of NaCl increased, the Debye lengths[6] decreased (Cerca et al., 2005).

Together these data support the phenomenon of physio-chemical approache in microbial adhesive interactions. Microbial adhesion to highly hydrophobic materials is caused by hydrophobic interaction and the combination of van der Waals' force and repulsive and attractive electrostatic forces. For example, as analysed in this study, GAG as a polycationic polysaccharide mediates adherence to negatively charged surfaces via charge-charge interactions. Immersing glass (SiO_2) in (deionised) water (PDB medium) decrease the pH of the water due to the unbound H^+ release from the glass surface to the water and hence make the glass surface negatively charged (SiO^-). Thus, the mycelia attachment to the glass surface is facilitating by GAG. The general physio-chemical affects, though, led to less mycelia (biofilm) attachment to the glass surface in triclosan-treated than AMB- treated samples. Thus, down-regulation of GAG biosynthesis induced by triclosan may decrease mycelia attachment to the glass surface. While an alternative mechanism (or molecule) might be present to cover for GAG function when AMB induces down-regulation of GAG biosynthesis.

Taken together, all the agents turned conidia surface property from hydrophobic to hydrophilic. Farnesol, though, functioned directly on the conidia cell wall to down-regulate or interrupt with rodlet layer protein translation. Triclosan and AMB turned conidia cell wall hydrophilic, independent from affecting the rodlet layer, through formation of a hydrophilic glycoprotein layer over the rodlet layer on the conidia cell wall. Lack of hydrophobicity led to less conidia aggregation and hence less biofilm formation on any type of surfaces. In the case of coating surfaces with the antifungal agents, farnesol-coated hydrophobic surfaces became hydrophilic. Accordingly, under dynamic growth, using flow-cell transmission device farnesol-coated hydrophobic surfaces provided an unsuitable substrate for conidia attachment.

[6] The Debye length characterizes the length scale of ionic interactions in solution. Debye length is determined by the ratio of the temperatures of the electrons and ions, to the electron (or ion) number density. It is a crucial parameter in the description of aqueous systems that include ions, charged colloids, surfactants, polyelectrolytes, and biopolymers (Bryant 1996; Tadmor et al., 2002)

Chapter 6

Fututre work

6.1 Studying QQrs (e.g. triclosan, tyrosol and farnesol) antifungal effect against *A.fumigatus*

This has been already reported in bacteria that the cell death pathway might be controlled by a QS mechanism (Peeters and Jonge, 2018). Kolodkin-Gal and Engelberg-Kulka (2008), for instance, showed that in *E. coli* cell death is dependent on a quorum-sensing factor that they have named it as EDF (extracellular death factor) (Kolodkin-Gal and Engelberg-Kulka, 2008). As discussed in sections 4.1 and 4.2, the antifungal role of the agents against *A. fumigatus* might be through necrosis or apoptosis. Autophagy is another mechanism in the cells, which might be trigerred by the agents. Two type of autophagy, which involve dynamic rearrangement of a sequestering eukaryotic membrane have been identified; microautophagy and macroautophagy. Microautophagy includes the engulfment of cytoplasm directly at the lysosomal surface. Macroautophagy, in contrast, contains the formation of cytosolic double-membrane vesicles that sequester portions of the cytoplasm (Levine and Klionsky, 2004).

Taken together, each of this regulatory mechanism (apoptosis, necrosis, autophagy) in the cells can be affected by QS. Thus, assaying the agents' effect on these regulatory mechanisms can add further evidence for studying the agents' mechanism of action and that whether QS signalling pathway is interrupted by the agents.

6.1.1 Microscopic analysis

- Necrosis and apoptosis in *A. fumigatus* treated with QQrs can be analysed microscopically. Collins et al., (1997) revealed that necrotic cells swell and lyse, whereas apoptotic cells show intense cell surface zeotic blebbing (Collins et al., 1997).
- Autophagy in filamentous fungi is characterized by the presence of autophagosomes in the cytoplasm and autophagic bodies in the vacuoles. For microscopic analysis of autophagosome accumulation in vacuoles, overnight cultures are washed in sterile distilled water, and the medium is replaced either with sterile distilled water containing 2mM phenylmethylsulfonyl fluoride (PMSF) or with YG containing 2mM PMSF and 0.5mM EDTA. After 4 hr of incubation at 37°C, the presence of autophagic bodies within vacuoles is visualized by Differential interference contrast (DIC) microscopy.

6.1.2 Molecular analysis

- Apoptotic DNA fragmentation can be detected by the TUNEL (Terminal deoxynucleotidyl transferase-mediated dUTP nick end labelling) assay to analyse the apoptotic markers. TUNEL (terminal deoxynucleotidyl transferase dUTP nick end labeling) and annexin V-FITC can be used as markers of apoptosis, and uptake of PI can be used as a marker of cell-membrane integrity. In order to detect the expression of these apoptotic markers, the cell wall is first removed by digesting mycelium taken from mid-exponential-phase of growth, and protoplasts are then treated with various concentrations of QQrs. Following treatment, protoplasts are washed twice by centrifugation (1500 xg) for 10 min and resuspended in an equal volume of regeneration buffer (0.1M phosphate buffer, pH 7.0, 0.9M sorbitol). To determine protoplast viability, protoplasts are regenerated by spreading gently over the surface of modified Vogel's medium solidified with 1.5% (w/v) agar (supplemented with 0.9 M sorbitol), and plates incubated at 37°C until colonies became visible. To inhibit metacaspase activity or protein synthesis, respectively, 25 μg/mL of the broad-spectrum caspase inhibitor Z-VAD-fmk or 50μg/ mL cycloheximide are added to the protoplast suspension, 1h prior to treatment with the QQrs. DAPI (4′,6-diamidino-2-phenylindole) staining can be used to determine the percentage of protoplasts containing nuclei (Mousavi & Robson, 2003).
- Autophagy in filamentous fungi is controlled by Tor (Target of Rapamycin) kinase and its activity upon treatment with QQrs can be studied.

6.2 In vitro durability of coated catheters

The actual catheters can be studied for the agents' effects on fungal growth on them. The catheters, then, are subjected to human blood to provide an environment one step closer to in vivo conditions. A possible methodology could include the following (Darouiche et al., 2009):

Catheters are coated by dipping in a solution that contained triclosan MIC_{50} and then gas sterilized with ethylene oxide. Catheter segments (1 cm) are dipped overnight in the triclosan solution at 48°C to coat both internal and external catheter surfaces and left to dry for 8 hr at room temperature. The dipping and drying procedure are repeated twice. The catheter segments are then left to dry for an additional 24 hr.

One-centimetre long segments of uncoated control, triclosan-coated catheters are placed in separate 250 mL flasks containing 100 mL of PDB at 37°C with agitation at 100 rpm. Half of the PDB are replaced by fresh medium daily. Catheter segments are removed from the flask after 1, 4 and 7days to perform the adhesion assay against *A. fumigatus*.

Segments (1cm long; 3 mm external diameter) of uncoated control and agent-coated catheters are pressed onto the centre of agar plates containing 5% human blood that have been freshly inoculated with *A. fumigatus* and incubated at 37°C for 24 hr. The zone of inhibition is determined by measuring the diameter of the clear zone perpendicular to the long axis of the catheter segment. The actual zones of inhibition are recorded by subtracting the external diameter of the catheter (3 mm) from each measurement.

Appendix 1

Table 1 Materials used in this study

Item	Source
6-mm Whatman® antibiotic assay discs	Merck, Dorset, UK
7500 Real-Time PCR System	Fisher Scientific Ltd, Loughborough, UK
96-well tissue culture plates	Corning Inc., Corning, NY
AxioVert 100, fluorescence microscope	Carl Zeiss, Jena, Germany
Cell Culture Flasks	Thermo Fisher Scientific, UK, CAS 156340
Cell scraper, Falcon®	VWR, Brooklyn, NY
Centrifuge tubes	Merck, Dorset, UK, CAS CLS430829
Centrifuge, Heraeus Primo R	Thermo Fisher Scientific, UK, CAS 75005441
Chromatography Compartment, Dionex™ ICS-5000+ DC Detector	Thermo Fisher Scientific, UK, CAS 075941
Corning® Costar® TC-treated 6-well plates	Merck, Dorset, UK
Disposable tips	Greiner Bio One Ltd, UK
Dynamic Contact Angle Analyze, FTA100	First Ten Ångstroms, Portsmouth, UK
Eppendorf centrifuge	(SLS) Scientific Laboratory Supplies Ltd, UK, CAS E5418000068
Eppendorf Tubes	Eppendorf UK Limited, Item no. 0030125150
Falcon™ Round-Bottom (Polystyrene Tubes)	Fisher Scientific Ltd, Loughborough, UK
Flow Cytometer, NovoCyte Benchtop	ACEA Biosciences, UK
Gradient Thermal Cycler, Techne™ 5PrimeG	Fisher Scientific Ltd, Loughborough, UK

Item	Source
Horizontal gel tank, Mini-Sub® Cell GT Cell	BIO-RAD, CAS 1640300
Leica DMRE confocal microscope	Leica Microsystems Ltd, Milton Keynes, UK
MF-Millipore Membrane Filter, 0.22 µm pore size	Merck, Dorset, UK, CAS GSWP04700
Micropipettes (2, 20, 200 and 1000 µL)	Cole-Parmer, US
Miracloth	Merck, Dorset, UK
NanoDrop™ 1000 Spectrophotometer	Thermo Fisher Scientific, UK
Pestle and mortar	Eppendorf UK Limited, no. 0030120973
PowerPac Basic Power Supply	BIO-RAD, CAS 1640300
Refrigerated incubator shaker	Marshall Scientific, US, CAS NB-4430
RHM-Monosaccharide H+ (8%), LC Column 300 x 7.8 mm	Phenomenex Rezex, UK, Part no. 00H-0132-K0
Serological Pipets (Polystyrene Disposable)	Fisher Scientific Ltd, Loughborough, UK
SnakeSkin™ dialysis tubing	Thermo Fisher Scientific, Leicestershire, UK
Spectrophotometer, Jenway 6300 visible	Camlab Limited, UK, CAS 1191468
Strip PCR Tubes and Caps	Merck, Dorset, UK
Tranmission Flow-cell, FC 281	BioSurface Technologies Corporation (BST), Montana, USA
UV transilluminator	UVITEC, UK
Vertical Electrophoresis Cell, Mini-PROTEAN® Tetra	BIO-RAD, CAS 1658004
Whatman® qualitative filter paper, 22 µm pore size, Grade 54 circles, diam. 55mm	Merck, Dorset, UK, CAS WHA1454055

Table 2 Chemicals and reagents used in this study

Item	Source
1,4-dithiothreitol	Merck , Dorset, UK, CAS 3483-12-3
2-Mercaptoethanol	Merck , Dorset, UK, CAS 60-24-2
Acetic acid (glacial) 100%	Merck , Dorset, UK, CAS 64-19-7
Acrylamide/Bis-acrylamide, 30% solution	Merck, Dorset, UK, CAS A3574
Agar	Merck, Dorset, UK, CAS 9002-18-0
Agarose	Fisher scientific, UK, CAS 9012-36-6
Allrep fungal DNA/RNA/protein ki	Qiagen, Manchester, UK, Cat. no. 47154
Ammonium bicarbonate	Merck, Dorset, UK, CAS 1066-33-7
Bromophenol Blue	Sigma-Aldrich, UK, CAS B0126
Calcofluor white stain	Merck, Dorset, UK, CAS 18909
Cetyl trimethylammonium bromide (CTAB)	Merck , Dorset, UK , CAS 57-09-0
Coomassie brilliant blue	BIO-RAD, CAS 64-19-7
Crystal violet	Merck, Dorset, UK, CAS 50-00-0
CsCl (Cesium chloride)	Merck, Dorset, UK, CAS 7647-17-8
D-(+) Glucose	Merck, Dorset, UK, CAS 47829
D-galacto-D-mannan, from ceratonia Siliqua	Merck, Dorset, UK, Cat. no. 48230
D-Glucose	Sigma, CAS 50-99-7
D-Sorbitol	Sigma, S1876 – CAS 50-70-4
Dimethyl sulfoxide	Merck, Dorset, UK, CAS 548-62-9
EDTA	Merck, Dorset, UK, CAS 6381-92-6
Ethanol (96%v/v)	VWR, Brooklyn, NY
Ethylene diamine tetra	Merck , Dorset, UK, CAS 6381-92-6
FastStart SYBR Green Master	Merck, Dorset, UK, CAS 4673484001

Item	Source
Formaldehyde solution	Merck, Dorset, UK, CAS 8.18708
FUN® 1 cell stain	Molecular Probes, Life Tech, CAS F7030
Gel loading dye	Omega Corporation, Southampton, Cat. no. G1881
GelRed Nucleic Acid Stain	Merck, Dorset, UK, CAS SCT122
Glutaraldehyde solution; 70% in H2O	Sigma-Aldrich, UK, CAS G7776
Glycerol	Merck, Dorset, UK, CAS G5516
HaltTM Protease Inhibitor Cocktail	Thermo Fisher Scientific, UK, Cat. no. 78429
Hexadecane	Merck , Dorset, UK, CAS 544-76-3
Hexadecyltrimethylammonium bromide	Merck, Dorset, UK, CAS 57-09-0
In Vitro Toxicology Assay Kit, Resazurin based	Merck , Dorset, UK, CAS 263-718-5
Isopropanol	Merck , Dorset, UK, CAS 67-63-0
KCl (potassium chloride)	VWR, Brooklyn, NY
KH_2PO_4 (Monopotassium phosphate)	Merck , Dorset, UK, CAS 778-77-0
MOPS (3-(N-morpholino) propanesulfonic acid)	Merck, Dorset, UK, CAS 1132-61-2
N,N,N′,N′-Tetramethylethylenediamine, TEMED	Merck , Dorset, UK, CAS 110-18-9
Na_2HPO_4 (Disodium phosphate)	Merck , Dorset, UK, CAS 7558-79-4
NaCl (Sodium chloride)	VWR, Brooklyn, NY
Phenol: Chloroform: Isoamylalcohol	Merck , Dorset, UK, P3803
Polyvinylpyrrolidone (PVP)	Merck , Dorset, UK, CAS 9003-39-8
Potato Dextrose Agar	Merck, Dorset, UK, CAS 70139
Potato dextrose broth	Fisher scientific, UK, CAS 9012-36-6
Potato glucose agar	Merck, Dorset, UK, CAS 70139

Item	Source
Propidium Iodide	Abcam, Cambridge, UK, ab139418
Protein Assay Dye Reagent	BIO-RAD, CAS 5000006
Qiuck start bradford 1X dye reagent	BIO-RAD, CAS 5000205
QuantiTect Reverse Transcription Kit	Qiagen, Manchester, UK, Cat. no. 205311
Quick Start Bovine Serum Albumin Standard Set	BIO-RAD, Hertfordshire, UK, CAS 5000207
RPMI-1640 Medium with L Glutamine, without sodium bicarbonate	Merck, Dorset, UK, CAS R6504
Silver nitrate solution (2.5 % (w/v) AgNO3 in H2O)	Merck, Dorset, UK, CAS 85193
Sodium carbonate	Merck, Dorset, UK, CAS 451614
Sodium Chloride (NaCl)	AppliChem, CAS 7647-14-5
Sodium dodecyl sulfate	Merck, Dorset, UK, CAS 74255
Sodium hypochlorite	Merck, Dorset, UK, CAS 1.05614
Sucrose	Merck, Dorset, UK, CAS 1.07651
Sulfuric acid, 95.0-98.0%	Merck, Dorset, UK, CAS 258105
Trisma-Base	Merck, Dorset, UK, CAS 77-86-1
Trizma® hydrochloride	Merck, Dorset, UK, CAS 1185-53-1
Urea	Merck, Dorset, UK, CAS U4883

Table 3 Nucleotide sequences of primers used in RT-PCR experiments. They all were provided by Eurofins Genomics, Germany

Gene	Primer	Sequence (5' -> 3')	Product Size (bp)	Reference
*sph3**	Forward	GGGCATATGTCCAAGGTCTTTGTGCCTCTCTATGTG	657	Bamford et al., 2015
	Reverse	GGCTCGAGCTATTTTCCCATCAAATCCACAAACTC		
*ags3***	Forward	CGGCAGTCTCTACCTTGGTC	1700	Maubon et al., 2006
	Reverse	TCGTTCTTCAGCTTGACAGC		
Rho GTPase activator (*sac7*)	Forward	AGGAGGATGAAAGTAAAGGACCCC	159	Llanos, François and Parrou, 2015
	Reverse	AAACCCCACACTTGGCGAC		

* encodes a protein belonging to the spherulin-4 family

**encodes cell wall α (1–3) glucan biosynthesis

Appendix 2

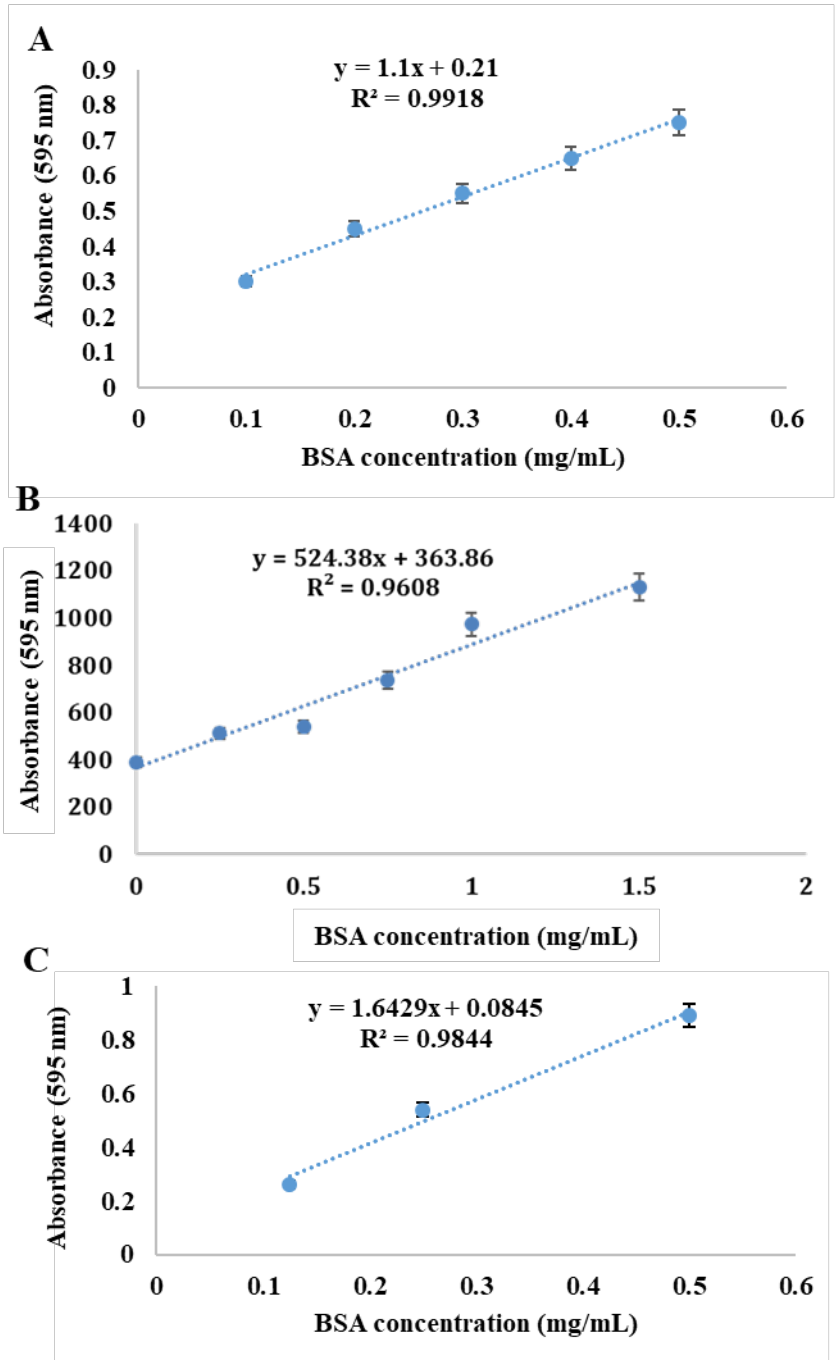

Figure 1 Bradford assay standard curves for protein

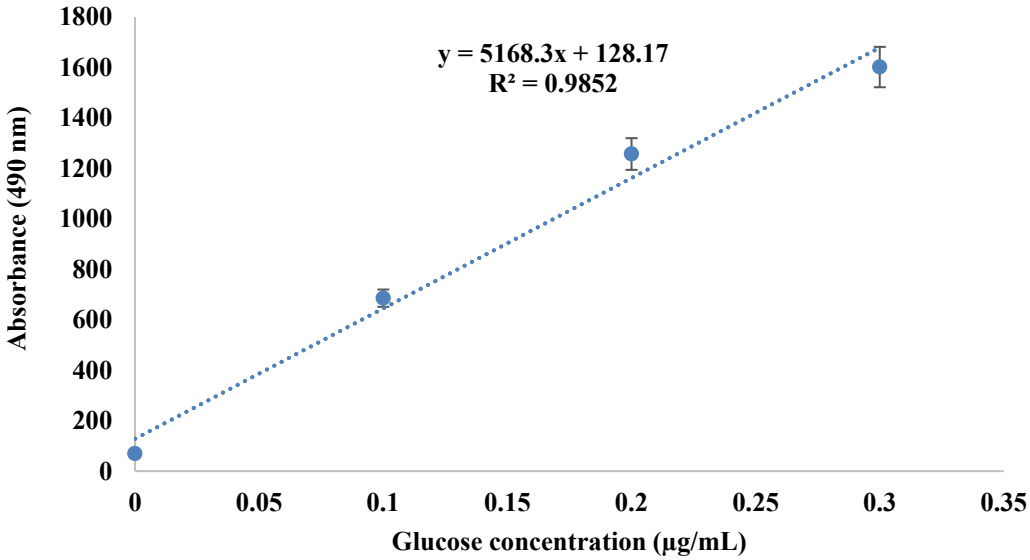

Figure 2 Total carbohydrate assay standard curve

References

Abdel-Rhman SH., El-Mahdy AM., and El-Mowafy M. (2015) Effect of Tyrosol and Farnesol on Virulence and Antibiotic Resistance of Clinical Isolates of Pseudomonas aeruginosa. *BioMed Research International* 2015: 1–7.

Abreu AC., Tavares RR., Borges A., Mergulhão F., Simões M. (2013). Current and emergent strategies for disinfection of hospital environments. J. Antimicrob. Chemother.; 68:2718–2732

Adams DJ. (2004) Fungal cell wall chitinases and glucanases. *Microbiology* 150(7): 2029–2035.

Adav, S., Lee, D., Show, K., and Tay, J. (2005). "Microstructural optimization of wastewater treatment by aerobic granular sludge," in Aerobic Granular Sludge, eds S. Bathe, M. K. de Kreuk, B. McSwain, and N. Schwarzenbeck (London: IWA Publishing), 213–219.

Affeldt KJ., Brodhagen M. and Keller NP. (2012) Aspergillus Oxylipin Signaling and Quorum Sensing Pathways Depend on G Protein-Coupled Receptors. *Toxins* 4(9): 695–717.

Aimanianda V., Bayry J., Bozza S., Kniemeyer O., Perruccio K., Elluru SR., Clavaud C., Paris S., Brakhage AA., Kaveri SV., Romani L., Latge JP (2009). Surface hydrophobin prevents immune recognition of airborne fungal spores. Nature; 460:1117–1121.

Alberts B, Johnson A, Lewis J, et al. (2002). Molecular Biology of the Cell. 4th edition. New York: Garland Science. Innate Immunity.

Albuquerque P and Casadevall A (2012) Quorum sensing in fungi – a review. *Medical Mycology* 50(4): 337–345.

Al-Dhaheri RS and Douglas LJ (2009) Apoptosis in Candida biofilms exposed to amphotericin B. *Journal of Medical Microbiology*59(2): 149–157.

Alem MAS, Oteef MDY, Flowers TH and Douglas LJ (2006) Production of Tyrosol by Candida albicans Biofilms and Its Role in Quorum Sensing and Biofilm Development. *Eukaryotic Cell* 5(10): 1770–1779.

Ali Abdul Hussein S Al Janabi (2015) In vitro Antagonistic Activity of Candida albicans against Filamentous Fungi. *Medical Mycology: Open Access* 1(1).

Allen U. 2010. Antifungal agents for the treatment of systemic fungal infections in children. *Paediatrics & Child Health* 15:603–608.

Almeida-Paes R, Figueiredo-Carvalho MHG, Brito-Santos F, Almeida-Silva F, Oliveira MME and Zancopé-Oliveira RM (2016) Melanins Protect Sporothrix brasiliensis and Sporothrix schenckii from the Antifungal Effects of Terbinafine. *Plos One*11(3).

Al-Samarrai, T. H., and Schmid, J. (2000). A simple method for extraction of fungal genomic DNA. *Letters in Applied Microbiology, 30*(1), 53-56.

Alsteens D, Aimanianda V, Hegde P, Pire S, Beau R, et al. (2013) Unraveling the Nanoscale Surface Properties of Chitin Synthase Mutants of Aspergillus fumigatus and Their Biological Implications. Biophys J 105(2):320–7.

Ambati S, Ferarro AR, Kang SE, Lin J, Lin X, Momany M, Lewis ZA and Meagher RB (2019) Dectin-1-Targeted Antifungal Liposomes Exhibit Enhanced Efficacy.*mSphere* 4(1).

Arai T, Ueda T, Sugiyama T and Sakurai K (2009) Inhibiting microbial adhesion to denture base acrylic resin by titanium dioxide coating. *Journal of Oral Rehabilitation* 36(12): 902–908.

Assis LJD, Manfiolli A, Mattos E, Fabri JHTM, Malavazi I, Jacobsen ID, Brock M, Cramer RA, Thammahong A, Hagiwara D, Ries LNA and Goldman GH (2018) Protein Kinase A and High-Osmolarity Glycerol Response Pathways Cooperatively Control Cell Wall Carbohydrate Mobilization in Aspergillus fumigatus. *mBio* 9(6).

Avbelj M, Zupan J and Raspor P (2016) Quorum-sensing in yeast and its potential in wine making. *Applied Microbiology and Biotechnology* 100(18): 7841–7852.

Badaruddin M, Holcombe LJ, Wilson RA, Wang ZY, Kershaw MJ, Talbot NJ. 2013. Glycogen metabolic genes are involved in trehalose-6- phosphate synthase-mediated regulation of pathogenicity by the rice blast fungus Magnaporthe oryzae. PLoS Pathog 9:e1003604.

Balajee SA and Marr KA (2002) Conidial Viability Assay for Rapid Susceptibility Testing of Aspergillus Species. *Journal of Clinical Microbiology* 40(8): 2741–2745.

Baldin C, Valiante V, Krüger T, Schafferer L, Haas H, Kniemeyer O and Brakhage AA (2015) Comparative proteomics of atorinducibleAspergillus fumigatusmutant reveals involvement of the Tor kinase in iron regulation. *Proteomics* 15(13): 2230–2243.

Bamford NC, Snarr BD, Gravelat FN, Little DJ, Lee MJ, Zacharias CA, Chabot JC, Geller AM, Baptista SD, Baker P, Robinson H, Howell PL and Sheppard DC (2015) Sph3 Is a Glycoside Hydrolase Required for the Biosynthesis of Galactosaminogalactan in Aspergillus fumigatus. *Journal of Biological Chemistry* 290(46): 27438–27450.

Bandara HMHN, Lam OLT, Jin LJ and Samaranayake L (2012) Microbial chemical signaling: a current perspective. *Critical Reviews in Microbiology* 38(3): 217–249.

Barhoom S and Sharon A (2004) cAMP regulation of “pathogenic” and “saprophytic” fungal spore germination. *Fungal Genetics and Biology* 41(3): 317–326.

Barriuso J (2015) Quorum sensing mechanisms in fungi. *AIMS Microbiology* 1(1): 37–47.

Bartnicki-Garcia, S., & Nickerson, W. J. (1962). NUTRITION, GROWTH, AND MORPHOGENESIS OF *MUCOR ROUXII*. *Journal of Bacteriology*, *84*(4), 841–858.

Bayry J., Beaussart A., Dufrêne Y. F., Sharma M., Bansal K., Kniemeyer O., et al. (2014). Surface structure characterization of *Aspergillus fumigatus* conidia mutated in the melanin synthesis pathway and their human cellular immune response. *Infect. Immun.* 82 3141–3153.

Bayry, J.; Aimanianda, V.; Guijarro, J.I.; Sunde, M.; Latge, J.P. (2012) Hydrophobins—Unique fungal proteins. PLoS Pathog, 8.

Beauvais A and Latgé J-P (2015) Aspergillus Biofilm In Vitro and In Vivo. *Microbiology Spectrum* 3(4).

Beauvais A, Bozza S, Kniemeyer O, Formosa C, Balloy V, Henry C, Roberson RW, Dague E, Chignard M, Brakhage AA, Romani L and Latgé J-P (2013) Deletion of the α-(1,3)-Glucan Synthase Genes Induces a Restructuring of the Conidial Cell Wall Responsible for the Avirulence of Aspergillus fumigatus. *PLoS Pathogens* 9(11).

Beauvais, A., and Latgé, J. (2018). Special Issue: Fungal Cell Wall. *Journal of Fungi, 4*(3), 91.

Beauvais A, Maubon D, Park S, Morelle W, Tanguy M, Huerre M, Perlin DS and Latge JP (2005) Two (1-3) Glucan Synthases with Different Functions in Aspergillus fumigatus. *Applied and Environmental Microbiology* 71(3): 1531–1538.

Beauvais, A., Schmidt, C., Guadagnini, S., Roux, P., Perret, E., Henry, C., Paris, S., Mallet, A., Prévost, M. C., and Latgé, J. P. (2007) An extracellular matrix glues together the aerial-grown hyphae of Aspergillus fumigatus. Cell Microbiol 9, 1588–1600.

Becker, M.J., et al., Effect of amphotericin B treatment on kinetics of cytokines and parameters of fungal load in neutropenic rats with invasive pulmonary aspergillosis. J Antimicrob Chemother, 2003. 52(3): p. 428-34. 145.

Beggs WH, Sarosi GA and Walker MI (1976) Synergistic Action of Amphotericin Band Rifampin against Candida Species. *Journal of Infectious Diseases* 133(2): 206–209.

Behrens SH and Grier DG (2001) The charge of glass and silica surfaces. The Journal of Chemical Physics 115(14): 6716–6721.

Benvenuto MA (2015) *Industrial chemistry: for advanced students*. De Gruyter.

Berlanga M and Guerrero R (2016) Living together in biofilms: the microbial cell factory and its biotechnological implications. *Microbial Cell Factories* 15(1).

Bernard M and Latgé J-P (2001) Aspergillus fumigatus cell wall: composition and biosynthesis.*Medical Mycology* 39(1): 9–17.

Bhardwaj AK, Vinothkumar K and Rajpara N (2013) Bacterial Quorum Sensing Inhibitors: Attractive Alternatives for Control of Infectious Pathogens Showing Multiple Drug Resistance. *Recent Patents on Anti-Infective Drug Discovery* 8(1): 68–83.

Bok JW and Keller NP (2004) LaeA, a Regulator of Secondary Metabolism inAspergillusspp. *Eukaryotic Cell* 3(2): 527–535.

Bom VL, de Castro PA, Winkelströter LK, Marine M, Hori JI, Ramalho LN, dos Reis TF, Goldman MH, Brown NA, Rajendran R, Ramage G, Walker LA, Munro CA, Rocha MC, Malavazi I, Hagiwara D, Goldman GH (2015). The Aspergillus fumigatus sitA Phosphatase Homologue Is Important for Adhesion, Cell Wall Integrity, Biofilm Formation, and Virulence. *Eukaryot Cell*. Aug;14(8):728-44.

Bonaventura GD, Pompilio A, Picciani C, Iezzi M, D'antonio D and Piccolomini R (2006) Biofilm Formation by the Emerging Fungal Pathogen Trichosporon asahii: Development, Architecture, and Antifungal Resistance. *Antimicrobial Agents and Chemotherapy* 50(10): 3269–3276.

Boniatti MM, Friedman G, Castilho RK, Vieira SRR and Fialkow L (2011) Characteristics of chronically critically ill patients: comparing two definitions. *Clinics* 66(4): 701–704.

Bortel K and Szewczyk P (1996) Studies on the effect of processing of unplasticized PVC on the polymer structure. *Polimery*41(11/12): 643–646.

Bradford, M. M. (1976). A rapid and sensitive method for the quantitation of microgram quantities of protein utilizing the principle of protein-dye binding. *Analytical Biochemistry, 72*(1-2), 248-254.

Brilhante RSN, Caetano ÉP, Lima RACD, Marques FJDF, Débora De Souza Collares Maia Castelo-Branco, Melo CVSD, Guedes GMDM, Oliveira JSD, Camargo ZPD, Moreira JLB, Monteiro AJ, Tereza De Jesus Pinheiro Gomes Bandeira, Cordeiro RDA, Rocha MFG and Sidrim JJC (2016) Terpinen-4-ol, tyrosol, and β-lapachone as potential antifungals against dimorphic fungi. *Brazilian Journal of Microbiology* 47(4): 917–924.

Brilhante RSN, Lima RACD, Caetano EP, Leite JJG, D. D. S. C. M. Castelo-Branco, Ribeiro JF, T. D. J. P. G. Bandeira, Cordeiro RDA, Monteiro AJ, Sidrim JJC and Rocha MFG (2013) Effect of Farnesol on Growth, Ergosterol Biosynthesis, and Cell Permeability in Coccidioides posadasii. *Antimicrobial Agents and Chemotherapy* 57(5): 2167–2170.

Brilhante RSN, Lima RACD, Marques FJDF, Silva NF, Caetano EP, D. D. S. C. M. Castelo-Branco, T. D. J. P. G. Bandeira, Moreira JLB, Cordeiro RDA, Monteiro AJ, Camargo ZPD, Sidrim JJC and Rocha MFG (2015) Histoplasma capsulatum in planktonic and biofilm forms: in vitro susceptibility to amphotericin B, itraconazole and farnesol. *Journal of Medical Microbiology* 64(Pt_4): 394–399.

Brooks, J., and Flint, S. (2008). Biofilms in the food industry: problems and potential solutions. Int. J. Food Sci. Technol. 43, 2163–2176.

Brosnahan J, Jull A and Tracy C (2002) Types of urethral catheters for management of short-term voiding problems in hospitalised adults. *Cochrane Database of Systematic Reviews*.

Brown GD, Denning DW, Gow NA, Levitz SM, Netea MG,White TC. 2012. Hidden killers: human fungal infections. *Sci Transl Med* 4:165rv113.

Brunke S, Seider K, Almeida RS, Heyken A, Fleck CB, Brock M, Barz D, Rupp S and Hube B (2010) Candida glabrata tryptophan-based pigment production via the Ehrlich pathway. *Molecular Microbiology* 76(1): 25–47.

Bryant DA (1996) Debye length in a kappa-distribution plasma. Journal of Plasma Physics 56(1): 87–93.

Budovskaya YV, Stephan JS, Reggiori F, Klionsky DJ and Herman PK (2004) The Ras/cAMP-dependent Protein Kinase Signaling Pathway Regulates an Early Step of the Autophagy Process in Saccharomyces cerevisiae. *Journal of Biological Chemistry* 279(20): 20663–20671.

Bugli F, Sterbini FP, Cacaci M, Martini C, Lancellotti S, Stigliano E, Torelli R, Arena V, Caira M, Posteraro P, Sanguinetti M and Posteraro B (2014) Increased production of gliotoxin is related to the formation of biofilm byAspergillus fumigatus: an immunological approach. *Pathogens and Disease* 70(3): 379–389.

Bugli F, Sterbini Paroni F, Cacaci M, Martini C, Lancellotti S, Stigliano E, Torelli R, Arena V, Caira M, Posteraro P, et al. (2014) Increased production of gliotoxin is related to the formation of biofilm by Aspergillus fumigatus: An immunological approach. Pathog Dis.;70:379–389.

Busscher, H. J., Weerkamp, A. H., van der Mei, H. C., van Pelt, A. W., de Jong, H. P., & Arends, J. (1984). Measurement of the surface free energy of bacterial cell surfaces and its relevance for adhesion. *Applied and environmental microbiology*, *48*(5), 980–983.

Cabib E., Arroyo J., 2013. How carbohydrates sculpt cells: chemical control of morphogenesis in the yeast cell wall. Nat Rev Microbiol 11:648 – 655.

Campos RP, do Nascimento MM, Chula DC, Riella MC. (2011) Minocycline-EDTA lock solution prevents catheter-related bacteremia in hemodialysis. J Am Soc Nephrol;22:1939–45.

Cannizzo FT, Eraso E, Ezkurra PA, Villar-Vidal M, Bollo E, Castellá G, Cabañes FJ, Vidotto V and Quindós G (2007) Biofilm development by clinical isolates ofMalassezia pachydermatis. *Medical Mycology* 45(4): 357–361.

Catalli, A., Kulka, M., 2010. Chitin and β-Glucan Polysaccharides as Immunomodulators of Airway Inflammation and Atopic Disease. Recent Patents on Endocrine, Metabolic & Immune Drug Discovery, 4(3), 175-189.

Cerca, N., Pier, G., Vilanova, M., Oliveira, R., and Azeredo, J. (2005). Quantitative analysis of adhesion and biofilm formation on hydrophilic and hydrophobic surfaces of clinical isolates of Staphylococcus epidermidis. Res. Microbiol. 156, 506–514.

Chakarborty, S., Mukhejri, S., and Murkherji, S. (2010). Surface hydrophobicity of petroleum hydrocarbon degrading Burkholderia strains and their interactions with NAPLs and surfaces. Colloids Surf. B Biointerfaces 78, 102–108.

Chakrabarty G, Vashishtha M and Leeder D (2015) Polyethylene in knee arthroplasty: A review. *Journal of Clinical Orthopaedics and Trauma* 6(2): 108–112.

Chandra J, Mukherjee PK and Ghannoum MA (2012) Candida biofilms associated with CVC and medical devices. *Mycoses* 55: 46–57.

Chandra, J., Kuhn, D.M., Mukherjee, P.K., Hoyer, L.L., et al., 2001. Biofilm formation by the fungal pathogen Candida albicans: development, architecture, and drug resistance. J. Bacteriol., 183, 5385–5394.

Chandrasekar PH and Manavathu EK (2008) DoAspergillusspecies produce biofilm? *Future Microbiology* 3(1): 19–21.

Chatzinikolaou I, Zipf TF, Hanna H, Umphrey J, Roberts WM, Sherertz R, et al. Minocycline-ethylenediaminetetraacetate lock solution for the prevention of implantable port infections in children with cancer. Clin Infect Dis 2003; 36:116 – 9.

Chauhan A, Bernardin A, Mussard W, Kriegel I, Esteve M, Ghigo J-M, et al. Preventing biofilm formation and associated occlusion by biomimetic glycocalyxlike polymer in central venous catheters. J Infect Dis 2014; 210:1347–56.

Chauhan NM, Shinde RB and Karuppayil SM (2013) Effect of alcohols on filamentation, growth, viability and biofilm development in Candida albicans. *Brazilian Journal of Microbiology* 44(4): 1315–1320.

Chen H (2006) Feedback control of morphogenesis in fungi by aromatic alcohols. *Genes & Development* 20(9): 1150–1161.

Chen H, Fujita M, Feng Q, Clardy J & Fink GR (2004) Tyrosol is a quorum-sensing molecule in Candida albicans. P Natl Acad Sci USA 101: 5048–5052

Cheng J, Park T-S, Chio L-C, Fischl AS and Ye XS (2003) Induction of Apoptosis by Sphingoid Long-Chain Bases in Aspergillus nidulans. *Molecular and Cellular Biology* 23(1): 163–177.

Chitarra GS, Abee T, Rombouts FM, Posthumus MA & Dijksterhuis J (2004) Germination of Penicillium paneum conidia is regulated by 1-octen-3-ol, a volatile self-inhibitor. Appl Environ Microb 70: 2823–2829.

Chou, T. (2010). Drug Combination Studies and Their Synergy Quantification Using the Chou-Talalay Method. *Cancer Research, 70*(2), 440-446.

Collins JA, Schandl CA, Young KK, Vesely J and Willingham MC (1997) Major DNA Fragmentation Is a Late Event in Apoptosis. *Journal of Histochemistry & Cytochemistry*45(7): 923–934.

Cordeiro RDA, Teixeira CE, Brilhante RS, Castelo-Branco DS, Alencar LP, Oliveira JSD, Monteiro AJ, Bandeira TJ, Sidrim JJ, Moreira JLB and Rocha MF (2015) Exogenous tyrosol inhibits planktonic cells and biofilms of Candida species and enhances their susceptibility to antifungals. *FEMS Yeast Research* 15(4).

Cordeiro, R.A., Teixeira, C.E., Brilhante, R.S., Castelo- Branco, D.S., et al., 2015. Exogenous tyrosol inhibits planktonic cells and biofilms of Candida species and enhances their susceptibility to antifungals. FEMS Yeast Res., 15, fov012.

Cortese YJ, Wagner VE, Tierney M, Devine D and Fogarty A (2018) Review of Catheter-Associated Urinary Tract Infections and In Vitro Urinary Tract Models. *Journal of Healthcare Engineering* 2018: 1–16.

Corvis Y, Brezesinski G, Rink R, Walcarius A, Heyden AVD, Mutelet F and Rogalska E (2006) Analytical Investigation of the Interactions between SC3 Hydrophobin and Lipid Layers: Elaborating of Nanostructured Matrixes for Immobilizing Redox Systems. *Analytical Chemistry* 78(14): 4850–4864.

Cottier F and Mühlschlegel FA (2012) Communication in Fungi. *International Journal of Microbiology* 2012: 1–9.

Cugini C, Calfee MW, Farrow JM, Morales DK, Pesci EC and Hogan DA (2007) Farnesol, a common sesquiterpene, inhibits PQS production in Pseudomonas aeruginosa. *Molecular Microbiology* 65(4): 896–906.

Cullen PJ and Sprague GF (2012) The Regulation of Filamentous Growth in Yeast. *Genetics* 190(1): 23–49.

D'Antonio D, Parruti G, Pontieri E, Bonaventura G, Manzoli L, Sferra R, Vetuschi A, Piccolomini R, Romano F and Staniscia T (2004) Slime production by clinical isolates of Blastoschizomyces capitatus from patients with hematological malignancies and catheter-related fungemia. *European Journal of Clinical Microbiology & Infectious Diseases* 23(10): 787–789.

Dagenais TRT, Chung D, Giles SS, Hull CM, Andes D and Keller NP (2008) Defects in Conidiophore Development and Conidium-Macrophage Interactions in a Dioxygenase Mutant of Aspergillus fumigatus. Infection and Immunity76(7): 3214–3220.

Dague E, Alsteens D, Latgé J-P and Dufrêne YF (2008) High-Resolution Cell Surface Dynamics of Germinating Aspergillus fumigatus Conidia. *Biophysical Journal* 94(2): 656–660.

Darouiche RO, Mansouri MD, Gawande PV and Madhyastha S (2009) Antimicrobial and antibiofilm efficacy of triclosan and DispersinB(R) combination. *Journal of Antimicrobial Chemotherapy* 64(1): 88–93.

Das S, Saha R, Rani M, Ramachandran V, Chaudhary S and Gupta C (2014) Biofilm formation by fvCandida species on intrauretheral catheter and its antifungal susceptibility profile. *Indian Journal of Medical Microbiology* 32(4): 467.

Das S.C.and Kapoor K.N., (2004) Effect of growth medium on hydrophobicity of Staphylococcus epidermidis. Indian J. Med. Res. 119: 107 – 109.

Davey ME and O'toole GA (2000) Microbial Biofilms: from Ecology to Molecular Genetics. *Microbiology and Molecular Biology Reviews* 64(4): 847–867.

Davis LE (2002) Biofilm on Ventriculo-Peritoneal Shunt Tubing as a Cause of Treatment Failure in Coccidioidal Meningitis. *Emerging Infectious Diseases* 8(4): 376–379.

Davis-Hanna A, Piispanen AE, Stateva LI and Hogan DA (2007) Farnesol and dodecanol effects on the Candida albicans Ras1-cAMP signalling pathway and the regulation of morphogenesis. *Molecular Microbiology* 67(1): 47–62. Davis LE (2002) Biofilm on Ventriculo-Peritoneal Shunt Tubing as a Cause of Treatment Failure in Coccidioidal Meningitis. *Emerging Infectious Diseases* 8(4): 376–379.

Defoirdt, T., Miyamoto, C. M., Wood, T. K., Meighen, E. A., Sorgeloos, P., Verstraete, W. and Bossier, P. 2007. The natural furanone (5Z)-4-bromo-5-(bromomethylene)-3-butyl-2(5H)-furanone disrupts quorum sensing-regulated gene expression in Vibrio harveyi by decreasing the DNA-binding activity of the transcriptional regulator protein luxR Environmental Microbiology 9(10): 2486-2495.

Deng, D., Sun, P., Yan, C. Ke, M., Jiang, X., Xiong, L., Ren, W., Hirata, K., Yamamoto, M., Fan, S., Yan, N (2015). Molecular basis of ligand recognition and transport by glucose transporters. *Nature* 526, 391–396.

Derengowski LS, De-Souza-Silva C, Braz SV, Mello-De-Sousa TM, Báo SN, Kyaw CM and Silva-Pereira I (2009) Antimicrobial effect of farnesol, a Candida albicans quorum sensing molecule, on Paracoccidioides brasiliensis growth and morphogenesis. *Annals of Clinical Microbiology and Antimicrobials* 8(1): 13.

Deveau A and Hogan DA (2010) Linking Quorum Sensing Regulation and Biofilm Formation by Candida albicans. *Methods in Molecular Biology Quorum Sensing* 219–233.

Dichtl K, Ebel F, Dirr F, Routier FH, Heesemann J and Wagener J (2010) Farnesol misplaces tip-localized Rho proteins and inhibits cell wall integrity signalling in Aspergillus fumigatus. *Molecular Microbiology* 76(5): 1191–1204.

Dixit S, Dubey RC, Maheshwari DK, Seth PK and Bajpai VK (2017) Roles of quorum sensing molecules from Rhizobium etli RT1 in bacterial motility and biofilm formation. *Brazilian Journal of Microbiology* 48(4): 815–821.

Dong Y-H, Wang L-H and Zhang L-H (2007) Quorum-quenching microbial infections: mechanisms and implications. *Philosophical Transactions of the Royal Society B: Biological Sciences* 362(1483): 1201–1211.

Donlan RM (2002) Biofilms: Microbial Life on Surfaces. *Emerging Infectious Diseases* 8(9): 881–890.

Donlan RM and Costerton JW (2002) Biofilms: Survival Mechanisms of Clinically Relevant Microorganisms. *Clinical Microbiology Reviews* 15(2): 167–193.

Dos Reis, T. F., Menino, J. F., Bom, V. L., Brown, N. A., Colabardini, A. C., Savoldi, M., Goldman M.H., Rodrigues, F., Goldman, G. H., (2013). Identification of glucose transporters in *Aspergillus nidulans*. *PloS one*, *8*(11), e81412.

Doyle, R. (2000). Contribution of the hydrophobic effect to microbial infection. Microb. Infect. 2, 391–400

Dranginis AM, Rauceo JM, Coronado JE and Lipke PN (2007) A Biochemical Guide to Yeast Adhesins: Glycoproteins for Social and Antisocial Occasions. *Microbiology and Molecular Biology Reviews* 71(2): 282–294.

Dunne WM (2002) Bacterial Adhesion: Seen Any Good Biofilms Lately? *Clinical Microbiology Reviews* 15(2): 155–166.

Dupont B and Drouhet E (1979) In vitro synergy and antagonism of antifungal agents against yeast-like fungi. *Postgraduate Medical Journal* 55(647): 683–686.

Dupont B. (2002). Overview of the lipid formulations of amphotericin B. *J Antimicrob Chemother* 49 Suppl 1:31–36

Dynesen J and Nielsen J (2003) Surface Hydrophobicity of Aspergillus nidulans Conidiospores and Its Role in Pellet Formation. *Biotechnology Progress* 19(3): 1049–1052.

Egbe NE, Paget CM, Wang H and Ashe MP (2015) Alcohols inhibit translation to regulate morphogenesis in C. albicans. *Fungal Genetics and Biology* 77: 50–60.

Ellis M (1999) Therapy of *Aspergillus fumigatus*-Related Diseases. *Aspergillus fumigatus Contributions to Microbiology* 105–129.

Estrela A and Abraham W-R (2016) Fungal Metabolites for the Control of Biofilm Infections. *Agriculture* 6(3): 37.

Falde EJ, Yohe ST, Colson YL and Grinstaff MW (2016) Superhydrophobic materials for biomedical applications. *Biomaterials* 104: 87–103.

Ferriols VMEN, Yaginuma R, Adachi M, Takada K, Matsunaga S and Okada S (2015) Cloning and characterization of farnesyl pyrophosphate synthase from the highly branched isoprenoid producing diatom Rhizosolenia setigera. *Scientific Reports* 5(1).

Fillinger S, Chaveroche M-K, Shimizu K, Keller N, d'Enfert C. (2002). cAMP and ras signaling independently control spore germination in the filamentous fungus Aspergillus nidulans. Mol Microbiol 44:1001–1016.

Fink SL, Cookson BT. 2005. Apoptosis, pyroptosis, and necrosis: mechanistic description of dead and dying eukaryotic cells. Infect. Immun. 73: 1907–1916

Flemming H-C and Wingender J (2010) The biofilm matrix. *Nature Reviews Microbiology* 8(9): 623–633.

Fontaine T, Beauvais A, Loussert C, Thevenard B, Fulgsang CC, Ohno N, Clavaud C, Prevost M-C and Latgé J-P (2010) Cell wall α1-3glucans induce the aggregation of germinating conidia of Aspergillus fumigatus. *Fungal Genetics and Biology* 47(8): 707–712.

Fontaine T., Delangle A., Simenel C., Coddeville B., van Vliet S. J., van Kooyk Y., Bozza S., Moretti S., Schwarz F., Trichot C., Aebi M., Delepierre M., Elbim C., Romani L., and Latgé J. P. (2011) Galactosaminogalactan, a new immunosuppressive polysaccharide of *Aspergillus fumigatus*. PLoS Pathog. 7, e1002372.

Foster AJ, Jenkinson JM, Talbot NJ. (2003). Trehalose synthesis and metabolism are required at different stages of plant infection by Magnaporthe grisea. EMBO J 22:225–235.

Fournel I, Sautour M, Lafon I, Sixt N, L'ollivier C, Dalle F, Chavanet P, Couillaud G, Caillot D, Astruc K, Bonnin A and Aho-Glélé L-S (2010) Airborne Aspergillus contamination during hospital construction works: Efficacy of protective measures. *American Journal of Infection Control* 38(3): 189–194.

Freitas FZ, de Paula RM, Barbosa LCB, Terenzi HF, Bertolini MC. 2010. cAMP signaling pathway controls glycogen metabolism in Neurospora crassa by regulating the glycogen synthase gene expression and phosphorylation. Fungal Genet Biol 47:43–52.

Fuglsang, C.C., Berka, R.M., Wahleithner, J.A., Kaupinnen, S., Shuster, J.R., Rasmussen, G., et al. (2000) Biochemical analysis of recombinant fungal mutanases. A new family of α-1,3-glucanases with novel carbohydrate-binding domains. J Biol Chem 275: 2009–2018.

Fuller KK, Richie DL, Feng X, Krishnan K, Stephens TJ, Wikenheiser Brokamp KA, Askew DS, Rhodes JC. 2011. Divergent protein kinase A isoforms co-ordinately regulate conidial germination, carbohydrate metabolism and virulence in Aspergillus fumigatus. Mol Microbiol 79: 1045–1062.

Fuqua WC, Winans SC and Greenberg EP (1994) Quorum sensing in bacteria: the LuxR-LuxI family of cell density-responsive transcriptional regulators. *Journal of Bacteriology* 176(2): 269–275.

Gastebois A, Clavaud C, Aimanianda V, Latgé J-P. (2009). Aspergillus fumigatus: cell wall polysaccharides, their biosynthesis and organization. Future Microbiol 4:583–595.

Gersuk, G.M., Underhill, D.M., Zhu, L., and Marr, K.A. (2006) Dectin-1 and TLRs permit macrophages to distinguish between different Aspergillus fumigatus cellular states. J Immunol 176: 3717–3724.

Gestel JV, Kolter R and Vlamakis H (2015) Division of Labor in Biofilms: the Ecology of Cell Differentiation. *Microbiology Spectrum* 3(2).

Ghannoum MA and Isham NC (2009) Dermatophytes and dermatophytoses. Chapter 16, *Clinical Mycology* 375–384.

Ghosh S, Kebaara BW, Atkin AL and Nickerson KW (2008) Regulation of Aromatic Alcohol Production in Candida albicans. *Applied and Environmental Microbiology* 74(23): 7211–7218.

Giaouris E., Chapot-Chartier M., Briandet R. (2009). Surface physicochemical analysis of natural *Lactococcus lactis* strains reveals the existence of hydrophobic and low charged strains with altered adhesive properties. Int. J. Food. Microbiol. 131, 2–9

Gibbons, J. G., Beauvais, A., Beau, R., McGary, K. L., Latge, J. P., and Rokas, A. (2012). Global transcriptome changes underlying colony growth in the opportunistic human pathogen *Aspergillus fumigatus*. *Eukaryot. Cell* 11, 68–78.

Gilbert P and Mcbain AJ (2002) Literature-Based Evaluation of the Potential Risks Associated with Impregnation of Medical Devices and Implants with Triclosan. *Surgical Infections* 3(s1).

Girardin H, Paris S, Rault J, Bellon-Fontaine MN, Latge´ JP (1999). The role of the rodlet structure on the physicochemical properties of Aspergillus conidia. Lett Appl Microbiol; 29: 364–369.

Glass N (2004) Hyphal homing, fusion and mycelial interconnectedness. *Trends in Microbiology* 12(3): 135–141

Gominet M, Compain F, Beloin C and Lebeaux D (2017) Central venous catheters and biofilms: where do we stand in 2017? *Apmis*125(4): 365–375.

González-Ramírez AI, Ramírez-Granillo A, Medina-Canales MG, Rodríguez-Tovar AV and Martínez-Rivera MA (2016) Analysis and description of the stages of Aspergillus fumigatus biofilm formation using scanning electron microscopy. *BMC Microbiology* 16(1).

Gori K, Knudsen PB, Nielsen KF, Arneborg N and Jespersen L (2011) Alcohol-based quorum sensing plays a role in adhesion and sliding motility of the yeast Debaryomyces hansenii. *FEMS Yeast Research* 11(8): 643–652.

Granick S and Bae SC (2008) CHEMISTRY: A Curious Antipathy for Water. Science 322(5907): 1477–1478.

Gravelat F. N., Beauvais A., Liu H., Lee M. J., Snarr B. D., Chen D., Xu W., Kravtsov I., Hoareau C. M., Vanier G., Urb M., Campoli P., Al Abdallah Q., Lehoux M., Chabot J. C., et al. (2013) Aspergillus galactosaminogalactan mediates adherence to host constituents and conceals hyphal β-glucan from the immune system. PLoS Pathog. 9, e1003575.

Gravelat FN, Doedt T, Chiang LY, Liu H, Filler SG, Patterson TF and Sheppard DC (2008) In Vivo Analysis of Aspergillus fumigatus Developmental Gene Expression Determined by Real-Time Reverse Transcription-PCR. *Infection and Immunity* 76(8): 3632–3639.

Gray KC, Palacios DS, Dailey I, Endo MM, Uno BE, Wilcock BC, Burke MD. (2012). Amphotericin primarily kills yeast by simply binding ergosterol. Proc. Natl. Acad. Sci. U. S. A. 109:2234 –2239

Graybill JR, Burgess DS and Hardin TC (1997) Key issues concerning fungistatic versus fungicidal drugs. *European Journal of Clinical Microbiology & Infectious Diseases* 16(1): 42–50.

Gresnigt MS, Bozza S, Becker KL, Joosten LAB, Abdollahi-Roodsaz S, Berg WBVD, Dinarello CA, Netea MG, Fontaine T, Luca AD, Moretti S, Romani L, Latge J-P and Veerdonk FLVD (2014) A Polysaccharide Virulence Factor from Aspergillus fumigatus Elicits Anti-inflammatory Effects through Induction of Interleukin-1 Receptor Antagonist. *PLoS Pathogens* 10(3).

Grosse C, Heinekamp T, Kniemeyer O, Gehrke A, Brakhage AA. 2008. Protein kinase A regulates growth, sporulation, and pigment formation in Aspergillus fumigatus. Appl Environ Microbiol 74:4923– 4933.

Grundke K, Pöschel K, Synytska A, Frenzel R, Drechsler A, Nitschke M, Cordeiro A, Uhlmann P and Welzel P (2015) Experimental studies of contact angle hysteresis phenomena on polymer surfaces — Toward the understanding and control of wettability for different applications. Advances in Colloid and Interface Science 222: 350–376.

Grunér MS, Szilvay GR, Berglin M, Lienemann M, Laaksonen P and Linder MB (2012) Self-assembly of Class II Hydrophobins on Polar Surfaces. *Langmuir* 28(9): 4293–4300.

Guilhen C, Charbonnel N, Parisot N, Gueguen N, Iltis A, Forestier C and Balestrino D (2016) Transcriptional profiling of Klebsiella pneumoniae defines signatures for planktonic, sessile and biofilm-dispersed cells. *BMC Genomics* 17(1).

Guo B, Zou Q, Lei Y and Jia D (2009) Structure and Performance of Polyamide 6/Halloysite Nanotubes Nanocomposites. *Polymer Journal* 41(10): 835–842.

Guo J, Pan L-H, Li Y-X, Yang X-D, Li L-Q, Zhang C-Y and Zhong J-H (2016) Efficacy of triclosan-coated sutures for reducing risk of surgical site infection in adults: a meta-analysis of randomized clinical trials. *Journal of Surgical Research* 201(1): 105–117.

Guruceaga X, Ezpeleta G, Mayayo E, Sueiro-Olivares M, Abad-Diaz-DeCerio A, Aguirre-Urízar JM, Liu HG, Wiemann P, Bok JW, Filler SG, Keller NP, Hernando FL, Ramirez-Garcia A, Rementeria A (2018) A possible role for fumagillin in cellular damage during host infection by Aspergillus fumigatus. Virulence 9:1548–1561.

Hakanpää J., Paananen A., Askolin S., Nakari-Setälä T., Parkkinen T., Penttilä M., Linder M.B., Rouvinen J. 2004. Atomic resolution structure of the HFBII hydrophobin, a self-assembling amphiphile. J. Biol. Chem. 279: 534–539.

Hall-Stoodley L, Costerton JW and Stoodley P (2004) Bacterial biofilms: from the Natural environment to infectious diseases. *Nature Reviews Microbiology* 2(2): 95–108.

Han T-L, Cannon RD and Villas-Bôas SG (2012) The metabolic response of Candida albicansto farnesol under hyphae-inducing conditions. *FEMS Yeast Research* 12(8): 879–889.

Harding MW, Marques LL, Howard RJ and Olson ME (2009) Can filamentous fungi form biofilms? *Trends in Microbiology* 17(11): 475–480.

Hardwick JM (2018) Do Fungi Undergo Apoptosis-Like Programmed Cell Death? *mBio* 9(4).

Harmsen P, Huijgen W, Bermudez L, Bakker R (2010) Literature review of physical and chemical pretreatment processes for lignocellulosic biomass. Report no. 1184, pp 1–49

Harris SD and Momany M (2004) Polarity in filamentous fungi: moving beyond the yeast paradigm. *Fungal Genetics and Biology* 41(4): 391–400.

Hazen KC and Cutler JE (1983) Isolation and Purification of Morphogenic Autoregulatory Substance Produced by Candida albicans1. *The Journal of Biochemistry* 94(3): 777–783.

Hediger, M. A., Clemencon, B., Burrier, R. E., Bruford, E. A., (2013). The ABCs of membrane transporters in health and disease (SLC series): introduction. Mol. Aspects Med.34, 95–107.

Heilmann C, Schweitzer O, Gerke C, Vanittanakom N, Mack D and Götz F (1996) Molecular basis of intercellular adhesion in the biofilm-forming Staphylococcus epidermidis. *Molecular Microbiology* 20(5): 1083–1091.

Heinekamp T, Schmidt H, Lapp K, Pähtz V, Shopova I, Köster-Eiserfunke N, Krüger T, Kniemeyer O and Brakhage AA (2014) Interference of Aspergillus fumigatus with the immune response. *Seminars in Immunopathology* 37(2): 141–152.

Helou GE, Viola GM, Hachem R, Han XY and Raad II (2013) Rapidly growing mycobacterial bloodstream infections. *The Lancet Infectious Diseases* 13(2): 166–174.

Hengge R, Gründling A, Jenal U, Ryan R and Yildiz F (2015) Bacterial Signal Transduction by Cyclic Di-GMP and Other Nucleotide Second Messengers. *Journal of Bacteriology* 198(1): 15–26.

Henry C, Latgé J-P and Beauvais A (2011) α1,3 Glucans Are Dispensable in Aspergillus fumigatus. *Eukaryotic Cell* 11(1): 26–29.

Hentzer M and Givskov M (2003) Pharmacological inhibition of quorum sensing for the treatment of chronic bacterial infections. Journal of Clinical Investigation 112(9): 1300–1307.

Hentzer M, Rice SA, Givskov M, Høiby N, Parsek MR, Riedel K, Heydorn A, Eberl L, Andersen JB, Molin S, Kjelleberg S and Rasmussen TB (2002) Inhibition of quorum sensing in Pseudomonas aeruginosa biofilm bacteria by a halogenated furanone compound. *Microbiology* 148(1): 87–102.

Hoiby N, Ciofu O, Johansen HK, Song ZJ, Moser C, Jensen PO, Molin S, Givskov M, Tolker-Nielsen T, Bjarnsholt T (2011). The clinical impact of bacterial biofilms. Int J Oral Sci.; 3(2):55–65.

Hope, W.W., et al., (2007) Pathogenesis of Aspergillus fumigatus and the kinetics of galactomannan in an in vitro model of early invasive pulmonary aspergillosis: implications for antifungal therapy. J Infect Dis.; 195(3): p. 455-66.

Hopewell J, Dvorak R and Kosior E (2009) Plastics recycling: challenges and opportunities. *Philosophical Transactions of the Royal Society B: Biological Sciences* 364(1526): 2115–2126.

Hornby JM, Jacobitz-Kizzier SM, Mcneel DJ, Jensen EC, Treves DS and Nickerson KW (2004) Inoculum Size Effect in Dimorphic Fungi: Extracellular Control of Yeast-Mycelium Dimorphism in Ceratocystis ulmi. *Applied and Environmental Microbiology* 70(3): 1356–1359.

Hornby JM, Jensen EC, Lisec AD, Tasto JJ, Jahnke B, Shoemaker R, Dussault P and Nickerson KW (2001) Quorum Sensing in the Dimorphic Fungus Candida albicans Is Mediated by Farnesol. *Applied and Environmental Microbiology* 67(7): 2982–2992.

Houck MM (2001) *Mute witnesses: trace evidence analysis*. Academic Press.

Howard, S.J., et al., Pharmacokinetics and pharmacodynamics of posaconazole for invasive pulmonary aspergillosis: clinical implications for antifungal therapy. J Infect Dis, 2011. 203(9): p. 1324-32.

Hsu CY, Lin MH, Chen CC, Chien SC, Cheng YH, Su IN, and Shu JC (2011) Vancomycin promotes the bacterial autolysis, release of extracellular DNA, and biofilm formation in vancomycin-non-susceptible Staphylococcus aureus. FEMS Immunol Med Microbiol., 63 (2): 236-247.

Huhtamäki T, Tian X, Korhonen JT and Ras RHA (2018) Surface-wetting characterization using contact-angle measurements. *Nature Protocols* 13(7): 1521–1538.

Ibrahim NH, Melake NA, Somily AM, Zakaria AS, Baddour MM and Mahmoud AZ (2015) The effect of antifungal combination on transcripts of a subset of drug-resistance genes in clinical isolates of Candida species induced biofilms. *Saudi Pharmaceutical Journal* 23(1): 55–66.

Imamura Y, Chandra J, Mukherjee PK, Lattif AA, Szczotka-Flynn LB, Pearlman E, Lass JH, O'donnell K and Ghannoum MA (2007) Fusarium and Candida albicans Biofilms on Soft Contact Lenses: Model Development, Influence of Lens Type, and Susceptibility to Lens Care Solutions. *Antimicrobial Agents and Chemotherapy* 52(1): 171–182.

Iwahori K, Tokutomi T, Miyata N and Fujita M (2001) Formation of stable foam by the cells and culture supernatant of Gordonia (Nocardia) amarae. *Journal of Bioscience and Bioengineering* 92(1): 77–79.

Jacobsen SM, Stickler DJ, Mobley HLT and Shirtliff ME (2008) Complicated Catheter-Associated Urinary Tract Infections Due to Escherichia coli and Proteus mirabilis. *Clinical Microbiology Reviews* 21(1): 26–59.

Jaganathan SK, Supriyanto E, Murugesan S, Balaji A and Asokan MK (2014) Biomaterials in Cardiovascular Research: Applications and Clinical Implications. *BioMed Research International* 2014: 1–11.

Jensen BG, Andersen MR, Pedersen MH, Frisvad JC and Søndergaard I (2010) Hydrophobins from Aspergillus species cannot be clearly divided into two classes. *BMC Research Notes* 3(1).

Jones RD, Jampani HB, Newman JL and Lee AS (2000) Triclosan: A review of effectiveness and safety in health care settings. *American Journal of Infection Control* 28(2): 184–196.

Joo JH and Jetten AM (2010) Molecular mechanisms involved in farnesol-induced apoptosis. *Cancer Letters* 287(2): 123–135.

Jordan L, Adams-Graves P, Kanter-Washko J, Oneal PA, Sasane M, Vekeman F, Bieri C, Magestro M, Marcellari A and Duh MS (2014) Multicenter COMPACT study of COMplications in Patients with sickle cell disease And utilization of iron Chelation Therapy. *Current Medical Research and Opinion* 31(3): 513–523.

Joung Y-H (2013) Development of Implantable Medical Devices: From an Engineering Perspective. *International Neurourology Journal* 17(3): 98.

Kalia VC (2013) Quorum sensing inhibitors: An overview. *Biotechnology Advances* 31(2): 224–245.

Kamiński DM (2014) Recent progress in the study of the interactions of amphotericin B with cholesterol and ergosterol in lipid environments. European Biophysics Journal 43(10-11): 453–467.

Kaplan J (2010) Biofilm Dispersal: Mechanisms, Clinical Implications, and Potential Therapeutic Uses. *Journal of Dental Research* 89(3): 205–218.

Katragkou, A., McCarthy, M., Alexander, E.L., Antachopoulos, C., et al., (2015). In vitro interactions between farnesol and fluconazole, amphotericin B or micafungin against Candida albicans biofilms. J. Antimicrob. Chemother., 70, 470–478.

Kaur S and Singh S (2013) Biofilm formation byAspergillus fumigatus. *Medical Mycology* 1–8.

Kavosi Z, Sarikhani Khorrami M, Keshavarz K, Jafari A, Hashemi Meshkini A, Safaei HR, et al. (2016) Is Taurolidine-citrate an effective and cost-effective hemodialysis catheter lock solution? A systematic review and cost- effectiveness analysis. Med J Islam Repub Iran; 30:347.

Kaye, D., and M. T. Hessen. (1994). Infections associated with foreign bodies in the urinary tract. In A. L. Bisno and F. A. Waldovogel (ed.), Infections associated with indwelling medical devices, 2nd ed. American Society for Microbiology, Washington, D.C. p. 291–307.

Kelly S, Grimm LH, Jonas R, Hempel DC and Krull R (2006) Investigations of the Morphogenesis of Filamentous Microorganisms. *Engineering in Life Sciences* 6(5): 475–480.

Keren, I., N. Kaldalu, A. Spoering, Y. Wang, and K. Lewis (2004). Persister cells and tolerance to antimicrobials. *FEMS Microbiol. Lett.* 230:13-18

Khot, P. D., P. A. Suci, R. L. Miller, R. D. Nelson, and B. J. Tyler. (2006). A small subpopulation of blastospores in *Candida albicans* biofilms exhibit resistance to amphotericin B associated with differential regulation of ergosterol and β-1,6-glucan pathway genes. *Antimicrob. Agents Chemother.* 50:3708-3716.

Kim SA, Moon H, Lee K and Rhee MS (2015) Bactericidal effects of triclosan in soap both in vitro and in vivo. *Journal of Antimicrobial Chemotherapy*.

Kisko, K.; Szilvay, G. R.; Vuorimaa, E.; Lemmetyinen, H.; Linder, M. B.; Torkkeli, M.; Serimaa, R. (2009). Self-assembled films of hydrophobin proteins HFBI and HFBII studied in situ at the air/water interface. Langmuir, 25 (3), 1612−9.

Kitahara M, Seth VK, Medoff G and Kobayashi GS (1976). Activity of Amphotericin B, 5-Fluorocytosine, and Rifampin Against Six Clinical Isolates of Aspergillus. *Antimicrobial Agents and Chemotherapy* 9(6): 915–919.

Kitazumi I and Tsukahara M (2010) Regulation of DNA fragmentation: the role of caspases and phosphorylation. *FEBS Journal* 278(3): 427–441.

Kobayashi, H., Takami, H., Hirayama, H., Kobata, K., Usami, R., and Horikoshi, K. (1999). Outer membrane changes in a toluene-sensitive mutant of toluenetolerant Pseudomonas putida IH-2000. J. Bacteriol. 181, 4493–4498.

Kobayashi, H., Takami, H., Hirayama, H., Kobata, K., Usami, R., and Horikoshi, K. (1999). Outer membrane changes in a toluene-sensitive mutant of toluenetolerant Pseudomonas putida IH-2000. J. Bacteriol. 181, 4493–4498

Kochkodan V., Tsarenko S., Potapchenko N., Kosinova V., Goncharuk V. (2008). Adhesion of microorganisms to polymer membranes: a photobactericidal effect of surface treatment with TiO_2. Desalination 220, 380–385

Kohler JR, Casadevall A and Perfect J (2014) The Spectrum of Fungi That Infects Humans. *Cold Spring Harbor Perspectives in Medicine* 5(1).

Kolodkin-Gal I and Engelberg-Kulka H (2008) The Extracellular Death Factor: Physiological and Genetic Factors Influencing Its Production and Response in Escherichia coli. *Journal of Bacteriology* 190(9): 3169–3175.

Korstgens V, Flemming HC, Wingender J, Borchard W (2001). Influence of calcium ions on the mechanical properties of a model biofilm of mucoid Pseudomonas aeruginosa. Water Sci Technol; 43:49–57.

Köseoğlu VK, Heiss C, Azadi P, Topchiy E, Güvener ZT, Lehmann TE, Miller KW and Gomelsky M (2015) L isteria monocytogenes exopolysaccharide: origin, structure, biosynthetic machinery and c-di-GMP-dependent regulation. *Molecular Microbiology* 96(4): 728–743.

Kostakioti M, Hadjifrangiskou M and Hultgren SJ (2013) Bacterial Biofilms: Development, Dispersal, and Therapeutic Strategies in the Dawn of the Postantibiotic Era. *Cold Spring Harbor Perspectives in Medicine* 3(4).

Kovács R, Tóth Z, Nagy F, Daróczi L, Bozó A and Majoros L (2017) Activity of exogenous tyrosol in combination with caspofungin and micafungin against Candida parapsilosis sessile cells. *Journal of Applied Microbiology* 122(6): 1529–1536.

Kragelund, C., Kong, Y., van der Waarde, J., Thelen, K., Eikelboom, D., Tandoi, V., et al. (2006). Ecophysiology of different filamentous Alphaproteobacteria in industrial wastewater treatment plants. Microbiology 152, 3003–3012

Krijgsheld P, Bleichrodt R, van Veluw GJ, Wang F, Müller WH, Dijksterhuis J, Wösten HAB. 2013. Development in Aspergillus. Stud Mycol 74:1–29

Krom BP, Levy N, Meijler MM and Jabra-Rizk MA (2015) Farnesol and Candida albicans: Quorum Sensing or Not Quorum Sensing? *Israel Journal of Chemistry* 56(5): 295–301.

Kulkarni VS and Shaw C (2016) Surfactants, Lipids, and Surface Chemistry. Essential Chemistry for Formulators of Semisolid and Liquid Dosages 5–19.

Kvasničková E, Paulíček V, Paldrychová M, Ježdík R, Maťátková O and Masák J (2016) Aspergillus fumigatus DBM 4057 biofilm formation is inhibited by chitosan, in contrast to baicalein and rhamnolipid. *World Journal of Microbiology and Biotechnology* 32(11).

Kwon-Chung KJ and Sugui JA (2013) Aspergillus fumigatus—What Makes the Species a Ubiquitous Human Fungal Pathogen? *PLoS Pathogens* 9(12).

Lamarre C, Sokol S, Debeaupuis J-P, Henry C, Lacroix C, Glaser P, Coppée J-Y, François J-M and Latgé J-P (2008) Transcriptomic analysis of the exit from dormancy of Aspergillus fumigatus conidia. *BMC Genomics* 9(1): 417.

Langford ML, Atkin AL and Nickerson KW (2009) Cellular interactions of farnesol, a quorum-sensing molecule produced by Candida albicans. *Future Microbiology* 4(10): 1353–1362.

Langford ML, Hasim S, Nickerson KW and Atkin AL (2009). Activity and Toxicity of Farnesol towards Candida albicans Are Dependent on Growth Conditions. Antimicrobial Agents and Chemotherapy 54(2): 940–942.

Lappann M, Claus H, van Alen T, Harmsen M, Elias J, Molin S, Vogel U. 2010. A dual role of extracellular DNA during biofilm formation of Neisseria meningitidis. Mol. Microbiol. 75: 1355–1371

Larsen P, Nielsen JL, Dueholm MS, Wetzel R, Otzen D and Nielsen PH (2007). Amyloid adhesins are abundant in natural biofilms. *Environmental Microbiology* 9(12): 3077–3090.

Lasarre B and Federle MJ (2013) Exploiting Quorum Sensing To Confuse Bacterial Pathogens. *Microbiology and Molecular Biology Reviews* 77(1): 73–111.

Latgé Jean-Paul and Steinbach WJ (2009) *Aspergillus fumigatus and aspergillosis*. Washington, D.C.: ASM Press.

Latge, J.P., et al., Chemical and immunological characterization of the extracellular galactomannan of Aspergillus fumigatus. Infect Immun, 1994. 62(12): p. 5424-33.

Lebeaux D, Ghigo J-M, Beloin C (2014). Biofilm-related infections: bridging the gap between clinical management and fundamental aspects of recalcitrance toward antibiotics. Microbiol Mol Biol Rev ;78:510–43.

Lee H, Chang YC, Nardone G & Kwon-Chung KJ (2007) TUP1 disruption in Cryptococcus neoformans uncovers a peptidemediated density-dependent growth phenomenon that mimics quorum sensing. Mol Microbiol 64: 591–601.

Lee MJ and Sheppard DC (2016) Recent advances in the understanding of the Aspergillus fumigatus cell wall. *Journal of Microbiology* 54(3): 232–242.

Lee MJ, Geller AM, Bamford NC, Liu H, Gravelat FN, Snarr BD, Mauff FL, Chabot J, Ralph B, Ostapska H, Lehoux M, Cerone RP, Baptista SD, Vinogradov E, Stajich JE, Filler SG, Howell PL and Sheppard DC (2016) Deacetylation of Fungal Exopolysaccharide Mediates Adhesion and Biofilm Formation. *mBio* 7(2).

Lee MJ, Gravelat FN, Cerone RP, Baptista SD, Campoli PV, Choe S-I, Kravtsov I, Vinogradov E, Creuzenet C, Liu H, Berghuis AM, Latgé J-P, Filler SG, Fontaine T and Sheppard DC (2013) Overlapping and Distinct Roles ofAspergillus fumigatusUDP-glucose 4-Epimerases in Galactose Metabolism and the Synthesis of Galactose-containing Cell Wall Polysaccharides. *Journal of Biological Chemistry* 289(3): 1243–1256.

Lee MJ., Sheppard DC. (2016). Recent advances in the understanding of the Aspergillus fumigatus cell wall. J Microbiol 54:232–242.

Leekha S, Terrell CL and Edson RS (2011) General Principles of Antimicrobial Therapy. *Mayo Clinic Proceedings* 86(2): 156–167.

Leeuwen MV, Krijgsheld P, Bleichrodt R, Menke H, Stam H, Stark J, Wösten H and Dijksterhuis J (2013) Germination of conidia of Aspergillus niger is accompanied by major changes in RNA profiles.*Studies in Mycology* 74: 59–70.

Lefebvre CA, Wataha JC, Cibirka RM, Schuster GS and Parr GR (2001) Effects of triclosan on the cytotoxicity and fungal growth on a soft denture liner. *The Journal of Prosthetic Dentistry* 85(4): 352–356.

Léger T, Garcia C, Ounissi M, Lelandais G and Camadro J-M (2014) The Metacaspase (Mca1p) has a Dual Role in Farnesol-induced Apoptosis inCandida albicans. *Molecular & Cellular Proteomics* 14(1): 93–108.

Lestner, J.M., et al., Pharmacokinetics and pharmacodynamics of amphotericin B deoxycholate, liposomal amphotericin B, and amphotericin B lipid complex in an in vitro model of invasive pulmonary aspergillosis. Antimicrob Agents Chemother, 2010. 54(8): p. 3432-41.

Levine B and Klionsky DJ (2004) Development by Self-Digestion. Developmental Cell 6(4): 463–477.

Lewis, K. 2007. Persister cells, dormancy and infectious disease. *Nat. Rev. Microbiol.* 5:48-56.

Li Y and Bhushan B (2015) The effect of surface charge on the boundary slip of various oleophilic/phobic surfaces immersed in liquids. Soft Matter 11(38): 7680–7695.

Li, Z., Luo, R., Zhang, Y., Yan, X., & Pang, Q. (2018). Effective protein extraction from mycelium and fruiting body of Auricularia auricula for proteomics studies. *International Journal of Food Properties, 21*(1), 2156-2166.

Liebmann B, Mu M, Braun A, Brakhage AA. 2004. The cyclic AMPdependent protein kinase A network regulates development and virulence in Aspergillus fumigatus. Infect Immun 72:5193–5203.

Lin P-J, Grimm L, Wulkow M, Hempel D and Krull R (2007) Population balance modeling of the conidial aggregation ofAspergillus niger. *Biotechnology and Bioengineering* 99(2): 341–350.

Linder MB, Szilvay GR, Nakari-Setälä T and Penttilä ME (2005) Hydrophobins: the protein-amphiphiles of filamentous fungi. *FEMS Microbiology Reviews* 29(5): 877–896.

Littlejohn KA, Hooley P and Cox PW (2012) Bioinformatics predicts diverse Aspergillus hydrophobins with novel properties. *Food Hydrocolloids* 27(2): 503–516.

Liu H, Liu H, Deng J, Chen L, Yuan L, Wu Y. Preventing catheter-related bacteremia with taurolidine-citrate catheter locks: a systematic review and meta-analysis. Blood Purif 2014; 37:179–87.

Liu P, Deng B, Long C-A and Min X (2009) Effect of farnesol on morphogenesis in the fungal pathogenPenicillium expansum. *Annals of Microbiology* 59(1): 33–38.

Liu, X., Sheng, G., and Yu, H. (2009). Physicochemical characteristics of microbial granules. Biotechnol. Adv. 27, 1061–1070.

Llanos A, François J and Parrou J-L (2015) Tracking the best reference genes for RT-qPCR data normalization in filamentous fungi. *BMC Genomics* 16(1): 71.

Lo V, Ren Q, Pham C, Morris V, Kwan A and Sunde M (2014) Fungal Hydrophobin Proteins Produce Self-Assembling Protein Films with Diverse Structure and Chemical Stability. *Nanomaterials*4(3): 827–843.

Lo W-S and Dranginis AM (1998) The Cell Surface Flocculin Flo11 Is Required for Pseudohyphae Formation and Invasion by Saccharomyces cerevisiae. *Molecular Biology of the Cell* 9(1): 161–171.

Lorek J, Pöggeler S, Weide MR, Breves R and Bockmühl DP (2008) Influence of farnesol on the morphogenesis of Aspergillus niger. *Journal of Basic Microbiology* 48(2): 99–103.

Loussert C, Schmitt C, Prevost M-C, Balloy V, Fadel E, Philippe B, Kauffmann-Lacroix C, Latgé JP and Beauvais A (2010) In vivo biofilm composition of Aspergillus fumigatus. *Cellular Microbiology* 12(3): 405–410.

Lu Y, Deng J, Rhodes JC, Lu H and Lu LJ (2014) Predicting essential genes for identifying potential drug targets in Aspergillus fumigatus. *Computational Biology and Chemistry* 50: 29–40.

Luther K, Torosantucci A, Brakhage AA, Heesemann J and Ebel F (2007) Phagocytosis of Aspergillus fumigatus conidia by murine macrophages involves recognition by the dectin-1 beta-glucan receptor and Toll-like receptor 2. *Cellular Microbiology* 9(2): 368–381.

Ly, M., Naïtali-Bouchez, M., Meylheuc, T., Bellon-Fontaine, M., Le, T., Belin, J., et al. (2006). Importance of bacterial surface properties to control the stability of emulsions. Int. J. Food Microbiol. 112, 26–34.

Madeo, F., Fro¨ hlich, E., Ligr, M., Grey, M., Sigrist, S. J. & Wolf, D. H. (1999). Oxygen stress: a regulator of apoptosis in yeast. J Cell Biol 145, 757–767.

Manny AJ, Kjelleberg S, Kumar N, Nys RD, Read RW and Steinberg P (1997) Reinvestigation of the sulfuric acid-catalysed cyclisation of brominated 2-alkyllevulinic acids to 3-alkyl-5-methylene-2(5H)-furanones. *Tetrahedron* 53(46): 15813–15826.

Marqués-Calvo MS (2002) In vitro colonization of hydrophilic contact lenses by Aspergillus niger. *Journal of Industrial Microbiology & Biotechnology* 29(1): 6–9.

Martãnez LC and Vadyvaloo V (2014) Mechanisms of post-transcriptional gene regulation in bacterial biofilms. *Frontiers in Cellular and Infection Microbiology*4.

Martinet, W., van den Plas, D., Raes, H., Reekmans, R. & Contreras, R. (1999). Bax-induced cell death in Pichia pastoris. Biotechnol Lett 21, 821–829.

Martinez LR and Fries BC (2010) Fungal Biofilms: Relevance in the Setting of Human Disease. *Current Fungal Infection Reports* 4(4): 266–275.

Martino, P. D. (2018). Extracellular polymeric substances, a key element in understanding biofilm phenotype. *AIMS Microbiology, 4*(2), 274-288.

Martins M, Henriques M, Lopez-Ribot JL and Oliveira R (2011) Addition of DNase improves the in vitro activity of antifungal drugs against Candida albicans biofilms. *Mycoses* 55(1): 80–85.

Martins M, Uppuluri P, Thomas DP, Cleary IA, Henriques M, Lopez-Ribot JL and Oliveira R (2009) Presence of Extracellular DNA in the Candida albicans Biofilm Matrix and its Contribution to Biofilms. *Mycopathologia* 169(5): 323–331.

Masuko T, Minami A, Iwasaki N, Majima T, Nishimura S-I and Lee YC (2005) Carbohydrate analysis by a phenol–sulfuric acid method in microplate format. *Analytical Biochemistry* 339(1): 69–72.

Maubon D, Park S, Tanguy M, Huerre M, Schmitt C, Prévost M, Perlin D, Latgé J and Beauvais A (2006) AGS3, an α(1–3)glucan synthase gene family member of Aspergillus fumigatus, modulates mycelium growth in the lung of experimentally infected mice.*Fungal Genetics and Biology* 43(5): 366–375.

Mcdougald D, Rice SA, Barraud N, Steinberg PD and Kjelleberg S (2011) Should we stay or should we go: mechanisms and ecological consequences for biofilm dispersal. *Nature Reviews Microbiology* 10(1): 39–50.

McKeen LW (2017) *Permeability properties of plastics and elastomers*. Elsevier.

Medoff, G., Comfort, M., Kobayashi, G. S (1971). Synergistic action of amphotericin Band 5-fluorocytosine against yeast-like organisms. Proc. Soc. Exp. BioI. Med. 138:571-574.

Mehmood A, Liu G, Wang X, Meng G, Wang C and Liu Y (2019) Fungal Quorum-Sensing Molecules and Inhibitors with Potential Antifungal Activity: A Review. *Molecules* 24(10): 1950.

Meletiadis J, Meis JFGM, Mouton JW and Verweij PE (2001) Analysis of Growth Characteristics of Filamentous Fungi in Different Nutrient Media. *Journal of Clinical Microbiology* 39(2): 478–484.

Menon V, Thomas R, Ghale AR, Reinhard C and Pruszak J (2014) Flow Cytometry Protocols for Surface and Intracellular Antigen Analyses of Neural Cell Types. *Journal of Visualized Experiments* (94).

Mesquita N, Portugal A, Piñar G, Loureiro J, Coutinho A, Trovão J, Nunes I, Botelho M and Freitas H (2013) Flow cytometry as a tool to assess the effects of gamma radiation on the viability, growth and metabolic activity of fungal spores. *International Biodeterioration & Biodegradation* 84: 250–257.

Metz B and Kossen NWF (1977) The growth of molds in the form of pellets-a literature review. *Biotechnology and Bioengineering* 19(6): 781–799.

Millard, P., Roth, B., Thi, H.P., Yue, S and Haugland, R. (1997). Development of the FUN-1 family of fluorescent probes for vacuole labeling and viability testing of yeasts. Applied and environmental microbiology. 63. 2897-905.

Miller AJ, Roman B and Norstrom E (2016) A method for easily customizable gradient gel electrophoresis. *Analytical Biochemistry* 509: 12–14.

Mirkes PE (1974). Polysomes, ribonucleic acid, and protein synthesis during germination of Neurospora crassa conidia. Journal of Bacteriology 117: 196– 202.

Mittal KL (2000) *Acid-base interactions: relevance to adhesion science and technology*. VSP.

Miyazawa K, Yoshimi A, Kasahara S, Sugahara A, Koizumi A, Yano S, Kimura S, Iwata T, Sano M and Abe K (2018) Molecular Mass and Localization of α-1,3-Glucan in Cell Wall Control the Degree of Hyphal Aggregation in Liquid Culture of Aspergillus nidulans. Frontiers in Microbiology 9.

Modjarrad K and Ebnesajjad S (2014) *Handbook of polymer applications in medicine and medical devices*. Elsevier/William Andrew.

Molin S and Tolker-Nielsen T (2003) Gene transfer occurs with enhanced efficiency in biofilms and induces enhanced stabilisation of the biofilm structure. *Current Opinion in Biotechnology* 14(3): 255–261.

Monod M, Capoccia S, Léchenne B, Zaugg C, Holdom M, Jousson O (2002) Secreted proteases from pathogenic fungi. Int J Med Microbiol 292:405–419

Mortz E, Krogh TN, Vorum H and Görg A (2001) Improved silver staining protocols for high sensitivity protein identification using matrix-assisted laser desorption/ionization-time of flight analysis. *Proteomics* 1(11): 1359–1363.

Mousavi SAA (2004) Oxidative and amphotericin B-mediated cell death in the opportunistic pathogen Aspergillus fumigatus is associated with an apoptotic-like phenotype. *Microbiology* 150(6): 1937–1945.

Mousavi, S. A. A. & Robson, G. D. (2003). Entry into the stationary phase is associated with a rapid loss of viability and an apoptoticlike phenotype in the opportunistic pathogen Aspergillus fumigatus. Fungal Genet Biol 39, 221–229

Movahed E, Tan GMY, Munusamy K, Yeow TC, Tay ST, Wong WF and Looi CY (2016) Triclosan Demonstrates Synergic Effect with Amphotericin B and Fluconazole and Induces Apoptosis-Like Cell Death in Cryptococcus neoformans. *Frontiers in Microbiology,* 7.

Mowat E, Butcher J, Lang S, Williams C and Ramage G (2007) Development of a simple model for studying the effects of antifungal agents on multicellular communities of Aspergillus fumigatus. *Journal of Medical Microbiology* 56(9): 1205–1212.

Mowat E, Lang S, Williams C, Mcculloch E, Jones B and Ramage G (2008) Phase-dependent antifungal activity against Aspergillus fumigatus developing multicellular filamentous biofilms. *Journal of Antimicrobial Chemotherapy* 62(6): 1281–1284.

Mowat E, Williams C, Jones B, Mcchlery S and Ramage G (2009) The characteristics of Aspergillus fumigatus mycetoma development: is this a biofilm? *Medical Mycology*47(s1).

Mueckler, M., Thorens, B., (2013). The SLC2 (GLUT) family of membrane transporters. Mol. Aspects Med. 34, 121–138.

Mulcahy, H., Charron-Mazenod, L., and Lewenza, S. (2008). Extracellular DNA chelates cations and induces antibiotic resistance in *Pseudomonas aeruginosa* biofilms. *PLoS Pathog.* 4:e1000213.

Mulcahy, H., Charron-Mazenod, L., and Lewenza, S. (2010). *Pseudomonas aeruginosa* produces an extracellular deoxyribonuclease that is required for utilization of DNA as a nutrient source. *Environ. Microbiol.* 12, 1621–1629.

Munro CA (2013) Chitin and Glucan, the Yin and Yang of the Fungal Cell Wall, Implications for Antifungal Drug Discovery and Therapy. *Advances in Applied Microbiology* 145–172.

Murray J, Muruko T, Gill CIR, Kearney MP, Farren D, Scott MG, Mcmullan G and Ternan NG (2017) Evaluation of bactericidal and anti-biofilm properties of a novel surface-active organosilane biocide against healthcare associated pathogens and Pseudomonas aeruginosa biolfilm. *Plos One* 12(8).

Nagamalleswari, E., Rao, S., Vasu, K., & Nagaraja, V. (2017). Restriction endonuclease triggered bacterial apoptosis as a mechanism for long time survival. *Nucleic Acids Research, 45*(14), 8423-8434.

Nakamura Y, Yamamoto N, Kino Y, Yamamoto N, Kamei S, Mori H, Kurokawa K and Nakashima N (2016) Establishment of a multi-species biofilm model and metatranscriptomic analysis of biofilm and planktonic cell communities. *Applied Microbiology and Biotechnology* 100(16): 7263–7279.

Nealson, K.H., Platt, T., and Hastings, J.W. (1970). Cellular control of the synthesis and activity of the bacterial luminescent system. J. Bacteriol. 104, 313–322.

Negri M, Silva S, Henriques M, Azeredo J, Svidzinski T and Oliveira R (2011) Candida tropicalisbiofilms: artificial urine, urinary catheters and flow model. *Medical Mycology* 1–9.

Nelson D.L., Cox M.M., (2012). Lehninger principles of biochemistry, 6th ed. W. H. Freeman, New York, NY.

Ng W-L and Bassler BL (2009) Bacterial Quorum-Sensing Network Architectures. *Annual Review of Genetics* 43(1): 197–222.

Nickerson KW, Atkin AL and Hornby JM (2006) Quorum Sensing in Dimorphic Fungi: Farnesol and Beyond. *Applied and Environmental Microbiology* 72(6): 3805–3813.

Nielsen, J., Mikkelsen, L., and Nielsen, P. (2001). In situ detection of cell surface hydrophobicity of probe-defined bacteria in activated sludge. Water Sci. Technol. 43, 97–103.

Nishinari K and Tipton CM (2000) *Hydrocolloids*. Amsterdam: Elsevier.

Norman KL, Shively CA, Rocha AJDL, Mutlu N, Basu S, Cullen PJ and Kumar A (2018) Inositol polyphosphates regulate and predict yeast pseudohyphal growth phenotypes. *PLOS Genetics* 14(6).

Nys RD, Wright AD, König GM and Sticher O (1993) New halogenated furanones from the marine alga delisea pulchra (cf. fimbriata). *Tetrahedron* 49(48): 11213–11220.

Ohyama K, Enn P, Uchide N, Bessho T and Yamakawa T (2001) Improvement of Separation Method of Fragmented DNA from an Apoptotic Cell DNA Sample for the Quantitation Using Agarose Gel Electrophoresis. *Biological & Pharmaceutical Bulletin* 24(4): 342–346.

Orosz A, Fekete E, Flipphi M, Karaffa L. (2014). Metabolism of D-galactose is dispensable for the induction of the beta-galactosidase (bgaD) and lactose permease (lacpA) genes in Aspergillus nidulans. FEMS Microbiol Lett 359:19 –25

Osherov N, May G. (2000). Conidial germination in Aspergillus nidulans requires RAS signaling and protein synthesis. Genetics. 155:647–656.

P.J. Millard, B.L. Roth, H.-P.T. Thi, S.T. Yue, R.P. HauglandDevelopment of the FUN-1 family of fluorescent probes for vacuole labeling and viability testing of yeasts. Appl. Environ. Microbiol., 63 (1997), pp. 2897-2905

Palacios DS, Anderson TM, Burke MD (2007) A post-PKS oxidation of the amphotericin B skeleton predicted to be critical for channel formation is not required for potent antifungal activity. J Am Chem Soc 129:13804–13805.

Pang X, Liu C, Lyu P, Zhang S, Liu L, Lu J, Ma C and Lv J (2016) Identification of Quorum Sensing Signal Molecule of Lactobacillus delbrueckii subsp. bulgaricus. *Journal of Agricultural and Food Chemistry* 64(49): 9421–9427.

Papagianni M (2004) Fungal morphology and metabolite production in submerged mycelial processes. *Biotechnology Advances* 22(3): 189–259.

Papenfort K and Bassler BL (2016) Quorum sensing signal–response systems in Gram-negative bacteria. *Nature Reviews Microbiology* 14(9): 576–588.

Parida S and Mishra S (2013) Urinary tract infections in the critical care unit: A brief review. *Indian Journal of Critical Care Medicine* 17(6): 370.

Paris, S., Debeaupuis, J., Crameri, R., Charlès, F., Prévost, M. C., Philippe, B., Latgé, J. P., Carey, M., Charle, F., Pre, M. C., Schmitt, C., and Latge, J. P. (2003) Conidial Hydrophobins of Aspergillus fumigatus. Appl. Environ. Microbiol. 69, 1581–1588.

Parsek MR and Greenberg E (2005) Sociomicrobiology: the connections between quorum sensing and biofilms. *Trends in Microbiology* 13(1): 27–33.

Pasqualotto AC (2009) Differences in pathogenicity and clinical syndromes due toAspergillus fumigatusandAspergillus flavus. *Medical Mycology* 47(s1).

Paulitz T, Nowak-Thompson B, Gamard P, Tsang E and Loper J (2000). *Journal of Chemical Ecology* 26(6): 1515–1524.

Peeters SH and Jonge MID (2018) For the greater good: Programmed cell death in bacterial communities. *Microbiological Research* 207: 161–169.

Peral-Cagigal B, Redondo-Gonzalez L and Verrier-Hernandez A (2014) Invasive maxillary sinus aspergillosis: A case report successfully treated with voriconazole and surgical debridement. *Journal of Clinical and Experimental Dentistry*.

Perez-Cuesta U, Aparicio-Fernandez L, Guruceaga X, Martin-Souto L, Abad-Diaz-De-Cerio A, Antoran A, Buldain I, Hernando FL, Ramirez-Garcia A and Rementeria A (2019) Melanin and pyomelanin in Aspergillus fumigatus: from its genetics to host interaction. *International Microbiology*.

Petraitiene, R., et al., Antifungal activity and pharmacokinetics of posaconazole (SCH 56592) in treatment and prevention of experimental invasive pulmonary aspergillosis: correlation with galactomannan antigenemia. Antimicrob Agents Chemother, 2001. 45(3): p. 857-69.

Philipp H (1997) Silicon Dioxide (SiO2) (Glass). Handbook of Optical Constants of Solids 749–763.

Platt R, Murdock B, Polk BF and Rosner B (1983) Reduction Of Mortality Associated With Nosocomial Urinary Tract Infection. *The Lancet* 321(8330): 893–897.

Priegnitz B-E, Wargenau A, Brandt U, Rohde M, Dietrich S, Kwade A, Krull R and Fleißner A (2012) The role of initial spore adhesion in pellet and biofilm formation in Aspergillus niger. *Fungal Genetics and Biology* 49(1): 30–38.

Prigent-Combaret C, Brombacher E, Vidal O, Ambert A, Lejeune P, Landini P and Dorel C (2001) Complex Regulatory Network Controls Initial Adhesion and Biofilm Formation in Escherichia coli via Regulation of the csgD Gene. *Journal of Bacteriology* 183(24): 7213–7223.

Promega Corporation. www.promega.co.uk.

Puttikamonkul S, Willger SD, Grahl N, Perfect JR, Movahed N, Bothner B, Park S, Paderu P, Perlin DS, Cramer RA, Jr. (2010). Trehalose 6-phosphate phosphatase is

required for cell wall integrity and fungal virulence but not trehalose biosynthesis in the human fungal pathogen Aspergillus fumigatus. Mol Microbiol 77:891–911.

PVCMed Alliance, in “PVC medical devices”, http://pvcmed.org/pvc-in-healthcare/pvc-medical-devices/, available on Feb. 11, 2017.

Quistgaard, E. M., Low, C., Moberg, P., Tresaugues, L., Nordlund, P., (2013). Structural basis for substrate transport in the GLUT-homology family of monosaccharide transporters. Nature Struct. Mol. Biol. 20, 766–768.

Raad I, Hachem R, Tcholakian RK, Sherertz R. Efficacy of minocycline and EDTA lock solution in preventing catheter-related bacteremia, septic phlebitis, and endocarditis in rabbits. Antimicrob Agents Chemother 2002;46:327–32.

Raina S, Vizio DD, Palonen EK, Odell M, Brandt AM, Soini JT and Keshavarz T (2012) Is quorum sensing involved in lovastatin production in the filamentous fungus Aspergillus terreus? *Process Biochemistry* 47(5): 843–852.

Rajendran R, Sherry L, Lappin DF, Nile CJ, Smith K, Williams C, Munro CA and Ramage G (2014) Extracellular DNA release confers heterogeneity in Candida albicans biofilm formation. *BMC Microbiology* 14(1).

Rajendran R, Williams C, Lappin DF, Millington O, Martins M and Ramage G (2013) Extracellular DNA Release Acts as an Antifungal Resistance Mechanism in Mature Aspergillus fumigatus Biofilms. *Eukaryotic Cell* 12(3): 420–429.

Ramage G, Rajendran R, Gutierrez-Correa M, Jones B and Williams C (2011) Aspergillus biofilms: clinical and industrial significance. *FEMS Microbiology Letters* 324(2): 89–97.

Ramage G, Saville SP, Wickes BL and Lopez-Ribot JL (2002) Inhibition of Candida albicans Biofilm Formation by Farnesol, a Quorum-Sensing Molecule. *Applied and Environmental Microbiology* 68(11): 5459–5463.

Ramphal L, Suzuki S, McCracken IM, Addai A. (2014) Improving hospital staff compliance with environmental cleaning behavior. Proc. (Bayl. Univ. Med. Cent); 27:88–91.

Reen FJ, Gutiérrez-Barranquero JA, Parages ML and O´gara F (2018) Coumarin: a novel player in microbial quorum sensing and biofilm formation inhibition. *Applied Microbiology and Biotechnology*102(5): 2063–2073.

Reeves EP, Murphy T, Daly P, Kavanagh K. 2004. Amphotericin B enhances the synthesis and release of the immunosuppressive agent gliotoxin from the pulmonary pathogen Aspergillus fumigatus. J. Med. Microbiol. 53:719 –725.

Remund KF, Best M and Egan JJ (2009) Infections Relevant to Lung Transplantation. *Proceedings of the American Thoracic Society* 6(1): 94–100.

Ren B, Dai H-Q, Pei G, Tong Y-J, Zhuo Y, Yang N, Su M-Y, Huang P, Yang Y-Z and Zhang L-X (2014) ABC transporters coupled with the elevated ergosterol contents contribute to the azole resistance and amphotericin B susceptibility. *Applied Microbiology and Biotechnology* 98(6): 2609–2616.

Rendueles O, Ghigo J-M. Mechanisms of competition in biofilm communities. Microbiol Spectr 2015;3:1–18.

Rendueles O, Ghigo J-M. Multi-species biofilms: how to avoid unfriendly neighbors. FEMS Microbiol Rev 2012;36:972–89.

Renko M, Paalanne N, Tapiainen T, Hinkkainen M, Pokka T, Kinnula S, Sinikumpu J-J, Uhari M and Serlo W (2017) Triclosan-containing sutures versus ordinary sutures for reducing surgical site infections in children: a double-blind, randomised controlled trial. *The Lancet Infectious Diseases* 17(1): 50–57.

Reyes-Montes MDR, Duarte-Escalante E, Frías-De-León MG, Martínez-Herrera EO and Acosta-Altamirano G (2018) Molecular Diagnosis of Invasive Aspergillosis. *Molecular Medicine [Working Title]*.

Reynolds TB (2001) Bakers' Yeast, a Model for Fungal Biofilm Formation. *Science* 291(5505): 878–881.

Riccardi, C., and Nicoletti, I. (2006). Analysis of apoptosis by propidium iodide staining and flow cytometry. *Nature Protocols, 1*(3), 1458-1461.

Rieux A, Soubeyrand S, Bonnot F, Klein EK, Ngando JE, Mehl A, Ravigne V, Carlier J and Bellaire LDLD (2014) Long-Distance Wind-Dispersal of Spores in a Fungal Plant Pathogen: Estimation of Anisotropic Dispersal Kernels from an Extensive Field Experiment. *PLoS ONE* 9(8).

Robbins N, Uppuluri P, Nett J, Rajendran R, Ramage G, Lopez-Ribot JL, Andes D and Cowen LE (2011) Hsp90 Governs Dispersion and Drug Resistance of Fungal Biofilms. *PLoS Pathogens* 7(9).

Rohde, M., Schwienbacher, M., Nikolaus, T., Heesemann, J., and Ebel, F. (2002) Detection of early phase specific surface appendages during germination of Aspergillus fumigatus conidia. FEMS Microbiol Lett 206: 99–105.

Rollet C, Gal L and Guzzo J (2008) Biofilm-detached cells, a transition from a sessile to a planktonic phenotype: a comparative study of adhesion and physiological characteristics in Pseudomonas aeruginosa. *FEMS Microbiology Letters* 290(2): 135–142.

Rosenberg M, Azevedo NF and Ivask A (2019) Propidium iodide staining underestimates viability of adherent bacterial cells. *Scientific Reports* 9(1).

Rowley T (2012) Flow Cytometry - A Survey and the Basics. *Materials and Methods* 2.

Ruiz-Herrera J and San-Blas G (2003) Chitin Synthesis as a Target for Antifungal Drugs. *Current Drug Target -Infectious Disorders* 3(1): 77–91.

Rumbo-Feal S, Gómez MJ, Gayoso C, Álvarez-Fraga L, Cabral MP, Aransay AM, Rodríguez-Ezpeleta N, Fullaondo A, Valle J, Tomás M, Bou G and Poza M (2013) Whole Transcriptome Analysis of Acinetobacter baumannii Assessed by RNA-Sequencing Reveals Different mRNA Expression Profiles in Biofilm Compared to Planktonic Cells. *PLoS ONE* 8(8).

Runguphan W and Keasling JD (2014) Metabolic engineering of Saccharomyces cerevisiae for production of fatty acid-derived biofuels and chemicals. *Metabolic Engineering* 21: 103–113.

Ruszkiewicz JA, Li S, Rodriguez MB and Aschner M (2017) Is Triclosan a neurotoxic agent?*Journal of Toxicology and Environmental Health, Part B* 20(2): 104–117.

Safdar N, Maki DG. The pathogenesis of catheter-related bloodstream infection with noncuffed short-term central venous catheters. Intensive Care Med 2004;30:62–7.

Saidi S, Luitaud C and Rouabhia M (2006) In vitro synergistic effect of farnesol and human gingival cells againstCandida albicans. *Yeast* 23(9): 673–687.

Sánchez-Gómez S and Martínez-De-Tejada G (2016) Antimicrobial Peptides as Anti-biofilm Agents in Medical Implants. *Current Topics in Medicinal Chemistry* 17(5): 590–603.

Sanchez-Gomez S, Martınez-de-Tejada G. Antimicrobial peptides as anti-biofilagents in medical implants. Curr Top Med Chem 2017;17:590–603.

Sande WWVD, Kat JD, Coppens J, Ahmed AO, Fahal A, Verbrugh H and Belkum AV (2007) Melanin biosynthesis in Madurella mycetomatis and its effect on susceptibility to itraconazole and ketoconazole. *Microbes and Infection* 9(9): 1114–1123.

Santangelo GM. 2006. Glucose signaling in Saccharomyces cerevisiae. Microbiol Mol Biol Rev 70:253–282.

Savoldi M, Malavazi I, Soriani FM, Capellaro JL, Kitamoto K, Ferreira MEDS, Goldman MHS and Goldman GH (2008) Farnesol induces the transcriptional accumulation of the Aspergillus nidulans Apoptosis-Inducing Factor (AIF)-like mitochondrial oxidoreductase. *Molecular Microbiology* 70(1): 44–59.

Schiavone M, Vax A, Formosa C, Martin-Yken H, Dague E, François JM. (2014). A combined chemical and enzymatic method to determine quantitatively the polysaccharide components in the cell wall of yeasts. FEMS Yeast Res 14:933–947.

Schmaler-Ripcke J, Sugareva V, Gebhardt P, Winkler R, Kniemeyer O, Heinekamp T and Brakhage AA (2008) Production of Pyomelanin, a Second Type of Melanin, via the Tyrosine Degradation Pathway in Aspergillus fumigatus. *Applied and Environmental Microbiology* 75(2): 493–503.

Schwienbacher M, Weig M, Thies S, Regula JT, Heesemann J and Ebel F (2005) Analysis of the major proteins secreted by the human opportunistic pathogenAspergillus fumigatusunderin vitroconditions. Medical Mycology 43(7): 623–630.

Sebastián-Pérez V, Manoli M-T, Pérez DI, Gil C, Mellado E, Martínez A, Espeso EA, Campillo NE. (2016). New applications for known drugs: human glycogen synthase kinase 3 inhibitors as modulators of Aspergillus fumigatus growth. Eur J Med Chem 116:281–289

Sedor, J., and S. G. Mulholland. (1999). Hospital-acquired urinary tract infections associated with the indwelling catheter. Urol. Clin. N. Am. 26: 821–828.

Sekiguchi Y, Yao Y, Ohko Y, Tanaka K, Ishido T, Fujishima A. (2007). Self- sterilizing catheters with titanium dioxide photocatalyst thin film for clean intermittent catheterization: basis and study of clinical use. Int J Urol.; 14:426–430.

Simpson, I. A., Dwyer, D., Malide, D., Moley, K. H., Travis, A., Vannucci, S. J (2008). The facilitative glucose transporter GLUT3: 20 years of distinction. *American Journal of Physiology-Endocrinology and Metabolism, 295*(2).

Tadmor R, Hernández-Zapata E, Chen N, Pincus P and Israelachvili JN (2002) Debye Length and Double-Layer Forces in Polyelectrolyte Solutions. Macromolecules 35(6): 2380–2388.

Selby H and Whistler RL (1993) Agar. Industrial Gums 87–103.

Selvam S, Andrews ME and Mishra AK (2009) A photophysical study on the role of bile salt hydrophobicity in solubilizing amphotericin B aggregates. Journal of Pharmaceutical Sciences 98(11): 4153–4160.

Semighini CP, Hornby JM, Dumitru R, Nickerson KW and Harris SD (2006) Farnesol-induced apoptosis in Aspergillus nidulans reveals a possible mechanism for antagonistic interactions between fungi. *Molecular Microbiology* 59(3): 753–764.

Semighini CP, Murray N and Harris SD (2008) Inhibition of Fusarium graminearum growth and development by farnesol. *FEMS Microbiology Letters* 279(2): 259–264.

Sengupta J, Saha S, Khetan A, Sarkar SK and Mandal SM (2012) Effects of lactoferricin B against keratitis-associated fungal biofilms. *Journal of Infection and Chemotherapy* 18(5): 698–703.

Seo K, Akiyoshi H, Ohnishi Y. (1999). Alteration of cell wall composition leads to amphotericin B resistance in Aspergillus flavus. Microbiol. Immunol. 43:1017–1025.

Shanmugam N, Baker MODG, Ball SR, Steain M, Pham CLL and Sunde M (2019) Microbial functional amyloids serve diverse purposes for structure, adhesion and defence. Biophysical Reviews 11(3): 287–302.

Shanmughapriya S, Sornakumari H, Lency A, Kavitha S and Natarajaseenivasan K (2014) Synergistic effect of amphotericin B and tyrosol on biofilm formed by Candida krusei and Candida tropicalis from intrauterine device users. *Medical Mycology* 52(8): 853–861.

Shareck J and Belhumeur P (2011) Modulation of Morphogenesis in Candida albicans by Various Small Molecules. *Eukaryotic Cell* 10(8): 1004–1012.

Sheppard DC (2011) Molecular mechanism of Aspergillus fumigatus adherence to host constituents. *Current Opinion in Microbiology* 14(4): 375–379.

Sheppard DC and Howell PL (2016) Biofilm Exopolysaccharides of Pathogenic Fungi: Lessons from Bacteria. *Journal of Biological Chemistry* 291(24): 12529–12537.

Sheppard DC and Howell PL (2016) Biofilm Exopolysaccharides of Pathogenic Fungi: Lessons from Bacteria. *Journal of Biological Chemistry* 291(24): 12529–12537.

Shirtliff ME, Krom BP, Meijering RAM, Peters BM, Zhu J, Scheper MA, Harris ML and Jabra-Rizk MA (2009) Farnesol-Induced Apoptosis in Candida albicans. *Antimicrobial Agents and Chemotherapy* 53(6): 2392–2401.

Shopova I, Bruns S, Thywissen A, Kniemeyer O, Brakhage AA and Hillmann F (2013) Extrinsic extracellular DNA leads to biofilm formation and colocalizes with matrix polysaccharides in the human pathogenic fungus Aspergillus fumigatus. *Frontiers in Microbiology* 4.

Sinde E., Carballo J. (2000). Attachment of *Salmonell*a spp. and *Listeria monocytogenes* to stainless steel, rubber and polytetrafluor-ethylenethe influence of free energy and the effect of commercial sanitizers. Food Microbiol. 17, 439–447 10.1006/fmic.2000.0339

Singh N and Paterson DL (2005) Aspergillus Infections in Transplant Recipients. *Clinical Microbiology Reviews* 18(1): 44–69.

Siqueira VM and Lima N (2013) Biofilm Formation by Filamentous Fungi Recovered from a Water System. *Journal of Mycology* 2013: 1–9.

Sletmoen M and Stokke BT (2008) Higher order structure of (1,3)-β-D-glucans and its influence on their biological activities and complexation abilities. *Biopolymers* 89(4): 310–321.

Sloothaak, J., Odoni, D. I., de Graaff, L. H., Martins Dos Santos, V., Schaap, P. J., Tamayo-Ramos, J. A., (2015). *Aspergillus niger* membrane-associated proteome analysis for the identification of glucose transporters. *Biotechnology for biofuels*, *8*, 150.

Smith RS, Zhang Z, Bouchard M, Li J, Lapp HS, Brotske GR, et al. (2012) Vascular catheters with a non-leaching poly-sulfobetaine surface modification reduce thrombus formation and microbial attachment. Sci Transl Med; 4:153ra132.

Sordi LD and Mühlschlegel FA (2009) Quorum sensing and fungal-bacterial interactions inCandida albicans: a communicative network regulating microbial coexistence and virulence. *FEMS Yeast Research* 9(7): 990–999.

Sorrentino F, Roy I and Keshavarz T (2010) Impact of linoleic acid supplementation on lovastatin production in Aspergillus terreus cultures. *Applied Microbiology and Biotechnology* 88(1): 65–73.

Souweine B, Lautrette A, Gruson D, Canet E, Klouche K, Argaud L. (2015) Ethanol lock and risk of hemodialysis catheter infection in critically ill patients. A randomized controlled trial. Am J Respir Crit Care Med;191:1024– 32.

Spoering, A. L., and Lewis, K. (2001). Biofilms and Planktonic Cells of *Pseudomonas aeruginosa* Have Similar Resistance to Killing by Antimicrobials. *Journal of Bacteriology, 183*(23), 6746-6751.

Sprague GF (2006) Eukaryotes learn how to count: quorum sensing by yeast. *Genes & Development* 20(9): 1045–1049.

Srinivasan, R., and Swain, G. (2007). Managing the use of copper-based antifouling paints. Environ. Manag. 39, 23–441

Steinbach WJ, Schell WA, Blankenship JR, Onyewu C, Heitman J and Perfect JR (2004) In Vitro Interactions between Antifungals and Immunosuppressants against Aspergillus fumigatus. *Antimicrobial Agents and Chemotherapy* 48(5): 1664–1669.

Stewart MJ, Parikh S, Xiao G, Tonge PJ et al (1999) Structural basis and mechanism of enoyl reductase inhibition by triclosan. J Mol Biol 290:859–865.

Stickler D (2012) Surface coatings in urology. *Coatings for Biomedical Applications* 304–335.

Stroud, P.A., Goodwin, J.S., Butko, P., Cannon, G.C., McCormick, C.L., (2003). Experimental evidence for multiple assembled states of Sc3 from Schizophyllum commune. Biomacromolecules 4, 956–967.

Sueiro-Olivares M, Fernandez-Molina JV, Abad-Diaz-de-Cerio A, Gorospe E, Pascual E, Guruceaga X, Ramirez-Garcia A, Garaizar J, Hernando FL, Margareto J, Rementeria A (2015) Aspergillus fumigatus transcriptome response to a higher temperature during the earliest steps of germination monitored using a new customized expression microarray. Microbiology 161:490–502.

Sun, L., Zeng, X., Yan, C., Sun, X., Gong, X., Rao, Y., Yan, N., (2012). Crystal structure of a bacterial homologue of glucose transporters GLUT1–4. *Nature, 490*(7420), 361-366.

Svensater G and Bergenholtz G (2004) Biofilms in endodontic infections. *Endodontic Topics* 9(1): 27–36.

Swartjes J, Sharma P, Kooten T, Mei H, Mahmoudi M, Busscher H and Rochford E (2015) Current Developments in Antimicrobial Surface Coatings for Biomedical Applications. *Current Medicinal Chemistry* 22(18): 2116–2129.

Szilagyi M, Kwon NJ, Dorogi C, Pocsi I, Yu JH, Emri T. (2010). The extracellular beta-1,3-endoglucanase EngA is involved in autolysis of Aspergillus nidulans. J. Appl. Microbiol. 109: 1498–1508.

Tabak, M., Scher, K., Hartog, E., Ro mLing, U., Matthews, K., Chikindas, M., et al. (2007). Effect of triclosan on Salmonella typhimurium at different growth stages and in biofilms. FEMS Microbiol. Lett. 267, 200–206

Taff, H.T., Mitchell, K.F., Edward, J.A., Andes, D.R., (2013). Mechanisms of Candida biofilm drug resistance. Future Microbiol., 8, 1325–1337.

Taheri-Talesh N, Horio T, Araujo-Bazan L, Dou X, Espeso EA, Penalva MA, Osmani SA and Oakley BR (2008) The Tip Growth Apparatus of Aspergillus nidulans. *Molecular Biology of the Cell* 19(4): 1439–1449.

Takahashi, T.; Maeda, H.; Yoneda, S.; Ohtaki, S.; Yamagata, Y.; Hasegawa, F.; Gomi, K.; Nakajima, T.; Abe, K. (2005) The fungal hydrophobin RolA recruits polyesterase and laterally moves on hydrophobic surfaces. Mol. Microbiol, 57 (6), 1780−1796.

Tamkovich S, Vlassov V, Laktionov P. (2008). Circulating DNA in the blood and its application in medical diagnosis. Mol. Biol. 42: 9–19

Tan TRM, Hoi KM, Zhang P and Ng SK (2016) Characterization of a Polyethylene Glycol-Amphotericin B Conjugate Loaded with Free AMB for Improved Antifungal Efficacy. Plos One 11(3).

Tepsic K (1997) Growth and mycotoxin production by Aspergillus fumigatus strains isolated from a saltern. *FEMS Microbiology Letters* 157(1): 9–12.

Thevelein JM. 1984. Regulation of trehalose mobilization in fungi. Microbiol Rev 48:42–59.

Thomas-White K, Brady M, Wolfe AJ and Mueller ER (2016) The Bladder Is Not Sterile: History and Current Discoveries on the Urinary Microbiome. *Current Bladder Dysfunction Reports* 11(1): 18–24.

Thormann, E., Simonsen, A., Hansen, P., and Mouritsen, O. (2008). Interactions between a polystyrene particle and hydrophilic and hydrophobic surfaces in aqueous solutions. Langmuir 24, 7278–7284.

Tonin FS, Steimbach LM, Borba HH, Sanches AC, Wiens A,Pontarolo R, Fernandez-Llimos F. 2017. Efficacy and safety of amphotericin B formulations: a network meta-analysis and a multicriteria decision analysis. *J Pharm Pharmacol* 69:1672–1683.

Torkkeli M., Serimaa R., Ikkala O., Linder M. (2002). Low-resolution structural models. *Biophys*. *J*. Trichoderma reesei 83: 2240–2247.

Torres, N. V., Riol-Cimas, J. M., Wolschek, M. Kubicek, C. P., (1996). Glucose transport by *Aspergillus niger*: the low-affinity carrier is only formed during growth on high glucose concentrations. Appl Microbiol Biotechnol 44, 790–794.

Trautner BW (2005) Colicins prevent colonization of urinary catheters. *Journal of Antimicrobial Chemotherapy* 56(2): 413–415.

Tseng CC and Fink GR (2008) Quorum Sensing in Fungi. *Chemical Communication among Bacteria* 443–451.

Tzoraki O and Lasithiotakis M (2018) Environmental Risks Associated with Waste Electrical and Electronic Equipment Recycling Plants. *Reference Module in Earth Systems and Environmental Sciences*.

Vahtera E, Crespo BG, Mcgillicuddy DJ, Olli K and Anderson DM (2014) Alexandrium fundyense cyst viability and ger mLing survival in light vs. dark at a constant low temperature. *Deep Sea Research Part II: Topical Studies in Oceanography* 103: 112–119.

Vallor, A.C., et al., (2008) Assessment of Aspergillus fumigatus burden in pulmonary tissue of guinea pigs by quantitative PCR, galactomannan enzyme immunoassay, and quantitative culture. Antimicrob Agents Chemother. 52(7): p. 2593-8.

Valsecchi I, Dupres V, Stephen-Victor E, Guijarro J, Gibbons J, Beau R, Bayry J, Coppee J-Y, Lafont F, Latgé J-P and Beauvais A (2017) Role of Hydrophobins in Aspergillus fumigatus. *Journal of Fungi* 4(1): 2.

Van Loosdrecht M., Norde W., Zehnder A. (1990). Physical chemical description of bacterial adhesion. J. Biomater. Appl. 5, 91–106

Vanhauteghem D, Demeyere K, Callaert N, Boelaert A, Haesaert G, Audenaert K and Meyer E (2017) Flow Cytometry Is a Powerful Tool for Assessment of the Viability of Fungal Conidia in Metalworking Fluids. *Applied and Environmental Microbiology* 83(16).

Verplanck N, Coffinier Y, Thomy V and Boukherroub R (2007) Wettability Switching Techniques on Superhydrophobic Surfaces. *Nanoscale Research Letters* 2(12): 577–596.

Villena GK and Gutierrez-Correa M (2007) Production of lignocellulolytic enzymes by Aspergillus niger biofilms at variable water activities. *Electronic Journal of Biotechnology* 10(1).

Viola GM and Sutton R (2010) Allergic fungal sinusitis complicated by fungal brain mass. *International Journal of Infectious Diseases* 14.

Voltersen V, Blango MG, Herrmann S, Schmidt F, Heinekamp T, Strassburger M, Krüger T, Bacher P, Lother J, Weiss E, Hünniger K, Liu H, Hortschansky P, Scheffold A, Löffler J, Krappmann S, Nietzsche S, Kurzai O, Einsele H, Kniemeyer O, Filler SG, Reichard U and Brakhage AA (2018) Proteome Analysis Reveals the Conidial Surface Protein CcpA Essential for Virulence of the Pathogenic Fungus Aspergillus fumigatus. *mBio* 9(5).

Walker L, Sood P, Lenardon MD, Milne G, Olson J, Jensen G,Wolf J, Casadevall A, Adler-Moore J, Gow NAR. (2018). The Viscoelastic Properties of the Fungal Cell Wall Allow Traffic of AmBisome as Intact Liposome Vesicles. *MBio* 9.

Walker LA, Gow NA, Munro CA (2013) Elevated chitin content reduces the susceptibility of Candida species to caspofungin. Antimicrob Agents Chemother, 57 (1): 146-154.

Walker LA, Munro CA, de Bruijn I, Lenardon MD, McKinnon A, Gow NA: Stimulation of chitin synthesis rescues Candida albicans from echinocandins.*PLoS Pathog* 2008, 4(4):e1000040.,

Walsh TJ and Dixon DM (1989) Nosocomial aspergillosis: Environmental microbiology, hospital epidemiology, diagnosis and treatment. *European Journal of Epidemiology* 5(2): 131–142.

Wang X, Wang Y, Zhou Y and Wei X (2014) Farnesol induces apoptosis-like cell death in the pathogenic fungus Aspergillus flavus. *Mycologia* 106(5): 881–888.

Wartenberg D, Lapp K, Jacobsen ID, Dahse HM, Kniemeyer O, Heinekamp T, Brakhage AA (2011) Secretome analysis of Aspergillus fumigatus reveals Asp-hemolysin as a major secreted protein. Int J Med Microbiol 301:602–611

Weatherly LM and Gosse JA (2017) Triclosan exposure, transformation, and human health effects. *Journal of Toxicology and Environmental Health, Part B* 20(8): 447–469.

Wei, H., Vienken, K., Weber, R., Bunting, S., Requena, N., Fischer R., (2004). A putative high affinity hexose transporter, hxtA, of *Aspergillus nidulans* is induced in vegetative hyphae upon starvation and in ascogenous hyphae during cleistothecium formation. Fungal Genet Biol (41), 148–156.

Welch K, Cai Y and Strømme M (2012) A Method for Quantitative Determination of Biofilm Viability. *Journal of Functional Biomaterials* 3(2): 418–431.

Westfall C, Flores-Mireles AL, Robinson JI, Lynch AJL, Hultgren S, Henderson JP and Levin PA (2019) The Widely Used Antimicrobial Triclosan Induces High Levels of Antibiotic Tolerance In Vitro and Reduces Antibiotic Efficacy up to 100-Fold In Vivo. *Antimicrobial Agents and Chemotherapy* 63(5).

Westwater C, Balish E and Schofield DA (2005) Candida albicans-Conditioned Medium Protects Yeast Cells from Oxidative Stress: a Possible Link between Quorum Sensing and Oxidative Stress Resistance. *Eukaryotic Cell* 4(10): 1654–1661.

Whitchurch CB (2002) Extracellular DNA Required for Bacterial Biofilm Formation. *Science* 295(5559): 1487–1487.

Wildgruber M, Lueg C, Borgmeyer S, Karimov I, Braun U, Kiechle M, Meier R, Koehler M, Ettl J and Berger H (2016) Polyurethane versus silicone catheters for central venous port devices implanted at the forearm. *European Journal of Cancer* 59: 113–124.

Williams HE, Steele JCP, Clements MO and Keshavarz T (2012) γ-Heptalactone is an endogenously produced quorum-sensing molecule regulating growth and secondary metabolite production by Aspergillus nidulans. *Applied Microbiology and Biotechnology* 96(3): 773–781.

Williams HE, Steele JCP, Clements MO and Keshavarz T (2012) γ-Heptalactone is an endogenously produced quorum-sensing molecule regulating growth and secondary metabolite production by Aspergillus nidulans. *Applied Microbiology and Biotechnology* 96(3): 773–781.

Wimpenny J, Manz W and Szewzyk U (2000) Heterogeneity in biofilms: Table 1. *FEMS Microbiology Reviews* 24(5): 661–671.

Winn WC and Koneman EW (2006) *Koneman's color atlas and textbook of diagnostic microbiology*. Lippincott Williams & Wilkins.

Wisedchaisri, G., Park, M. S., Iadanza, M. G., Zheng, H., Gonen T., (2014). Proton-coupled sugar transport in the prototypical major facilitator superfamily protein XylE. Nature Commun. 5, 4521.

Wö sten, H. A.; Schuren, F. H.; Wessels, J. G. (1994). Interfacial selfassembly of a hydrophobin into an amphipathic protein membrane mediates fungal attachment to hydrophobic surfaces. EMBO J., 13 (24), 5848−54.

Wongsuk T, Pumeesat P and Luplertlop N (2016) Fungal quorum sensing molecules: Role in fungal morphogenesis and pathogenicity. *Journal of Basic Microbiology* 56(5): 440–447.

Wösten HAB (2001) Hydrophobins: Multipurpose Proteins. *Annual Review of Microbiology* 55(1): 625–646.

Wuster A and Babu MM (2009) Transcriptional control of the quorum sensing response in yeast. *Mol. BioSyst.* 6(1): 134–141.

Yang MS and Li LK (2011) Preparation of High-Rigidity, High-Toughness Unplasticized Poly(vinyl Chloride) for Plastic Windows Profiles Reinforced and Toughened by Nano-CaCO3. Applied Mechanics and Materials 71-78: 1237–1241.

Yasir M, Willcox M and Dutta D (2018) Action of Antimicrobial Peptides against Bacterial Biofilms. *Materials* 11(12): 2468.

Yazdankhah, S., Scheie, A., Høiby, E., Lunestad, B., Heir, E., Fotland, T., et al. (2006). Triclosan and antimicrobial resistance in bacteria: an overview. Microb. Drug Res. 12, 83–89.

Yeagle PL (2016) Membrane Transport. The Membranes of Cells 335–378.

Yoda, Ryuichiro 1998, Elastomers for biomedical applications, Journal Of Biomaterials Science Polymer Edition. 9(6): 561-626.

Young T. (1805) III. An essay on the cohesion of fluids. *Philosophical Transactions of the Royal Society of London* 95: 65–87.

Yu J-H (2010) Regulation of Development inAspergillus nidulansandAspergillus fumigatus. *Mycobiology* 38(4): 229.

Yu L, Ling G, Deng X, Jin J, Jin Q and Guo N (2011) In Vitro Interaction between Fluconazole and Triclosan against Clinical Isolates of Fluconazole-Resistant Candida albicans Determined by Different Methods. *Antimicrobial Agents and Chemotherapy* 55(7): 3609–3612.

Yu, L.H., Wei, X., Ma, M., Chen, X.J.(2012). Possible inhibitory molecular mechanism of farnesol on the development of fluconazole resistance in Candida albicans biofilm. Antimicrob. Agents Chemother. 56, 770– 775.

Yuan, Y. and Lee, T. R., (2013). Contact angle and wetting properties, In: Surface science techniques, Eds: Springer, p. 3-34.

Zemke AC and Bomberger JM (2016) Microbiology: Social Suicide for a Good Cause. *Current Biology* 26(2).

Zhang Y and Lin Y-P (2014) Leaching of lead from new unplasticized polyvinyl chloride (uPVC) pipes into drinking water. *Environmental Science and Pollution Research* 22(11): 8405–8411.

Zhang Y, Yuan Z-P, Qin Y, Dai J and Zhang T (2018) Comparative Studies on Hydrophilic and Hydrophobic Segments Grafted Poly (vinyl chloride). *Chinese Journal of Polymer Science* 36(5): 604–611.

Zhao W, Panepinto JC, Fortwendel JR, Fox L, Oliver BG, Askew DS, Rhodes JC. 2006. Deletion of the regulatory subunit of protein kinase A in Aspergillus fumigatus alters morphology, sensitivity to oxidative damage, and virulence. Infect Immun 74:4865–4874.

Zhao, Q., and Liu, Y. (2006). Modification of stainless steel surfaces by electroless Ni-P and small amount of PTFE to minimize bacterial adhesion. J. Food Eng. 72, 266–272.

Zielińska, J., Wieczór, M., Bączek, T. *et al.* (2016). Thermodynamics and kinetics of amphotericin B self-association in aqueous solution characterized in molecular detail. *Sci Rep* **6,** 19109.

Zmantar, T., Bettaie, F., Chaieb, K., Ezzili, B., Mora-Ponsonnet, L., Othmane, A., et al. (2011). Atomic force microscopy and hydrodynamic characterization of the adhesion of Staphylococcus aureus to hydrophilic and hydrophobic substrata at different pH values. World J. Microbiol. Biotechnol. 27, 887–896.